

**Synthesis of Analogs of the Natural Product
Chondramide A. Mechanisms of Transition Metal
Catalyzed Reactions of Alkynes**

**Synthese von Analoga des Naturstoffes Chondramid A.
Mechanismen Übergangsmetall-katalysierter
Reaktionen von Alkinen**

Dissertation

der Mathematisch-Naturwissenschaftlichen Fakultät

der Eberhard Karls Universität Tübingen

zur Erlangung des Grades eines

Doktors der Naturwissenschaften

(Dr. rer. nat.)

vorgelegt von

Alexander G. Zhdanko

aus Kletsk, Weißrussland

Tübingen

2015

Tag der mündlichen Prüfung:

30.04.2015

Dekan:

Prof. Dr. W. Rosenstiel

1. Berichterstatter:

Prof. Dr. M. E. Maier

2. Berichterstatter:

Prof. Dr. H. F. Bettinger

3. Berichterstatter:

Prof. Dr. A. S. K. Hashmi

This doctoral thesis was carried out from September 2009 to August 2014 at the Institute of Organic Chemistry, Faculty of Natural Science, University of Tübingen, Germany, in the laboratory of Prof. Dr. Martin E. Maier.

First of all, I would like to thank Prof. Dr. Martin E. Maier for giving me an opportunity to work in a high level research laboratory, for giving me complete freedom to perform the work in a spirit of curiosity and creativity, and for supporting me in all my initiatives.

I thank Dr. Klaus Eichele and the Institute of Inorganic Chemistry at the University of Tübingen, for allowing me to use their 400 Bruker Avance II NMR spectrometer. Most of the research results were obtained using this instrument. And I apologise for any inconvenience I might have caused to other people during the time of very intensive use.

I thank all our group members for their friendly nature and for keeping a relaxed atmosphere in the lab. I specially thank Dr. Anton Khartulyari, Dr. Dmitry Ushakov, Petra Brozik, Dr. Natalia Fischer and Libra for fun and support during my stay in Tübingen.

I thank Maria Munari for well organized supply of chemicals, her great help in the laboratory and her wonderful cakes. I thank our secretaries Egidia Naiser and Magdalena Muresan for help with the office work.

I thank Dr. Dorothee Wistuba for performing HRMS analyses, Dr. Florenz Sasse (HZI Braunschweig) as well as Christopher I. Ma, and L. David Sibley (Department of Molecular Microbiology, Washington University School of Medicine, St. Louis, Missouri, USA) for biological experiments, Dr. Markus Ströbele and Dr. Cäcilia Maichle-Mössmer (Institut für Anorganische Chemie) for X-ray crystallography experiments, Paul Schuler and Dr. Markus Kramer for assistance with NMR.

I thank all my undergraduate students I assisted during several organic chemistry university lab courses for providing me with numerous chemicals for my research and for raising the level of my German language.

Finally, I am thankful to my mother for the love and support in my life and education. And I am thankful to my father for the kindly presence in my life despite the big distance between the countries.

My mother

CONTENTS

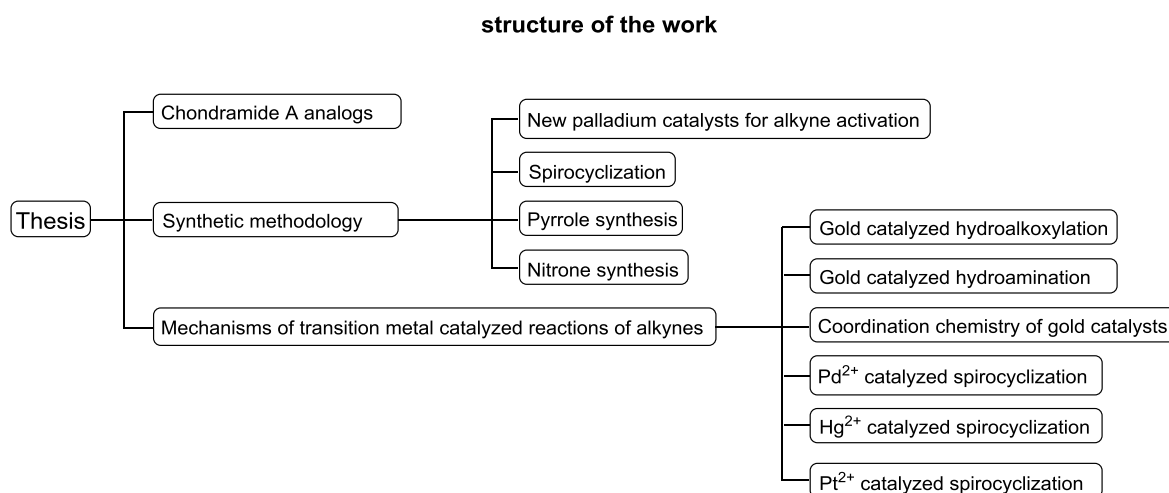
| | |
|---|-----------|
| 1. ABSTRACT (ENGLISH) | 3 |
| 2. ABSTRACT (GERMAN) | 5 |
| 3. PUBLICATIONS INCORPORATED INTO THIS THESIS | 6 |
| 4. PERSONAL CONTRIBUTION | 7 |
| 5. OBJECTIVE AND EXPECTED OUTPUT OF THE THESIS | 9 |
| 6. RESULTS AND DISCUSSION | 10 |
| 6.1. SYNTHESIS OF CHONDRAMIDE A ANALOGS WITH MODIFIED B-TYROSINE AND THEIR BIOLOGICAL EVALUATION | 10 |
| 6.2. SYNTHETIC METHODOLOGY | 13 |
| 6.2.1. GOLD(I), PALLADIUM(II), PLATINUM(II) AND MERCURY(II) CATALYZED SPIROCYCLIZATION OF 1,3-ENYNE DIOLS | 13 |
| 6.2.2. NEW PALLADIUM CATALYSTS FOR ALKYNE ACTIVATION | 15 |
| 6.2.3. CYCLIZATION OF ALKYNYL HYDROXYLAMINES. SYNTHESIS OF PYRROLES AND NITRONES | 17 |
| 6.3. MECHANISMS OF TRANSITION METAL CATALYZED REACTIONS OF ALKYNES | 18 |
| 6.3.1. COORDINATION CHEMISTRY OF GOLD CATALYSTS | 18 |
| 6.3.2. MECHANISM OF GOLD CATALYZED HYDROALKOXYLATION | 19 |
| 6.3.3. EXPLANATION OF COUNTERION EFFECTS IN GOLD(I)-CATALYZED HYDROALKOXYLATION OF ALKYNES | 21 |
| 6.3.4. EXPLANATION OF "SILVER EFFECT" ON GOLD(I)-CATALYZED HYDROALKOXYLATION OF ALKYNES | 22 |
| 6.3.5. MECHANISM OF GOLD CATALYZED HYDROAMINATION | 24 |
| 6.3.6. MECHANISM OF PALLADIUM CATALYZED SPIROCYCLIZATION | 25 |
| 6.3.7. MECHANISM OF PLATINUM CATALYZED SPIROCYCLIZATION | 27 |
| 6.3.8. MECHANISM OF MERCURY CATALYZED SPIROCYCLIZATION | 28 |
| 7. BIBLIOGRAPHY | 30 |
| 8. PUBLICATIONS 1-8 INCLUDED IN THIS THESIS | |
| 8A. MANUSCRIPTS 9-10 INCLUDED IN THIS THESIS | |
| 9. APPENDIX 1. SYNTHESIS OF HYDROXYLAMINE 19B AND PYRROLE 20A | |

Abbreviations

| | |
|-------------------|--|
| Ac | acetyl |
| aq. | aqueous |
| Bn | benzyl |
| br | broad (NMR) |
| b.p. | boiling point |
| Bz | benzoyl |
| COSY | correlation spectroscopy |
| Cy | cyclohexyl |
| DCM | dichloromethane |
| DEAD | diethyl azodicarboxylate |
| DIAD | diisopropyl azodicarboxylate |
| DIPEA | diisopropylethylamine |
| DMAP | 4-dimethylaminopyridine |
| DMF | N,N-dimethylformamide |
| DMSO | dimethylsulfoxide |
| dr | diastereomeric ratio |
| ee | enantiomeric excess |
| ESI | electrospray ionization |
| Et ₂ O | diethyl ether |
| EtOAc | ethyl acetate |
| HMBC | heteronuclear multiple bond correlation (NMR) |
| HOBt | N-hydroxybenzotriazole |
| HRMS | high resolution mass spectrometry |
| Hz | Hertz |
| iPr | isopropyl |
| J | coupling constant |
| LDA | lithium diisopropylamide |
| Ms | methanesulfonyl |
| NBS | N-bromosuccinimide |
| NMP | N-methylpyrrolidone |
| NOESY | nuclear Overhauser effect spectroscopy |
| OTFA | trifluoroacetate |
| PE | petroleum ether |
| Ph | phenyl |
| Py | pyridine |
| R _f | retention factor (TLC) |
| r.t. | room temperature |
| TBAF | tetrabutylammonium fluoride |
| TBS | tert-butyldimethylsilyl |
| TBTU | O-(Benzotriazol-1-yl)-N,N,N',N'-tetramethyluronium tetrafluoroborate |
| THF | tetrahydrofuran |
| TFA | trifluoroacetic acid |
| TfO (OTf) | triflate, trifluoromethanesulfonate |
| TMS | trimethylsilyl |
| TMTU | N,N,N',N'-tetramethylthiourea |
| TsOH | para-toluenesulfonic acid |

1. Abstract (English)

This thesis consists of several independent projects, covering three aspects of organic chemistry: total synthesis, development of new synthetic methodology and mechanistic investigation. The total synthesis part is devoted to the synthesis of chondramide A analogs and their biological evaluation. The methodology part describes several new catalytic transformations of alkynes and creation of new palladium catalysts for alkyne activation. The third and the biggest part describes experimental mechanistic investigations of gold, palladium, platinum and mercury catalyzed reactions of alkynes.



Chondramide A is a natural product belonging to the class of cyclodepsipeptides isolated from myxobacteria. It possesses antitumor activity due to its stabilizing effect on F-actin filaments. In 2009 our group reported the first total synthesis of Chondramide A. To better understand the mode of action, to establish which structural motifs are critical for its action and which parts could be modified without loss of biological activity, the synthesis and biological study of analogs of the above-mentioned cyclodepsipeptide was undertaken. Using the known route to chondramide A, seven unnatural analogues with modified β -tyrosine moiety were synthesized.

The synthesis of complex bioactive molecules would not be possible without having strong synthetic methods. Therefore, development of new synthetic methodology goes hand in hand with total synthesis. Within the great variety of all synthetic methods, the highest diversity and productivity is provided by catalytic methods. Besides the high synthetic potential, catalytic methods offer high versatility, and high atom economy, and low waste generation. These aspects make the catalytic methods favored for industrial applications.

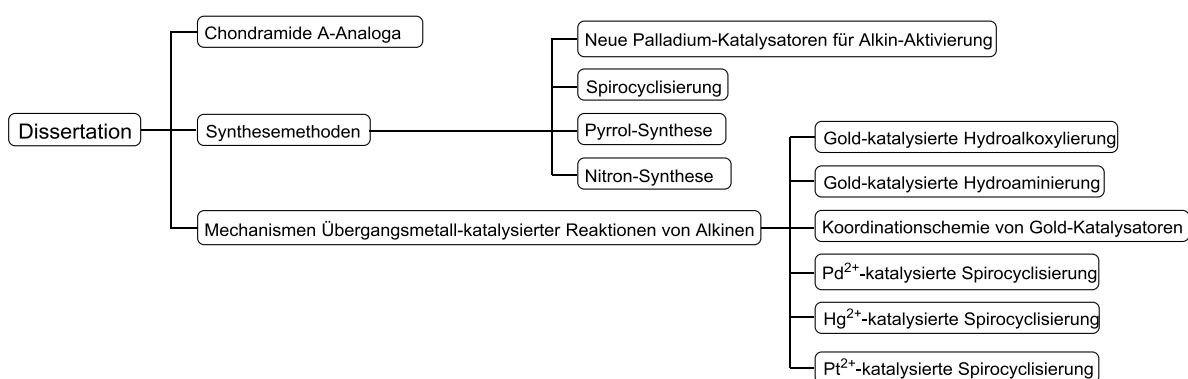
Homogeneous gold catalysis has emerged as a new flourishing area of research since around the year 2000. While the arsenal of synthetic methods based on gold catalysis significantly increased since then, the knowledge about the mechanisms of the corresponding transformations remained more limited and this area has actually just began to emerge. Indeed, most papers about new gold catalyzed reactions confine themselves to "proposed" mechanisms, without going into deep experimental mechanistic investigations and characterization of the actual gold intermediates. Often mechanistic investigation is conducted theoretically, using computational methods, without

getting strong support from experimental evidence. This might be partly caused by relatively low accessibility and the high expense of gold materials. It should be stressed, that the mechanistic knowledge obtained from computational methods is less reliable than the knowledge obtained directly from nature in appropriately designed experiments. Often theoretical viewpoints are controverted by subsequent experimental studies. There are numerous examples particularly in gold catalysis. That is the reason why it is preferable to investigate mechanisms also experimentally. The biggest part of this thesis is dedicated to purely experimental investigations of mechanisms of various gold catalyzed processes: hydroalkoxylation, hydroamination, and spirocyclization. All these processes are based on electrophilic activation of alkynes towards nucleophilic attack. The mechanistic study involves synthesis, characterization and study of relevant organogold intermediates, coordination chemistry of gold catalysts, determination and analysis of chemical kinetics and direct observation of actual organogold intermediates in situ during catalytic processes. The whole study uses NMR as the main research method to study reactions and species in solution. Additional compound characterization data was obtained from single crystal X-ray structure analysis and high resolution mass spectrometry (ESI HRMS).

2. Abstract (German)

Diese Arbeit besteht aus mehreren unabhängigen Projekten, die sich mit drei Aspekten der organischen Chemie befassen: Totalsynthese, die Entwicklung neuer Synthesemethoden und mechanistische Untersuchungen. Im Totalsynthese-Teil wird die Synthese von Chondramid A-Analoga und deren biologische Bewertung vorgestellt. Der Methodik-Teil beschreibt mehrere neue katalytische Umwandlungen von Alkinen und die Entwicklung von neuen Palladium-Katalysatoren für Alkin-Aktivierung. Der dritte und größte Teil beschreibt experimentelle mechanistische Untersuchungen Gold-, Palladium-, Platin- und Quecksilber-katalysierter Reaktionen von Alkinen.

Struktur der Arbeit



3. Publications incorporated into this thesis

- Paper 1** | Zhdanko, A.; Schmauder, A.; Ma, C. I.; Sibley, L. D.; Sept, D.; Sasse, F.; Maier, M. E.
Synthesis of Chondramide A Analogues with Modified β -Tyrosine and Their Biological Evaluation.
Chem. Eur. J. **2011**, *17*, 13349–13357.
- Paper 2** | Zhdanko, A.; Ströbele, M.; Maier, M. E.
Coordination Chemistry of Gold Catalysts in Solution: A Detailed NMR Study.
Chem. Eur. J. **2012**, *18*, 14732–14744.
- Paper 3** | Zhdanko, A.; Maier, M. E.
Synthesis of *gem*-Diaurated Species from Alkynols.
Chem. Eur. J. **2013**, *19*, 3932–3942.
- Paper 4** | Zhdanko, A.; Maier, M. E.
Quantitative Evaluation of the Stability of *gem*-Diaurated Species in Reactions with Nucleophiles.
Organometallics **2013**, *32*, 2000–2006.
- Paper 5** | Zhdanko, A.; Maier, M. E.
The Mechanism of Gold(I) Catalyzed Hydroalkoxylation of Alkynes: an Extensive Experimental Study.
Chem. Eur. J. **2014**, *20*, 1918–1930.
- Paper 6** | Zhdanko, A.; Maier, M. E.
Gold(I), Palladium(II), Platinum(II) and Mercury(II) catalyzed Spirocyclization of 1,3-Enynediols: Reaction Scope.
Eur. J. Org. Chem. **2014**, 3411–3422.
- Paper 7** | Zhdanko, A.; Maier, M. E.
Mechanistic Study of Gold(I)-Catalyzed Hydroamination of Alkynes: Outer or Inner Sphere Mechanism?
Angew. Chem. **2014**, *126*, 7894–7898; *Angew. Chem. Int. Ed.* **2014**, *53*, 7760–7764.
- Paper 8** | Zhdanko, A.; Maier, M. E.
Explanation of Counterion Effects in Gold(I) Catalyzed Hydroalkoxylation of Alkynes.
ACS Catal., **2014**, *4*, 2770–2775.
- Paper 9** | Zhdanko, A.; Maier, M. E.
Explanation of "Silver effect" on Gold(I) Catalyzed Hydroalkoxylation of Alkynes.
Manuscript.
- Paper 10** | Zhdanko, A.; Ströbele, M.; Maichle-Mössmer, C.; Maier, M. E.
Experimental mechanistic investigation on Gold(I), Palladium(II), Platinum(II) and Mercury(II) catalyzed spirocyclizations.
Manuscript.

4. Personal Contribution

Paper 1: Zhdanko, A.; Schmauder, A.; Ma, C. I.; Sibley, L. D.; Sept, D.; Sasse, F.; Maier, M. E. Synthesis of Chondramide A Analogues with Modified β -Tyrosine and Their Biological Evaluation, *Chem. Eur. J.* **2011**, *17*, 13349–13357.

I synthesized seven chondramide analogs (compounds **2e-k**) and wrote *ca.* 70% of the manuscript. Part of compound characterization (^1H , ^{13}C , H,H-COSY, HSQC, DEPT, HMBC, NOESY NMR spectra, optical rotation measurements) was performed by me.

A. Schmauder synthesized three chondramide analogs (compounds **2b-d**). C. I. Ma, L. D. Sibley, D. Sept, F. Sasse provided the biological study.

Paper 2: Zhdanko, A.; Ströbele, M.; Maier, M. E. Coordination Chemistry of Gold Catalysts in Solution: A Detailed NMR Study, *Chem. Eur. J.* **2012**, *18*, 14732–14744.

I designed and performed the complete project and wrote the complete manuscript. Compound characterization was performed by me (except X-ray analysis and HRMS).

Dr M. Ströbele performed two X-rays analyses and provided the structure solutions. Dr D. Wistuba performed the HRMS measurements.

Paper 3: Zhdanko, A.; Maier, M. E. Synthesis of *gem*-Diaurated Species from Alkynols, *Chem. Eur. J.* **2013**, *19*, 3932–3942.

I designed and performed the complete project and wrote the complete manuscript. Compound characterization was performed by me (except X-ray analysis and HRMS).

Dr M. Ströbele performed one X-rays analysis and provided the structure solution. Dr D. Wistuba performed the HRMS measurements.

Paper 4: Zhdanko, A.; Maier, M. E. Quantitative Evaluation of the Stability of *gem*-Diaurated Species in Reactions with Nucleophiles, *Organometallics* **2013**, *32*, 2000–2006.

I designed and performed the complete project and wrote the complete manuscript. Compound characterization was performed by me (except HRMS).

Dr. M. Kramer provided assistance for the various temperature NMR experiments (setting up the temperature in the instrument and running spectra). Dr D. Wistuba performed HRMS measurements.

Paper 5: Zhdanko, A.; Maier, M. E. The mechanism of gold(I) catalyzed hydroalkoxylation of alkynes: an extensive experimental study, *Chem. Eur. J.* **2014**, *20*, 1918–1930.

I designed and performed the complete project and wrote the complete manuscript. Compound characterization was performed by me (except HRMS). Dr D. Wistuba performed the HRMS measurements.

Paper 6: Zhdanko, A.; Maier, M. E. Gold(I), Palladium(II), Platinum(II) and Mercury(II) catalyzed Spirocyclization of 1,3-Enynediols: Reaction Scope, *Eur. J. Org. Chem.* **2014**, 3411–3422.

The initial idea to use a transition metal catalyst for the synthesis of mono unsaturated spiroketal structures was provided by Prof. Dr. M. E. Maier. This was the starting point for how I got involved in catalysis. I performed the complete project and wrote the major part of the manuscript. Some sections were written by Prof. M. E. Maier. Compound characterization was performed by me (except HRMS). Dr D. Wistuba performed HRMS.

Paper 7: Zhdanko, A.; Maier, M. E. Mechanistic Study of Gold(I)-Catalyzed Hydroamination of Alkynes: Outer or Inner Sphere Mechanism? *Angew. Chem.* **2014**, 126, 7894–7898; *Angew. Chem. Int. Ed.* **2014**, 53, 7760–7764.

I designed and performed the complete project and wrote the complete manuscript. Compound characterization was performed by me (except X-ray analysis and HRMS).

Dr. M. Kramer provided assistance for the various temperature NMR experiments (setting up the temperature in the instrument and running spectra). Dr M. Ströbele performed one X-rays analysis and provided the structure solution. Dr D. Wistuba performed HRMS measurements.

Paper 8: Zhdanko, A.; Maier, M. E. Explanation of counterion effects in gold(I) catalyzed hydroalkoxylation of alkynes, *ACS Catal.*, **2014**, 4, 2770–2775.

I designed and performed the complete project and wrote the complete manuscript.

Paper 9: Zhdanko, A.; Maier, M. E. Explanation of "Silver effect" on Gold(I) Catalyzed Hydroalkoxylation of Alkynes, *Manuscript*.

I designed and performed the complete project and wrote the complete manuscript.

Paper 10: Zhdanko, A.; Ströbele, M.; Maichle-Mössmer, C.; Maier, M. E. Experimental mechanistic investigation on Gold(I), Palladium(II), Platinum(II) and Mercury(II) catalyzed spirocyclizations, *Manuscript*.

I designed and performed the complete project and wrote the complete manuscript. Dr M. Ströbele performed one X-ray analysis and Dr. C. Maichle-Mössmer performed two X-ray analyses and provided the corresponding structure solutions.

In cases where I wrote the complete manuscripts, they were checked and corrected by Prof. Martin E. Maier before submission to the journals.

5. Objective and Expected Output of the Thesis

The primary objective of the thesis was to gain new knowledge and to have fun disclosing the secrets of Nature.

The knowledge obtained in my research enables a high level of understanding of mechanisms in gold catalysis. This information can be practically used to design catalytic conditions and explain the observed results in gold catalysis and also to better understand the scope and limitations of gold catalysis.

Besides gold, the work provides insights for Pd, Hg and Pt catalysis and it allows comparison of several aspects of catalysis by Au, Pd, Hg and Pt. In particular, a new Pd catalyst for alkyne activation was developed, which might expand the scope of catalytic reactions of alkynes.

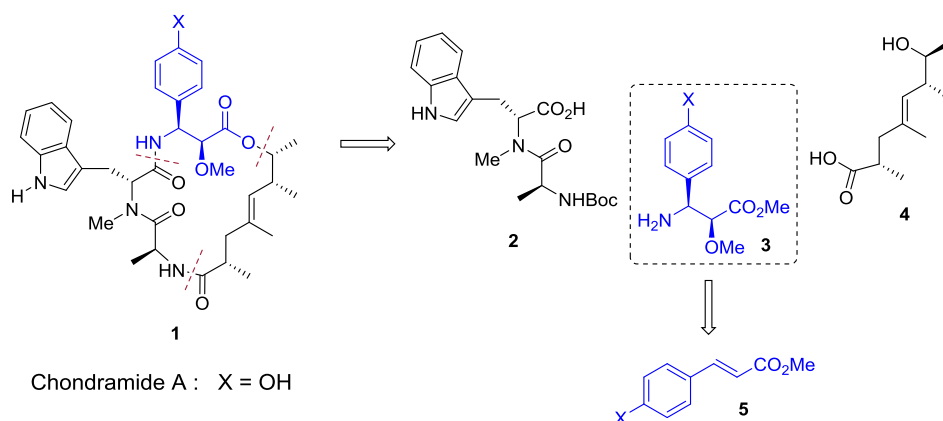
6. Results and Discussion

6.1. Synthesis of Chondramide A Analogs with Modified β -Tyrosine and Their Biological Evaluation

[This study was published in Paper N1, Chem. Eur. J. **2011**, 17, 13349–13357]

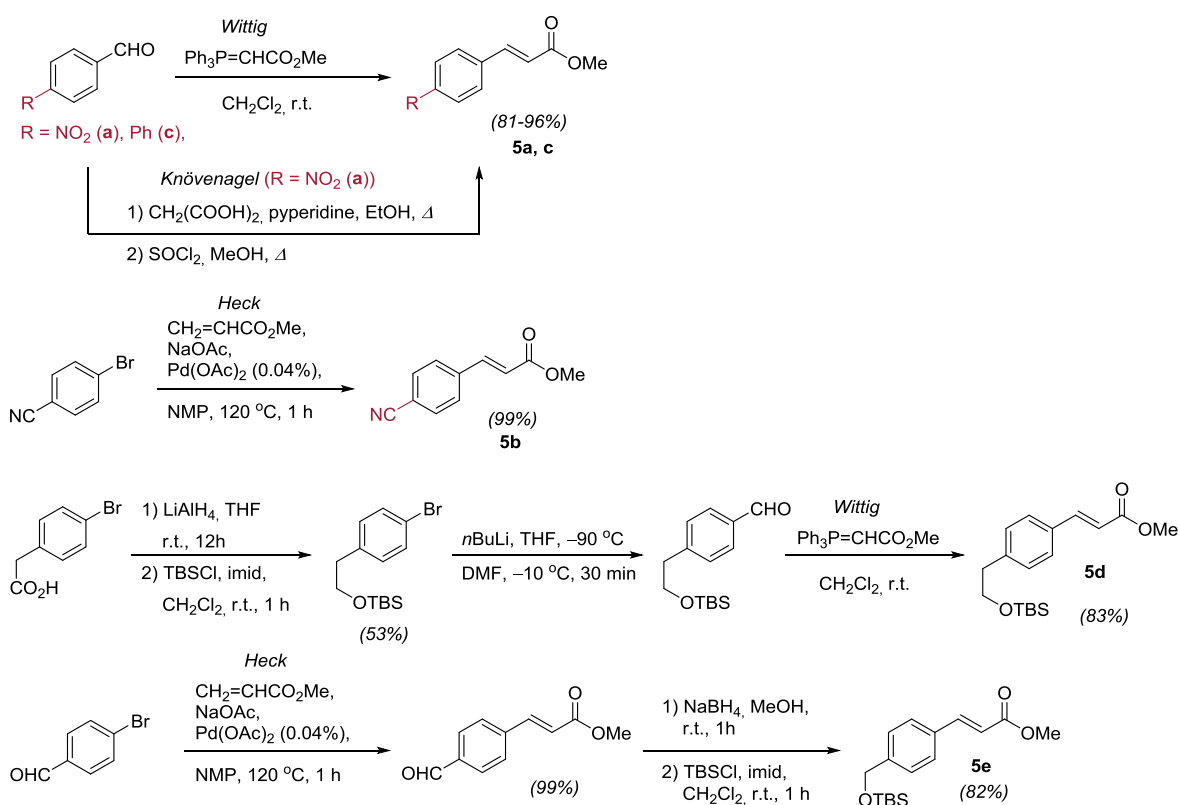
The reason for this project was to possibly find chondramide analogs that would bind preferentially to the F-actin of parasites. Because there is no high resolution X-ray structure of a chondramide/F-actin complex, the exact binding mode is not known. However, differences in amino acids that are in the binding region are known. Based on some molecular modelling the collaboration partners L. David Sibley and David Sept suggested to synthesize analogs with a modified tyrosine. In a later paper they indeed were able to show that our synthetic chondramide A analogs stabilize filamentous actin and block invasion by *Toxoplasma gondii*.¹

A total synthesis of chondramide A (**1**) was previously developed in our laboratory.² Originally this depsipeptide was synthesized from three building blocks (**2-4**) in a concise manner (Scheme 1). In order to synthesize several analogs of the natural product, the same synthetic approach was used.



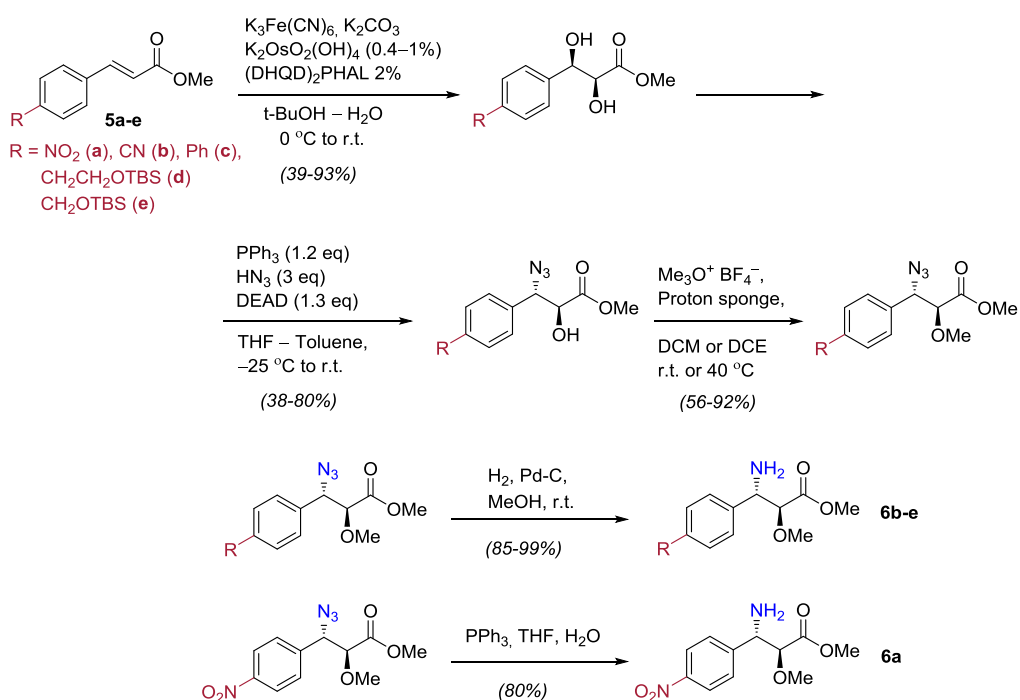
Scheme 1. Retrosynthetic analysis of chondramide A.

According to this synthetic plan, several *trans*-cinnamic esters (**5a-e**) were synthesized from easily accessible commercial starting materials using Wittig reactions, Knoevenagel reactions or Heck coupling (Scheme 2). In particular, the Heck coupling was performed according to a modern procedure, under low catalyst loading and ligand-free conditions, using Pd(OAc)₂ as a catalyst.³ This method is especially effective for electron deficient aryl bromides.

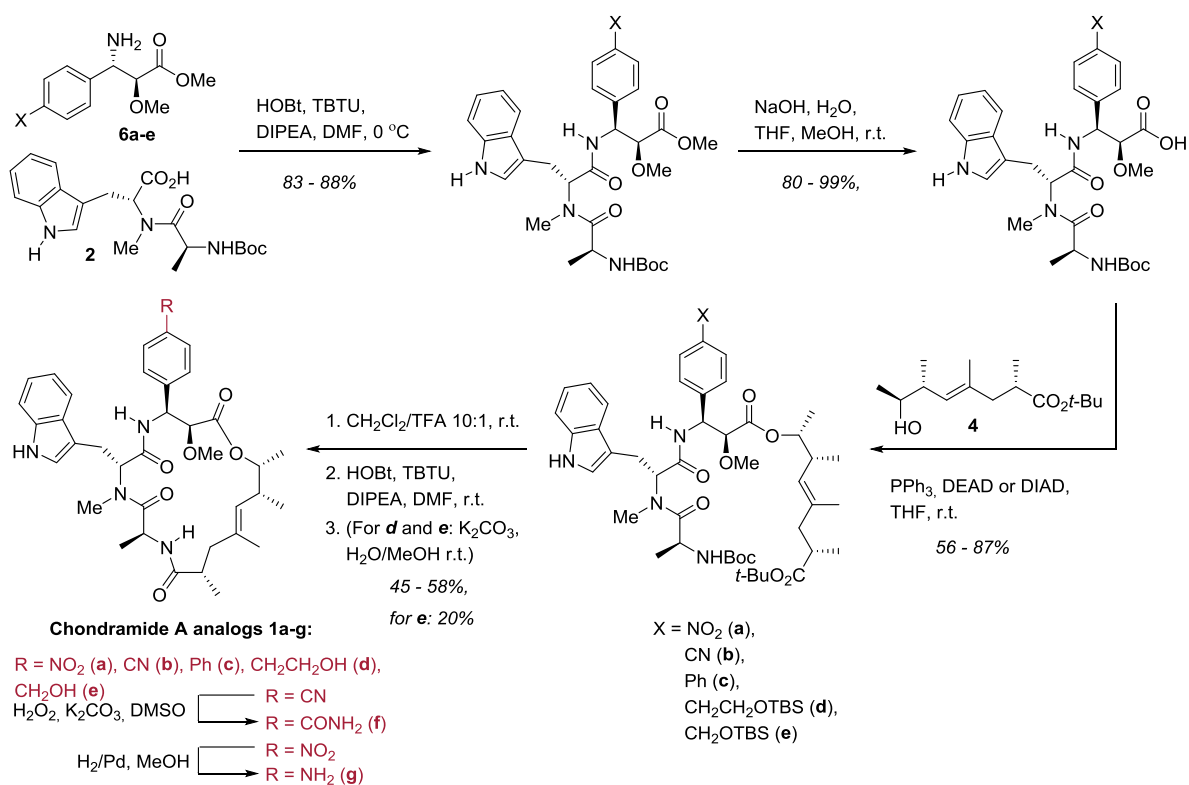


Scheme 2. Synthesis of *trans*-cinnamic esters **5a-e**.

The cinnamic esters were first elaborated into β -tyrosine esters **6a-e** (Scheme 3), that were further elaborated into seven chondramide analogs **1a-g** conveniently, using the methods known from the original chondramide A synthesis with only minor optimizations (Scheme 4). Noteworthy in this regard is the introduction of the amino function by a Mitsunobu reaction with hydrazoic acid.



Scheme 3. Synthesis of β -tyrosine esters **6a-e**.



Scheme 4. Synthesis of chondramide A analogues **1a-g**.

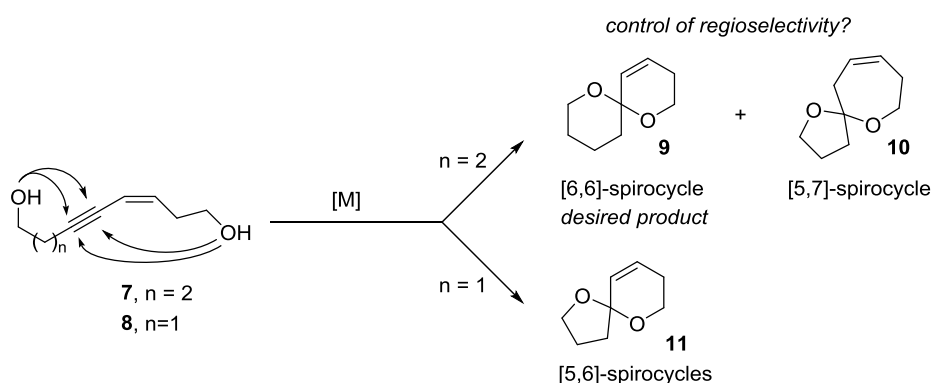
Upon the biological assays, most of the chondramide A analogs exhibited biological activity similar to the natural chondramide A. It was concluded that the 4-position of the aryl ring in the β -tyrosine of chondramide A can be structurally modified without significant loss of the biological activity. Surprisingly the amide derivative **1f** showed the weakest growth inhibition activity.

6.2. Synthetic Methodology

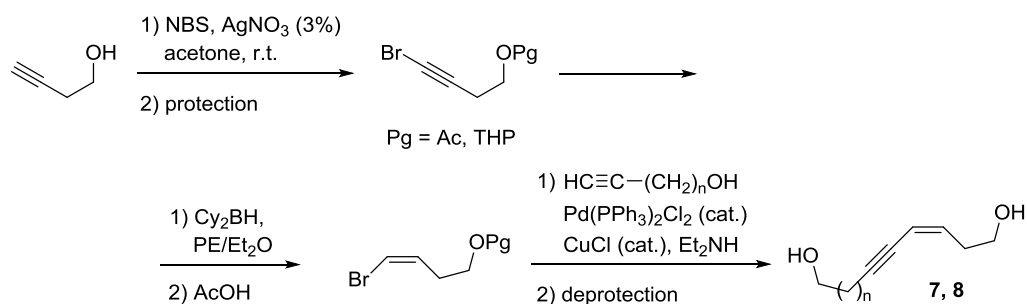
6.2.1. Gold(I), Palladium(II), Platinum(II) and Mercury(II) catalyzed Spirocyclization of 1,3-Enynediols

[This study was published in Paper N6, *Eur. J. Org. Chem.* **2014**, 3411–3422]

During investigations towards the total synthesis of natural products in our laboratory a method was needed that would allow to synthesize mono unsaturated spiroketal structures **9**, a common structural motif appearing in several natural products, from simple precursors. The desired spirocycles were suggested to be synthesized by a transition metal catalyzed double cyclization of 1,3-enynediols **7** (Scheme 5). Here, the potential problem to overcome is the regioselectivity of the cyclization that may occur at each carbon atom of the C≡C bond in case of $n = 2$. The starting materials are easily available by Sonogashira coupling between terminal alkynes and *cis*-vinyl bromides under mild conditions. The general approach to the starting enynediols **7** is shown in Scheme 6.



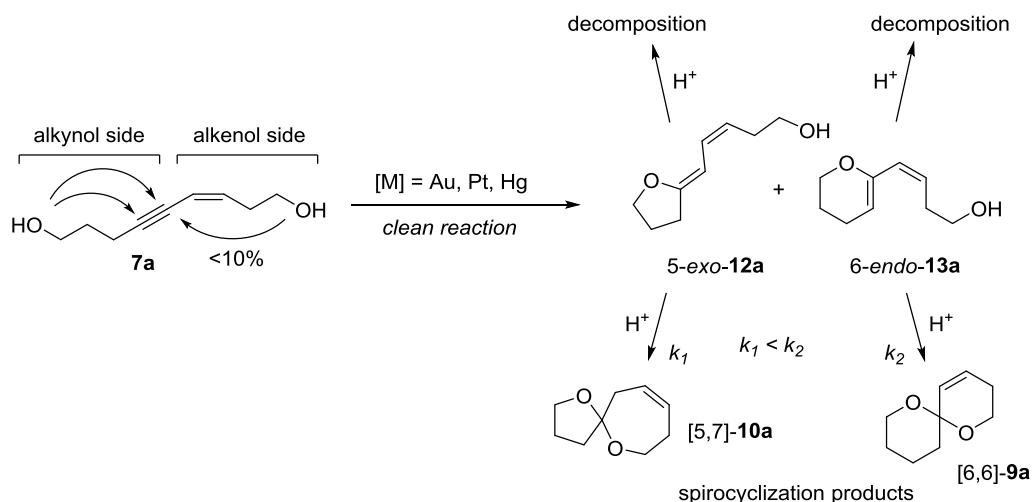
Scheme 5. Routes to unsaturated spiroacetals. The arrows indicate the formal cyclization modes.



Scheme 6. General approach to starting enynediols **7, 8** used in this study.

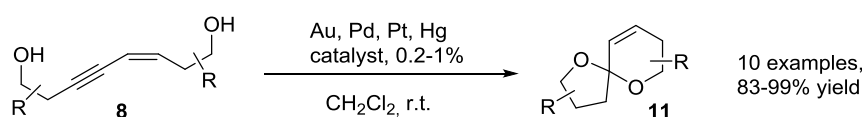
Unfortunately we could not achieve an efficient synthesis of the [6,6]-spirocycles **9** ($n = 2, m = 1$). The reason of this negative result is poor regioselectivity of the first cyclization event and competitive spirocyclization/decomposition of the intermediate dienol ethers **12, 13** upon the second cyclization event (Scheme 7). Obviously, the conjugated double bond in **7** has little or no impact on regioselectivity of the alcohol addition to the triple bond (reaction remains not selective). In addition, the hydroxyl group coming from the alkenol side and being seemingly well preorganized for cyclization was found to be the least reactive, making ~90% of cyclization to

originate from the saturated side (alkynol side). The inability of the alkenol side to selectively cyclize in a 6-*exo-dig* mode *ahead* of the alkynol side has made the selective synthesis of [6,6]-spirocycles principally impossible.

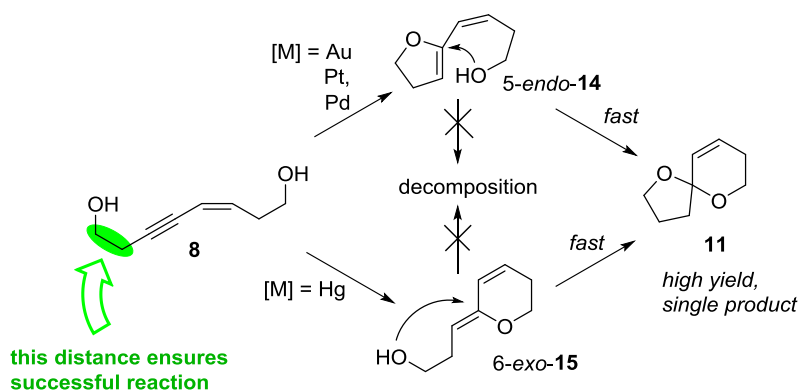


Scheme 7. Unselective first cyclization and competitive spirocyclization/decomposition of dienol ether intermediates **12**, **13** make the overall reaction unsuitable for synthetic purposes.

However, we found that spirocyclization of various (3*Z*)-oct-3-en-5-yne-1,8-diols **8** yields the corresponding [5,6]-spiroacetals **11** in almost quantitative yields. The reaction occurs under mild conditions at room temperature, and is characterized by short reaction times and low catalyst loading (0.5-1%). The reaction provides a thermodynamical mixture of epimers at the acetal carbon, subject to control by the side chain substituents (Scheme 8). Thus, simple shortening of the substrate by just one methylene unit completely eliminated the regioselectivity and decomposition problems as explained on Scheme 9.



Scheme 8. Highly efficient synthesis of [5,6]-spiroacetals **11**.

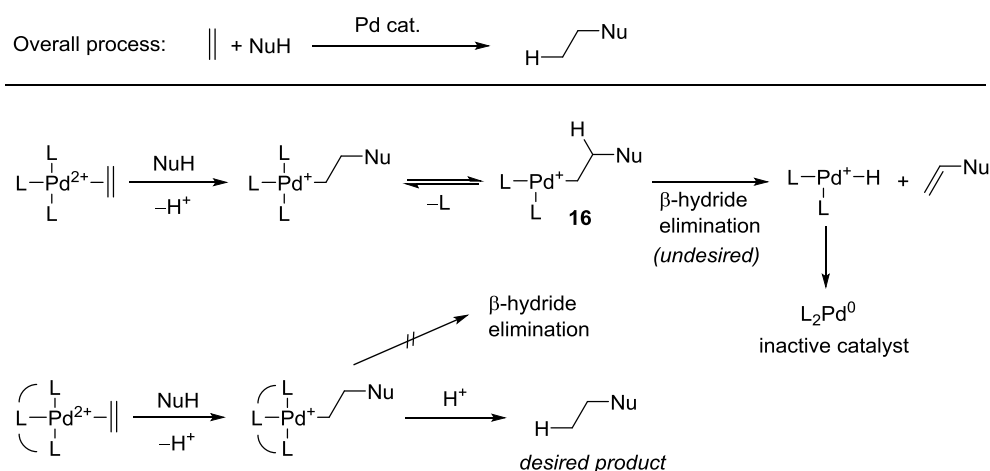


Scheme 9. Fast ring closure of dienol ether intermediates **14**, **15** saves them from decomposition.

6.2.2. New Palladium Catalysts for Alkyne Activation

[The information regarding synthesis and use of complex **18** was published in Paper N6, *Eur. J. Org. Chem.* **2014**, 3411–3422, other information has not yet been published]

This work was inspired by a report from Michael and Cochran concerning the hydroamination of alkenes catalyzed by cationic palladium pincer complexes.⁴ One of the complications of Pd-catalyzed additions to alkenes is the strong tendency for the alkylpalladium intermediates **16** to undergo β -hydride elimination (Scheme 10). Accordingly, the purpose of a tridentate pincer ligand is to block the open coordination site required for the β -hydride elimination, and thereby to prevent this process and promote other reactions of the alkylpalladium species. Simply saying, installation of a tridentate pincer ligand reduces the intrinsic "specialization" of the palladium center by blocking any Pd(II)/Pd(0) redox processes. After such a "restyle", cationic pincer complexes become similar to simple gold catalysts LAu⁺.



Scheme 10. Use of tridentate pincer ligands to prevent the undesired β -hydride elimination.

The original publication by Michael and Cochran uses dicationic pincer complexes bearing a neutral PNP pincer ligand, Figure 1. The catalyst is generated *in situ* upon action of 2 equivalents of AgBF₄ on **17**. In our work we created a new catalyst **18** that contains an easily accessible anionic bisphosphinite (PCP) ligand, which is also known from the literature. The synthesis of **18** is shown in Scheme 12. The known complex PdPCP-Cl was synthesized according to a modified literature procedure in one pot, using simple commercially available starting materials.⁵ Then, halogen abstraction using AgSbF₆ in the presence of acetone immediately gave rise to a new cationic palladium complex **18**.⁶ To our delight, this monocationic complex exhibited high catalytic activity in the synthesis of spiroacetals (see above). Successful application of this well-defined catalyst in the spirocyclization reaction (Section 6.2.1 and Paper N6) opens new perspectives for chemistry of alkynes, which could become complementary to modern gold catalysis.

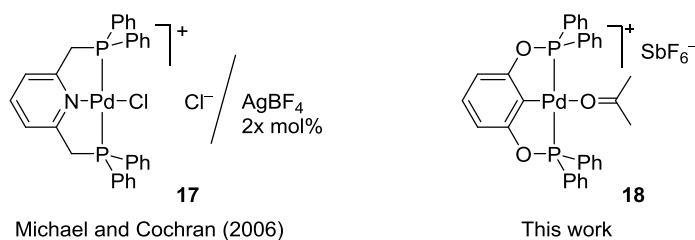
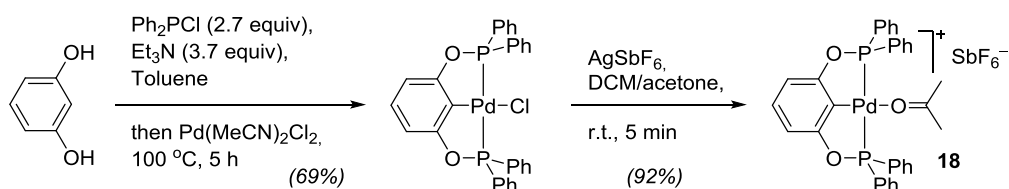
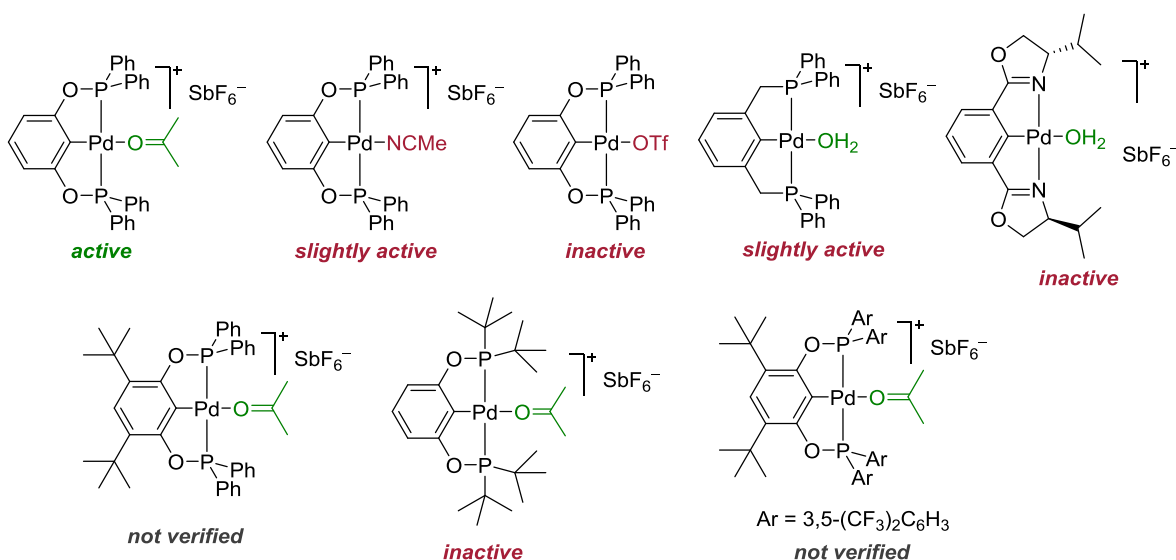


Figure 1. Pincer complexes used in the work of Michael and Cochran and our work.



Scheme 12. Synthesis of cationic palladium pincer complex **18**.

In addition to conventional gold catalysts, new palladium complexes may offer different reactivity and selectivity patterns, expanding the scope of catalytic reactions of alkynes. Encouraged by the successful initial result, we synthesized a number of new cationic palladium pincer complexes for future catalytic and mechanistic studies (Figure 2). Preliminary investigations indicated that the catalytic activity is strongly dependent on both the nature of the pincer ligand and the nature of the remaining counterion/ligand on the other side. We conducted ligand exchange reactions to find out, that MeCN and OTf bind the palladium center considerably stronger than hexyne-3, a model substrate. Not surprisingly, the cationic complex with MeCN or the corresponding triflate exhibits very low catalytic activity (at room temperature). It can be concluded, that palladium pincer complexes are much less alkynophilic than gold catalysts (which are compatible with MeCN and OTf⁻). In case of palladium, only cationic pincer complexes bearing a very weak remaining ligand (e.g. H₂O or acetone) and a non-nucleophilic anion (e.g. SbF₆⁻) can be highly active at room temperature. On the other hand, the nature of the pincer ligand also has strong influence on the catalytic activity of the complex. Increase of electron donation or steric hindrance around the palladium center leads to loss of catalytic activity. Use of an NCN type of pincer ligand led to an inactive catalyst.



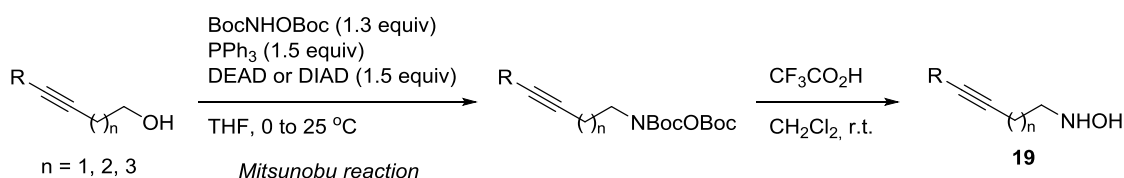
Binding affinity to Pd(PCP)⁺: water, acetone, hexyne << MeCN < OTf⁻

Figure 2. New palladium catalysts for alkyne activation. Preliminary assessment of catalytic activity is written below the structures.

6.2.3. Cyclization of Alkynyl Hydroxylamines. Synthesis of Pyrroles and Nitrones

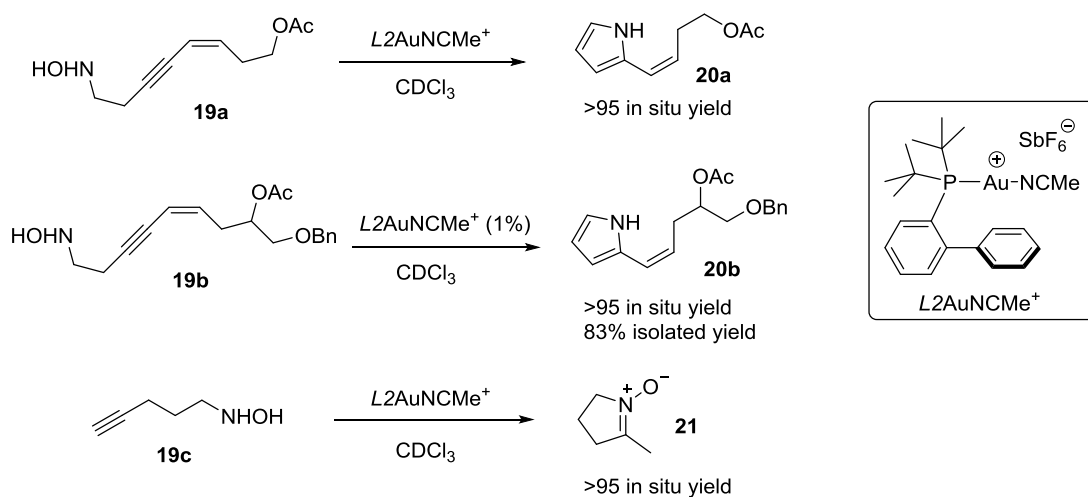
[The information of this section has not yet been published; see Appendix 1 for experimental details]

In the presence of gold catalysts alkynes are known to react with a variety of nucleophiles.⁷ However, reaction of alkynes with hydroxylamines has not been described in the literature. First of all, the occurrence of the intramolecular version was tested. For this purpose, a few alkynyl hydroxylamines **19** were synthesized. The general approach to these substrates is shown in Scheme 13. Here we utilized the Mitsunobu reaction with subsequent deprotection, a method known from literature.⁸ The Mitsunobu reaction with the sterically hindered hydroxylamine derivative BocNHOBoc occurs sluggishly. We found it only applicable if the substrate is a primary alcohol. In case of $n = 2, 3$ high yields are achievable. In case of homopropargylic alcohols ($n = 1$) the yields are somewhat lower because of elimination to a conjugated enyne ($\text{RC}\equiv\text{C}-\text{CH}=\text{CH}_2$) occurring as a competitive side reaction. Deprotection of the hydroxylamines by TFA occurs smoothly in CH_2Cl_2 .



Scheme 13. General approach to starting alkynyl hydroxylamines **19** used in this study.

Pleasingly, in the presence of $\text{L2AuNCMe}^+ \text{SbF}_6^-$ ($\text{L2} = o\text{-(di-tert-butylphosphino)biphenyl}$), alkynyl hydroxylamines **19a-c** underwent fast and efficient reactions (Scheme 14). Pyrrole derivatives **20a, b** were obtained from **19a, b** as a result of a 5-*endo-dig* reaction. Nitrone **21** was obtained from **19c** as a result of a 5-*exo-dig* reaction. These very first observations (achieved without any optimizations) demonstrated that gold catalyzed addition of hydroxylamine can be a promising new reaction, which may find applications in organic synthesis. High yield, selectivity, mild reaction conditions and the importance of pyrroles and nitrones in organic chemistry add value to this finding. However, the utility of the reaction may be diminished owing to the difficult accessibility of the starting alkynyl hydroxylamines.⁹



Scheme 14. New gold catalyzed transformations of hydroxylamines.

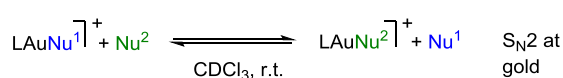
6.3. Mechanisms of Transition Metal Catalyzed Reactions of Alkynes

6.3.1. Coordination Chemistry of Gold Catalysts

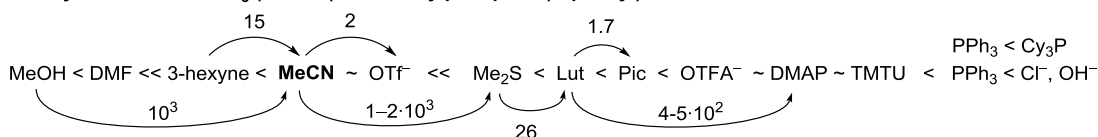
[This study was published in Paper N2, *Chem. Eur. J.* **2012**, *18*, 14732–14744]

Coordination chemistry of gold catalysts is essential for understanding mechanisms of gold catalyzed processes in general. Therefore, prior to our mechanistic investigations, we performed a thorough study of coordination chemistry of several gold catalysts. This study provided supplementary information which was used in the subsequent mechanistic studies of gold catalyzed processes. The following primary results were obtained:

1. Binding affinity of various ligands (negatively charged X^- or neutral Nu) to an LAu^+ unit was determined qualitatively and quantitatively.



affinity to $L2Au^+$ in $CDCl_3$ ($L2 = o$ -(di-*tert*-butylphosphino)biphenyl):



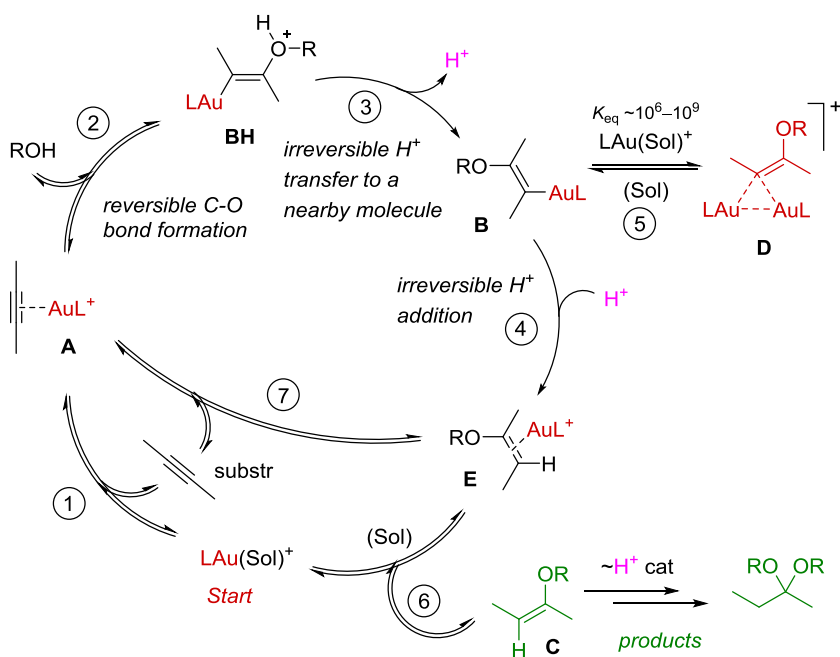
2. Acid/base dependent interconversions of gold hydroxide $LAuOH$ and oxonium species $(LAu)_3O^+$ and $(LAu)_2OH^+$ were established. Similar acid/base dependent interconversions of $LAuSH$, $(LAu)_2SH^+$, $(LAu)_3S^+$ were established.
3. NMR spectroscopic data of all new complexes $LAu(Nu)^+$, $LAuX$, $LAuOH$, $(LAu)_3O^+$, $(LAu)_2OH^+$, $LAuSH$, $(LAu)_2SH^+$, $(LAu)_3S^+$ were collected (often in various solvents).

6.3.2. Mechanism of Gold Catalyzed Hydroalkoxylation

[This study was published in the following papers: Paper N3, *Chem. Eur. J.* **2013**, *19*, 3932–3942; Paper N4, *Organometallics* **2013**, *32*, 2000–2006; Paper N5, *Chem. Eur. J.* **2014**, *20*, 1918–1930]

An extensive experimental study of the mechanism of gold(I) catalyzed hydroalkoxylation of internal alkynes was conducted using NMR spectroscopy. The study focused on the chemistry of organogold intermediates, observations of actual catalytic intermediates *in situ* and the reaction kinetics. Based on the experimental results a complete mechanistic picture was established. The reaction starts from a reversible *anti*-addition of an alcohol onto an alkyne gold π -complex **A** to form a highly unstable adduct **BH** which quickly undergoes proton transfer to give vinyl gold **B**. Subsequently, the vinyl gold species **B** undergoes protonation by the previously released acid to form enol ether π -complex **E** which participates in the global ligand exchange equilibrium, releasing product **C**. Competitively, **B** undergoes reversible addition of a second LAu^+ unit to form diaurated species **D**. Depending on the level of acidity in the system, **C** may stay as the end product or further transform into acetal **L** by means of a classical Brønsted acid catalysis.

We established, that **D** is an off-cycle intermediate. Its formation is a negative issue of gold catalysis. Structural factors controlling stability of diaurated species **D** were investigated. Electron donor substituents at the α -carbon atom of the enol ether core increase stability as well as electron donor ligands at gold. Any conjugation of the enol ether residue with a simple double bond or an aryl residue will decrease the stability. Steric factors play a crucial role on the stability of diaurated species and can readily dominate over the electronic factors. Therefore, it is preferred to use sterically hindered catalysts to prevent or reduce formation of **D**. In a kinetics study we determined, that formation/dissociation of **D** can be considered as an ordinary ligand exchange reaction, occurring through an associative $\text{S}_{\text{N}}2$ mechanism at gold.



Scheme 15. The mechanism of gold(I) catalyzed hydroalkoxylation of internal alkynes.

Ligand effects. In addition, we explained a number of effects for gold catalyzed hydroalkoxylation: ligand, counterion and silver effects. The overall ligand effect is determined by the following elementary ligand effects found in our research:

1. Use of electron poor ligands at gold catalysts increases electrophilicity of **A**, greatly enhancing transition from **A** to **B**.

2. Electron rich and/or sterically less demanding L increase stability of **D**, making its formation favored (or more likely). Favoring formation of **D** is a negative issue for the reaction.

3. Protodeauration is favored for electron rich L.

4. Because ligand exchange at gold occurs by an associative S_N2 mechanism, the ligand exchange will be faster in case of sterically less demanding LAu^+ than in case of sterically hindered ones. Nevertheless, the ligand exchange equilibria are established very fast even at LAu^+ bearing very sterically hindered L. We suggest, for the majority of gold catalyzed processes the influence of the ligand L on the rate of ligand exchange at LAu^+ will play only a minor role while the aforementioned factors 1-3 will play a dominant role, determining the overall ligand effect for the entire catalytic process.

5. To complete the picture, here one should place the effect of L on the stability of a catalyst and its organogold species towards irreversible decomposition, competitively occurring along the desired catalytic process. This factor was not systematically investigated in our research. Nevertheless, from our experience and from the data reported in the literature, simple ligands like PPh_3 , PMe_3 , IMes should generally not be recommended because of the reduced stability of derived organogold species, slowly decomposing to give gold mirrors.

According to these factors, a ligand can accelerate one part of catalytic cycle while diminishing the rate of another part. Since rate limiting step varies depending on a number of factors (nature of reactants, catalyst), it is not possible to recommend a ligand for the best catalyst, which would be most effective for all hydroalkoxylation. But it is possible to give some recommendations for particular types of hydroalkoxylation:

1. Sterically hindered electron deficient ligands are recommended for intermolecular hydroalkoxylation and intramolecular ones starting from *6-exo-dig* cyclization and larger ring formation. This ligand category is currently poorly represented in gold catalysis, some promising examples were recently introduced by Alcarazo.¹⁰

2. Sterically hindered electron donating ligands are recommended for intramolecular *5-endo-dig* and possibly *5-exo-dig*/*6-endo-dig* cyclizations (e.g. all electron-rich Buchwald ligands).

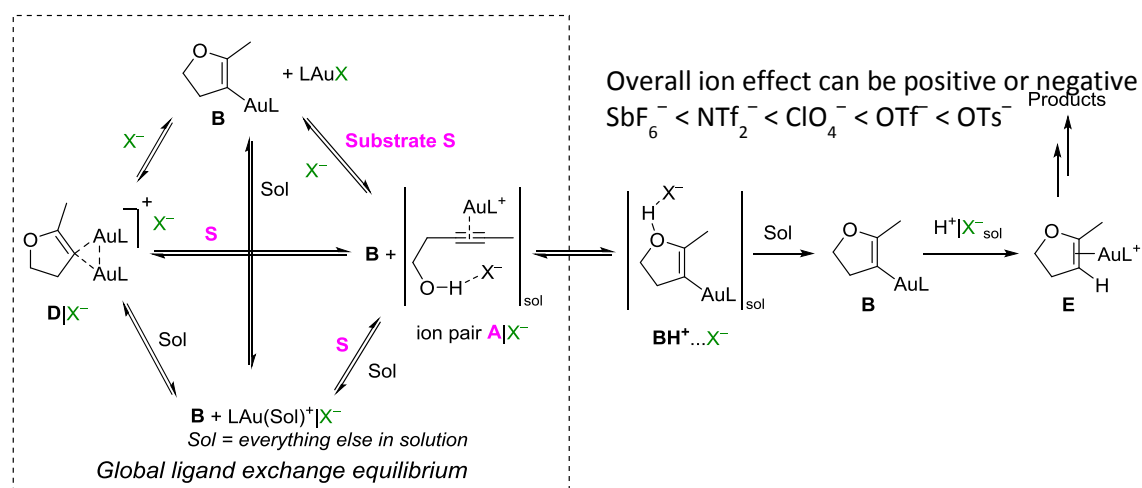
3. Because of increased probability of formation of **D**, the use of sterically less hindered catalysts is generally not recommended for any type of hydroalkoxylation (e.g. $L = PPh_3, PMe_3$).

6.3.3. Explanation of Counterion Effects in Gold(I)-Catalyzed Hydroalkoxylation of Alkynes

[This study was published in Paper N8, *ACS Catal.*, **2014**, 4, 2770–2775]

Cationic gold(I) complexes are typically applied with various anions (most often $X^- = \text{SbF}_6^-$, NTf_2^- , OTf^-). Dependence of a reaction from the counterion (the counterion effect) is well documented in many papers on gold catalysis methodology, but it is left without in depth explanation. Specific investigations into the counterion effects are scarce and mostly based on theoretical methods. Using purely experimental approaches and NMR spectroscopy as the main investigation method, we conducted a detailed investigation into the counterion effects occurring in the hydroalkoxylation of alkynes. We disclosed a number of simple counterion effects operating at different steps of the catalytic process and explained the overall counterion effect as a superposition of the elementary effects (Scheme 16), in a similar manner as was explained for the ligand effects.

Thus, counterions X^- facilitate the transition from **A** to **B** within ion pairs $\mathbf{A}|X^-$ in the order $\text{SbF}_6^- < \text{NTf}_2^- < \text{ClO}_4^- < \text{OTf}^- < \text{OTs}^-$. But use of anions with higher affinity to gold should be avoided because they disfavor formation of $\mathbf{A}|X^-$ simply by binding gold into LAuX (provided there are no stronger nucleophiles in the system and no diaurated species formed). Counterions X^- reduce the reactivity of H^+ in the order $\text{SbF}_6^- < \text{NTf}_2^- < \text{ClO}_4^- < \text{OTf}^- < \text{OTs}^-$, reducing the rate of protodeauration. Counterions X^- negligibly influence (if at all) simple ligand exchange equilibria at cationic gold species, unless there is specific interaction arising within the ion pairs or unless the counterion itself binds the metal to form neutral LAuX species.



General ion effects:

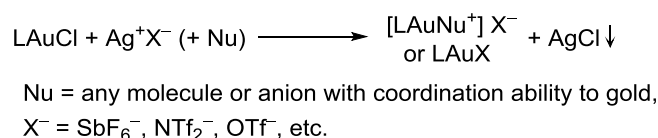
- 1) hydrogen bonding of ROH to X^- will enhance every equilibrium with alkyne **S** to the side of **A**. Besides that, there is no ion effect on any simple ligand exchange equilibria (not to confuse with binding of LAu^+ by X^- to form LAuX);
- 2) nucleophilicity of X^- enhances formation of LAuX (which should be avoided)
- 3) hydrogen bonding of ROH to X^- will enhance reactivity of **A** towards alcohol addition (valid for intra- and intermolecular alcohol addition);
- 4) solvation of H^+ with X^- will decrease reactivity of acid for protodeauration of **B**. Also any other parallel Brønsted acid catalyzed processes will be affected.

Scheme 16. Explanation of ion effects in gold catalyzed hydroalkoxylation.

6.3.4. Explanation of “Silver effect” on Gold(I)-Catalyzed Hydroalkoxylation of Alkynes

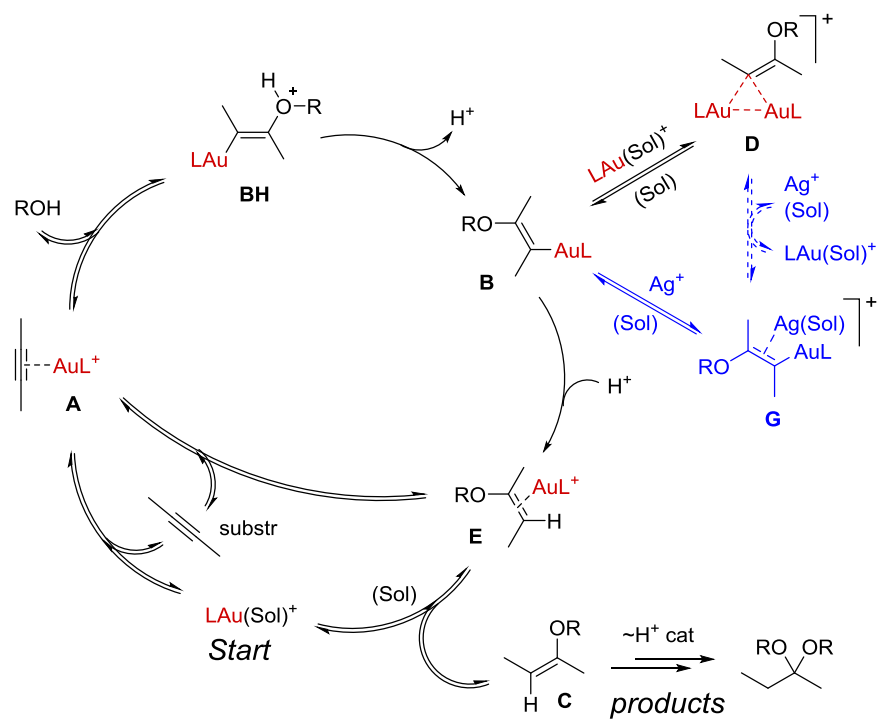
[This study is described in unpublished manuscript N9]

For a long time silver salts AgX have been routinely used to activate gold chloride complexes LAuCl by halogen abstraction for use in gold catalysis or synthesis of various gold complexes and the role of silver in gold catalysis has not been discussed beyond this simple ligand exchange process:



Since recently there has been increased amount of experimental observations suggesting that silver is not totally innocent in gold catalysis.¹¹ Moreover, these observations even questioned fundamental mechanistic principals of gold catalysis. Therefore, an in depth study is required to clarify the situation. In our research, we focused on the influence of silver salts (AgOTf or AgClO₄) on gold catalyzed hydroalkoxylation. We found that addition of a silver salt can cause a negative, positive or no effect on a reaction. Every time when a non-zero silver effect was observed, it was associated with formation of argento vinyl gold species **G**. Silver was found to be essentially innocent (plays no role) with regard to the mechanism of the catalytic process itself, exhibiting only off-cycle reactivity as summarized on Scheme 17. Considering material balance of the catalytic system, it can be seen that formation of **G** induces variations of concentrations of in-cycle intermediates, and these variations account for the silver effect.

No silver effect is observed if the catalytic system forms no **G**. This can take place in two cases. First, if a reaction is accompanied by complete formation of strong diaurated species **D** so that silver is unable to shift the equilibrium towards **G** (and cause change of the actual concentrations of the in-cycle intermediates). And second, when transition from **A** to **B** is the rate limiting step of the whole process so that no off-cycle intermediates **D** or **G** are formed.

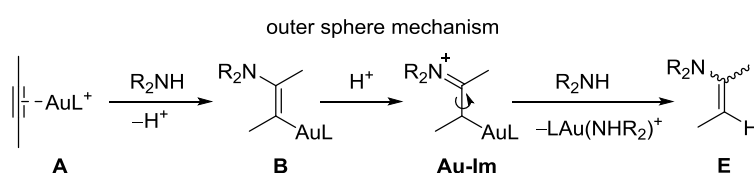


Scheme 17. The mechanism of hydroalkoxylation. The steps responsible for the silver effect are shown in blue.

6.3.5. Mechanism of Gold Catalyzed Hydroamination

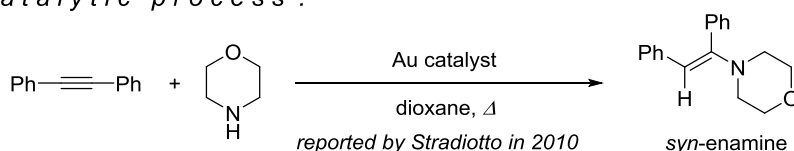
[This study was published in Paper N7, *Angew. Chem.* **2014**, 126, 7894–7898; *Angew. Chem. Int. Ed.* **2014**, 53, 7760–7764]

Using similar experimental approaches, a mechanistic study was conducted for the gold catalyzed hydroamination. This study revealed formation of conformationally flexible auro iminium salts **Au-Im**, which originate from protonation of vinyl gold species **B**. Rotation around the C–CAu is the fundamental reason of protodeauration of **B** being not stereospecific, unlike protodeauration of other vinyl gold species. Correspondingly, this can lead to loss of stereospecificity of the entire reaction, which results in formation of the enamine product as thermodynamic mixture or geometric isomers (or the most thermodynamically stable isomer as a main product), Scheme 18. In particular, the intermolecular hydroamination of alkynes was previously reported by Stradiotto to selectively yield *syn*-enamines, which was erroneously interpreted as evidence for an inner sphere mechanism being operative.¹² In contrary, the *syn*-enamine arises as a thermodynamically more stable isomer upon complete reversal of initially occurring *anti*-addition of amine onto a gold alkyne π -complex **A** (Scheme 19). Therefore, our study resolves a long standing ambiguity: should the entire reaction be described by outer or inner sphere mechanisms, in favor of the outer sphere mechanism.

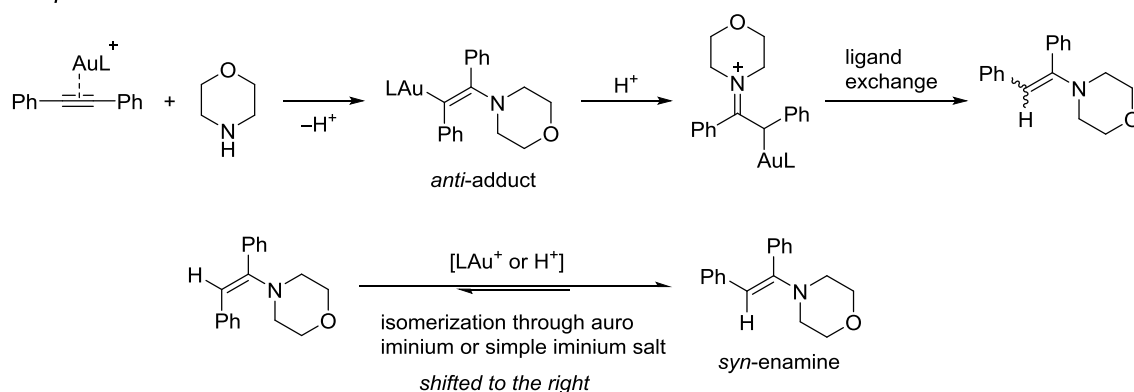


Scheme 18. Mechanism of gold catalyzed hydroamination.

Overall catalytic process :



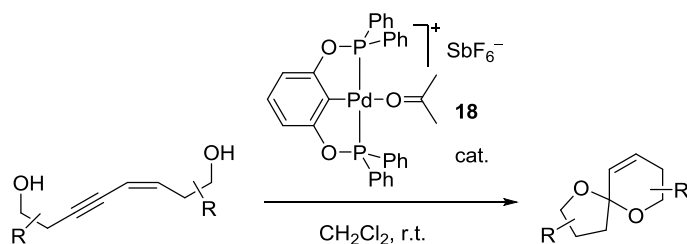
Explanation :



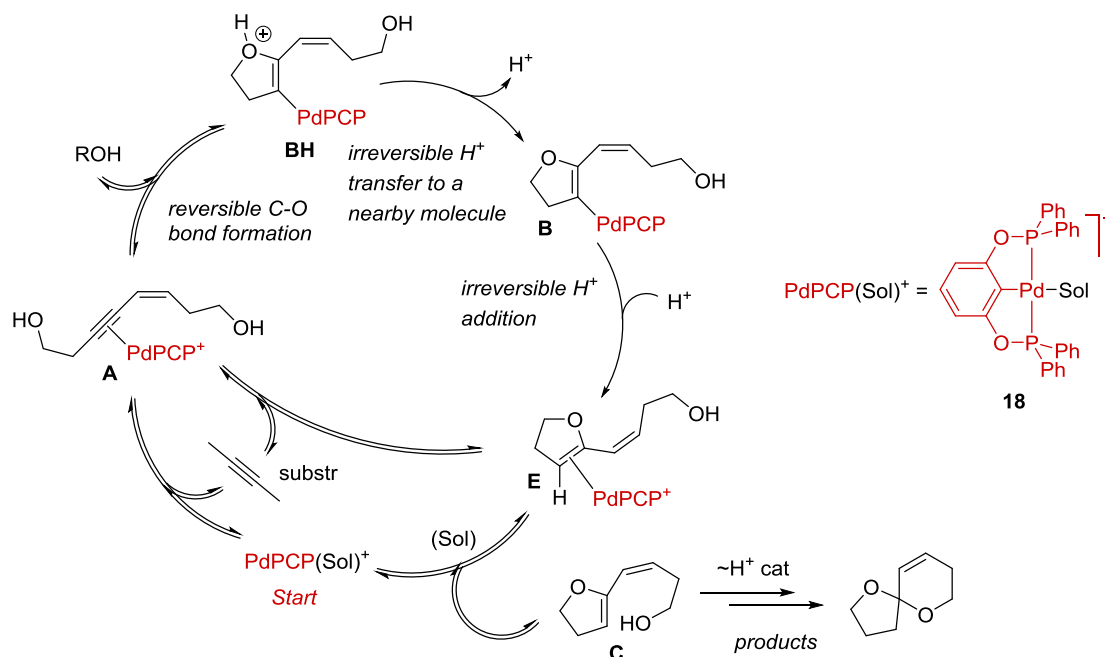
Scheme 19. Explanation of stereochemical outcome of gold-catalyzed hydroamination.

6.3.6. Mechanism of Palladium Catalyzed Spirocyclization

[This study is included in unpublished manuscript N10]



The mechanistic study of spirocyclization catalyzed by our cationic palladium pincer complex **18** revealed formation of vinyl palladium species **B** as a key intermediate. Strong inhibition of catalysis by MeCN or OTf, ligands with stronger binding affinity to palladium than an alkyne, indicates that formation of a cationic alkyne π -complex **A** is necessary for a catalytic reaction. These findings allow proposing the same mechanism for alcohol addition to an alkyne as found in the gold catalyzed variant (Scheme 20).



Species directly observable by NMR: PdPCP(Sol)⁺, A, B, E.

Scheme 20. The mechanism of palladium catalyzed spirocyclization.

Besides that, our experimental work revealed the following features of catalysis by cationic palladium pincer complex **18** that makes it different to gold catalysis:

1. In contrast to gold catalysis, the palladium pincer complex **18** is unable to inhibit itself by building up any sort of an off-cycle intermediate analogous to *gem*-diaurated species.
2. Catalysis by **18** is less tolerable to the presence of nucleophiles that are able to competitively bind the catalytic Pd center. For example, MeCN and OTf are well

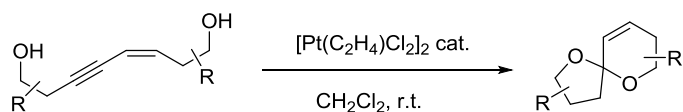
compatible with gold catalysis but not compatible with catalysis by **18** (at room temperature).

This aspect limits the scope of solvents applicable as a reaction medium. For example, palladium catalyzed reactions running fast in a non-coordinating solvent like CH₂Cl₂ become significantly inhibited in methanol (but yet possible). In case of gold catalysis, fast reactions are possible in either solvent.

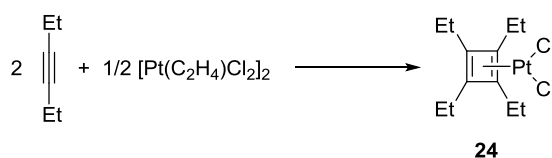
3. The palladium pincer complex **18** appears to have milder Lewis acidic character and its π -complexes with unsaturated hydrocarbons will possess less reactivity as compared to gold complexes. This is exemplified by the inability of PdPCP⁺ to catalyze isomerization of 5-*exo*-enol ether **C**.
4. Protodepalladation requires somewhat stronger acidic conditions as compared to protodeauration. Nevertheless, either gold catalysis or palladium catalysis is well compatible with the presence of mild bases (like TMU or *t*Bu₂Py).

6.3.7. Mechanism of Platinum Catalyzed Spirocyclization

[This study is included in unpublished manuscript N10]

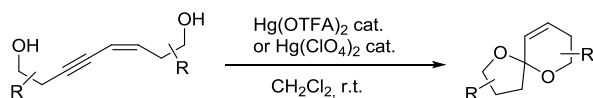


Mechanistic study of spirocyclization catalyzed by Zeise's dimer $[\text{Pt}(\text{C}_2\text{H}_4)\text{Cl}_2]_2$ was attempted. No organoplatinum intermediate could be identified. However, the *trans*-effects controlling the rate of the ligand exchange at platinum has been demonstrated to be crucial for catalytic activity of platinum complexes. This means that any ligand in a square platinum(II) complex directly influences the rate of ligand exchange specifically at the opposite position. The rate of ligand exchange may vary in a very broad range, from being immediate to taking many hours (consider compounds **22** and **23** as examples). The fast ligand exchange is the primary reason why Zeise's dimer $[\text{Pt}(\text{C}_2\text{H}_4)\text{Cl}_2]_2$ or complex **22** are by far more catalytically active than, for example, PtCl_2 or **23**. Formation of cyclobutadiene complexes (like **24**) was found to slowly occur in some catalytic reactions. This can be seen as a process of catalyst deactivation. Formation of cyclobutadiene complexes is unlikely for bigger alkyne substrates.

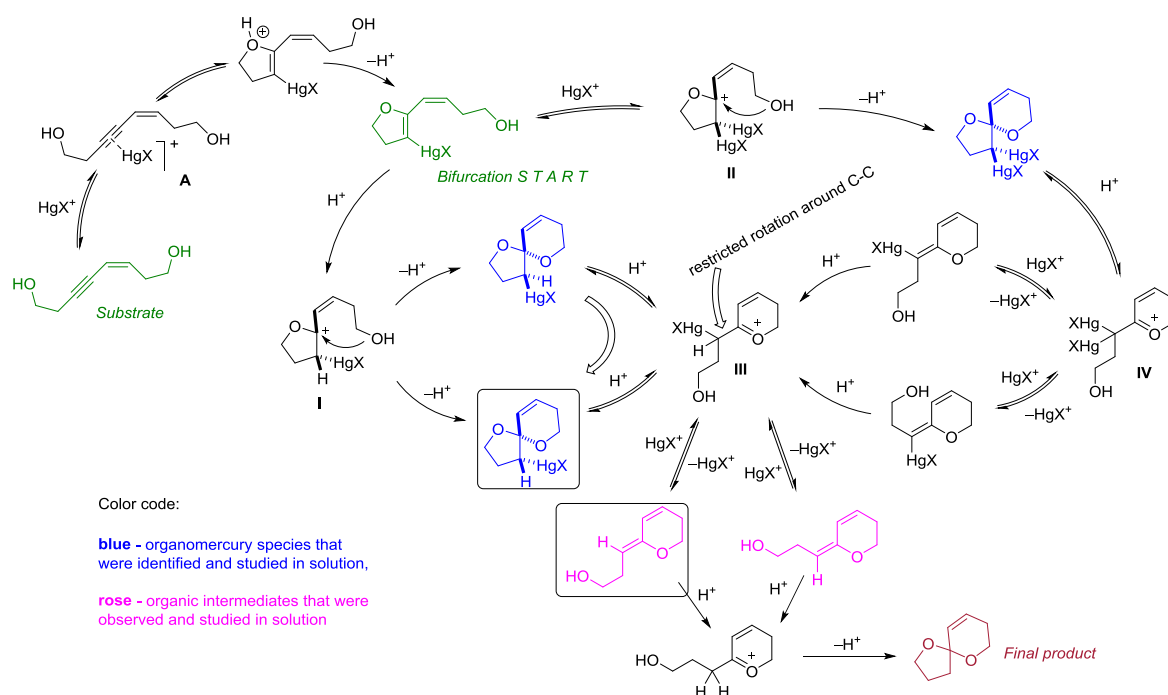


6.3.8. Mechanism of Mercury Catalyzed Spirocyclization

[This study is included in unpublished manuscript N10]



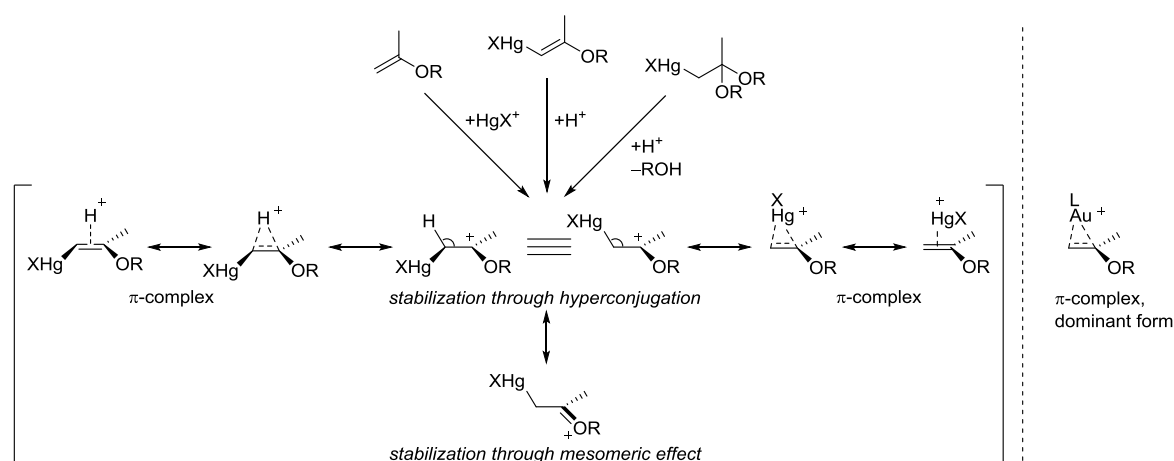
Mechanistic study of spirocyclization catalyzed by simple mercury salts was conducted. A number of organomercury intermediates were identified and characterized for the title reaction. Based on *in situ* NMR observations of catalytic reactions and stoichiometric studies the following mechanism was proposed:



Scheme 21. Mechanism of $\text{Hg}(\text{OTFA})_2$ catalyzed spirocyclization.

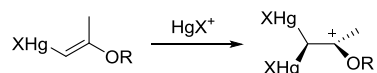
From a first sight this mechanism might look complicated. However, there are simple principals inside. This mechanism has much in common with other transition metal catalyzed hydroalkoxylation processes. The main common feature is that the whole reaction starts the same: from formation of acetylene π -complex **A**. However, this complex remains hypothetical. Some extra steps appear due to the reactivity of organomercury intermediates. Let's consider the reasons that make this mechanism look more complicated (in comparison with Au and Pd catalyzed versions).

At first, several steps include formation of a single type of intermediate: **α -mercurated oxonium ion** (species **I**, **III**). These species are formed by three processes, from three different types of precursor. The structure of the α -mercurated oxonium can be displayed as a series of resonance structures (Scheme 22). This species is believed to be involved in the known mercury(II)-catalyzed transesterification of enol ethers. The exact structure of this species was not established. But from the reactivity patterns we may suggest that it should be best described as α -mercurated oxonium ion and not as a π -complex (a situation similar to that of α -aurated iminium ion, Section 6.3.5). In contrast, gold complexes of enol ethers are qualified rather as π -complexes.

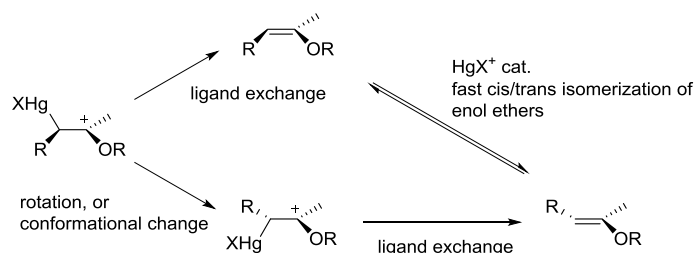


Scheme 22. Formation of α -mercured oxonium ion and its resonance structures. Comparison with gold enol ether π -complex.

In addition to α -mercured oxonium ion there are also α,α -dimercured oxonium ions possible (species **II**, **IV**), which is formed by mercuration of any vinyl mercury intermediate. These ions are even more stabilized by hyperconjugation with mercury:



The double bond character in α -mercured oxonium ions is at least partially lost; therefore they must give a mixture of alkene isomers upon ligand exchange. Therefore, protodemercuration should not be considered as a stereospecific process. The situation resembles that described for α -aurated iminium ion and conjuncted isomerization of enamines (Section 6.3.5). Without strong thermodynamic forces to control alkene configuration, an equilibrium mixture of alkenes will be eventually obtained. Under catalytic conditions the equilibrium is reached fast.



Scheme 23. The origin of *cis/trans* isomerization of an enol ether.

7. Bibliography

- ¹ Ma, C. I.; Diraviyam, K.; Maier, M. E.; Sept, D.; Sibley, L. D. *J. Nat. Prod.* **2013**, *76*, 1565-1572.
- ² Schmauder, A.; Sibley, L. D.; Maier, M. E. *Chem. Eur. J.* **2010**, *16*, 4328-4336.
- ³ de Vries, A. H. M.; Mulders, J. M. C. A.; Mommers, J. H. M.; Henderickx, H. J. W.; de Vries, J. G. *Org. Lett.* **2003**, *5*, 3285-3288.
- ⁴ Michael, F. E.; Cochran, B. M. *J. Am. Chem. Soc.* **2006**, *128*, 4246-4247.
- ⁵ Gong, J.-F.; Zhang, Y.-H.; Song, M.-P.; Xu, C. *Organometallics* **2007**, *26*, 6487-6492.
- ⁶ For a recent review on catalysis by Pd pincer complexes, see: a) Selander, N.; Szabó, K. J. *Chem. Rev.*, **2011**, *111*, 2048-2076. b) Szabo, K. J. *Top. Organomet. Chem.* **2013**, *40*, 203-242.
- ⁷ Hashmi, A. S. K. *Chem. Rev.* **2007**, *107*, 3180-3211.
- ⁸ a) Knight, D. W.; Leese, M. P. *Tetrahedron Lett.* **2001**, *42*, 2593-2595. b) Parry, R. J.; Tao, T.; Alemany, L. B. *Org. Lett.* **2003**, *5*, 1213-1215. c) Bourgeois, J.; Dion, I.; Cebrowski, P. H.; Loiseau, F.; Bédard, A. C.; Beauchemin, A. M. *J. Am. Chem. Soc.* **2009**, *131*, 874-875.
- ⁹ Melman, A. Synthesis of hydroxylamines, in "The Chemistry of Hydroxylamines, Oximes and Hydroxamic Acids", Patai's Chemistry of Functional Groups; Zvi Rappoport, Joel F. Liebman eds, John Wiley & Sons, **2008**, Vol. 175, 117-161.
- ¹⁰ Tinnermann, H.; Wille, C.; Alcarazo, M. *Angew. Chem., Int. Ed.* **2014**, *53*, 8732-8736.
- ¹¹ Wang, D.; Cai, R.; Sharma, S.; Jirak, J.; Thummanapelli, S. K.; Akhmedov, N. G.; Zhang, H.; Liu, X.; Petersen, J. L.; Shi, X. *J. Am. Chem. Soc.* **2012**, *134*, 9012-9019.
- ¹² Hesp, K. D.; Stradiotto, M. *J. Am. Chem. Soc.* **2010**, *132*, 18026-18029.

Paper 1

For the Section 6.1.

Synthesis of Chondramide A Analogs

Synthesis of Chondramide A Analogues with Modified β -Tyrosine and Their Biological Evaluation

Alexander Zhdanko,^[a] Anke Schmauder,^[a] Christopher I. Ma,^[b] L. David Sibley,^[b] David Sept,^[c] Florenz Sasse,^[d] and Martin E. Maier*^[a]

Abstract: Starting from cinnamates **9**, obtained by Wittig reaction or Heck coupling, the diols **17** were prepared by asymmetric dihydroxylation. This was followed by a regioselective substitution of the 3-OH group with hydrazoic acid under Mitsunobu conditions. Methylation of the 2-OH group and reduction of the azide group led to the β -tyrosine derivatives **8**. Condensation

with the dipeptide acid **6** furnished the tripeptide part of the chondramides. The derived acids **21** were combined with the hydroxy ester **7** to the esters **22**. Cleavage of the *tert*-butyl groups

and intramolecular lactam formation gave rise to the chondramide A analogues **2b–k**. Growth inhibition assays showed most of the analogues to be biologically active. Some of them even reach the activity of jasplakinolide. It can be concluded that the 4-position of the aryl ring in the β -tyrosine of chondramide A tolerates structural modifications quite well.

Keywords: chondramides • cyclopeptides • Mitsunobu reaction • total synthesis • tyrosine analogues

Introduction

Cyclodepsipeptides comprise a unique class of secondary metabolites. They frequently contain unusual amino acids, like D-amino acids or N-methylated amino acids and hydroxy acids that typically originate from the polyketide pathway. Incorporation of the hydroxy acid results in an ester bond, explaining the term “depsi”.^[1,2] Many cyclodepsipeptides have been isolated from marine sponges and found to display interesting biological activities.^[3] Thus, cyclodepsipeptides with anti-HIV or anti-tumor activity are known. With the peptide subunit cyclodepsipeptides are clearly protein-like and therefore it is not surprising that they very often modulate protein–protein interactions.^[4]

Very prominent examples of such cyclodepsipeptides, displaying anti-tumor activity are the jasplakinolides and the chondramides. Jasplakinolide (**1**) was isolated from the marine sponge *Jaspis splendans* many years ago (Figure 1).^[5]

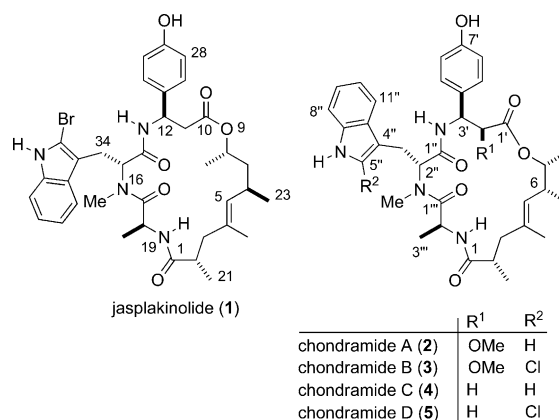


Figure 1. Structures of jasplakinolide (**1**) and the chondramides A–D (**2–5**).

Independently, it was also found in a *Jaspis* sponge and named jaspamide.^[6] In the meantime jasplakinolide was isolated from many other sponges. Furthermore, several additional jasplakinolides could be isolated by the groups of Zampella^[7] and Crews.^[8] In contrast, so far only four natural chondramides are known, namely chondramides A–D (**2–5**) (Figure 1). They were isolated by the Höfle/Reichenbach group from myxobacteria.^[9] The chondramides are quite similar in structure to jasplakinolide, in that they contain a tripeptide subunit consisting of an L-alanine, an N-methyl-D-tryptophan, and an L- β -tyrosine. Jasplakinolide and the

[a] Dipl.-Chem. A. Zhdanko, Dr. A. Schmauder, Prof. Dr. M. E. Maier
Institut für Organische Chemie
Universität Tübingen
Auf der Morgenstelle 18, 72076 Tübingen (Germany)
Fax: (+49) 7071-2975247
E-mail: martin.e.maier@uni-tuebingen.de

[b] Dr. C. I. Ma, Prof. Dr. L. D. Sibley
Department of Molecular Microbiology
Washington University School of Medicine
660 S. Euclid Ave., St. Louis, MO 63110-1093 (USA)

[c] Prof. Dr. D. Sept
Department of Biomedical Engineering
Center for Computational Medicine and Bioinformatics
University of Michigan
1101 Beal Ave.
Ann Arbor, MI 48109-2110 (USA)

[d] Dr. F. Sasse
Abteilung Chemische Biologie
Helmholtz-Zentrum für Infektionsforschung
Inhoffenstrasse 7, 38124 Braunschweig (Germany)

Supporting information for this article is available on the WWW under <http://dx.doi.org/10.1002/chem.201101978>.

chondramides differ essentially in the hydroxy acid that bridges the tripeptide part to form the cyclodepsipeptide. Whereas jasplakinolide contains an 8-hydroxy acid, in the chondramides the corresponding sector is a 7-hydroxy acid. Accordingly, jasplakinolide features a 19-membered macrocycle, while the chondramides are 18-membered.

Over the years several total syntheses of jasplakinolide have been achieved.^[10] Most of them close the macrocyclic ring by intramolecular amide or ester formation. The Waldmann/Arndt synthesis^[10g] relies on a relay ring-closing meta-thesis reaction. Furthermore, syntheses of simplified jasplakinolide analogues have been reported.^[11,12] Surprisingly, syntheses of chondramides were achieved only recently. The reason was that the configuration at the stereogenic centers was not given in the original article. Even though it could be assumed that the configurations in the peptide part and even the overlapping hydroxy acid might be similar to the ones in jasplakinolide. The Waldmann^[13] and Kalesse^[14] groups independently secured the configuration of the hydroxy acid in the chondramides by synthesizing various stereoisomers of chondramide C. Our group had developed a concise synthesis of the hydroxy acid through an asymmetric vinylogous aldol reaction.^[15] Subsequently, we reported the total synthesis of chondramide A (chon A).^[16] Instead of a β -tyrosine, this chondramide contains a 3-amino-2-methoxy-3-arylpropanoic acid, whose configuration was determined to be (2*S*,3*S*). The ester bond could be established either by Yamaguchi esterification or via a Mitsunobu reaction^[17] that was then followed by macrolactam formation. While the β -tyrosine derivative in chondramide A seems more complicated on first sight, it is easily available by asymmetric dihydroxylation of a cinnamic ester precursor.

The potent antitumor activity of these cyclodepsipeptides is due to their stabilizing effect on F-actin filaments.^[18] Because of this property jasplakinolide became an important tool in cell biology. Together with microtubules and the intermediate filaments, actin filaments (F-actin) make up the cytoskeleton which has a key role in cell shape and division. According to a binding model recently refined by the Waldmann group, chondramide C is located in a shallow binding pocket made up by three independent actin subunits in the filament.^[19] The binding site is identical to the one of the bicyclic heptapeptide phalloidin.^[20] There seems to be a hydrophobic interaction of the indole moiety with a loop region of one of the actin subunits (subunit X). The phenolic group of the β -tyrosine occupies a larger cavity with the hydroxyl group close to an Asp of G-actin monomer Y. It seems that the hydroxy acid not only serves to provide a scaffolding role, but rather parts (C1–C3) of it are close to the protein surface of subunit Z and contribute substantially to efficient binding. This model was supported by the activity of the available jasplakinolide and chondramide analogues (Figure 2).^[12] For example, omitting the phenolic ring essentially results in an inactive jasplakinolide analogue. With regard to the hydroxy acid, it turned out that the configuration at C2 of the methyl-bearing carbon and the *E*-configuration of the C4–C5 double bond are crucial. Jaspla-

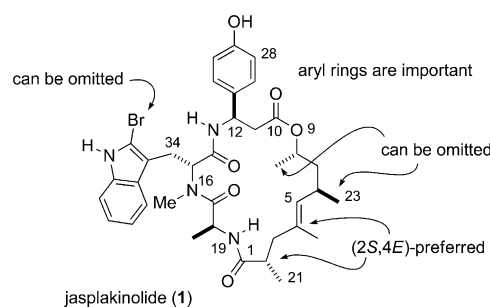


Figure 2. Key structure-activity relationships for good biological activity of jasplakinolides and chondramides illustrated with the jasplakinolide structure.

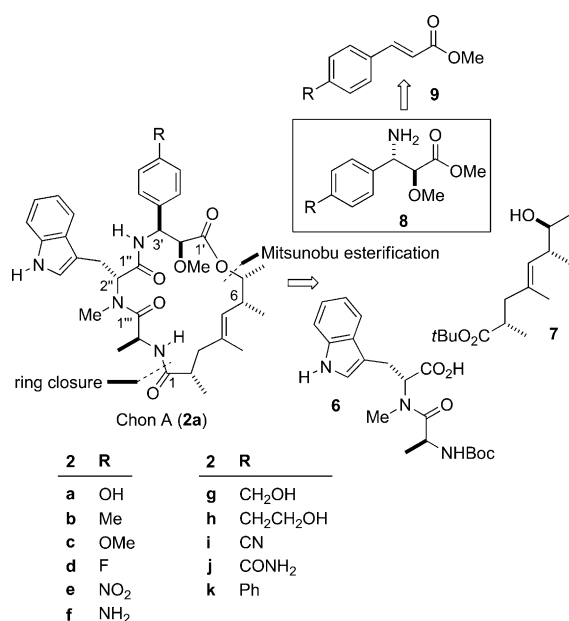
kinolide analogues with this feature are still active even if they lack some of the other methyl groups of the hydroxy acid. For chondramide C analogues it could be shown that the configuration at C6 and C7 of the hydroxy acid is less critical.

Due to their interesting biology and structural similarity analogues of the above-mentioned cyclodepsipeptides should help to understand protein–protein interactions and further advance the binding site model.^[12] With an efficient route to chondramide A we embarked on the synthesis of chondramide A analogues with modified β -tyrosine derivatives. In this paper we report on the synthesis of ten analogues and their biological activity.

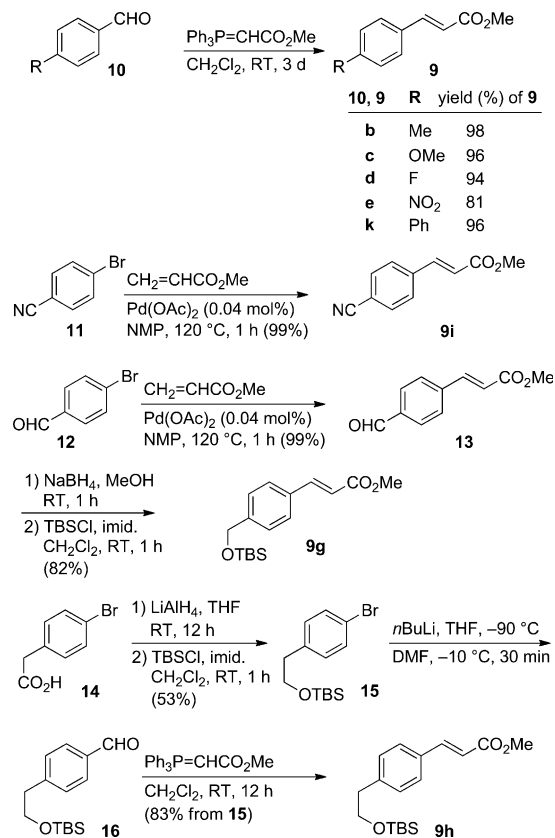
Results and Discussion

Synthesis of the analogues: The synthetic route towards natural chondramide A (**2a**), recently disclosed from our laboratory,^[16] was put as a basis for synthesis of new chondramide analogues, containing variations in the β -tyrosine unit.^[16] Accordingly, this implied the use of differently substituted β -amino esters **8** that had to be synthesized from substituted *trans*-cinnamic esters **9**. At this point, taking into account the compatibility of the substituents at the aromatic ring with all the synthetic steps, we have chosen eight cinnamic esters **9b–e**, **9g–i**, and **9k** as precursors for the desired chondramide analogues (Scheme 1).

All the *trans*-cinnamic esters **9** were synthesized from easily accessible commercial starting materials as outlined in Scheme 2. Enoates **9b–e**, **9k** were prepared by Wittig reaction of the corresponding aldehydes **10** with the stabilized ylide [(carbomethoxy)methylene]triphenylphosphorane^[21] in dichloromethane. Enoate **9e** could also be obtained by Knoevenagel condensation with subsequent esterification in high 93% yield. In case of enoate **9k**, its low solubility in methanol, allowed for efficient isolation of the product by simple filtration. The 4-cyanocinnamate **9i** was synthesized by Heck reaction from 4-bromobenzonitrile under low catalyst loading and ligand-free conditions, using Pd(OAc)₂ as catalyst.^[22] This method is especially efficient for electron deficient aromatic bromides and enoate **9i** was obtained in



Scheme 1. Synthetic strategy and key fragments for the synthesis of chondramide A analogues **2b-k**.

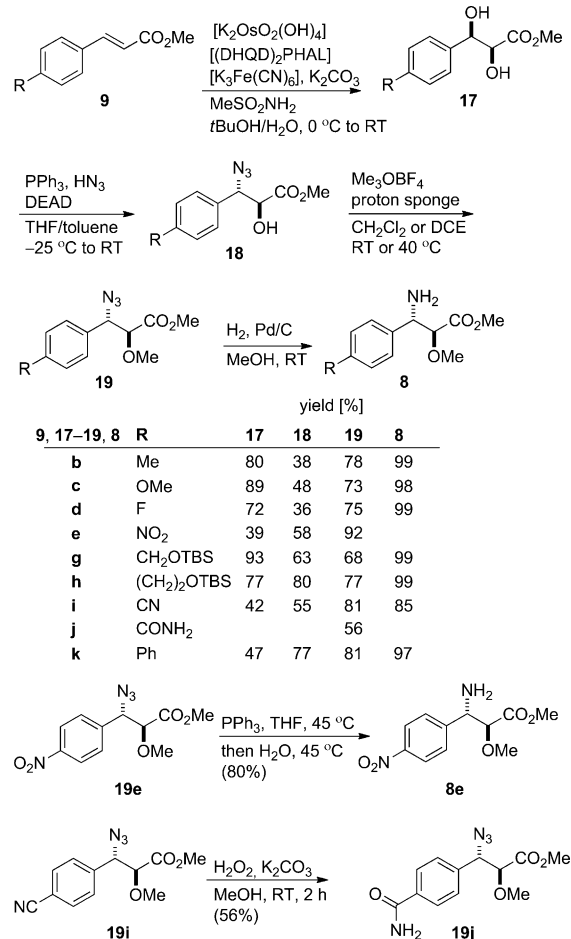


Scheme 2. Synthesis of cinnamic acid building blocks **9** by Wittig reaction or Heck coupling; NMP = *N*-methyl-2-pyrrolidone.

essentially quantitative yield. This result stipulated the choice of 4-bromobenzaldehyde as a precursor for preparation of the CH₂OTBS-substituted enoate **9g**, that was finally done in three steps in high overall yield. Thus, the Heck re-

action to (*E*)-methyl 4-formylcinnamate (**13**) was followed by NaBH₄ reduction of the aldehyde group and silylation of the primary alcohol. Cinnamate **9h** with a CH₂CH₂OTBS substituent in 4-position was prepared from the arylacetic acid **14** through reduction with LiAlH₄ and silylation of the resulting primary alcohol. A subsequent halogen-metal exchange on aryl bromide **15** and quenching the anion with DMF furnished aldehyde **16** which was extended via Wittig reaction in good yield. The synthesis of the last derivative, enoate **9h** initially was also attempted using Heck reaction, however, the corresponding substrate **15** did not react neither under ligand free conditions nor in the presence of PPh₃. Here, formation of palladium black was observed and starting material was recovered unchanged. This is explained by the low reactivity of the aromatic bromide, which is not activated by an electron-withdrawing substituent. In all cases the cinnamates **9** were obtained configurationally pure and no *cis*-isomers could be detected by NMR in the products.

With several cinnamic esters in hands we next turned to the synthesis of amino esters **8** (Scheme 3). Sharpless asymmetric dihydroxylation (AD)^[23] under standard conditions



Scheme 3. Conversion of the cinnamates **9** to the β -tyrosine derivatives **19**, respectively; DCE = dichloroethane, DEAD = diethyl azodicarboxylate.

(0.4 mol% Os catalyst, 2 mol% ligand) was used initially, but this proved problematic providing the diols only in moderate yield (30–68%). After some experimentation, possible reasons for these problems became clear. Due to the electron-deficient nature of the alkenes, especially of the nitro and cyano derivatives, dihydroxylation occurred with reduced rate and saponification of the methyl ester became a significant side reaction. In the case of the nitro-substituted diol **17e** the corresponding acid was partially isolated and characterized (see the supporting information). The dihydroxylation reactions with the NO₂-, Ph-, and CN-substituted cinnamates were additionally hampered by very limited solubility of the alkenes in the reaction medium. As soon as the ester saponification seemed to be the only problem and otherwise the reaction was clean, attempts were made to improve the yield by addition of KHCO₃ to the reaction mixture, to make it less alkaline, but this was again not sufficiently successful. Finally, the situation was significantly improved when increased catalyst loading was used together with buffering the reaction mixture with KHCO₃. Indeed, in the presence of 1 mol% K₂OsO₂(OH)₄/1.5 mol% chiral ligand, the reaction required somewhat shorter time and the diol **17g** was obtained in 93% yield. Although the synthesis of other diols was not attempted under the optimized conditions, we believe that increasing the catalyst loading (e.g., up to 2 mol%) should be the most efficient way to increase the yield in the AD of these relatively unreactive and hardly soluble alkenes. This is in line with the observations given in the literature.^[23] For three of the diols (**17e**, **17g**, **17i**) the optical purity was assessed by means of HPLC on a chiral column (see the Supporting Information), and in no case the opposite enantiomer could be detected, which implies at least 98% *ee* for these compounds.^[16] For the other diols the enantiomeric purity was tentatively assessed to be “high” by the observation of no significant side peaks in the ¹H and ¹³C NMR spectra on later steps when diastereomers would appear.

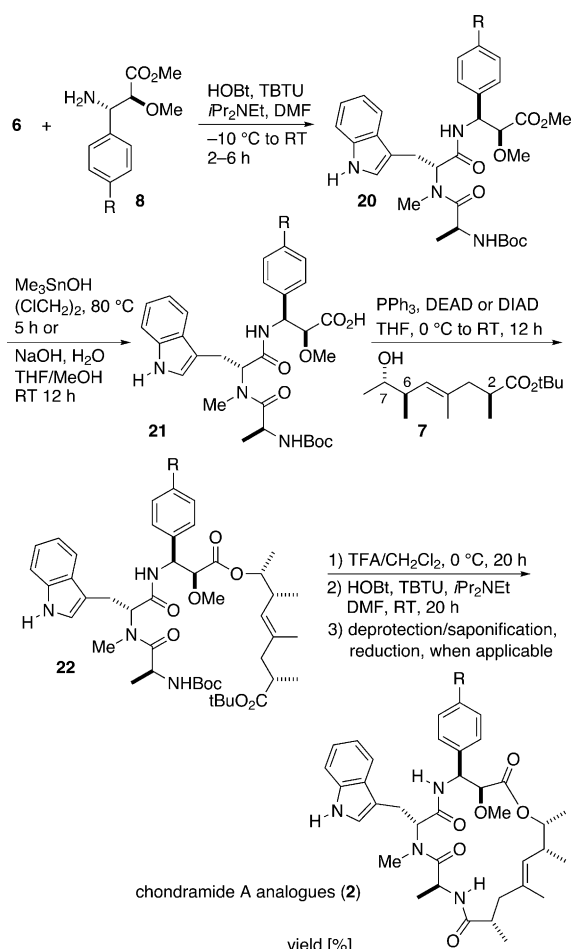
Diols **17** were next transformed to β-azides **18** by means of a Mitsunobu reaction with hydrazoic acid.^[24] Initial experiments revealed only moderate conversion of the diols, accompanied by significant nitrogen evolution. This side reaction was caused by hydrazoic acid decomposition of the ternary mixture in the presence of triphenylphosphine and DEAD. Mixing all three components together caused rapid nitrogen evolution, while the binary mixture of HN₃ and PPh₃ was stable at room temperature. This undesired side reaction was diminished when the DEAD solution was introduced into the reaction as the last component at –25°C rather than at 0°C. Thereafter, the mixture was allowed to stand at room temperature until the reaction stopped. Under these conditions, the desired azides were obtained in better yields as pure stereoisomers in accordance with literature data.^[24] The structure and purity were additionally confirmed by careful comparison of NMR spectra with previously described compounds (see supporting information). In these Mitsunobu reactions, diols **17e** (NO₂), **17i** (CN), and **17k** (Ph) were used as hardly separable mixtures, slightly

contaminated with MeSO₂NH₂, resulting from the previous step. We found MeSO₂NH₂ to have no influence on the reaction.

Subsequently, azides **18** were smoothly methylated by trimethyloxonium tetrafluoroborate in the presence of proton sponge to give the α-methoxy propanoates **19**. The cyano derivative **19i** was hydrolyzed with H₂O₂/K₂CO₃ to provide amide **19j**, the precursor for chondramide analogue **2j**. The hydrolysis was performed in DMSO, MeOH and DMF media and was found to be the fastest in DMSO (complete conversion was observed already in 1–2 min), but in this case the product was isolated only as inseparable mixture with dimethyl sulfone as by-product. Pure amide **19j** was obtained in MeOH, but in this case the reaction took much longer time and gave the product in reduced yield most likely due to hydrolysis of the ester.

Azides **19** were conveniently hydrogenated in presence of Pd/C to afford the amino esters **8**. Nitro derivative **19i** was selectively reduced by treatment with PPh₃ followed by hydrolysis of the iminophosphorane intermediate to afford amine **8e**, that was used without further purification.

In several steps amino esters were transformed into chondramide analogs **2b–k** (Scheme 4). First, peptide coupling with the known dipeptide acid,^[11c,25] **6** afforded tripeptides **20** in good yields. Subsequent saponification of the methyl ester, either with Me₃SnOH (**20b–d**) or simply with NaOH [**20e** (NO₂), **20i** (CN), **20j** (CONH₂), **20k** (Ph)] occurred in quantitative yields and without epimerization. But saponification of the CH₂OTBS- and (CH₂)₂OTBS-substituted tripeptide esters **20g** and **20h** was accompanied by partial deprotection of the alcohol functions. Still, pure acids **21g** and **21h** were successfully isolated by chromatography in reduced, but good yields (~80%). Thus, there was no need to call upon the milder Me₃SnOH procedure. On the next stage, acids **21b–d** were initially esterified with hydroxy ester *7-epi-7* under Yamaguchi conditions to give the *seco*-compounds **22b–d** in reasonable yields. However, later we found it more convenient to perform the esterification reaction under Mitsunobu conditions since the synthesis of hydroxy ester **7** is shorter than the one for *7-epi-7*.^[15] Therefore, the acids **21** were esterified with alcohol^[15] **7** under Mitsunobu conditions in quite good yields. Here, the correct use of either DEAD or DIAD reagents in each case is important for successful separation of the esterification product. Otherwise, the corresponding hydrazodicarboxylate by-product would be inseparable (or hardly separable) from the product. Unfortunately, the acid **21j** (CONH₂) could not be esterified under Mitsunobu conditions. Other methods (Yamaguchi esterification, DCC/DMAP conditions) were unsuccessful either. Eventually, the corresponding chon A derivative was prepared by nitrile hydrolysis on the macrocycle **2j** (see below). For macrolactam formation, the NBoc protected *tert*-butyl esters **22** were subjected to double deprotection under acidic conditions. Initially, the reaction was carried out in a mixture of TFA/CH₂Cl₂ (1:30) as previously described.^[16] The progress of the deprotection was easily monitored by TLC and NMR and under these conditions



| | | yield [%] | | | |
|----------------------|--------------------------------------|-----------|----|----|----------|
| 20–22, 2 | R | 20 | 21 | 22 | 2 |
| b | Me | 75 | – | 67 | 33 |
| c | OMe | 77 | – | 61 | 31 |
| d | F | 68 | – | 64 | 39 |
| e | NO ₂ | 76 | – | 86 | 48 |
| f | NH ₂ | | | | 47 |
| g^a | CH ₂ OTBS | 88 | 82 | 73 | 20 |
| h^a | (CH ₂) ₂ OTBS | 86 | 80 | 66 | 60 |
| i | CN | 86 | – | 78 | 45 |
| j | CONH ₂ | | | | 67 |
| k | Ph | 83 | – | 56 | 54 |

Scheme 4. Synthesis of chondramide A analogues **2b–j**. Esters **2b–d** were also prepared by Yamaguchi esterification using hydroxy ester 7-*epi*-**7**; TBTU = 2-(1*H*-benzotriazole-1-yl)-1,1,3,3-tetramethylammonium tetrafluoroborate, HOBt = 1-hydroxy-benzotriazole, DIAD = diisopropyl azodicarboxylate. [a] For compound **2**, R = CH₂OH and (CH₂)₂OH, respectively.

the conversion was not complete even after 2 d. In particular, the carboxylic ester cleavage is quite slow. However with more concentrated acid (1:10) complete and clean deprotection was observed for each compound after about 20 h. Interestingly, under these reaction conditions the TBS groups of **22g** and **22h** were quantitatively transformed to the corresponding TFA esters, as suggested by NMR of the crude products. In each case the crude amino acids were subjected to macrolactamization in the presence of TBTU, which afforded chondramide A analogs **2e** (NO₂), **2i** (CN), and **2k** (Ph) directly. In order to obtain the analogues **2g**

(CH₂OH) and **2h** [(CH₂)₂OH] the crude cyclization products were stirred in aqueous K₂CO₃/MeOH for 5–10 min before purification. This resulted in complete hydrolysis of the corresponding TFA esters. Unfortunately, the presence of the benzylic trifluoroacetate negatively affected cyclization of the amino acid generated from **22g** (CH₂OTBS), yielding after short hydrolysis with aqueous K₂CO₃/MeOH two products as judged by TLC. The more polar substance turned out to be the desired chondramide A analogue **2g**. The second substance was shown to be the corresponding benzotriazolyl ether that was characterized by ¹H NMR and HRMS analysis (see Supporting Information for details). Thus, for this analogue it can be concluded that the TBS group is not ideal and revision of the synthetic scheme would be required in this case for an optimized synthesis. But for the other cases the described synthetic Scheme is considered reliable. With the NO₂-substituted analogue **2e** we attempted reduction of the nitro group to obtain the NH₂ derivative **2f**. This was tried with catalytic hydrogenation and sodium dithionite. Both methods afforded the desired amino chondramide **2f** in moderate yield. Finally, the CONH₂-substituted analogue **2j** was prepared by hydrolysis of the cyano group of **2i** with H₂O₂/K₂CO₃/DMSO under mild conditions in good unoptimized yield.

Biology: The biological activity of the chondramide A (chon A) analogues **2** was evaluated in a cytotoxicity assay on human primary foreskin fibroblast (HFF) cells. These data are included in Table 1. We also included the natural prod-

Table 1. Cytotoxicity of jasplakinolide (**1**) and chondramide A derivatives **2**.^[a]

| Entry | Compound | EC ₅₀ (HFF) [μM] | IC ₅₀ (L-929) [μM] |
|-------|---|-----------------------------|-------------------------------|
| 1 | jasplakinolide_np (1) | 0.028 ± 0.004 | |
| 2 | chon A_np (2a) | 0.118 ± 0.023 | 0.056 ± 0.013 |
| 3 | chon B_np (3) | 0.044 ± 0.005 | |
| 4 | chon C_np (4) | 0.036 ± 0.007 | |
| 5 | chon A_synth (2a) | 0.109 ± 0.007 | |
| 6 | chon A_Me (2b) | 0.027 ± 0.002 | 0.0079 ± 0.0013 |
| 7 | chon A_OMe (2c) | 0.066 ± 0.008 | 0.0083 ± 0.0021 |
| 8 | chon A_F (2d) | 0.029 ± 0.002 | 0.0080 ± 0.0013 |
| 9 | chon A_NO ₂ (2e) | 0.040 ± 0.006 | 0.017 ± 0.005 |
| 10 | chon A_NH ₂ (2f) | 0.057 ± 0.001 | 0.031 ± 0.002 |
| 11 | chon A_CH ₂ OH (2g) | 0.052 ± 0.010 | 0.035 ± 0.002 |
| 12 | chon A_(CH ₂) ₂ OH (2h) | 0.059 ± 0.010 | 0.033 ± 0.004 |
| 13 | chon A_CN (2i) | 0.027 ± 0.001 | 0.011 ± 0.001 |
| 14 | chon A_CONH ₂ (2j) | 1.424 ± 0.017 | 0.223 ± 0.042 |
| 15 | chon A_Ph (2k) | 0.213 ± 0.016 | 0.025 ± 0.002 |

[a] np = natural product (isolated), synth = synthetic compound.

ucts jasplakinolide and other chondramides in this assay. As can be seen, several of the chon A analogues are slightly more active than the natural product itself. Three of the analogues [**2b** (Me), **2d** (F), **2i** (CN)] are even comparable to jasplakinolide (**1**) itself (EC₅₀ in the range of 30 nM). These are characterized by small substituents. Other analogues show intermediate activity, being about half as active as jasplakinolide (EC₅₀ in the range of 60 nM). These analogues

include **2c** (OMe), **2e** (NO₂), **2f** (NH₂), **2g** (CH₂OH), and **2h** ((CH₂)₂OH). Somewhat surprising is the activity of analogue **2k** (Ph) (EC₅₀=213 nm). With this large substituent one would not expect that the analogue would fit in the binding pocket.^[12] Although the amide substituent in **2j** is not very large, this compound is much less active. A similar trend in activity can be seen on the mouse fibroblast cell line L-929, which is more sensitive to these cyclodepsipeptides.

In general, it can be concluded that the aryl ring on the tyrosine derivative accepts a range of substituents. One explanation could be that the 4-position of the aryl ring protrudes out of the binding pocket. Thus, some of the prepared derivatives might be used for the preparation of labeled derivatives. The recent finding that jasplakinolide V with a catechol in place of the phenol substituent is also quite active shows this region to be less sensitive to structural modifications than the other parts.^[8b]

Conclusion

Based on our previous synthesis of chondramide A, a range of analogues was prepared that feature modifications in the 4-position of the β -tyrosine derivative. The required building blocks, 3-aryl-3-amino-2-methoxypropanoates **8** were prepared from cinnamates **9** by asymmetric dihydroxylation, regioselective Mitsunobu substitution with hydrazoic acid, O-methylation and reduction of the azide group. Subsequently, amino esters **8** were condensed with dipeptide acid **6**. After hydrolysis of the methyl ester function, esterification of the tripeptide acids **21** with the 7-hydroxy ester **7** or 7-*epi*-**7**, respectively furnished the *seco*-compounds **22**. Deprotection of both the amino and the ester group was followed by macrolactam formation to give analogues **2**.

In cell growth assays several of the derivatives surpassed natural chondramide A in its biological activity. Among the derivatives only the amide derivative **2j** was not very active. Otherwise, it appears that the aryl ring of the β -tyrosine tolerates a broad range of substituents in the 4-position. These derivatives should be useful for probing a number of cellular questions in different systems that rely on actin filaments for important aspects of biology.

Experimental Section

Only part of the experimental material is given here. For further details and for compound characterization see Supporting Information. Procedures are given for the sequence leading to chondramide A analogue **2e** (NO₂) and the reduction of **2e** to analogue **2f** (NH₂).

(E)-Methyl 4-nitrocinnamate (9e) (by Knoevenagel reaction): A solution of nitrobenzaldehyde (1.51 g, 0.01 mol), malonic acid (1.14 g, 1.1 equiv), and pyridine (0.25 mL, 0.31 equiv) in ethanol (2 mL) was heated at reflux. Already after 10–15 min a white solid began to precipitate. After 1.5 h, when TLC (EtOAc/petroleum ether, 1:2) indicated complete consumption of the aldehyde, the reaction mixture was cooled and acidified with diluted aqueous HCl. The precipitate was filtered, washed with

water and dried in vacuo to afford crude but pure (2E)-3-(4-nitrophenyl)acrylic acid in quantitative yield (Note: the free acid is soluble in acetone, DMSO, but hardly soluble in CH₂Cl₂, EtOAc). It was taken up in methanol (20 mL), thionyl chloride (1.3 equiv) was carefully added and the resulting suspension was heated at reflux for 1 h. At this time TLC (EtOAc/petroleum ether, 1:2) indicated complete consumption of the acid and the volume of precipitates visually increased. The product was obtained by recrystallization directly from the reaction mixture as follows. The reaction mixture was concentrated in vacuo till a thick suspension resulted, that was filtered on a glass frit and the precipitate was washed with a small amount of cold methanol to afford 1.52 g (93%) of pure methyl (2E)-3-(4-nitrophenyl)acrylate (**9e**) as a slightly yellow solid. Analytical data were in agreement with literature data.^[26]

(2S,3R)-Methyl 3-(4-cyanophenyl)-2,3-dihydroxypropanoate (17e): A mixture of K₃Fe(CN)₆ (7.22 g, 22.0 mmol, 3 equiv), K₂CO₃ (3.04 g, 22.0 mmol, 3 equiv), MeSO₂NH₂ (0.70 g, 7.37 mmol, 1 equiv), K₂OsO₂(OH)₄ (10 mg, 0.027 mmol, 0.0037 equiv), and the ligand (DHQD)₂PHAL (57 mg, 0.073 mmol, 0.01 equiv) was stirred in a mixture of water (35 mL) and *t*BuOH (35 mL) until dissolved and then the solution was cooled to 0°C in an ice bath. At this point cinnamate **9e** (1.52 g, 7.34 mmol) was added and the reaction mixture was allowed to reach room temperature slowly while being stirred overnight, at which time a yellow suspension was formed and complete or almost complete conversion was observed according to TLC (petroleum ether/EtOAc, 1:1). Then solid Na₂SO₃ (9.2 g, 73.4 mmol, 10 equiv) was added and the mixture was stirred for several min. The suspension was filtered, and the filter cake was washed with EtOAc. The filtrate was transferred to a separatory funnel, the organic phase was separated, and the water phase was extracted twice with EtOAc. The combined organic extracts were washed with saturated NaCl solution, dried with Na₂SO₄, filtered, and evaporated. The residue was purified by flash chromatography (CH₂Cl₂/MeOH, 95:5) to afford pure diol **17e** (0.698 g, 39%) as a colorless solid. Sometimes it was difficult to purify the diol from CH₃SO₂NH₂ (as a contaminant in different compounds comes at δ =3.08–3.10 (s, 3H), 4.67–4.79 ppm (brs, 2H)), but the sulfone amide impurity did not influence the next Mitsunobu azidation as was established later. Also, a better procedure but for another substrate (**17g**) utilizing 1% of the catalyst is described in the Supporting information. ¹H NMR (400 MHz, CDCl₃): δ =2.81 (brs, 1H, OH), 3.13 (brs, 1H, OH), 3.86 (s, 3H, OCH₃), 4.39 (brs, 1H, 2-H), 5.14 (brs, 1H, 3-H), 7.59 (d, *J*=8.4 Hz, 2H, Ar), 8.23 ppm (d, *J*=8.4 Hz, 2H, Ar).

Preparation of hydrazoic acid solution: CAUTION: Hydrazoic acid is a highly volatile, toxic and explosive liquid in individual state. However, in solution it is stable and safe. In this study solutions up to 5M were used. Sodium azide (3.0 g, 46 mmol) was mixed with water (1.5 mL) and toluene (10 mL). The suspension was cooled to near 0°C and concentrated H₂SO₄ (~2 g, ~1.09 mL, 20 mmol) was carefully added while cooling and shaking the round bottom flask (stirring with magnetic stirring bar is not sufficient). Crystals were kneaded with a spatula shortly after the addition of the acid. Then the mixture was filtered under positive pressure and dried with Na₂SO₄ (there was no water phase remained, and no need to separate it from toluene solution). To rapidly estimate the resulting concentration of hydrazoic acid, a known amount of NaOH was dissolved in a small amount of water, phenolphthalein was added and the pink solution was titrated with the hydrazoic acid solution from an analytical pipette (the concentration was found to be 3.3M against theoretical 4.0M).

(2S,3S)-Methyl 3-azido-2-hydroxy-3-(4-nitrophenyl)propanoate (18e): To a stirred solution of diol **17e** (0.228 g, 0.946 mmol), triphenylphosphine (0.297 g, 1.14 mmol, 1.2 equiv), hydrazoic acid (0.86 mL, 3.3M in toluene, 3 equiv) in THF (2.0 mL) at –25°C was added DEAD (0.56 mL, 0.535 g, 1.23 mmol, 40% wt. solution in toluene, 1.3 equiv), then the cooling bath was removed (slight evolution of N₂ was observed) and the resulting mixture was stirred overnight at ambient temperature (TLC control: petroleum ether/EtOAc, 1:1; NMR control: a sample portion was taken from the reaction mixture, evaporated and directly analyzed by NMR). Then the reaction mixture was concentrated in vacuo. The residue was purified by flash chromatography (petroleum ether/EtOAc, 4:1 to 2:1) to yield

18e (0.145 g, 58%) as a slightly orange oil which solidified into a waxy solid upon standing. R_f (petroleum ether/EtOAc, 1:1) = 0.55; $[\alpha]_D^{20} = +101.1$ ($c = 1.00$, CH_2Cl_2); $^1\text{H NMR}$ (400 MHz, CDCl_3): $\delta = 3.11$ (brs, 1H, OH), 3.73 (s, 3H, OCH_3), 4.58 (d, 1H, 2-H), 5.08 (d, $J = 3.8$ Hz, 1H, 3-H), 7.53 (d, $J = 8.7$ Hz, 2H, Ar), 8.23 ppm (d, $J = 8.7$ Hz, 2H, Ar); $^{13}\text{C NMR}$ (100 MHz, CDCl_3): $\delta = 53.1$ (OCH_3), 66.4 (C-3), 73.7 (C-2), 123.7 (C_{ar}), 128.7 (C_{ar}), 141.8 (C_{ar}), 148.1 (C_{ar}), 171.3 ppm (CO_2CH_3); HMRS (ESI): m/z calcd for $\text{C}_{10}\text{H}_{10}\text{N}_4\text{O}_5$ $[M + \text{Na}]^+$: 289.05434; found: 289.05431. *Note.* The product **18e** was slightly contaminated with diethyl hydrazodicarboxylate (~3–5 mol%), having signals $\delta = 1.28 \pm 0.01$ (t, 6H), 4.22 ± 0.01 ppm (q, 4H). This impurity did not cause problems in the subsequent steps.

(2S,3S)-Methyl 3-azido-2-methoxy-3-(4-nitrophenyl)propanoate (19e): To a solution of α -hydroxy ester **18e** (0.495 g, 1.86 mmol) in dry 1,2-dichloroethane (1.9 mL) was added trimethylxonium tetrafluoroborate (0.495 g, 3.35 mmol, 1.8 equiv) and proton sponge (0.876 g, 4.09 mmol, 2.2 equiv). The flask was covered with alumina foil. After stirring the suspension at 40 °C overnight, a small probe was taken from the reaction mixture and quenched with EtOAc/ HCl_{aq} for TLC (petroleum ether/EtOAc, 1:1), that indicated full conversion. The reaction mixture was cooled, treated with EtOAc/ H_2O , and acidified with 1N HCl to pH 2–3. The precipitate was filtered off and the filtrate was separated. The aqueous phase was extracted once with EtOAc and the combined organic extracts were washed with water, and saturated NaCl solution, dried with Na_2SO_4 , filtered, and concentrated in vacuo. The residue was chromatographed (petroleum ether/EtOAc, 3:1 to 2:1) to yield **19e** (0.48 g, 92%) as a slightly orange oil. R_f (petroleum ether/EtOAc, 2:1) = 0.54; $[\alpha]_D^{20} = +49.5$ ($c = 1.00$, CH_2Cl_2); $^1\text{H NMR}$ (400 MHz, CDCl_3): $\delta = 3.38$ (s, 3H, OCH_3), 3.75 (s, 3H, CO_2CH_3), 3.99 (d, $J = 6.1$ Hz, 1H, 2-H), 4.89 (d, $J = 6.1$ Hz, 1H, 3-H), 7.55 (d, $J = 8.7$ Hz, 2H, Ar), 8.22 ppm (d, $J = 8.7$ Hz, 2H, Ar); $^{13}\text{C NMR}$ (100 MHz, CDCl_3): $\delta = 52.5$ (OCH_3), 59.3 (OCH_3), 65.0 (C-3), 83.0 (C-2), 123.8 (C_{ar}), 129.0 (C_{ar}), 142.4 (C_{ar}), 148.1 (C_{ar}), 169.6 ppm (CO_2CH_3); HMRS (ESI): m/z calcd for $\text{C}_{11}\text{H}_{12}\text{N}_4\text{O}_5$ $[M + \text{Na}]^+$: 303.06999; found: 303.07002.

Reduction of azide 19e and coupling of amine 8e with acid 6 to tripeptide 20e (NO₂): A solution of azide **19e** (89.6 mg, 0.32 mmol) and PPh_3 (92.2 mg, 0.352 mmol, 1.1 equiv) in THF (1 mL) was stirred at 40–50 °C for 1 h for clean and complete conversion to the corresponding iminophosphorane (TLC control: $\text{CH}_2\text{Cl}_2/\text{MeOH}/\text{NH}_3$, 10:1:0.1, R_f 0.5 for the iminophosphorane). Selected $^1\text{H NMR}$ (400 MHz, CDCl_3) data for the iminophosphorane: $\delta = 7.91$ (d, 2H), 3.67 (s, 3H), 3.13 ppm (s, 3H). Then water (0.1 mL) was added and the mixture was further stirred at 40–50 °C for ~8 h. Because the R_f values of the iminophosphorane, $\text{Ph}_3\text{P}=\text{O}$ and the resulting amine were all the same, the reaction progress was conveniently monitored by analyzing small evaporated probes taken from the reaction mixture by NMR. Selected $^1\text{H NMR}$ (400 MHz, CDCl_3) data for the amine: $\delta = 8.15$ (d, 2H), 3.65 (s, 3H), 3.39 ppm (s, 3H). When appropriately clean and high (~86%) conversion was achieved, the mixture was evaporated to yield 0.166 g of a sticky oil, containing ~36% w/w amine **8e** (assuming the conversion was 80% as the lowest). Then, to a solution of this crude mixture (108 mg), containing amine **8e** (approx. 38.9 mg, 0.153 mmol, 1.24 equiv of the amine) in DMF (2.3 mL) were added acid **6** (47.7 mg, 0.123 mmol), HOBt (24.9 mg, 0.184 mmol, 1.5 equiv), $i\text{Pr}_2\text{NEt}$ (0.064 mL, 0.369 mmol, 3 equiv). At –10 °C TBTU (59 mg, 0.184 mmol, 1.5 equiv) was added and the reaction was stirred for 5–6 h at room temperature. The mixture was diluted with water (5 mL) and extracted with ethyl acetate (3 × 8 mL). The combined organic layers were washed with 1N NaHSO_4 solution (5 mL), saturated NaHCO_3 solution (5 mL), saturated NaCl solution (5 mL), dried with Na_2SO_4 , filtered, and concentrated in vacuo. Purification of the residue by flash chromatography (petroleum ether/EtOAc, 2:1) gave tripeptide **20e** (58.7 mg, 76%) as a white foam. R_f (petroleum ether/EtOAc, 2:1) = 0.48; $[\alpha]_D^{20} = +4.0$ ($c = 1.00$, CH_2Cl_2); $^1\text{H NMR}$ (400 MHz, CDCl_3): $\delta = 0.97$ (d, $J = 6.9$ Hz, 3H, Ala CH_3), 1.40 (s, 9H, $t\text{Bu}$), 2.98 (s, 3H, NCH_3), 3.17 (dd, $J = 15.5$, 9.4 Hz, 1H, CH_2), 3.38 (s, 3H, OCH_3), 3.38 (m, 1H, CH_2), 3.61 (s, 3H, CO_2CH_3), 4.07 (d, $J = 5.1$ Hz, 1H, CHOCH_3), 4.48–4.54 (m, 1H, Ala CH), 5.33 (d, $J = 7.4$ Hz, 1H, Ala NH), 5.44 (dd, $J = 8.1$, 5.1 Hz, 1H, β -Tyr CH), 5.53 (dd, $J = 8.9$, 7.4 Hz, 1H, Trp CH), 6.89 (s, 1H, Trp H_{Ar}), 7.08 (ddd, $J = 7.9$, 7.1, 0.8 Hz, 1H, Trp H_{Ar}), 7.16 (ddd, $J =$

7.9, 7.1, 0.8 Hz, 1H, Trp H_{Ar}), 7.21 (d, $J = 8.1$ Hz, 1H, β -Tyr NH), 7.31 (d, $J = 7.9$ Hz, 1H, Trp H_{Ar}), 7.34 (d, $J = 8.3$ Hz, 2H, Ar), 7.57 (d, $J = 7.9$ Hz, 1H, Trp H_{Ar}), 8.06 (d, $J = 8.3$ Hz, 2H, Ar), 8.21 ppm (s, 1H, Trp NH); $^{13}\text{C NMR}$ (100 MHz, CDCl_3): $\delta = 17.8$ (Ala CH_3), 23.5 (CH_2), 28.3 ($\text{C}(\text{CH}_3)_3$), 30.9 (NCH_3), 46.7 (Ala CH), 52.1 (OCH_3), 53.8 (β -Tyr CH), 56.8 (Trp CH), 59.3 (OCH_3), 79.7 ($\text{C}(\text{CH}_3)_3$), 81.8 (CHOCH_3), 110.5 (quat. Trp), 111.2, 118.5, 119.5, 122.2 (2C, Trp), 123.4 (2C, Ar), 127.1 (quat. Trp), 128.7 (2C, Ar), 136.1 (quat. Trp), 144.3 (quat. Ar), 147.5 (quat. Ar), 155.2 (Boc), 169.5, 169.6, 174.5 ppm; HMRS (ESI): m/z calcd for $\text{C}_{31}\text{H}_{39}\text{N}_5\text{O}_9$ $[M + \text{Na}]^+$: 648.26400; found: 648.26502.

Tripeptide acid 21e (NO₂): To a solution of methyl ester **20e** (55.3 mg, 0.0884 mmol) in THF (0.4 mL) were added water (0.6 mL), methanol (0.3 mL) and NaOH (7.5 mg, 0.188 mmol, 2.1 equiv). The initial biphasic mixture became homogeneous with progressing saponification. After being stirred for 1 h at room temperature until complete conversion (controlled by TLC), the mixture was diluted with water (5 mL) and ethyl acetate (8 mL). It was carefully acidified with 1M NaHSO_4 to pH ~2 before the layers were separated and the aqueous phase extracted once with ethyl acetate (8 mL). The combined organic layers were washed with water, saturated NaCl solution, dried with Na_2SO_4 , filtered, and concentrated in vacuo to afford the crude acid **21e** as a colorless foam. R_f (EtOAc/AcOH 100:1) = 0.4; $^1\text{H NMR}$ (400 MHz, CDCl_3): $\delta = 0.83$ (d, $J = 6.9$ Hz, 3H, Ala CH_3), 1.39 (s, 9H, $t\text{Bu}$), 2.93 (s, 3H, NCH_3), 3.18 (dd, $J = 15.3$, 9.9 Hz, 1H, CH_2), 3.28–3.34 (m, 1H, CH_2), 3.34 (s, 3H, OCH_3), 3.98 (d, $J = 6.3$ Hz, 1H, CHOCH_3), 4.42–4.49 (m, 1H, Ala CH), 5.40 (dd, $J = 7.6$, 7.1 Hz, 1H, β -Tyr CH), 5.46 (d, $J = 7.4$ Hz, 1H, Ala NH), 5.59 (dd, $J = 9.9$, 7.4 Hz, 1H, Trp CH), 6.88 (s, 1H, Trp H_{Ar}), 7.05 (app t, $J = 7.0$ Hz, 1H, Trp H_{Ar}), 7.13 (app t, $J = 7.0$ Hz, 1H, Trp H_{Ar}), 7.21 (d, $J = 8.6$ Hz, 1H, β -Tyr NH), 7.28 (d, $J = 7.9$ Hz, 1H, Trp H_{Ar}), 7.41 (d, $J = 8.4$ Hz, 2H, Ar), 7.53 (d, $J = 7.9$ Hz, 1H, Trp H_{Ar}), 8.04 (d, $J = 8.4$ Hz, 2H, Ar), 8.36 ppm (s, 1H, Trp NH); $^{13}\text{C NMR}$ (100 MHz, CDCl_3): $\delta = 17.0$ (Ala CH_3), 23.2 (CH_2), 28.3 ($\text{C}(\text{CH}_3)_3$), 30.6 (NCH_3), 46.6 (Ala CH), 54.0 (β -Tyr CH), 56.7 (Trp CH), 58.8 (OCH_3), 80.8 ($\text{C}(\text{CH}_3)_3$), 82.5 (CHOCH_3), 110.2 (quat. Trp), 111.2, 118.4, 119.5, 122.1, 122.3, 123.5 (2C, Ar), 127.1 (quat. Trp), 128.4 (2C, Ar), 136.1 (quat. Trp), 145.2 (quat. Ar), 147.4 (quat. Ar), 156.3 (Boc), 169.5, 170.7, 174.8 ppm; HMRS (ESI): m/z calcd for $\text{C}_{30}\text{H}_{37}\text{N}_5\text{O}_9$ $[M + \text{Na}]^+$: 634.24835; found: 634.24819.

Depsipeptide 22e (NO₂): The crude acid **21e** (52 mg, 0.0851 mmol) and alcohol **7** (32.8 mg, 0.128 mmol, 1.5 equiv) were dissolved in THF (1 mL) and Ph_3P (40 mg, 0.152 mmol, 1.8 equiv) was added at 0 °C. This was followed by the dropwise addition of DIAD (0.030 mL, 0.152 mmol, 1.8 equiv). The cooling bath was removed and the mixture stirred overnight at room temperature. The reaction mixture was concentrated in vacuo and the residue purified by flash chromatography (petroleum ether/EtOAc 2:1 to 1:1) to give ester **22e** (62 mg, 86%) as a colorless foam. R_f (petroleum ether/EtOAc 1:1) = 0.30; $[\alpha]_D^{20} = -4.0$ ($c = 1.00$, CH_2Cl_2); $^1\text{H NMR}$ (400 MHz, CDCl_3): $\delta = 0.77$ (d, $J = 6.6$ Hz, 3H, CH_3), 0.91 (d, $J = 6.1$ Hz, 3H, CH_3), 0.96 (d, $J = 6.8$ Hz, 3H, Ala CH_3), 1.01 (d, $J = 6.8$ Hz, 3H, CH_3), 1.40 (s, 9H, $t\text{Bu}$), 1.41 (s, 9H, $t\text{Bu}$), 1.56 (s, 3H, CH_3), 1.92 (dd, $J = 13.9$, 7.6 Hz, 1H, CH_2), 2.33 (dd, $J = 13.9$, 6.8 Hz, 1H, CH_2), 2.40–2.51 (m, 2H, 2 CH), 2.97 (s, 3H, NCH_3), 3.17 (dd, $J = 15.4$, 9.6 Hz, 1H, CH_2), 3.37 (dd, $J = 15.4$, 7.1 Hz, 1H, CH_2), 3.40 (s, 3H, OCH_3), 4.06 (d, $J = 4.5$ Hz, 1H, CHOCH_3), 4.46–4.61 (m, 2H, Ala CH, CO_2CH), 4.84 (d, $J = 9.9$ Hz, 1H, =CH), 5.34 (d, $J = 7.3$ Hz, 1H, Ala NH), 5.43 (dd, $J = 8.3$, 4.5 Hz, 1H, β -Tyr CH), 5.52 (dd, $J = 9.6$, 7.1 Hz, 1H, Trp CH), 6.88 (s, 1H, Trp H_{Ar}), 7.07 (ddd, $J = 7.8$, 7.1, 0.8 Hz, 1H, Trp H_{Ar}), 7.15 (ddd, $J = 8.1$, 7.1, 0.8 Hz, 1H, Trp H_{Ar}), 7.21 (d, $J = 8.3$ Hz, 1H, β -Tyr NH), 7.30 (d, $J = 8.1$ Hz, 1H, Trp H_{Ar}), 7.39 (d, $J = 8.6$ Hz, 2H, Ar), 7.56 (d, $J = 7.8$ Hz, 1H, Trp H_{Ar}), 8.04 (d, $J = 8.6$ Hz, 2H, Ar), 8.25 ppm (s, 1H, Trp NH); $^{13}\text{C NMR}$ (100 MHz, CDCl_3): $\delta = 16.4$, 16.6, 17.1, 17.6, 17.9, 23.5 (CH_2), 28.0 ($\text{C}(\text{CH}_3)_3$), 28.3 ($\text{C}(\text{CH}_3)_3$), 30.9 (NMe), 37.5, 38.6, 43.4 (CH_2), 46.7 (Ala CH), 53.8 (β -Tyr CH), 56.8 (Trp CH), 59.3 (OCH_3), 76.4 (CO_2CH), 79.6 ($\text{C}(\text{CH}_3)_3$), 79.9 ($\text{C}(\text{CH}_3)_3$), 81.4 (CHOCH_3), 110.5 (quat. Trp), 111.1, 118.4, 119.5, 122.1, 122.2, 123.3 (2C, Ar), 127.1 (quat. Trp), 127.5 (=CH), 129.1 (2C, Ar), 134.0 (=C<), 136.1 (quat. Trp), 144.3, 147.4, 155.2 (Boc), 168.6, 169.5, 174.5, 175.7 ppm; HMRS (ESI): m/z calcd for $\text{C}_{45}\text{H}_{63}\text{N}_5\text{O}_{11}$ $[M + \text{Na}]^+$: 872.44163; found: 872.44212.

Chondramide 2e (NO₂): To a stirred solution of compound **2e** (62.7 mg, 0.0738 mmol) in CH₂Cl₂ (2.2 mL) was added TFA (0.22 mL, 0.34 g, 2.98 mmol) at 0°C. The reaction mixture was allowed to warm to room temperature and after stirring for 22 h, the solvent was removed in vacuo (TLC control: CH₂Cl₂/MeOH/NH₃, 10:1:0.1). For azeotropic removal of TFA the residue was taken up in toluene (3×0.5 mL) and concentrated in vacuo each time. The crude product was dissolved in DMF (30 mL) and *i*Pr₂NEt (64 μL, 47.7 mg, 0.369 mmol, 5 equiv), HOBt (19.9 mg, 0.147 mmol, 2 equiv) and TBTU (47.4 mg, 0.147 mmol, 2 equiv) were added. The solution was stirred at room temperature for 20 h and then diluted with water (20 mL) and EtOAc (20 mL). The aqueous layer was extracted with EtOAc (3×20 mL) and the combined organic layers were washed with 5% aqueous KHSO₄ solution (20 mL), water (20 mL), saturated NaHCO₃ solution (20 mL), water (2×20 mL) and saturated NaCl solution (20 mL). The combined organic extracts were dried over Na₂SO₄, filtered, and concentrated in vacuo. The crude product was purified by flash chromatography (petroleum ether/EtOAc, 1:3 to 0:1) to give depsipeptide **2e** (27.3 mg, 48%) as a colorless foam. *R*_f (EtOAc) = 0.41; [α]_D²⁰ = +18.5 (*c* = 1.00, CH₂Cl₂); ¹H NMR (400 MHz, CDCl₃): δ = 0.84 (d, *J* = 6.6 Hz, 3H, CH₃), 0.85 (d, *J* = 6.1 Hz, 3H, CH₃), 1.07 (d, *J* = 6.8 Hz, 3H, CH₃), 1.17 (d, *J* = 6.8 Hz, 3H, CH₃), 1.64 (s, 3H, CH₃), 1.88 (d, *J* = 13.1 Hz, 1H, CH₂), 2.36–2.51 (m, 3H, 2 CH, CH₂), 2.95 (s, 3H, NCH₃), 3.17 (dd, *J* = 15.2, 8.6 Hz, 1H, CH₂), 3.22 (s, 3H, OCH₃), 3.31 (dd, *J* = 15.2, 7.8 Hz, 1H, CH₂), 3.75 (d, *J* = 8.1 Hz, 1H, CHOCH₃), 4.77–4.83 (m, 2H, Ala CH, CO₂CH), 4.90 (d, *J* = 9.1 Hz, 1H, =CH), 5.30 (t, *J* = 8.3 Hz, 1H, β-Tyr CH), 5.60 (t, *J* = 8.1 Hz, 1H, Trp CH), 6.50 (d, *J* = 7.3 Hz, 1H, Ala NH), 6.82 (s, 1H, Trp H_{Ar}), 7.06 (d, *J* = 8.8 Hz, 1H, β-Tyr NH), 7.10 (ddd, *J* = 8.1, 7.1, 0.8 Hz, 1H, Trp H_{Ar}), 7.17 (ddd, *J* = 8.1, 7.1, 0.8 Hz, 1H, Trp H_{Ar}), 7.24 (d, *J* = 8.6 Hz, 2H, Ar), 7.32 (d, *J* = 8.1 Hz, 1H, Trp H_{Ar}), 7.59 (d, *J* = 8.1 Hz, 1H, Trp H_{Ar}), 8.06 (d, *J* = 8.6 Hz, 2H, Ar), 8.11 ppm (s, 1H, Trp NH); ¹³C NMR (100 MHz, CDCl₃): δ = 15.8, 16.6, 17.3, 18.6, 20.0, 23.6 (CH₂), 30.2 (NCH₃), 37.0, 40.2, 44.1 (CH₂), 45.2 (Ala CH), 54.4 (β-Tyr CH), 56.0 (Trp CH), 58.2 (OCH₃), 76.8 (CO₂CH), 81.9 (CHOCH₃), 110.2 (quat. Trp), 111.2, 118.5, 119.6, 122.2, 122.3, 123.4, 127.1 (quat. Trp), 127.8 (=CH), 127.9, 134.3 (=C<), 136.1 (quat. Trp), 144.5, 147.3, 169.77, 169.82, 174.1, 174.5 ppm; HMRS (ESI): *m/z* calcd for C₃₆H₄₄N₅O₈ [*M*+Na]⁺: 698.31603; found: 698.31672.

Chondramide 2f (NH₂): By catalytic hydrogenation: A solution of chondramide **2e** (6.1 mg, 9.03 μmol) in methanol (0.5 mL) was hydrogenated overnight in a round bottom flask connected to a hydrogen filled balloon, using 10% Pd on carbon (TLC control: CH₂Cl₂/MeOH, 10:1). Upon complete conversion, the solvent was evaporated and the residue purified by flash chromatography (CH₂Cl₂/MeOH, 30:1 to 20:1) to afford chondramide **2f** (2.7 mg, 47%) as white foam. A mixed fraction, containing **2f** and another unknown compound as major component was also isolated. Complete conversion was observed, but the reaction was not very clean, likely because of formation of RNO and/or RNHOH, as suggested by LC/MS examination of the mixed fraction. No evidence for competitive hydrogenation of the double bond was found (by ¹H NMR).

By reduction with sodium dithionite: Alternatively, reduction of chondramide **2e** (5.8 mg, 8.58 μmol) was carried out in THF (0.5 mL), H₂O (0.5 mL) in the presence of Na₂S₂O₄ (20 mg, 0.115 mmol) overnight at room temperature. Conversion was high but not complete. The reaction mixture was diluted with saturated NaCl solution and EtOAc with addition of some saturated NaHCO₃ solution. The water phase was extracted once more with EtOAc. The combined organic extracts were dried with Na₂SO₄, filtered, and evaporated. The desired NH₂-chondramide **2f** (2 mg, 36%) was isolated successfully by flash chromatography (CH₂Cl₂/MeOH 30:1 to 20:1) as a white foam. *R*_f (CH₂Cl₂/MeOH 20:1) = 0.26; [α]_D²⁰ = +24.9 (*c* = 0.35, CH₂Cl₂); ¹H NMR (400 MHz, CDCl₃): δ = 0.80 (d, *J* = 6.3 Hz, 3H, CH₃), 0.85 (d, *J* = 6.8 Hz, 3H, CH₃), 1.03 (d, *J* = 6.8 Hz, 3H, Ala CH₃), 1.15 (d, *J* = 7.1 Hz, 3H, CH₃), 1.63 (s, 3H, CH₃), 1.80 (d, *J* = 13.9 Hz, 1H, CH₂), 2.33–2.40 (m, 2H, 2 CH), 2.53 (d, *J* = 10.4, 13.6 Hz, 1H, CH₂), 2.94 (s, 3H, NCH₃), 3.14 (dd, *J* = 15.5, 9.2 Hz, 1H, CH₂), 3.23 (s, 3H, OCH₃), 3.27 (dd, *J* = 15.5, 6.8 Hz, 1H, CH₂), 3.68 (brs, 2H, NH₂), 3.75 (d, *J* = 7.3 Hz, 1H, CHOCH₃), 4.77–4.84 (m, 2H, Ala CH, 7-H), 4.90 (d, *J* = 8.8 Hz, 1H, =CH), 5.25 (dd, *J* = 7.3, 9.1 Hz, 1H, β-Tyr CH), 5.60 (dd, *J* = 7.1, 9.1 Hz, 1H, Trp CH), 6.58 (d, *J* = 7.3 Hz, 1H, Ala NH), 6.58 (d, *J* = 8.3 Hz, 2H, Ar), 6.81 (d, *J* = 2.2 Hz, 1H, Trp H_{Ar}), 6.92–

6.96 (m, 3H, β-Tyr NH, Ar), 7.11 (ddd, *J* = 8.1, 7.8, 1.0 Hz, 1H, Trp H_{Ar}), 7.17 (ddd, *J* = 8.1, 7.8, 1.0 Hz, 1H, Trp H_{Ar}), 7.30 (d, *J* = 7.8 Hz, 1H, Trp H_{Ar}), 7.90 (d, *J* = 7.8 Hz, 1H, Trp H_{Ar}), 7.87 ppm (s, 1H, Trp NH); ¹³C NMR (100 MHz, CDCl₃): δ = 15.3, 16.6, 17.6, 18.6, 20.5, 23.3 (CH₂), 30.1 (NCH₃), 37.1, 40.3, 43.8 (CH₂), 45.3 (Ala CH), 53.9 (β-Tyr CH), 55.7 (Trp CH), 58.0 (OCH₃), 77.2 (CO₂CH), 82.6 (CHOCH₃), 110.7 (quat. Trp), 111.0, 115.0 (2C, Ar), 118.6, 119.4, 122.05, 122.11, 127.2 (quat. Trp), 127.7 (quat. Ar), 127.9 (2C, Ar), 128.4 (=CH), 134.1 (=C<), 136.1 (quat. Trp), 145.9, 169.6, 170.6, 174.0, 174.5 ppm; HMRS (ESI): *m/z* calcd for C₃₆H₄₇N₅O₆ [*M*+Na]⁺: 668.34186; found: 668.34224.

Cytotoxicity assay and EC₅₀ determination: Human foreskin fibroblast (HFF) cells grown in Dulbecco's modified Eagle's medium with 10% fetal bovine serum and 10 μg mL⁻¹ gentamicin were seeded at 2000 cells per well in 96-well microtiter plates. After 2 h of incubation at 37°C in a humidified atmosphere with 5% CO₂, jasplakinolide and chon A analogues were added to reach the final concentrations of 0.0049–5 μM (in two-fold increments). The number of viable cells was determined 72 h later using the CellTiter 96 AQ_{ueous} One Solution Cell Proliferation Assay (Promega). Absorbance at 570 nm (A₅₇₀) measured was normalized to percentage of control (untreated) and plotted against logarithmic conversions of compound concentrations using Prism 5.0 (GraphPad Software). The log (inhibitor) vs. response curve with variable slope was generated from triplicates of data to calculate EC₅₀ values with Prism 5.0.

MTT test with the L-929 mouse fibroblasts: Growth inhibitory activity on L-929 mouse fibroblasts were determined after incubation with serial dilutions of the compounds for 5 d using an MTT assay.^[27,28] The IC₅₀ was estimated from the concentration dependent activity curves.

Acknowledgements

Financial support by the Deutsche Forschungsgemeinschaft, an NIH (grant AI073155) and the Fonds der Chemischen Industrie is gratefully acknowledged. We thank Dr. Dorothee Wistuba (Institute of Organic Chemistry, Tübingen) for measuring the HRMS spectra. In addition, we acknowledge help with chiral separations from Dr. Silvia Marten, Head of Applications and Columns Department, Knauer GmbH, Berlin, Germany. Furthermore, we would like to thank Wera Collisi (HZI Braunschweig) for excellent technical assistance with cytotoxicity assays.

- [1] *depsi*” comes from the Greek word, *depsidi*, which refers to an ester.
- [2] S. Deechongkit, S.-L. You, J. W. Kelly, *Org. Lett.* **2004**, *6*, 497–500.
- [3] For a recent review, see: G. S. Bagavananthem Andavan, R. Lemmens-Gruber, *Mar. Drugs* **2010**, *8*, 810–834.
- [4] For some reviews, see: a) M. R. Arkin, J. A. Wells, *Nat. Rev. Drug Discovery* **2004**, *3*, 301–317; b) A. Lorigian, G. Palu, *J. Cell. Physiol.* **2005**, *204*, 750–762; c) D. C. Fry, *Biopolymers* **2006**, *84*, 535–552; d) S. Patel, M. R. Player, *Expert Opin. Invest. Drugs* **2008**, *17*, 1865–1882; e) S. N. Haydar, H. Yun, R. G. W. Staal, W. D. Hirst, *Annu. Rep. Med. Chem.* **2009**, *44*, 51–69.
- [5] P. Crews, L. V. Manes, M. Boehler, *Tetrahedron Lett.* **1986**, *27*, 2797–2800.
- [6] T. M. Zabriskie, J. A. Klocke, C. M. Ireland, A. H. Marcus, T. F. Molinski, D. J. Faulkner, C. Xu, J. C. Clardy, *J. Am. Chem. Soc.* **1986**, *108*, 3123–3124.
- [7] a) A. Zampella, C. Giannini, C. Debitus, C. Roussakis, M. V. D'Auria, *J. Nat. Prod.* **1999**, *62*, 332–334; b) F. Gala, M. V. D'Auria, S. De Marino, F. Zollo, C. D. Smith, J. E. Copper, A. Zampella, *Tetrahedron* **2007**, *63*, 5212–5219; c) F. Gala, M. V. D'Auria, S. De Marino, V. Sepe, F. Zollo, C. D. Smith, J. E. Copper, A. Zampella, *Tetrahedron* **2008**, *64*, 7127–7130; d) F. Gala, M. V. D'Auria, S. De Marino, V. Sepe, F. Zollo, C. D. Smith, S. N. Keller, A. Zampella, *Tetrahedron* **2009**, *65*, 51–56.
- [8] a) S. J. Robinson, B. I. Morinaka, T. Amagata, K. Tenney, W. M. Bray, N. C. Gassner, R. S. Lokey, P. Crews, *J. Med. Chem.* **2010**, *53*,

- 1651–1661; b) K. R. Watts, B. I. Morinaka, T. Amagata, S. J. Robinson, K. Tenney, W. M. Bray, N. C. Gassner, R. S. Lokey, J. Media, F. A. Valeriotte, P. Crews, *J. Nat. Prod.* **2011**, *74*, 341–351.
- [9] a) B. Kunze, R. Jansen, F. Sasse, G. Höfle, H. Reichenbach, *J. Antibiot.* **1995**, *48*, 1262–1266; b) R. Jansen, B. Kunze, H. Reichenbach, G. Höfle, *Liebigs Ann.* **1996**, 285–290.
- [10] a) P. A. Grieco, Y. S. Hon, A. Perez-Medrano, *J. Am. Chem. Soc.* **1988**, *110*, 1630–1631; b) K. S. Chu, G. R. Negrete, J. P. Konopelski, *J. Org. Chem.* **1991**, *56*, 5196–5201; c) A. V. Rama Rao, M. K. Gurjar, B. R. Nallaganachu, A. Bhandari, *Tetrahedron Lett.* **1993**, *34*, 7085–7088; d) Y. Hirai, K. Yokota, T. Momose, *Heterocycles* **1994**, *39*, 603–612; e) P. Ashworth, B. Broadbelt, P. Jankowski, P. Kocienski, A. Pimm, R. Bell, *Synthesis* **1995**, 199–206; f) A. K. Ghosh, D. K. Moon, *Org. Lett.* **2007**, *9*, 2425–2427; g) R. Tannert, T.-S. Hu, H.-D. Arndt, H. Waldmann, *Chem. Commun.* **2009**, 1493–1495.
- [11] a) S. Terracciano, I. Bruno, G. Bifulco, J. E. Copper, C. D. Smith, L. G. Paloma, R. Riccio, *J. Nat. Prod.* **2004**, *67*, 1325–1331; b) S. Terracciano, I. Bruno, G. Bifulco, E. Avallone, C. D. Smith, L. Gomez-Paloma, R. Riccio, *Bioorg. Med. Chem.* **2005**, *13*, 5225–5239; c) S. Marimganti, S. Yasmeen, D. Fischer, M. E. Maier, *Chem. Eur. J.* **2005**, *11*, 6687–6700; d) T.-S. Hu, R. Tannert, H.-D. Arndt, H. Waldmann, *Chem. Commun.* **2007**, 3942–3944; e) S. Terracciano, I. Bruno, E. D'Amico, G. Bifulco, A. Zampella, V. Sepe, C. D. Smith, R. Riccio, *Bioorg. Med. Chem.* **2008**, *16*, 6580–6588.
- [12] R. Tannert, L.-G. Milroy, B. Ellinger, T.-S. Hu, H.-D. Arndt, H. Waldmann, *J. Am. Chem. Soc.* **2010**, *132*, 3063–3077.
- [13] H. Waldmann, T.-S. Hu, S. Renner, S. Menninger, R. Tannert, T. Oda, H.-D. Arndt, *Angew. Chem.* **2008**, *120*, 6573–6577; *Angew. Chem. Int. Ed.* **2008**, *47*, 6473–6477; Corrigendum: H. Waldmann, T.-S. Hu, S. Renner, S. Menninger, R. Tannert, T. Oda, H.-D. Arndt, *Angew. Chem.* **2009**, *121*, 1554; *Angew. Chem. Int. Ed.* **2009**, *48*, 1526.
- [14] U. Eggert, R. Diestel, F. Sasse, R. Jansen, B. Kunze, M. Kalesse, *Angew. Chem.* **2008**, *120*, 6578–6582; *Angew. Chem. Int. Ed.* **2008**, *47*, 6478–6482.
- [15] A. Schmauder, S. Müller, M. E. Maier, *Tetrahedron* **2008**, *64*, 6263–6269.
- [16] A. Schmauder, L. D. Sibley, M. E. Maier, *Chem. Eur. J.* **2010**, *16*, 4328–4336.
- [17] For recent reviews, see: a) R. Dembinski, *Eur. J. Org. Chem.* **2004**, 2763–2772; b) K. C. K. Swamy, N. N. B. Kumar, E. Balaraman, K. V. P. P. Kumar, *Chem. Rev.* **2009**, *109*, 2551–2651.
- [18] M. R. Bubba, A. M. Senderowicz, E. A. Sausville, K. L. Duncan, E. D. Korn, *J. Biol. Chem.* **1994**, *269*, 14869–14871.
- [19] T. Oda, M. Iwasa, T. Aihara, Y. Maeda, A. Narita, *Nature* **2009**, *457*, 441–445.
- [20] R. Bai, D. G. Covell, C. Liu, A. K. Ghosh, E. Hamel, *J. Biol. Chem.* **2002**, *277*, 32165–32171.
- [21] a) E. Diekmann, K. Friedrich, J. Lehmann, *Liebigs Ann. Chem.* **1989**, 1247–1250; b) R. W. Lang, H. J. Hansen, *Org. Synth.* **1984**, *62*, 202–209; *Org. Synth. Coll. Vol.* **1990**, *7*, 232–236.
- [22] A. H. M. de Vries, J. M. C. A. Mulders, J. H. M. Mommers, H. J. W. Henderickx, J. G. de Vries, *Org. Lett.* **2003**, *5*, 3285–3288.
- [23] a) H. C. Kolb, M. S. VanNieuwenhze, K. B. Sharpless, *Chem. Rev.* **1994**, *94*, 2483–2547; b) N. J. Lawrence, S. Brown, *Tetrahedron* **2002**, *58*, 613–619; c) P. Liu, W. He, Y. Zhao, P.-A. Wang, X.-L. Sun, X.-Y. Li, S.-Y. Zhang, *Chirality* **2008**, *20*, 75–83.
- [24] S. Y. Ko, *J. Org. Chem.* **2002**, *67*, 2689–2691.
- [25] Y. Hirai, K. Yokota, T. Momose, *Heterocycles* **1994**, *39*, 603–612.
- [26] Z. Zhang, Z. Wang, *J. Org. Chem.* **2006**, *71*, 7485–7487.
- [27] C. A. Staton, S. M. Stribbling, S. Tazzyman, R. Hughes, N. J. Brown, C. E. Lewis, *Int. J. Exp. Pathol.* **2004**, *85*, 233–248 and references therein.
- [28] V. V. Vintonyak, M. Calà, F. Lay, B. Kunze, F. Sasse, M. E. Maier, *Chem. Eur. J.* **2008**, *14*, 3709–3720.

Received: June 27, 2011
Published online: October 20, 2011

Paper 2

For the Section 6.3.1.

Coordination Chemistry of Gold

DOI: 10.1002/chem.201201215

Coordination Chemistry of Gold Catalysts in Solution: A Detailed NMR Study

Alexander Zhdanko,^[a] Markus Ströbele,^[b] and Martin E. Maier*^[a]

Abstract: Coordination chemistry of gold catalysts bearing eight different ligands [L = PPh₃, JohnPhos (L2), Xphos (L3), DTBP, IMes, IPr, dppf, S-tolBINAP (L8)] has been studied by NMR spectroscopy in solution at room temperature. Cationic or neutral mononuclear complexes LAuX (L = L2, L3, IMes, IPr; X = charged or neutral ligand) underwent simple ligand exchange without giving any higher coordinate complexes. For L2AuX the following ligand strength series was determined: MeOH ≪ hex-3-yne < MeCN ≈ OTf⁻ ≪ Me₂S < 2,6-lutidine < 4-picoline < CF₃CO₂⁻ ≈ DMAP < TMTU < PPh₃ < OH⁻ ≈ Cl⁻. Some heteroligand complexes DTBPAuX exist in solution in equilibrium with the corresponding symmetrical species. Binuclear com-

plexes dppf(AuOTf)₂ and S-tolBINAP(AuOTf)₂ showed different behavior in exchange reactions with ligands depending on the ligand strength. Thus, PPh₃ causes abstraction of one gold atom to give mononuclear complexes LLAuPPh₃⁺ and (Ph₃P)_nAu⁺, but other N and S ligands give ordinary dicationic species LL(AuNu)₂²⁺. In reactions with different bases, LAu⁺ provided new oxonium ions whose chemistry was also studied: (DTBPAu)₃O⁺, (L2Au)₂OH⁺, (L2Au)₃O⁺, (L3Au)₂OH⁺, and (IMesAu)₂OH⁺. Ultimately, formation of gold hydroxide

LAuOH (L = L2, L3, IMes) was studied. Ligand- or base-assisted interconversions between (L2Au)₂OH⁺, (L2Au)₃O⁺, and L2AuOH are described. Reactions of dppf(AuOTf)₂ and S-tolBINAP(AuOTf)₂ with bases provided more interesting oxonium ions, whose molecular composition was found to be [dppf(Au)₂]₃O₂²⁺, L8(Au)₂OH⁺, and [L8(Au)₂]₃O₂²⁺, but their exact structure was not established. Several reactions between different oxonium species were conducted to observe mixed heteroligand oxonium species. Reaction of L2AuNCMe⁺ with S²⁻ was studied; several new complexes with sulfide are described. For many reversible reactions the corresponding equilibrium constants were determined.

Keywords: gold • ligand effects • ligand exchange • NMR spectroscopy • oxonium ions

Introduction

Gold catalysis has emerged as an extensive area of research that continues to evolve very rapidly today.^[1] However, while the arsenal of synthetic methods available to an organic chemist benefited enormously from gold catalysis, knowledge about the mechanism of the corresponding transformations remains more limited, and this area has just begun to emerge as a major topic in gold catalysis.^[2] Indeed, most papers dealing with gold-catalyzed reactions confine themselves to “proposed” mechanisms, without going into deep experimental mechanistic investigation and characteri-

zation of the gold intermediates. Often, instead of experimental elucidation of mechanisms, computational investigations are conducted to support the mechanism.^[3]

Although general coordination chemistry of gold as a subject of inorganic chemistry has been investigated with a broad range of ligands, the coordination chemistry of gold compounds that are used nowadays as catalysts in organic transformations is largely unexplored.^[4] This actually is not too surprising, since many of them appeared after 2000.^[5] Here we present our pure coordination-chemistry investigations, which were conducted in parallel with our mechanistic studies.

The present paper describes reactions of gold complexes of the types LAuX and LAuNu⁺, where L is a strong, base or parent ligand, respectively, X is a negatively charged group in neutral complexes and Nu is a neutral weaker ligand in cationic complexes.^[6] Abbreviations, widely adopted in the text, are clear from the starting materials depicted in Figure 1. Almost all reactions were conducted in deuterated solvents (CDCl₃, C₆D₆, [D₈]THF (used pure or as a 15 vol% mixture with simple THF), CD₂Cl₂, MeOD) and were directly monitored by ¹H and ³¹P NMR spectroscopy at room temperature. Most of the reactions were conducted as NMR titrations, which allowed us to get the necessary information from changes observed in the spectra. We classify all

[a] Dipl.-Chem. A. Zhdanko, Prof. Dr. M. E. Maier
Institut für Organische Chemie
Universität Tübingen
Auf der Morgenstelle 18, 72076 Tübingen (Germany)
Fax: (+49) 7071-295137
E-mail: martin.e.maier@uni-tuebingen.de

[b] Dr. M. Ströbele
Institut für Anorganische Chemie
Universität Tübingen
Auf der Morgenstelle 18, 72076 Tübingen (Germany)
Fax: (+49) 7071-295702

Supporting information for this article is available on the WWW under <http://dx.doi.org/10.1002/chem.201201215>.

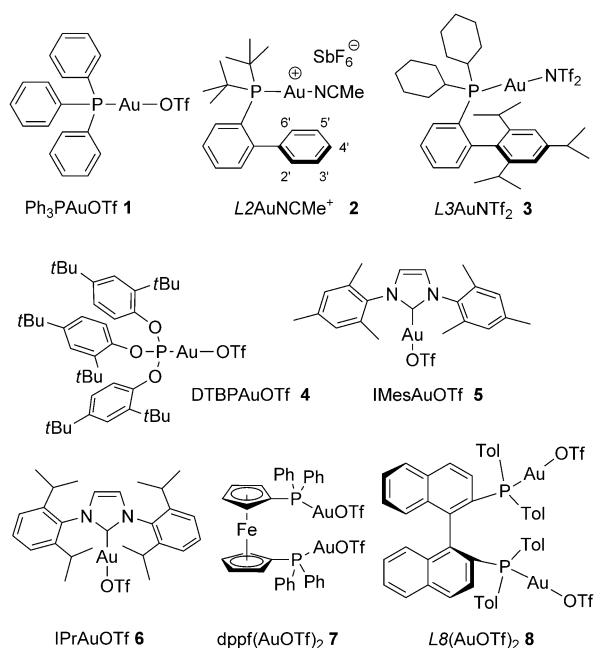


Figure 1. Structures of gold complexes together with ligand abbreviations used in the text.

homoligand exchanges $LAuNu^+/Nu$ as “fast” if Nu gives a single set of broadened signals, and as “slow” if bound and free Nu give clear or broadened separate signals. Complexes **1** and **4–8** were prepared by reaction of the corresponding chlorides with silver triflate.

Results and Discussion

Simple ligand exchange chemistry of gold catalysts: It has long been known that Ph_3PAu^+ (with weakly or noncoordinating anions) reacts with PPh_3 to provide mixtures of higher coordinate complexes $(Ph_3P)_nAu^+$ ($n=2-4$). However, individual components of the equilibria [Figure 2, Eqs. (2), (3)] could not be observed by NMR spectroscopy at room temperature because of fast exchange. The system simply gives one broadened phosphorus resonance averaged for all species.^[7] We reproduced this situation and describe it with detailed spectra in the Supporting Information. Since many of Ph_3PAu -containing complexes had been previously described, we largely focused on new species derived from other ligands. The following known species were considered of relevance for this study: Ph_3PAuNu^+ ($Nu = Me_2S$,^[8] 2,6-lutidine,^[9] 2,6-di-*tert*-butylpyridine, NMe_3 ,^[10] PPh_3), $Ph_3PAuN(SiMe_3)_2$ ^[11] and $(Ph_3PAu)_3O^+$.^[12]

Initially, we studied the reaction of $L2AuNCMe^+SbF_6^-$ (**2**) with different ligands: MeOH, hex-3-yne, Me_2S , 2,6-lutidine, 4-picoline, DMAP, TMTU, PPh_3 and Cy_3P in $CDCl_3$. All ligands except MeOH and hex-3-yne stoichiometrically substituted acetonitrile from **2** to give 1:1 products whose composition was established as $L2AuNu^+SbF_6^-$ [Figure 2, Eq. (4)], and in all these cases, before the equivalence point,

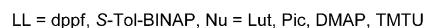
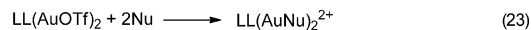
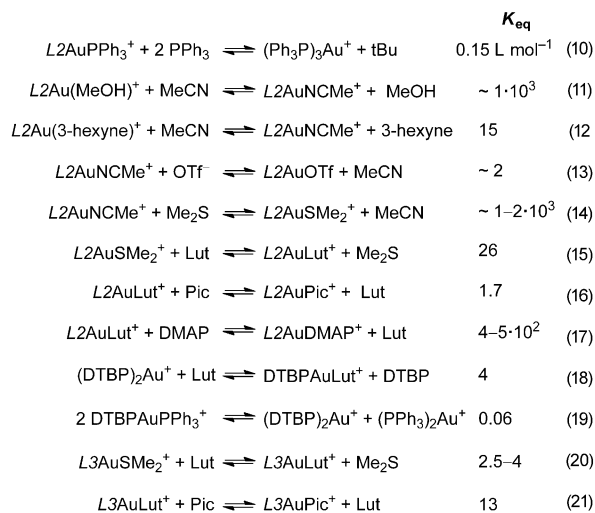
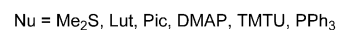
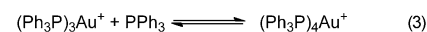
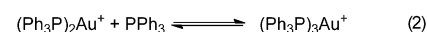
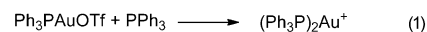
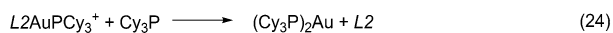


Figure 2. Equations (1)–(23) for the reactions of gold(I) complexes with nucleophiles; Lut = 2,6-lutidine, Pic = 4-picoline, DMAP = 4-dimethylaminopyridine, TMTU = tetramethylthiourea.

MeCN gave a single broad resonance, indicating fast ligand exchange in the $L2AuNCMe^+/MeCN$ system. After the equivalence point, MeCN became completely free, giving the normal sharp signal at 2.00 ppm in the 1H NMR spectrum. For example, in the reaction of **2** with PPh_3 the corresponding heteroligand complex $L2AuPPh_3^+$ was formed as sole product, giving two doublets in the ^{31}P NMR spectrum due to P–P coupling. As a characteristic feature of the 1H NMR spectrum, the protons at the 3',5'- and 4'-positions of the biphenyl ring are significantly shifted upfield, presumably due to the influence of the inductive currents in the triphenylphosphine rings situated in close proximity. Beyond the equivalence point gradual substitution of the $L2$ ligand started to occur. Experimentally we found also that this process can be better described as Equation (10) in Figure 2, with an equilibrium constant of approximately 0.15 L mol^{-1} . This demonstrates much higher preference of $L2$ versus the PPh_3 ligand for gold. Even 17.5 equiv PPh_3 were able to substitute only one-half of $L2$. Formation of stable $L2AuPPh_3^+$

heteroligand complex in solution was confirmed also by ESI HRMS analysis, while the presence of higher coordinate $L2Au(PPh_3)_2^+$ could not be confirmed. The absence of $L2Au(PPh_3)_2^+$ was also evident from the NMR spectra. Thus, if any appreciable amount thereof was formed in solution, it would either give new signals or shift the $L2AuPPh_3^+$ signals due to the dynamic equilibrium that would be established. However, even in the presence of such a large excess of PPh_3 , the resonances of $L2AuPPh_3^+$ broadened only slightly and appeared at constant chemical shift, which also points to a “slow” mode of exchange in the $L2AuPPh_3^+/PPh_3$ system. The significant kinetic stability of the $L2AuPPh_3^+$ complex is in sharp contrast to the behavior of the corresponding triphenylphosphine analogue $(Ph_3P)_2Au^+$ and must be a consequence of increased steric hindrance of the $L2$ ligand. If liberated, the free $L2$ ligand also gave a sharp constant resonance, while an excess of PPh_3 gave a broadened resonance due to fast exchange with the partially liberated gold in the classical $(Ph_3P)_nAu^+/Ph_3P$ dynamic system [Figure 2, Eqs. (2) and (3)].

Similarly, in the reaction with Cy_3P , formation of the corresponding $L2AuPCy_3^+$ occurred, which in the presence of excess Cy_3P readily underwent substitution of $L2$ from gold to give $(Cy_3P)_2Au^+$ [Eq. (24)].



Other $L2AuNu^+$ complexes with $Nu=Me_2S$, Lut, Pic, DMAP, and TMTU were readily obtained by reaction of **2** with the corresponding ligand; they all were completely stable in the presence of excess of ligand, giving neither higher coordinate complexes nor liberating the original phosphine ligand. For $Nu=Me_2S$, Lut, Pic, DMAP, and TMTU, fast ligand exchange between $L2AuNu^+$ and Nu was observed, but for $Nu=Lut$, remarkably, both free and bound forms gave separate clear resonances indicating a “slow” mode of ligand exchange, which is probably a consequence of increased steric bulk of this ligand.

Reactions of **2** with MeOH and hex-3-yne in $CDCl_3$ did not reveal stoichiometric substitution of MeCN, that is, the resulting complexes would be weaker than the starting one. We determined that MeOH is a weaker ligand than hex-3-yne, and both are weaker than MeCN [Figure 2, Eqs. (11) and (12)]. The complex with methanol is so weak that only in pure MeOD solution (≈ 7000 equiv) does it exist as predominant form over acetonitrile. Complexes of **2** with several alkynes and alkenes were recently studied by Widenhofer et al., and hex-3-yne exhibited the strongest binding among a range of several alkynes and alkenes.^[13] Therefore, it can be taken as a general rule for gold catalysis that binding of a cationic gold catalyst to a $C=C$ or $C\equiv C$ bond of a substrate would be generally weaker than with acetonitrile by a factor of 10–100. This provides a ready explanation why acetonitrile is often not a preferable solvent for a gold(I)-catalyzed reaction: obviously, it would seriously compete with an alkyne substrate for the gold center, slowing down the overall process.^[14]

Since gold catalysts are often prepared and used as triflates or trifluoroacetates, it was of interest to compare their binding abilities. For this purpose we prepared $L2AuOTf$ and $L2AuOTFA$ and found that OTf^- as a ligand is bound to gold slightly more strongly than MeCN [Figure 2, Eq. (13)], but more weakly than Me_2S . The OTFA salt was found to be quite strong, comparable to the complex with DMAP. This finding directly correlates with efficacy of catalysis: while triflates still provide fast reactions, the trifluoroacetates are in fact very sluggish catalysts. However, although binding of a catalyst to a substrate is important, it is not the only factor determining the efficacy of gold catalysis.

Similar studies using Me_2S , 2,6-lutidine, 4-picoline, DMAP, TMTU, and PPh_3 in $CDCl_3$ were conducted with $L3AuNTf_2$ (**3**), which displayed exactly the same properties [Figure 2, Eq. (5)]. The corresponding heteroligand complex $L3AuPPh_3^+$ was formed as a sole product with triphenylphosphine, and beyond the equivalence point gradual substitution of the $L3$ ligand started to occur. As in the case of $L2$, $L3$ proved to be a much better ligand for gold than PPh_3 , comparable to $L2$, but the equilibrium constant could not be found due to signal overlaps. With $Nu=Me_2S$, Lut, Pic, DMAP, and TMTU the corresponding complexes $L3AuNu^+$ were formed, which revealed fast $L3AuNu^+/Nu$ ligand exchange for $Nu=Me_2S$, DMAP, and TMTU and slow ligand exchange for $Nu=Lut$ and Pic. Ligand exchange in $L3AuNu^+/Nu$ was always slower than in $L2AuNu^+/Nu$, as was evident from the line shapes, and this can be regarded as a consequence of increased steric hindrance of the $L3$ ligand in comparison to $L2$.

Then we studied reactions of $DTBPAuOTf$ (**4**) having a phosphite ligand, which revealed several unexpected differences from the chemistry described above. First, **4** was found to give a heteroligand complex $DTBPAuPPh_3^+$, which does not exist in individual state but undergoes reversible ligand metathesis to $(Ph_3P)_2Au^+$ and $(DTBP)_2Au^+$, so that all three species are simultaneously observed in solution. The equilibrium constant was estimated to be $K_{eq} \approx 0.06$ [Figure 2, Eq. (19)]. On further addition of PPh_3 , DTBP is completely displaced from gold to give $(Ph_3P)_2Au^+$ as a sole product. During this process higher coordinate species $(DTBP)_2AuPPh_3^+$ and $DTBPAu(PPh_3)_2^+$ were not detected. The homoligand complex $(DTBP)_2Au^+$ was generated in the reaction between **4** and DTBP and revealed slow ligand exchange in the presence of excess DTBP. Here again, no higher coordinate $(DTBP)_nAu^+$ ($n > 2$) complexes were detected. One of the phosphite ligands in $(DTBP)_2Au^+$ is bound rather weakly: it is already substituted by 2,6-lutidine with an equilibrium constant $K_{eq} \approx 4$ [Figure 2, Eq. (18)]. We believe that such weak binding is a consequence of both high steric hindrance and weak donor ability of the DTBP ligand. Rather in contrast with the previous chemistry, complex **4** reacts with Me_2S and TMTU to give no clear picture of what is really happening in solution. In the case of Me_2S a complex dynamic mixture of $DTBPAuSM_2^+$, $(DTBP)_2Au^+$, and $(Me_2S)_{n=1,2}Au^+$ is formed due to ligand exchange [Figure 2, Eq. (8)]. In contrast, lutidine reacted

cleanly to give DTBPAuLut⁺ as a single product undergoing fast DTBPAuLut⁺/Lut exchange [Figure 2, Eq. (9)].

Next, IMesAuOTf (5) was treated with PPh₃ to give the expected IMesAuPPh₃⁺, which beyond the equivalence point displayed fast exchange with PPh₃. No other compounds were formed, that is, IMesAuPPh₃⁺/PPh₃ continues to be a simple binary system with PPh₃ exchange as the only process, which is not surprising, since N-heterocyclic carbene (NHC) cannot be easily substituted by a phosphine. With other ligands Nu=Lut, Pic the corresponding complexes IMesAuNu⁺ were formed, and both revealed slow IMesAuNu⁺/Nu ligand exchange [Figure 2, Eq. (6)]. Another similar NHC carbene complex, namely, IPrAuOTf (6), displayed exactly the same chemistry as 5. Ligand exchange in the IMesAuNu⁺/Nu system was found to be fast only for Nu=Me₂S and slow for other cases [Nu=Lut, Pic, DMAP, TMTU, PPh₃; Figure 2, Eq. (7)].

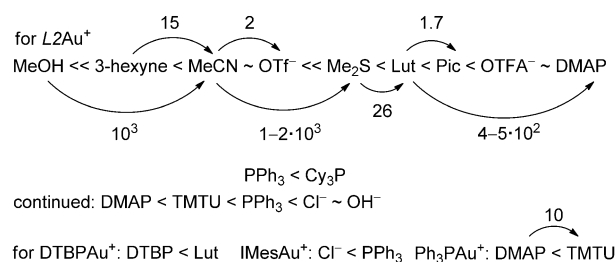
Further, we studied ligand-exchange chemistry of two binuclear complexes of gold. For example, when dppf(AuCl)₂ was titrated with PPh₃, the system displayed dynamic behavior with single sets of broad signals for dppf and PPh₃, but at some point sharp signals for the dppf unit were observed, together with broad signals for PPh₃ (in both ¹H and ³¹P NMR spectra), indicating formation of a single dppf complex. This can be either dppfAuCl or [dppfAuPPh₃]⁺Cl⁻. Complex dppfAuCl was previously described and its spectra did not match those observed by us, so we suppose [dppfAuPPh₃]⁺Cl⁻ could be formed in our case. The complex [dppfAuPPh₃]⁺ was previously described as the perchlorate salt and its spectra matched those observed by us pretty well.^[15]

When dppf(AuOTf)₂ (7) was titrated with PPh₃, the early-stage spectra were complicated, indicating formation of a multicomponent mixture. However already at three equivalents of PPh₃, sharp signals for the dppf unit arose, together with broad signals for PPh₃ (in both ¹H and ³¹P NMR spectra), indicating formation of a single dppf complex. Similar properties were displayed by another binuclear complex, namely, L8(AuOTf)₂ (8). The observed behavior was clear from the NMR spectra and additionally supported by ESI MS. The observations were consistent with complete abstraction of one gold atom from the initial complex and formation of mononuclear complexes LLAuPPh₃⁺ and (Ph₃P)_nAu⁺ [Figure 2, Eq. (22)]. In case of dppfAuPPh₃⁺ the spectra matched those reported in the literature.^[15] All sharp signals (in both ¹H and ³¹P NMR spectra) were assigned to the LL unit of LLAuPPh₃⁺, and broad, time-averaged signals were assigned to a PPh₃ unit which experiences fast exchange between all the species. This also causes the phosphorus resonance of LL to appear as a singlet rather than a doublet. Formation of free LL was not observed with an excess of PPh₃, that is, while abstraction of one gold cation from the initial dicationic complex was easy, abstraction of the second gold ion is rather difficult. This might be explained by a cooperative action of both phosphorus atoms rather than the nature of each of them. Such an interaction

might be described as a chelate or fast jumping of gold between the two phosphorus atoms.

In contrast to PPh₃, reactions with weaker N and S ligands revealed formation of the corresponding dicationic complexes dppf(AuTMTU)₂²⁺, dppf(AuLut)₂²⁺, L8(AuLut)₂²⁺, L8(AuPic)₂²⁺, L8(AuDMAP)₂²⁺, and L8(AuTMTU)₂²⁺, without any sign of gold abstraction [Figure 2, Eq. (23)]. Interestingly, the complexes with TMTU were slightly reactive in the presence of excess TMTU, and this suggests a further reversible unidentified process but with the equilibrium shifted to the left.

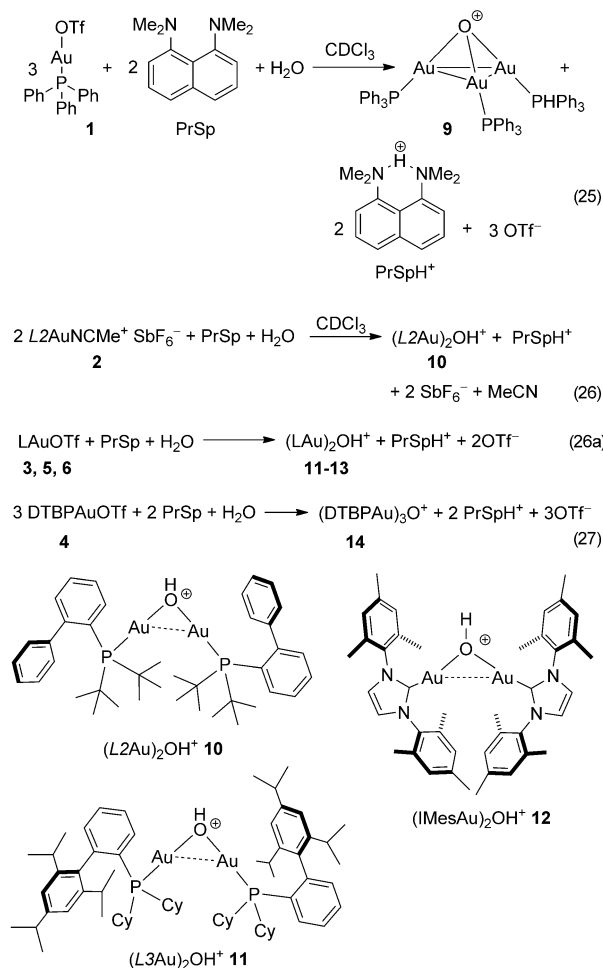
As a result of this study, the following ligand strength series was established, with some key *K*_{eq} values indicated (Scheme 1). Conveniently, the ligands before OTf⁻ can be



Scheme 1. Ligand strength series for cationic gold complexes with some key *K*_{eq} values.

regarded as weak, from Me₂S till TMTU as moderately strong and beyond PPh₃ very strong. The range of binding affinities from MeOH till DMAP spans approximately ten orders of magnitude. During further research we were able to determine indirectly the equilibrium constant for DMAP/TMTU exchange at Ph₃PAu⁺, which appears to be 10 in favor of TMTU. Unfortunately, it was not possible to quantitatively determine the difference in binding affinities for TMTU/PPh₃, but we suppose this may reach several (2–4) orders of magnitude.

Reaction of gold catalysts with bases: formation of LAuOH and oxonium species and their transformations: It has long been known that Ph₃PAu⁺ reacts with base and water to give triaurated oxonium salts (Ph₃PAu)₃O⁺ (9) stable in solution and in the solid state.^[12] Indeed, when proton sponge (PrSp) was added to a freshly prepared solution of Ph₃PAuOTf (1) in CDCl₃, a fast and quantitative reaction with traces of water (naturally contained in CDCl₃) occurred to give (Ph₃PAu)₃O⁺ as the sole product [Scheme 2, Eq. (25)]. Before the equivalence point, ³¹P NMR showed a single broadened resonance indicating fast exchange in the Ph₃PAuOTf/(Ph₃PAu)₃O⁺ system. In sharp contrast, 2 reacted with proton sponge to give diaurated oxonium ion (L2Au)₂OH⁺ (10) as a single product together with the proton sponge salt (PrSpH⁺) [Scheme 2, Eq. (26)]. Its proton spectrum exhibits a characteristic triplet at -0.42 ppm (²J_{H,P}=1.7 Hz) corresponding to a single OH proton. The stoichiometry of the whole reaction was deter-

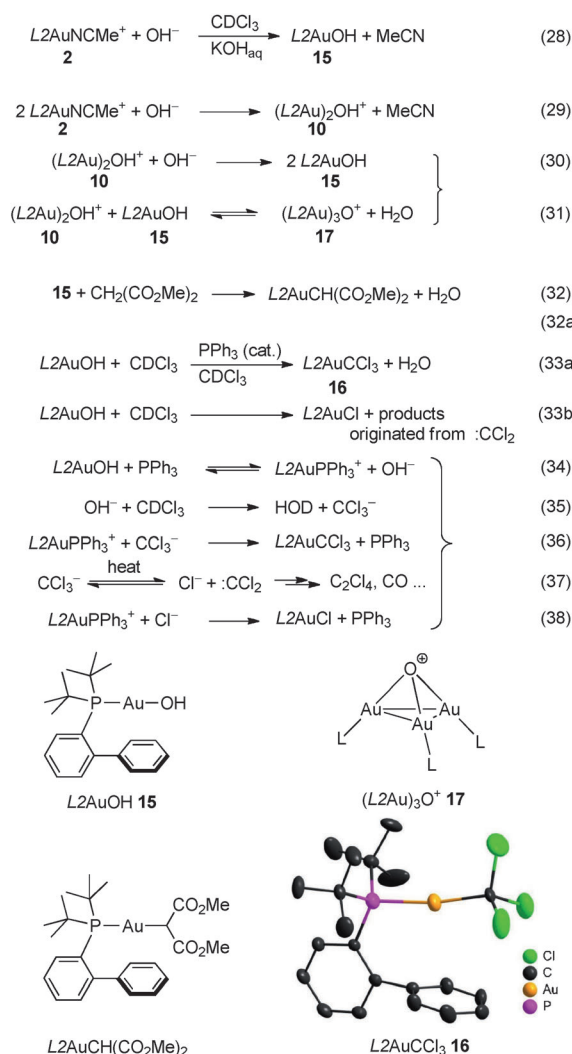


Scheme 2. Reactions of gold complexes with proton sponge.

mined by integration, which showed that 1 mol of **10** is generated together with 1 mol of proton sponge salt. Observation of a single resonance in the ^{31}P NMR and a triplet for OH suggests a symmetrical structure for this cation with two equal Au–O interactions, possibly stabilized by a single aurophilic interaction. Other diaurated oxonium ions $(\text{LAu})_2\text{OH}^+$ were obtained also with ligands $\text{L} = \text{L}_3$ (**11**), IMes (**12**), IPr (**13**) as sole products of reactions of **3**, **5**, and **6** with proton sponge according to Equation (26a) in Scheme 2. However, DTBPAuOTf (**4**) reacted with proton sponge to give triaurated oxonium ion $(\text{DTBPAu})_3\text{O}^+$ (**14**) [Scheme 2, Eq. (27)]. Proof of the molecular composition of oxonium ions obtained by these reactions comes not only from the presence or absence of OH protons, but simply from reaction stoichiometry, easily established by integration of relevant peaks in their spectra. $(\text{IPrAu})_2\text{OH}^+$ (**13**) was previously described by Nolan et al. in 2010 and until now was the only known example of diaurated oxonium ions.^[16] According to Nolan et al., the X-ray structure of **13** contained Au...Au interactions somewhat longer than it would be expected for aurophilic interactions. Therefore, it is doubtful whether they contribute to the stability of this type of structures in our case.

The cation $(\text{L}_2\text{Au})_2\text{OH}^+$ (**10**) can also be generated with other bases. For example, even 2,6-di-*tert*-butylpyridine reacts with **2** to give **10**, but the reaction is reversible: two equivalents of the base are able to transform only half of the starting complex. Solid LiOH, and even simple water extraction, trigger quantitative formation of **10**, but when a solution of **2** in CDCl_3 is treated with 10% aqueous KOH, fast reaction occurs to give L_2AuOH **15** as sole product [Scheme 3, Eq. (28)]. Its proton spectrum exhibits a characteristic broad singlet at -0.73 to -0.76 ppm corresponding to the OH proton. The exact chemical shift of the proton is slightly affected by the presence of water, which forms strong hydrogen bonds and causes exchange of the protons, so that no coupling to phosphorus is observable.^[17] Indeed, in an extra-dry solution of **15** in C_6D_6 (above solid KOH) the OH proton could be observed as a doublet at -0.20 ppm ($^3J_{\text{H-P}} = 4.8$ Hz), and the doublet was also nicely observed in the NMR spectrum of **15** in C_6D_6 layered above saturated aqueous KOH solution.

Complex L_2AuOH (**15**) is an example of a gold hydroxide, a new class of gold complexes. Currently, only a single

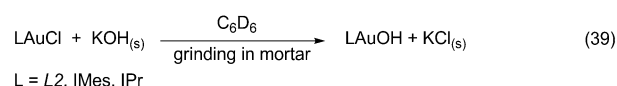


Scheme 3. Formation of gold hydroxide and its transformations.

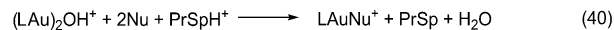
example is known in the literature. In 2010 Nolan described IPrAuOH and studied the chemistry of this compound, which exhibited strongly basic properties.^[2e,18] In complete accordance with expectations, $L2\text{AuOH}$ appeared to be a strong base as well. It readily reacted with dimethyl malonate to give $L2\text{AuCH}(\text{CO}_2\text{Me})_2$ [Scheme 3, Eq. (32)]. In CDCl_3 solution $L2\text{AuOH}$ slowly reacts with the solvent (over many hours at room temperature), but the reaction can be strongly accelerated by PPh_3 [Scheme 3, Eqs. (33a) and (33b)]. Thus, when a catalytic amount of PPh_3 ($\approx 1\text{--}5\%$) was added to a solution of $L2\text{AuOH}$ in CDCl_3 and the solution concentrated in vacuo, the residue already contained only the products of the reaction. Normally, a mixture of $L2\text{AuCl}$ and $L2\text{AuCCl}_3$ (**16**) is formed. The chloride ion in $L2\text{AuCl}$ must come from CDCl_3 [Scheme 3, Eq. (37)]. We found that the ratio of the products can be controlled by temperature. Thus, when evaporation of the reaction mixture was conducted below room temperature, **16** could be obtained as a main product ($\approx 95\%$), only slightly contaminated with $L2\text{AuCl}$, while formation of $L2\text{AuCl}$ is favored at higher temperature. Interestingly, **16** has exactly the same phosphorus chemical shift as **10** and $L2\text{AuDMAP}^+$ (57.43 ppm) in CDCl_3 solution, but the proton spectra differ sufficiently to allow differentiation. Unfortunately, a ^{13}C spectrum did not prove the presence of the CCl_3 residue. However the structure was unambiguously established by X-ray analysis (Scheme 3). The catalytic action of PPh_3 in this reaction is explained by its enhancing dissociation of $L2\text{AuOH}$, to provide OH^- , which is very reactive in organic solution due to lack of solvation and should deprotonate chloroform more readily [Scheme 3, Eq. (34) and (35)]. Control experiments in C_6D_6 revealed that PPh_3 is unable to stoichiometrically displace OH^- from gold (even in excess) and the reaction is thus highly reversible [Scheme 3, Eq. (34)]. Another test performed on **15** with TMTU indicated no sign of any exchange even if TMTU was present in excess. Rather, prolonged warming of the reaction mixture caused hydrolysis of TMTU to give $(\text{Me}_2\text{N})_2\text{CO}$ and some complexes with sulfur. These results might seem surprising, given the general low oxophilicity of gold, but on the other hand OH^- is a highly nucleophilic ion whose elimination from a covalent compound like LAuOH is disfavored in the absence of good OH^- acceptors. Obviously, the OH of gold hydroxide has strong desire to interact with more suitable electrophiles, (e.g., with a proton). In other words, LAuOH can be viewed as soluble covalent organic analogue of KOH .

Since gold hydroxides are promising catalyst precursors activated by protonation and useful reagents for the synthesis of various organogold compounds,^[19] we turned our attention towards their improved synthesis. Thus, the previously described example IPrAuOH was synthesized by heating a solution of IPrAuCl in THF/toluene with solid KOH for 24 h, which is a rather long and harsh procedure but nevertheless gave the product in high yield. We were pleased to find that the analogous reaction of $L2\text{AuCl}$ with solid KOH occurred in less than 1 min at room temperature under me-

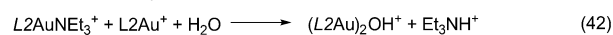
chanical stimulation. Thus, when a benzene solution of the starting gold complex was ground in a small mortar with solid KOH followed by simple filtration through Celite, a solution of about 95% pure product was obtained [Eq. (39)]. We were even more surprised when we found that this reaction occurs within 5 min at room temperature upon shaking a benzene solution of $L2\text{AuCl}$ with concentrated aqueous KOH . It appears that OH^- can displace Cl^- from gold even in solution, which was not previously recognized. In the same way, IPrAuOH and IMesAuOH were prepared as well. However the corresponding chlorides reacted more sluggishly than $L2\text{AuCl}$. Notably, neither of these methods was successful for the preparation of Ph_3PAuOH , whose existence has so far not been confirmed.



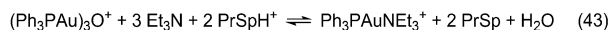
We further studied the chemistry of $(L2\text{Au})_2\text{OH}^+$ (**10**) and $L2\text{AuOH}$ (**15**). When a solution of **10**, generated by reaction of **2** with PrSp , was treated with another nucleophile (Nu), quantitative formation of $L2\text{AuNu}^+$ occurred [Eq. (40)]. Accordingly, PrSp is completely restored from the salt. This transformation is triggered already by Me_2S , which demonstrates high reactivity of **10** in the presence of a proton donor. In the absence of a proton donor, however, other pathways are followed (see below).



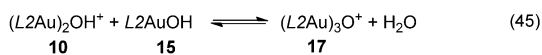
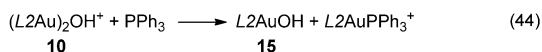
With regard to chemoselectivity, an interesting subject would be the reaction with simple amines, as they can act both as bases and ligands. To check this possibility, we conducted NMR titration of **2** with triethylamine. An interesting situation occurred before the equivalence point: $L2\text{AuNEt}_3^+$, **10**, and the remaining **2** were all simultaneously observed, together with the corresponding amount of Et_3NH^+ . Closer to the equivalence point, the amount of $(L2\text{Au})_2\text{OH}^+$ (**10**) and **2** decreased, while $L2\text{AuNEt}_3^+$ was formed as the major product. This situation can be described by Equations (41) and (42). Traces of $(L2\text{Au})_2\text{OH}^+$ were still detectable in the presence of 1.5 equivalents of Et_3N . This experiment demonstrated that initially some competition took place, but with increasing amount of Et_3N it reacted preferentially as a ligand and not a base.^[20] When TMTU was added to this solution, complete substitution of Et_3N occurred to give the $L2\text{AuTMTU}^+$ complex. In contrast, Lut, Pic, and DMAP reacted with **2** exclusively as ligands and not as bases, regardless of the molar ratios, as was described above [Figure 2, Eq. (4)].



Then we titrated a freshly prepared $(\text{Ph}_3\text{PAu})_3\text{O}^+$ (**9**)/ PrSpH^+ mixture with triethylamine and found that gradual formation of $\text{Ph}_3\text{PAuNEt}_3^+$ occurred, but the equilibrium now lay on the left: approximately nine equivalents of Et_3N were able to transform only about 60% of **9** into the triethylamine complex [Eq. (43)]. During this experiment both **9** and $\text{Ph}_3\text{PAuNEt}_3^+$ were observed clearly by ^{31}P NMR. When TMTU was added to the final solution, one broad phosphorus resonance was observed for all the species. This suggests that Et_3N was completely substituted from gold, but then $\text{Ph}_3\text{PAuTMTU}^+$ got involved in a fast exchange process, together with $(\text{Ph}_3\text{P})_2\text{Au}^+$, which was present in solution as impurity from the beginning but was not involved in any fast exchange before TMTU was added. Also, this experiment allowed the stability of the two species $(\text{LAu})_3\text{O}^+$ and $(\text{LAu})_2\text{OH}^+$ to be compared. Obviously $(\text{LAu})_3\text{O}^+$ should be more stable because it is stabilized by three aurophilic interactions, while $(\text{LAu})_2\text{OH}^+$ has only one, albeit doubtfully. The situation may change with the size of the ligand, and we postulate that this accounts for the relative instability of $(\text{LAu})_3\text{O}^+$ when a bulky phosphine ligand is present; there is simply not enough space around the oxygen atom for three big fragments, and only formation of less aurated $(\text{LAu})_2\text{OH}^+$ is possible.



Also, we studied conversions of $(\text{L}2\text{Au})_2\text{OH}^+$ (**10**) and $\text{L}2\text{AuOH}$ in both directions in three different solvents (CDCl_3 , CD_2Cl_2 , $[\text{D}_8]\text{THF}$). When PPh_3 was added to a solution of $(\text{L}2\text{Au})_2\text{OH}^+$, formation of new species was observed, which eventually were converted to $\text{L}2\text{AuOH}$ when more PPh_3 was added [overall Eq. (44) in Scheme 4]. The same species were detected during the synthesis of $\text{L}2\text{AuOH}$, when a solution of **2** in CDCl_3 was shaken briefly with 10% aqueous KOH. On further brief shaking, $\text{L}2\text{AuOH}$ was cleanly formed, according to Equation (28) in Scheme 3. From these observations, we concluded that these new species adopt the intermediate position between $(\text{L}2\text{Au})_2\text{OH}^+$ and $\text{L}2\text{AuOH}$ during the reaction with hydroxide ions. From general Equations (46)–(48) in Scheme 4 it becomes clear that the quantity of hydroxide ions per



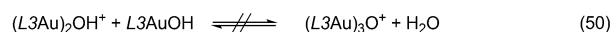
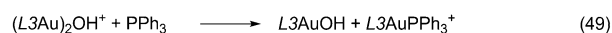
base per 1 mol gold

Scheme 4. Reaction of $(\text{L}2\text{Au})_2\text{OH}^+$ with PPh_3 .

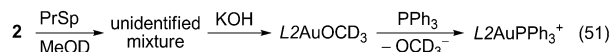
mole of gold increases for the following syntheses: $(\text{LAu})_2\text{OH}^+ < (\text{LAu})_3\text{O}^+ < \text{LAuOH}$. Hence, we concluded that the new species intermediately arising and disappearing on the way from $(\text{L}2\text{Au})_2\text{OH}^+$ (**10**) to $\text{L}2\text{AuOH}$ (**15**) must be $(\text{L}2\text{Au})_3\text{O}^+$ (**17**). We automatically concluded that **10** and **15** react with each other to give $(\text{L}2\text{Au})_3\text{O}^+$ (**17**) according to Equation (45) in Scheme 4. This process was found to be reversible, because **17** was often observed in mixture simultaneously with both **10** and **15** and not just with one of them or pure. Accordingly, brief appearance of **17** during the synthesis of $\text{L}2\text{AuOH}$ by Equation (28) in Scheme 3 corresponds to incomplete reaction when a mixture of **10** and **15** arises [Scheme 3, Eqs. (29)–(31)]. However, only in THF was $(\text{L}2\text{Au})_3\text{O}^+$ observed free of **10** and **15**. It remains unclear if this is due to better stability of $(\text{L}2\text{Au})_3\text{O}^+$ in this solvent or some kinetic circumstances. Note that $(\text{L}2\text{Au})_3\text{O}^+$ is not an intermediate on the way from **10** to **15**; it is rather a temporary side product. The same is valid when **15** is transformed into **10** by addition of **2**. Formation of $(\text{L}2\text{Au})_3\text{O}^+$ was rather unexpected given the increased steric bulk of the building blocks, but this ion is stable enough to be detected by ESI MS.

Compound $(\text{L}2\text{Au})_2\text{OH}^+$ (**10**) can be viewed as a complex of $\text{L}2\text{Au}^+$ with $\text{L}2\text{AuOH}$ as ligand, and thus Equation (44) in Scheme 4 can be viewed as simple ligand exchange. To get an idea how strong $\text{L}2\text{AuOH}$ is as a ligand, we conducted reactions with weaker nucleophiles in place of PPh_3 and found that this reaction reversibly occurs already with Me_2S , and with lutidine the equilibrium is much shifted to the right.

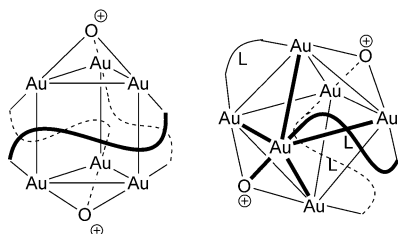
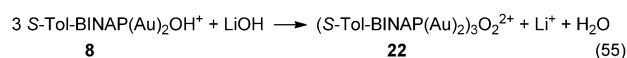
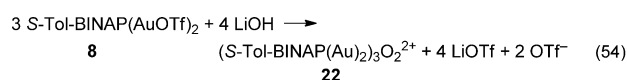
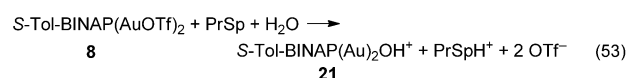
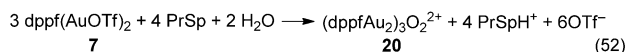
Thereafter, the analogous interconversion of $(\text{L}3\text{Au})_2\text{OH}^+$ (**11**) and $\text{L}3\text{AuOH}$ (**18**) was studied [Eq. (49)], but in contrast to the previous case it appears to be a mechanistically “clean” transformation giving no intermediate species. In no situation was the corresponding triaurated oxonium ion $(\text{L}3\text{Au})_3\text{O}^+$ observed [Eq. (50)]. Possibly, it cannot exist at all given the increased steric hindrance in comparison to $(\text{L}2\text{Au})_3\text{O}^+$.



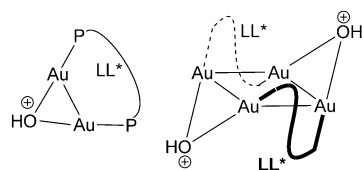
Finally, we studied reaction of **2** with proton sponge in methanol [Eq. (51)]. In contrast to the previous solvents, no clear situation was observed. Possibly, an equilibrium mixture of several oxonium and methoxonium species was formed. However, when solid KOH was added to this mixture, $\text{L}2\text{AuOMe}$ (**19**) was generated cleanly. Its identity was established by reaction with PPh_3 , giving clean substitution and no other products. Obviously, proton sponge was not strong enough to generate this methoxide.



So far no oxonium species have been described for binuclear gold complexes. Therefore, in line with the previous chemistry, we studied reactions of **7** and **8** with proton sponge. As above, by integration it was established that **7** reacts with proton sponge to give triaurated oxonium ions for which the simplest molecular composition was established to be $(\text{dppfAu}_2)_3\text{O}_2^{2+}$ (**20**) according to Equation (52) in Scheme 5, while **8** gave a kind of diaurated oxonium ion, for



possible structures for $(\text{dppfAu}_2)_3\text{O}_2^{2+}$ **20**
and $(\text{S-Tol-BINAP}(\text{Au})_2)_3\text{O}_2^{2+}$ **22**

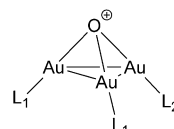
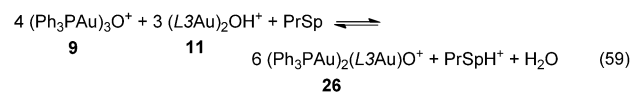
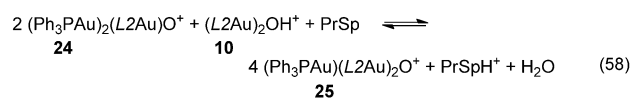
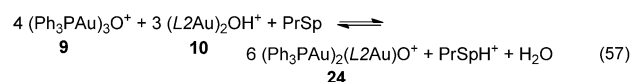
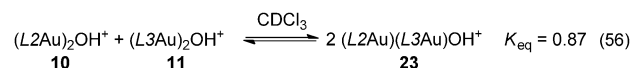


possible structures for $\text{S-Tol-BINAP}(\text{Au})_2\text{OH}^+$ **21**

Scheme 5. Reactions of binuclear gold complexes with bases.

which the simplest molecular composition was established as $\text{L}8(\text{Au})_2\text{OH}^+$ **21**, [Scheme 5, Eq. (53)]. In the ^1H NMR spectrum **21** exhibits a characteristic, slightly broad singlet at +5.36 ppm, corresponding to a single OH proton (in relation to 2Au), while in the ^{31}P NMR spectrum it shows a single sharp resonance at 22.85 ppm. In comparison with other such species the position of the OH signal is abnormal. On addition of solid LiOH to a solution of **21** a new species is formed, which was tentatively assigned the formula $[\text{L}8(\text{Au})_2]_3\text{O}_2^{2+}$ (**22**). This can be directly obtained by reaction of **8** with solid LiOH, its ^1H NMR spectrum exhibits no protons assignable to OH, and its ^{31}P NMR spectrum exhibits a single sharp resonance at 21.35 ppm. However, exact structures were not determined for either of these species. Based on the information on structures of known oxonium species, and from the fact that **20**, **21**, and **22** all exhibit a single phosphorus resonance, symmetric structures are proposed (Scheme 5).

So far we described homoleptic aurated oxonium species and it is of interest to check whether some mixed aurated oxonium complexes, a previously unknown type of compounds, can be observed. For this purpose we studied the reaction of $(\text{L}3\text{Au})_2\text{OH}^+$ (**11**) with **2** in the presence of excess proton sponge and found that **11** and **10** exist in equilibrium with the mixed species $(\text{L}2\text{Au})(\text{L}3\text{Au})\text{OH}^+$ (**23**), and the equilibrium constant was determined to be 0.87 [Scheme 6,



24: $\text{L}_1 = \text{PPh}_3$, $\text{L}_2 = \text{L}2$

25: $\text{L}_1 = \text{L}2$, $\text{L}_2 = \text{PPh}_3$

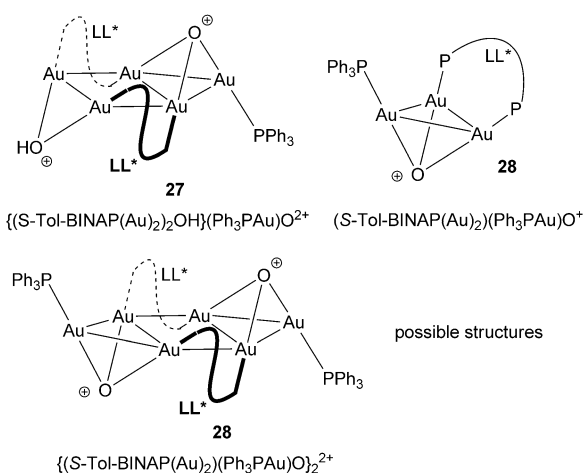
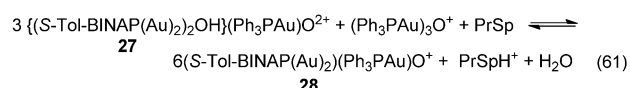
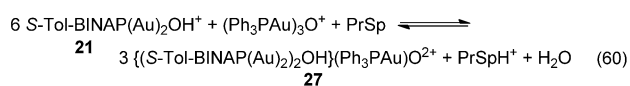
26: $\text{L}_1 = \text{PPh}_3$, $\text{L}_2 = i\text{Pr}$

Scheme 6. Formation of mixed oxonium species.

Eq. (56)].^[21] In the ^1H spectrum **23** exhibits a triplet for the OH proton with a chemical shift (−0.36 ppm) between the corresponding values for the homoleptic species. In the ^{31}P NMR spectrum **23** exhibits two singlets in a 1:1 ratio. Further, we conducted titration of $(\text{Ph}_3\text{PAu})_3\text{O}^+$ (**9**) with **2** in the presence of excess proton sponge. In the early stage, formation of **10** did not occur at all. Rather, formation of a single product $(\text{Ph}_3\text{PAu})_2(\text{L}2\text{Au})\text{O}^+$ (**24**) occurred quantitatively until almost all **9** had reacted [Scheme 6, Eq. (57)]. Interestingly, in the ^{31}P NMR spectrum this compound exhibits no P-P coupling and gives two singlets in 2:1 ratio. On further addition of **2**, the simultaneous formation of two compounds (**10** as major and $(\text{Ph}_3\text{PAu})(\text{L}2\text{Au})_2\text{O}^+$ **25** as minor product) indicates a reversible process [Scheme 6, Eq. (58)]. Obviously, formation of $(\text{Ph}_3\text{PAu})_2(\text{L}2\text{Au})\text{O}^+$ (**24**) with three possible aurophilic interactions is rather favored over formation of **10** in the presence of **9**, but this does not hold true for $(\text{Ph}_3\text{PAu})(\text{L}2\text{Au})_2\text{O}^+$ (**25**). This directly reflects the stability of these species, which decreases as they become more crowded. Thus, in the case of $(\text{L}3\text{Au})_2\text{OH}^+$ (**11**) formation of **26** is already highly reversible [Scheme 6, Eq. (59)], while formation of $(\text{Ph}_3\text{PAu})(\text{L}3\text{Au})_2\text{O}^+$ was not observed at all. Notably, phosphorus chemical shifts of the ligand residues in these mixed oxonium species are very close (within 0.3 ppm) to those observed in $(\text{Ph}_3\text{PAu})_3\text{O}^+$ and $(\text{L}2\text{Au})_3\text{O}^+$, which demonstrates similarities between all of these compounds. Assuming that the equilibrium

[Scheme 6, Eq. (58)] is pH-dependent, we attempted to shift it to the right with KOH, a stronger base. However, the equilibrium did not change significantly: both **24** and **25** were still observed; however, **10** completely transformed into L_2AuOH . We suppose that reaction of **10** with KOH to give **15** [Scheme 3, Eq. (30)] simply happened much faster than complex rearrangement by Equation (58) in Scheme 6.

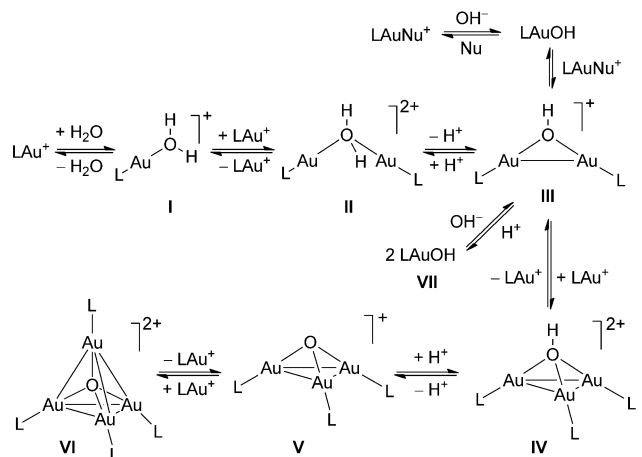
Finally, we titrated $L_8(Au)_2OH^+$ (**21**) with **9** in the presence of proton sponge and found that two new products were formed simultaneously, [Scheme 7, Eqs. (60), (61)].



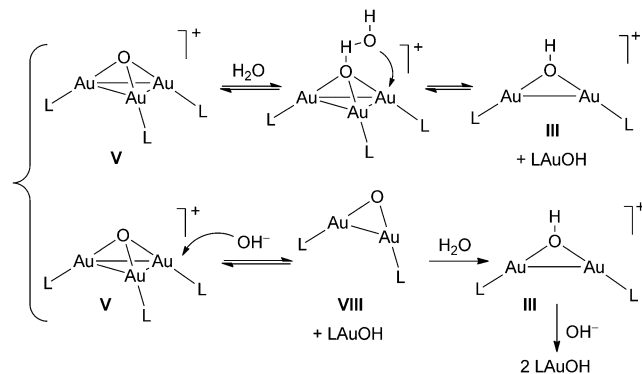
Scheme 7. Formation of mixed oxonium species bearing bidentate ligands.

However, one of them completely transformed into another species when more **9** was added. The molecular composition of this intermediate species was established as $\{L_8(Au)_2OH\}(Ph_3PAu)O^{2+}$ (**27**) since in the 1H spectrum it exhibits OH and Me signals in the ratio 1:12:12. The final product did not contain any OH signals, and its simplest molecular composition was established as $\{L_8(Au)_2\}(Ph_3PAu)O^+$ (**28**) which can be a monomer or dimer. The exact structures of these ions were not determined; possibly, symmetric structures are formed.

The interconversion between different kinds of oxonium ions and gold hydroxide can be explained by a general mechanism outlined in Scheme 8, consisting of principally all reversible steps, so that position of the real system at equilibrium primarily depends on the molar ratio and nature of reactants. Accordingly, reaction between LAu^+ and a base might begin with formation of a hydrate **I**, which would undergo a second addition of LAu^+ to give tetracoordinate oxonium ion **II**, which would readily expel one proton to give intermediate $(LAu)_2OH^+$ (**III**). If high OH^-



interconversion between $LAuOH$, $(LAu)_2OH$, $(LAu)_3O^+$ in the presence of OH^- :



Scheme 8. General mechanism of formation and transformation of oxonium species and gold hydroxide.

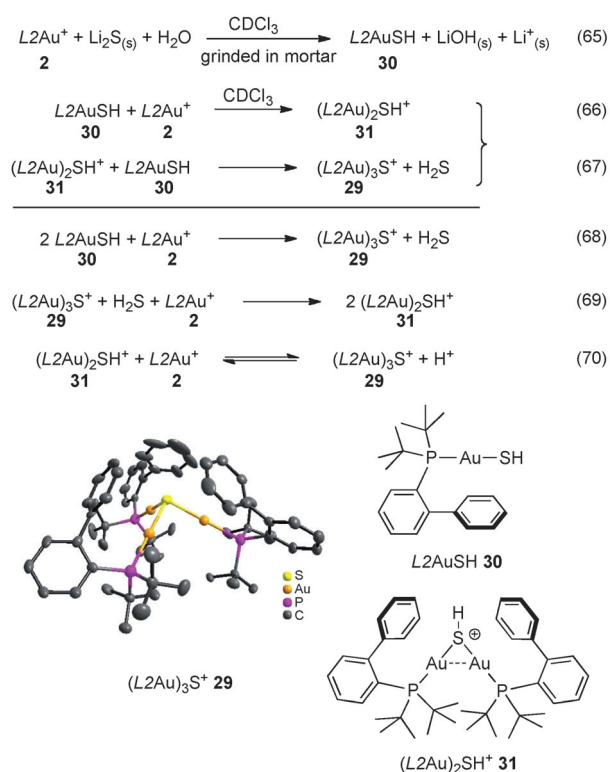
concentration is provided from the beginning, direct substitution at gold might take place as ordinary ligand exchange. Further, **III** reacts with LAu^+ to finally give oxonium ion **V** via tetracoordinate oxonium ion **IV** or, alternatively, **III** reacts with OH^- to give two equivalents of $LAuOH$. This process can be viewed as a simple ligand exchange at gold, if one considers **III** as a complex of LAu^+ with $LAuOH$ as a ligand. Correspondingly, it is easy to trace the process back when acid is added to $LAuOH$ or **V**. The intermediacy of tetracoordinate oxonium species like **II** and **IV** is postulated, but gains support from the ability of **V** to form isolable tetracoordinate oxonium ion **VI**, which has been known since 1995.^[22] Obviously, despite the cationic character of **III** and **V**, the oxygen atom still can act as a nucleophile, providing its fourth electronic pair to a proton or gold. The relative nucleophilic nature of oxygen in these species becomes clearer if one considers electronic density distribution within a molecule. Indeed, according to the concept of hard and soft Lewis acids and bases, there should be relatively weak interaction between Au and O, with little positive charge transfer from gold to oxygen. It can be argued that the oxygen atom in **V** is more electron rich than that in H_3O^+ , despite the fact that gold is more electronegative than hydrogen. This hy-

pothesis gains further support from NMR spectra, which typically show chemical shift of OH in **III** below 0 ppm. The same statements can be made to account for the strongly basic properties of LAuOH.

However, to account for reversible formation of **V** during transformation of $(\text{LAu})_2\text{OH}^+$ into LAuOH under basic conditions, equilibria $\text{V} \rightleftharpoons \text{IV} \rightleftharpoons \text{III}$ are not feasible, due to the absence of H^+ . In this case we propose alternative mechanisms, which are also given in Scheme 8. Thus, one might consider direct reaction of **V** with water, through hydrogen-bond activation, to give an equilibrium mixture of **III** and LAuOH. From here, transformation of **III** to LAuOH in the presence of OH^- is clear. Alternatively, one can consider the possibility of **V** reacting directly with OH^- , but then formation of gold oxide **VIII** would follow. However, at present, such gold derivatives remain unknown and their intermediacy is thus highly speculative. But if formed, they would be highly basic substances and would react immediately with water to give initially **III** and OH^- and finally lead to LAuOH. We conclude that, depending on the availability of H^+ and OH^- , gold may undergo transformations in different directions through different pathways, but the final outcome of a reaction would be dependent on the molar ratio and nature of reactants.

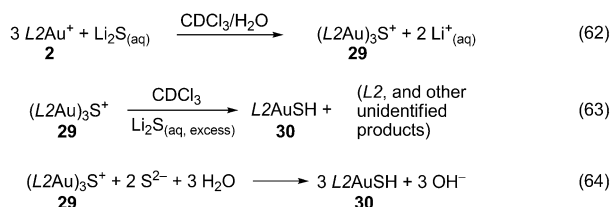
Formal LAu^+ exchange at oxygen between $(\text{LAu})_3\text{O}^+$ and $(\text{L}'\text{Au})_3\text{O}^+$ was previously observed, but nothing was said about formation of any mixed intermediate species on the way.^[23] In our study, due to the presence of at least one large unit, such exchanges were observed as stepwise processes for the first time.

Reaction of 2 with Li_2S : complexes with sulfur and their interconversion: When **2** was allowed to react with substoichiometric amounts of Li_2S in a biphasic $\text{CDCl}_3/\text{H}_2\text{O}$ mixture, $(\text{L}2\text{Au})_3\text{S}^+$ (**29**) was formed as a sole product [Eq. (62)]. Under these reaction conditions formation of tetraaurated sulfonium ion $(\text{L}2\text{Au})_4\text{S}^{2+}$ could be expected, and exclusive formation of **29** evidences for inability of any higher coordinated compound to exist due to steric reasons.^[24] On further addition of excess Li_2S , multiple processes occurred. Thus, **29** predominantly transformed into hydrosulfide $\text{L}2\text{AuSH}$ (**30**), but the reaction was also accompanied by formation of several minor products [Eqs. (63) and (64)]. Among them, free ligand *L*2 was identified. Liberation of free *L*2 implies that part of the gold was converted to Au_2S , and this idea gains support from the fact that some brown precipitate was indeed observed. The same decomposition was described in the case of $(\text{Ph}_3\text{PAu})_2\text{S}$ long ago,^[25] and later the structure of this compound could be established by X-ray analysis.^[26] Accordingly, we concluded that neutral sulfide $(\text{L}2\text{Au})_2\text{S}$ would also be unstable: it either decomposes to Au_2S and *L*2 or is hydrolyzed back to hydrosulfide **30**. Notably, complete precipitation of Au_2S and liberation of *L*2 could not be achieved, at least within a short time interval. The structure of $(\text{L}2\text{Au})_3\text{S}^+$ was established by X-ray analysis (Scheme 9). The ligand residues are located in such a way that the cation can be described as having



Scheme 9. Formation and transformations of complexes with sulfur.

a C_3 symmetry axis passing through the central sulfur atom and perpendicular to the base of the Au_3S pyramid.



Interestingly, when a chloroform solution of **2** was ground in a mortar together with excess of solid Li_2S (even without addition of water), clean formation of $\text{L}2\text{AuSH}$ (**30**) occurred and no brown Au_2S color or free *L*2 was observed, [Scheme 9, Eq. (65)]. Based on this fact, we suppose that **30** is the only stable ultimate product of the reaction with sulfide (correspondingly, formation of LiOH should be invoked to account for this process). In the ^1H NMR spectrum **30** exhibits a characteristic doublet at -1.44 ppm corresponding to a single SH proton.

Transformations of $\text{L}2\text{AuSH}$ (**30**) were further studied in the following experiment. When **2** was added to a fresh solution of **30** in CDCl_3 , $(\text{L}2\text{Au})_3\text{S}^+$ (**29**) was formed as sole product [Scheme 9, Eq. (68)]. This reaction is accompanied by liberation of H_2S , which could be also recognized by smell. On further addition of **2**, **29**, H_2S , and **2** reacted to give $(\text{L}2\text{Au})_2\text{SH}^+$ (**31**) as sole product, [Scheme 9, Eq. (69)].

In the ^1H NMR spectrum it exhibited a characteristic triplet at -0.41 ppm ($^3J_{\text{H-P}}=5.3$ Hz), corresponding to a single SH proton. Ultimately, when more **2** was added, **29** reappeared again, but now reversibly [Scheme 9, Eq. (70)]. These interesting transformations are explained as follows. Initially, when $L2\text{AuSH}$ reacts with **2**, $(L2\text{Au})_2\text{SH}^+$ would be expected as a direct product [Scheme 9, Eq. (66)]. Observation of **29** at an early stage implies that $(L2\text{Au})_2\text{SH}^+$ quantitatively reacted with **29** to give $(L2\text{Au})_3\text{S}^+$ and H_2S [Scheme 9, Eq. (67)], and only when no more **30** is present in solution is further reaction possible. Next, when $(L2\text{Au})_2\text{SH}^+$ reacted with an excess of **2**, formation of $(L2\text{Au})_3\text{S}^+$ occurred, but now liberation of super acid HSbF_6 makes this process reversible. However, the equilibrium could be completely shifted to the right on extraction with water. Such an interesting appearance, disappearance, and reappearance of $(L2\text{Au})_3\text{S}^+$ **29** is completely understandable if one considers material balance in the system. Thus, the initial formation of **29** happens before one equivalent of gold is added according to Equation (68) in Scheme 9. At this moment the molar ratio of elements in the system is $\text{Au}^+/\text{S}^{2-}/\text{H}^+=3/2/2$ (1S and 2H are present as H_2S and unreactive). Stoichiometric formation of **31** happens exactly when the molar ratio is $\text{Au}^+/\text{S}^{2-}/\text{H}^+=2/1/1$, as in the compound. Finally, **29** reappears again when $\text{Au}/\text{S} > 2/1$ and becomes complete provided $\text{Au}^+/\text{S}^{2-}=3/1$ and no acid is present.

From these two experiments it can be concluded that the outcome of the reaction between **2** and S^{2-} depends on the molar ratio of reactants and availability of reactive protons. The mechanism of these transformations would resemble the previously described mechanism for oxonium species.

An attempt was made to synthesize the elusive neutral $(L2\text{Au})_2\text{S}$ by reaction of **30** and **15** in C_6D_6 , but this led to mixtures of products. Interestingly, liberation of free $L2$ was observed, but now it was not accompanied by any brown precipitate, which suggests that formation of colorless products of general formula $(L2\text{Au})_2\text{S}\cdot x\text{Au}_2\text{S}$ could be possible. Four new components were observed in the NMR spectra of these mixtures; two of the compounds contained characteristic singlets at -0.61 and -0.66 ppm (in C_6D_6); none of them was identified. One of the products precipitated from benzene. The solid was soluble in chloroform and did not exhibit any signals below 0 ppm. The crystals, however, were not analyzed by X-ray analysis leaving this puzzle to be solved in the future.

Conclusion

We have thoroughly investigated the coordination chemistry of modern gold catalysts by NMR spectroscopy in solution. This included simple ligand-exchange reactions at gold, as well as formation and transformations of different oxonium and sulfonium species. Success in this study relied on the presence of bulky ligands in gold complexes, which allowed the transformations to be traced by NMR clearly without being spoiled by the dynamic situations that often happen

with complexes bearing small ligands. By observation of discrete rather than continuous changes in NMR spectra, we were able to detect and characterize intermediates and got closer insight to mechanisms of processes involving multiple reactive species.

Experimental Section

Synthesis of 2: An improved literature procedure was used.^[27] AgSbF_6 (0.213 g, 0.620 mmol) was quickly weighed in a vial. To this was added cold MeCN (≈ 0.3 mL) and CH_2Cl_2 (0.3 mL) to make a clear solution (dissolution of AgSbF_6 in MeCN is rather exothermic). To this solution was added a solution of $L2\text{AuCl}$ (0.329 g, 0.620 mmol) in CH_2Cl_2 (3 mL). A white precipitate immediately formed. The reaction mixture was allowed to stand in the dark for about 15 min (rather than overnight as is often given in the literature) before it was passed through Celite (we recommend conducting halogen abstraction reactions by silver in CH_2Cl_2 as a main co-solvent; see our remarks on synthesis of $L\text{AuOTf}$ in the Supporting Information). The reaction flask and filter cake were washed with copious CH_2Cl_2 . The clear colorless filtrate was evaporated in vacuo till dryness and redissolved in a minimum amount of MeCN (≈ 0.2 mL). This solution was layered with benzene (≈ 1.5 mL) to allow for slow crystallization. First crystals appeared rather slowly, but then crystal growth occurred faster and rather big crystals were obtained. The supernatant was removed by Pasteur pipette and the crystals washed once with benzene and dried in vacuo to yield **2** in about 95% yield. We note that both commercial and self-made **2** normally contain only 0.93 equiv MeCN rather than 1 equiv, and some **10** ($\approx 3\%$) as impurity or as hydrolysis product. However, when the final product was moistened with MeCN and dried in vacuo immediately, but not strongly at first, and then mixed with pentane and finally dried thoroughly, it was possible to obtain the product with 1 equiv MeCN as in the formula.

Synthesis of dppf(AuCl)₂ (7): Solid dppf (0.170 g, 1 equiv) was added to a suspension of Me_2SAuCl (0.101 g, 0.343 mmol, 2.02 equiv) in CH_2Cl_2 (2 mL). All insoluble material soon dissolved to give an almost clear orange solution containing trace amounts of a tiny dark precipitate. The solution was filtered through Celite into a 10 mL flask and additional amounts of CH_2Cl_2 were used to quantitatively transfer all of the material. The filtrate was concentrated in vacuo to about 0.5 mL. At this point a major part of $\text{dppf}(\text{AuCl})_2$ may already precipitate from the solution. The filtrate was triturated with MeOH to enhance precipitation of the product. The supernatant solution was carefully sucked out (by a Pasteur pipette with a piece of cotton at the end) and the residue washed once with MeOH and dried in vacuo (all in the same flask) to give the desired complex as orange microcrystalline solid in quantitative yield (0.173 g).

Note: Me_2SAuCl , dppf and $\text{dppf}(\text{AuCl})_2$ are all practically insoluble in MeOH; therefore it is not recommended to keep more significant deviations from 2/1 molar ratio of the reactants.

S -TolBINAP(AuCl)₂ **8** was synthesized by the same method in quantitative yield. It is also insoluble in MeOH.

Synthesis of (Ph₃PAu)₃O⁺ OTf⁻ (9): A solution of Ph_3PAuCl (171.3 mg, 0.345 mmol) in THF (2 mL) was added to a solution of AgOTf (89.2 mg, 0.347 mmol) in THF (2 mL). AgCl immediately precipitated. The reaction mixture was kept in the dark for 5 min and filtered through a pad of Celite. To the clear colorless filtrate was added a solution of NaOH (15 mg) in water (0.4 mL) and the emulsion was shaken briefly. The product formed as a gray precipitate. The resulting suspension was evaporated almost till dryness. The residue was taken up in CH_2Cl_2 and water. Any remaining precipitate was filtered off and washed with portions of CH_2Cl_2 . The clear biphasic filtrate was collected, the water phase separated, and the organic phase dried with Na_2SO_4 . After filtration, the clear filtrate was transferred to a weighed round-bottomed flask. Most of the solvent was removed in vacuo and the residue diluted with THF to cause spontaneous precipitation of the pure product as white crystals. The supernatant solution was decanted by Pasteur pipette and the precipitate

washed with THF once, decanted, and the product dried in vacuo to yield 0.166 g (93%) of the title compound. *Note:* Clearly, the synthesis would be better performed in CH₂Cl₂ solution (change of the solvent from THF to CH₂Cl₂ would be not necessary).

Synthesis of gold hydroxides LAuOH (L=L2, IMes, IPr), mechanochemical method: A suspension of L2AuCl (33.8 mg, 43.8 μmol) and KOH (23.5 mg, 420 μmol, 9.6 equiv) in C₆D₆ (0.5 mL) was ground in a small mortar for 30–60 s (10 s is enough for smaller loadings, and less KOH can also be used). On filtration through Celite (prewashed with C₆D₆) a clear solution of **15** was obtained, which was used directly without isolation. IPrAuCl reacted more slowly, but complete conversion was reliably achieved. Surprisingly, IMesAuCl reacted even more slowly, and complete conversion was not achieved. However, the reaction was clean, and this suggests that prolonged reaction time should achieve complete conversion. We suppose that solubility of the initial and final gold complexes in benzene would be important. We found that L2AuCl and L2AuOH are quite soluble, while IPrAuCl and IMesAuCl are less soluble.

Extractive variant: A solution of LAuCl in CH₂Cl₂/benzene (1/5) was shaken with concentrated (but not saturated) aqueous KOH for 5 min. The small amount of CH₂Cl₂ was used to improve the solubility of IPrAuCl and IMesAuCl. In principal, pure CH₂Cl₂ can be used, but the efficacy of emulsion generation on shaking and determination of phase separation is lower, while benzene is much better suited. No phase-transfer catalysts are required. Again, reaction of IMesAuCl was found to be rather sluggish. We recommend the mechanochemical method as the simplest and most reliable for synthesis of **15**, while for larger scale synthesis of IPrAuOH some adaptation would be required due to lower solubility in benzene. More remarks on these two procedures are given in the Supporting Information.

Generation of oxonium species (LAu)₂OH⁺ (10–13); comparison of different reagents: Of all bases used in this study only proton sponge generated this species essentially in 100% yield according to Equation (26a) in Scheme 2 regardless of the excess of base. In case of water extraction of a chloroform solution of **2**, reaction naturally does not reach completion, but was at least 95% complete (trace amounts of unconverted **2** always remained, as evidenced by the MeCN resonance not exactly at 2.00 ppm and broadening of the OH triplet). When a chloroform solution of **2** was extracted with dilute NaHCO₃ solution, the resulting solution contained traces of products of reaction beyond **10**, that is, **15** and **17** (as evidenced by the MeCN resonance exactly at 2.00 ppm and broadening of the OH triplet). The use of solid inorganic bases such as LiOH or KOH gave different results depending on the amount of base, particle size, and reaction time. Thus, on brief shaking of a chloroform solution of **2** with relatively coarse LiOH powder, **10** was observed cleanly (at least 95%), while on shaking with bigger amounts of finer powder reaction occurred till exclusive formation of **15**. Despite these ambiguities, shaking of a solution of **10** generated by reaction of **2** and PrSp according to Equation (26a) in Scheme 2 with LiOH powder was reliably used several times to get rid of PrSpH⁺ while not disturbing **10**.

Acknowledgements

We thank Dr. K. Eichele (Univ. Tübingen, Institut für Anorganische Chemie) and P. Schuler (Univ. Tübingen, Institut für Organische Chemie) for allowing us to use additional NMR spectrometers and Dr. D. Wistuba for HRMS analysis.

- [1] For reviews on gold catalysis, see: a) A. Corma, A. Leyva-Peréz, M. J. Sabater, *Chem. Rev.* **2011**, *111*, 1657–1712; b) M. Bandini, *Chem. Soc. Rev.* **2011**, *40*, 1358–1367; c) T. C. Boorman, I. Larrosa, *Chem. Soc. Rev.* **2011**, *40*, 1910–1925; d) A. S. K. Hashmi, M. Bührle, *Aldrichimica Acta* **2010**, *43*, 27–33; e) N. D. Shapiro, F. D. Toste, *Synlett* **2010**, 675–691; f) S. Sengupta, X. Shi, *ChemCatChem* **2010**, *2*, 609–619; g) N. Bongers, N. Krause, *Angew. Chem.* **2008**,

- 120*, 2208–2211; *Angew. Chem. Int. Ed.* **2008**, *47*, 2178–2181; h) D. J. Gorin, B. D. Sherry, F. D. Toste, *Chem. Rev.* **2008**, *108*, 3351–3378; i) E. Jiménez-Núñez, A. M. Echavarren, *Chem. Rev.* **2008**, *108*, 3326–3350; j) Z. Li, C. Brouwer, C. He, *Chem. Rev.* **2008**, *108*, 3239–3265; k) A. Arcadi, *Chem. Rev.* **2008**, *108*, 3266–3325; l) J. Muzart, *Tetrahedron* **2008**, *64*, 5815–5849; m) A. S. K. Hashmi, M. Rudolph, *Chem. Soc. Rev.* **2008**, *37*, 1766–1775; n) H. C. Shen, *Tetrahedron* **2008**, *64*, 7847–7870; o) H. C. Shen, *Tetrahedron* **2008**, *64*, 3885–3903; p) R. A. Widenhoefer, *Chem. Eur. J.* **2008**, *14*, 5382–5391; q) D. J. Gorin, F. D. Toste, *Nature* **2007**, *446*, 395–403; r) A. Fürstner, P. W. Davies, *Angew. Chem.* **2007**, *119*, 3478–3519; *Angew. Chem. Int. Ed.* **2007**, *46*, 3410–3449; s) E. Jiménez-Núñez, A. M. Echavarren, *Chem. Commun.* **2007**, 333–346; t) A. S. K. Hashmi, *Chem. Rev.* **2007**, *107*, 3180–3211.
- [2] For a recent review on intermediates in gold catalysis, see: A. S. K. Hashmi, *Angew. Chem.* **2010**, *122*, 5360–5369; *Angew. Chem. Int. Ed.* **2010**, *49*, 5232–5241. Recent highlight about diaurated species: A. Gómez-Suárez, S. P. Nolan, *Angew. Chem.* **2012**, *124*, 8278–8281; *Angew. Chem. Int. Ed.* **2012**, *51*, 8156–8159. Most recent research on mechanisms includes also: a) W. Wang, G. B. Hammond, B. Xu, *J. Am. Chem. Soc.* **2012**, *134*, 5697–5705; b) Z. J. Wang, D. Benitez, E. Tkatchouk, W. A. Goddard III, F. D. Toste, *J. Am. Chem. Soc.* **2010**, *132*, 13064–13071; c) T. J. Brown, D. Weber, M. R. Gagné, R. A. Widenhoefer, *J. Am. Chem. Soc.* **2012**, *134*, 9134–9137; d) A. S. K. Hashmi, I. Braun, M. Rudolph, F. Rominger, *Organometallics* **2012**, *31*, 644–661; e) A. S. K. Hashmi, A. M. Schuster, S. Gaillard, L. Cavallo, A. Poater, S. P. Nolan, *Organometallics* **2011**, *30*, 6328–6337; f) A. S. K. Hashmi, A. M. Schuster, S. Litters, F. Rominger, M. Pernpointner, *Chem. Eur. J.* **2011**, *17*, 5661–5667.
- [3] a) *Top. Curr. Chem. Vol. 302* (Eds.: E. Soriano, J. Marco-Contelles), Springer, Berlin, **2011**, pp. 252; b) C. M. Krauter, A. S. K. Hashmi, M. Pernpointner, *ChemCatChem* **2010**, *2*, 1226–1230; c) T. de Haro, E. Gómez-Bengoa, R. Cribiú, X. Huang, C. Nevado, *Chem. Eur. J.* **2012**, *18*, 6811–6824; d) R. Fang, L. Yang, *Organometallics* **2012**, *31*, 3043–3055; e) T. Fan, X. Chen, J. Sun, Z. Lin, *Organometallics* **2012**, *31*, 4221–4227; f) G. Mazzone, N. Russo, E. Sicilia, *Organometallics* **2012**, *31*, 3074–3080.
- [4] M. C. Gimeno, A. Laguna, in *Comprehensive Coordination Chemistry II, Vol. 6*, (Eds.: J. A. McCleverty, T. J. Meyer), Pergamon, Oxford, **2003**, pp. 911–1145.
- [5] The true rise of homogenous gold catalysis essentially started with the following two papers: a) A. S. K. Hashmi, L. Schwarz, J.-H. Choi, T. M. Frost, *Angew. Chem.* **2000**, *112*, 2382–2385; *Angew. Chem. Int. Ed.* **2000**, *39*, 2285–2288; b) A. S. K. Hashmi, T. M. Frost, J. W. Bats, *J. Am. Chem. Soc.* **2000**, *122*, 11553–11554.
- [6] With “parent ligand” we refer to heteroleptic two-coordinate gold complexes consisting of L-Au-Nu units in which gold is bound to two different ligands L and Nu. In their transformations the L-Au unit remains integral while the Au–Nu bond is disconnected. Thus, L can be considered the non-exchangeable ligand. In most situations L is the stronger ligand. In some rare cases it appears that the newly incoming Nu is stronger than L (e.g., exchange of MeCN by Cy₃P at L2AuNCMe⁺), but Cy₃P is still considered to be Nu with respect to the parent precursor.
- [7] a) C. B. Colburn, W. E. Hill, C. A. McAuliffe, R. V. Parish, *J. Chem. Soc. Chem. Commun.* **1979**, 218–219; b) R. V. Parish, O. Parry, C. A. McAuliffe, *J. Chem. Soc. Dalton Trans.* **1981**, 2098–2104; c) R. Colton, K. L. Harrison, Y. A. Mah, J. C. Traeger, *Inorg. Chim. Acta* **1995**, *231*, 65–71.
- [8] A. Sladek, H. Schmidbaur, *Z. Naturforsch., B: Chem. Sci.* **1996**, *51b*, 1207–1209.
- [9] M. Munakata, S.-G. Yan, M. Maekawa, M. Akiyama, S. Kitagawa, *J. Chem. Soc. Dalton Trans.* **1997**, 4257–4262.
- [10] J. Vicente, M.-T. Chicote, R. Guerrero, P. G. Jones, *J. Chem. Soc. Dalton Trans.* **1995**, 1251–1254.
- [11] G. L. Wegner, A. Jockisch, A. Schier, H. Schmidbaur, *Z. Naturforsch., B: Chem. Sci.* **2000**, *55b*, 347–351.

- [12] A. N. Nesmeyanov, E. G. Perevalova, Y. T. Struchkov, M. Y. Antipin, K. I. Grandberg, V. P. Dyadhenko, *J. Organomet. Chem.* **1980**, *201*, 343–349.
- [13] a) T. J. Brown, R. A. Widenhoefer, *J. Organomet. Chem.* **2011**, *696*, 1216–1220; b) T. J. Brown, M. G. Dickens, R. A. Widenhoefer, *Chem. Commun.* **2009**, 6451–6453.
- [14] For example, gold(I)-catalyzed hydroalkoxylation fails in MeCN: V. Belting, N. Krause, *Org. Lett.* **2006**, *8*, 4489–4492; in contrast, some gold(III) reactions were performed in MeCN: G. Dyker, E. Muth, A. S. K. Hashmi, L. Ding, *Adv. Synth. Catal.* **2003**, *345*, 1247–1252.
- [15] M. C. Gimeno, A. Laguna, C. Sarroca, P. G. Jones, *Inorg. Chem.* **1993**, *32*, 5926–5932.
- [16] a) S. Gaillard, J. Bosson, R. S. Ramón, P. Nun, A. M. Z. Slawin, S. P. Nolan, *Chem. Eur. J.* **2010**, *16*, 13729–13740; b) R. S. Ramón, S. Gaillard, A. Poater, L. Cavallo, A. M. Z. Slawin, S. P. Nolan, *Chem. Eur. J.* **2011**, *17*, 1238–1246.
- [17] Fast exchange and strong hydrogen bonding were previously documented for LAuOR/ROH systems: a) S. Komiya, M. Iwata, T. Sone, A. Fukuoka, *J. Chem. Soc. Chem. Commun.* **1992**, 1109–1110; b) T. Sone, M. Iwata, N. Kasuga, S. Komiya, *Chem. Lett.* **1991**, *20*, 1949–1952.
- [18] S. Gaillard, A. M. Z. Slawin, S. P. Nolan, *Chem. Commun.* **2010**, *46*, 2742–2744.
- [19] S. Gaillard, C. S. J. Cazin, S. P. Nolan, *Acc. Chem. Res.* **2012**, *45*, 778–787; see also refs. [16] and [18].
- [20] A similar IPrAuNEt₃⁺ complex has recently been described. Such complexes are important in the context of dual catalysis because they dissociate to give active gold and the base NEt₃. See ref. [2d].
- [21] For a related heteroleptic diaurated vinyl gold compound, see: A. S. K. Hashmi, I. Braun, P. Nösel, J. Schädlich, M. Wietek, M. Rudolph, F. Rominger, *Angew. Chem.* **2012**, *124*, 4532–4536; *Angew. Chem. Int. Ed.* **2012**, *51*, 4456–4460.
- [22] H. Schmidbaur, S. Hofreiter, M. Paul, *Nature* **1995**, *377*, 503–504.
- [23] Y. Yang, V. Ramamoorthy, P. R. Sharp, *Inorg. Chem.* **1993**, *32*, 1946–1950.
- [24] F. Canales, M. C. Gimeno, P. G. Jones, A. Laguna, *Angew. Chem.* **1994**, *106*, 811–812; *Angew. Chem. Int. Ed. Engl.* **1994**, *33*, 769–770.
- [25] C. Kowala, J. M. Swan, *Aust. J. Chem.* **1966**, *19*, 547–554. In contrast to (Ph₃PAu)₂S and (L₂Au)₂S, (Et₃PAu)₂S was reported to be stable.
- [26] C. Lensch, P. G. Jones, G. M. Sheldrick, *Z. Naturforsch., B: Org. Chem.* **1982**, *37B*, 944–949.
- [27] C. Nieto-Oberhuber, M. P. Muñoz, S. López, E. Jiménez-Núñez, C. Nevado, E. Herrero-Gómez, M. Raducan, A. M. Echavarren, *Chem. Eur. J.* **2006**, *12*, 1677–1693.

Received: April 10, 2012

Revised: July 30, 2012

Published online: September 27, 2012

Paper 3

For the Section 6.3.2.

Gold-Catalyzed Hydroalkoxylation

Synthesis of *gem*-Diaurated Species from Alkynols

Alexander Zhdanko and Martin E. Maier*^[a]

Abstract: A number of enol ether-derived diaurated species were synthesized directly from different alkynols and cationic gold complexes in the presence of a non-nucleophilic base (proton sponge). The reaction can be easily applied for in situ generation of diaurated species from all common types of hydroalkoxylation substrates: *5-endo*, *5-exo/6-endo*, *6-exo/7-endo* and intermolecular types. Six examples were also synthesized in individual state as stable hexafluoroantimonate

salts. Whereas diaurated species are obtained reliably from all conventional mononuclear gold catalysts, application of binuclear ones often gave diaurated species with unusual properties. The preliminary results point to complexities of behavior of binuclear gold catalysts and would require more research

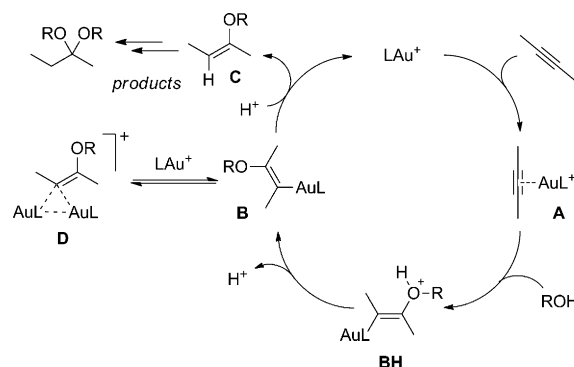
Keywords: alkynes • diaurated species • enol ethers • gold • gold intermediates

in future for this subclass. The formation of diaurated species from various gold-oxo compounds $(\text{LAu})_2\text{OH}^+$, $(\text{LAu})_3\text{O}^+$, and LAuOH (L = phosphine ligand) was also studied. Of these three types, only $(\text{LAu})_2\text{OH}^+$ is reactive, whereas $(\text{LAu})_3\text{O}^+$ and LAuOH are not reactive alone but require acidic promoters to enable the reaction. These differences in reactivity were explained by ability of these compounds to generate the necessary acetylene π -complex intermediate.

Introduction

Molecules containing an alkyne functionality allow a number of useful transformations.^[1] A classical reaction is the hydration of alkynes to ketones, which typically is performed in presence of Hg^{II} salts and acid. Related to this is the hydroalkoxylation of alkynes. In recent years, addition reactions to alkynes have benefited a lot from gold catalysis. For example, alkynes with internal hydroxyl functions can be converted to cyclic enol ethers by using an Au^{I} catalyst. However, knowledge about the mechanism of gold-catalyzed transformations involving alkynes remains much more limited.^[2] This also holds true for the hydroalkoxylation of alkynes. The current understanding of this mechanism still largely relies on computational methods. The addition is thought to proceed through the following steps: 1) coordination of gold onto an alkyne to give a π -complex **A**,^[3] 2) nucleophilic attack of an alcohol to give a vinyl gold intermediate **B**, and 3) subsequent protodeauration to give the primary product **C** (Scheme 1).^[4] The last event liberates the gold catalyst, ready to start the next catalytic cycle.

However, it is known by now that vinyl gold complexes exhibit strong aurophilic properties that may result in formation of *gem*-diaurated species **D**. Although the phenomenon of *gem*-diauration has long been known (since 1974),^[5]



Scheme 1. Key steps in the gold-catalyzed hydroalkoxylation and concurrent formation of *gem*-diaurated species **D**.

it was somehow overlooked by the gold catalysis community until 2009 when Gagné and co-workers observed the *gem*-diaurated species for the first time in a catalytic allene hydroarylation.^[6] Later, diaurated species were detected in other catalytic processes.^[7] Since diaurated species do not undergo protodeauration as easily as vinyl gold species, it was soon realized that they should be inhibitory for catalysis. Therefore, the knowledge about formation of these species and their behavior within a catalytic cycle is of fundamental importance for practical applications of gold catalysis, because avoiding this species should decrease the catalyst loadings and benefit the catalytic cycle. The current knowledge about this problem still primarily relies on model systems, that is, the aryl diaurated species $\text{Ar}(\text{AuL})_2^+$.^[8] In contrast, direct experimental elucidation of the role of diaurated species in a catalytic process has only begun to emerge, as exemplified by mechanistic investigations of

[a] A. Zhdanko, Prof. Dr. M. E. Maier
Institut für Organische Chemie, Universität Tübingen
Auf der Morgenstelle 18, 72076 Tübingen (Germany)
Fax: (+49) 7071-295137
E-mail: martin.e.maier@uni-tuebingen.de

Supporting information for this article is available on the WWW under <http://dx.doi.org/10.1002/chem.201204491>.

gold-catalyzed hydroalkoxylation of allenes recently published by Wiedenhofer, Gagné, and co-workers.^[9] Nevertheless, catalytic intermediates of the gold-catalyzed hydroalkoxylation of alkynes still remain to be experimentally explored.^[10]

In connection with the gold-catalyzed spiroacetal formation of certain alkyne diols, we discovered that enol ether-derived diaurated species **D** are formed directly if an alkyne is allowed to react with a gold catalyst in the presence of a base. The intermediacy of this kind of species in a catalytic hydroalkoxylation process was first suggested by Fürstner and co-workers in 2010.^[11] In that report, a boron-to-gold exchange reaction, rather than direct synthesis from an alkyne, was used for the synthesis of diaurated species and only one example of enol ether-derived diaurated species was described, which still remains the only example up to now.

Prompted by the fact that nothing else is known about chemical properties of this kind of diaurated species, the properties of the enol ether-derived vinyl gold species, the ligand effects during their formation, or the exact pathways of transformations of the diaurated species within the catalytic cycle, we embarked on a project with the aim to understand the role of diaurated species in more detail, at least for catalytic hydroalkoxylation. Subsequent investigation on the behavior of this species should provide important insights on their role in Au^I-catalyzed hydroalkoxylation reactions. In the current paper we describe the formation of enol ether-derived diaurated species from alkynols by using ten gold complexes bearing different ligands (Figure 1).

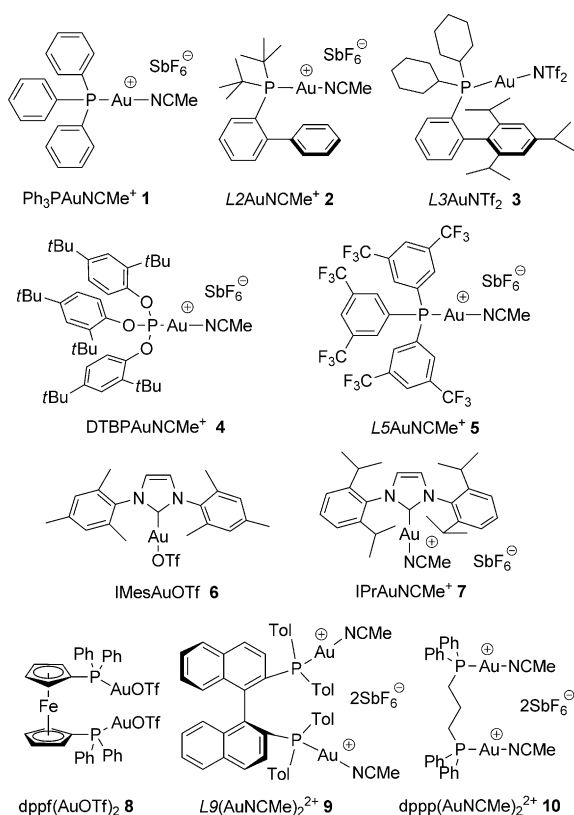


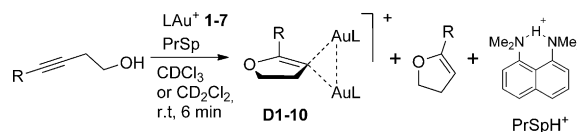
Figure 1. Gold catalysts used in this study.

Since only methodologies towards the synthesis of model diaurated species Ar(AuL)₂⁺ have been described so far,^[5,8b] our strategy can be considered as the first to target diaurated species that are real intermediates in gold catalysis.

Results and Discussion

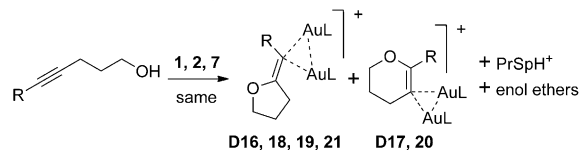
Formation of diaurated species from mononuclear catalysts:

Thus, simple addition of a gold catalyst (substoichiometric amount) to a solution of 3-heptyn-1-ol and proton sponge in CDCl₃ triggered an immediate reaction resulting in formation of diaurated species **D** as a single organogold product (Scheme 2).^[12] Under such conditions, the transformation was accompanied by competitive enol ether formation. Analogously, the diaurated species could be directly generated in [D₈]THF by using MeLi or another soluble strong base to stoichiometrically generate the alkoxide, which would then react with two equivalents of gold in a strictly stoichiometric manner. An important requirement for the successful formation of diaurated species is that the base should be well soluble in the reaction media, otherwise simple gold-catalyzed hydroalkoxylation will predominantly occur with (almost) complete regeneration of the initial catalyst. After some experimentation, we concluded that the use of proton sponge as a base in CDCl₃ or CD₂Cl₂ as sol-



| Species | R | Cat | Yield ^[a] | Species | R | Cat |
|---------|-------------|-----|----------------------|---------|-------------|-----|
| D1 | <i>n</i> Pr | 2 | 90% | D6 | Me | 7 |
| D2 | <i>n</i> Pr | 5 | 47% | D7 | <i>n</i> Pr | 7 |
| D3 | Me | 1 | 80% | D8 | Ph | 2 |
| D4 | <i>n</i> Pr | 1 | | D9 | <i>n</i> Pr | 3 |
| D5 | Me | 2 | 88% | D10 | <i>n</i> Pr | 4 |

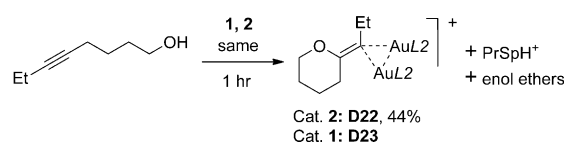
^[a]Isolated yield of the corresponding SbF₆⁻ salts is given. In other cases diaurated species were observed in situ.



| R | Cat | Species | Yield ^[a] |
|--|-----|---------------------------------|----------------------|
| Me | 1 | D16, D17 (1:1.6) ^[b] | |
| <i>n</i> -C ₅ H ₁₁ | 2 | D18 | |
| Me | 2 | D19, D20 (1:0.07) | D19 (69%) |
| Me | 7 | D21 | |

^[a]Isolated yield is given

^[b]Molar ratio of the species obtained in situ



Scheme 2. Synthesis of diaurated species from alkynols.

vents provided the most practically simple and reliable route for generation of diaurated species not only for characterization purposes, but also for the subsequent direct study in solution. This is associated with the following benefits: mixtures of proton sponge and its salt (bearing weakly and non-nucleophilic counterions such as OTf^- or SbF_6^-), which are present as byproducts in solution, form separate, sharp, easily integrated signals that enable accurate quantitative analysis of the NMR spectra (a representative NMR spectrum of the reaction mixture is given on Figure 2). Next, PrSpH^+ can be easily neutralized by using a base that is not soluble in the organic solvent. This provided, after filtration, clear solutions of untouched diaurated species free of active protons, which is necessary for the subsequent generation of vinyl gold species and for study of the equilibrium between vinyl gold and diaurated species. For this purpose, LiOH or K_2CO_3 were successfully used. Further, in case of volatile enol ethers, they can be completely evaporated from the reaction mixture in vacuo to provide simplification of the mixture upon subsequent dissolution. Since diaurated species are formed in competitive conditions, an excess of alkynol should be used, typically 2 equiv. It can be said that the use of proton sponge simply ensures strong inhibition of the catalytic reaction, which virtually stops as soon as all the gold is bound in the form of diaurated species.

We applied these conditions to a series of 3-alkyne-1-ols and a series of mononuclear gold catalysts **1–7** and found that 5-*endo* diaurated species **D1–D10** were successfully formed as the only organogold products in all the cases without exclusion in 99% in situ yield (Scheme 2). With cat-

alysts **1–3**, **5**, and **7** the reaction is essentially clean, generating the diaurated species, enol ethers, PrSpH^+ , and free MeCN as the only new components of the mixture (also shown in Figure 2).^[13]

In a completely similar manner as was performed with 3-alkyne-1-ols, we conducted reactions with other alkynols with the aim of collecting characterization data for the corresponding diaurated species **D16–D23** (Scheme 2). Interestingly, 4-alkynols reacted with catalysts **2** and **7** selectively providing 5-*exo* diaurated species **D18**, **D19**, and **D21** (however the corresponding enol ethers are still obtained as mixtures of 5-*exo*/6-*endo* isomers with low selectivity). This indicates that even if the cyclization event is not selective, the corresponding 5-*exo*/6-*endo* isomers of vinyl gold **B** bearing the bulky ligands differ enough in reactivity so that the 5-*exo* diaurated species is formed preferentially or even exclusively (Scheme 3). In contrast, catalyst **1** normally provided a mixture 5-*exo*/6-*endo* species **D16** and **D17** with low selectivity (1:1.6 ratio). The following general reactivity series was observed for substrates: 3-yne-1-ols > 4-yne-1-ols \gg 5-yne-1-ols. The former two types reacted rather instantly (ca. 5 min), whereas the latter required prolonged time and/or heating.

The described approach is not only applicable for the efficient generation of diaurated species in situ, but also for synthesis of these compounds in their individual state. In this study, six examples of diaurated species (**D1–3**, **D5**, **D19**, and **D22**) were isolated as stable hexafluoroantimonate solid salts in 44–90% yields (Scheme 2). Even though complete conversion of the starting gold complexes to diaurated

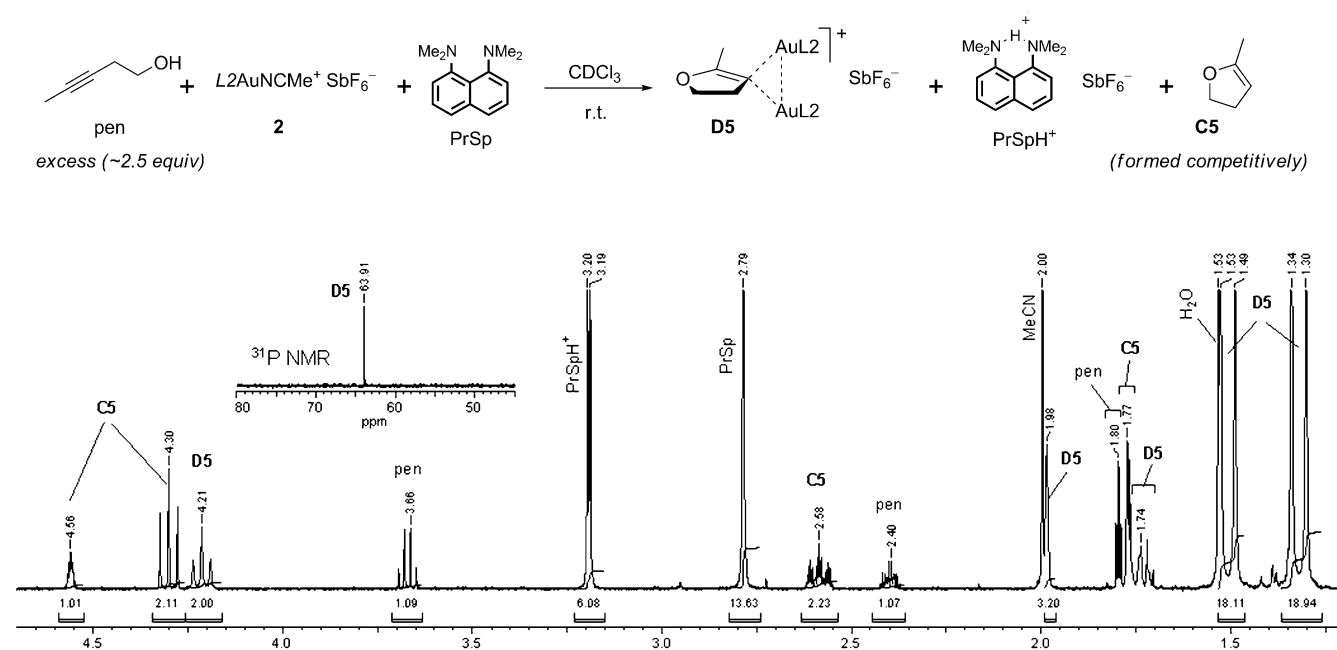
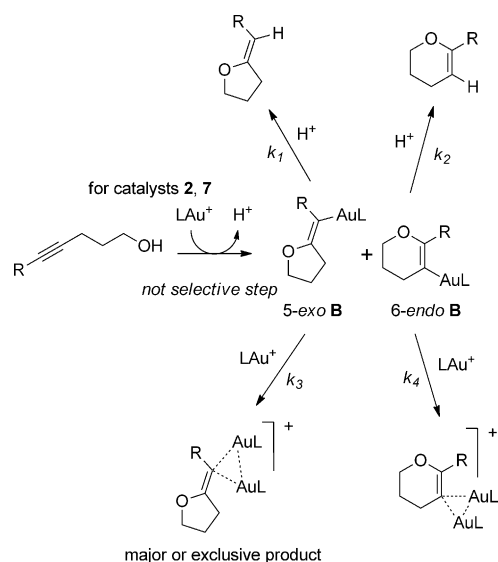


Figure 2. Representative ^1H NMR spectrum of the reaction mixture generated from pentynol (pen), gold catalyst **2**, and the proton sponge (PrSp) in CDCl_3 . Assignments of all peaks are given. The spectrum shows the presence of enol ether **C5** and diaurated species **D5** in a ratio of about 1.05:1. The $\text{CH}_2\text{-OR}$ peaks appear as apparent triplets at $\delta = 4.30$ and 4.21 ppm, respectively. The *tert*-butyl groups in each of the phosphine ligands are diastereotopic and additionally are split up due to the coupling with the phosphorus atom. They integrate well with regard to the protons in **D5**. The ^{31}P NMR (inset) confirms the formation of **D5** as a single organogold product.



Scheme 3. Kinetic resolution concept to explain predominant formation of 5-*exo* diaurated species.

species was always reached in situ, the yield of the isolated species was naturally dependent on the success in recrystallization, which was performed on a 20–100 mg reaction scale.

All new diaurated species were characterized by various NMR spectroscopic methods and ESI mass spectra (see the Experimental Section and the Supporting Information). In the ESI mass spectra, the species show a strong, easily detectable signal of the cation in the positive mode and the corresponding anion signal in the negative mode. Their common feature in ¹H NMR spectra is always the simple pattern of enol ether signals (e.g., always one triplet for CH₂O unit), whereas the pattern of ligand signals may be different depending on molecular dynamics and symmetry. For example, the diaurated species derived from *L*2 always exhibit two doublets for *t*Bu residues instead of only one in the catalyst. This is a consequence of the symmetrical structure of diaurated species, which possesses only one symmetry element: the symmetry plane passing through the enol ether unit, as exemplified in Figure 3.

This symmetry plane is now perpendicular to the symmetry planes of the ligands, meaning that the elements of the ligands being previously in equivalent environments are now no longer equivalent and exhibit different chemical shifts, that is, they are diastereotopic. The enol core/ligand 1:2 ratio is simply established in all cases by integration and is indicative to the overall molecular composition of the species.

In the ³¹P NMR spectra, all diaurated species (derived from mononuclear catalysts 1–5) exhibit a single resonance, which is in accordance with the symmetry of the species.

In the ³¹P NMR spectra, all diaurated species (derived from mononuclear catalysts 1–5) exhibit a single resonance, which is in accordance with the symmetry of the species.

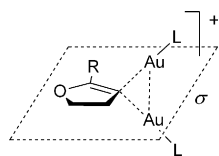


Figure 3. Symmetry plane passing through the enol ether unit accounts for the NMR spectroscopic features observed.

Several attempts to measure the ¹⁹F resonance of SbF₆[−], either in diaurated species or in starting catalysts, were all unsuccessful as no signal appeared. ¹⁹F NMR data is applicable only for *L*5 derivatives; giving signals of the CF₃ group around $\delta = -63$ ppm.

In four cases (**D1–3** and **D19**) ¹³C NMR spectra were recorded. Here, the observation of the CAu₂ *ipso*-carbon signal is very intriguing since this signal is often not found, especially in case of known aryl diaurated species Ar(AuL)₂⁺. In our case, a small triplet, almost equal to noise, was observed around $\delta = 100$ ppm in all the four carbon spectra. In the HMBC spectra of **D1** and **D2** this signal shows no cross-peaks, but in the other two cases clear cross-peaks were observed, proving that this weak signal is not noise, but the necessary carbon signal (Figure 4). The ²*J*_{C–P}

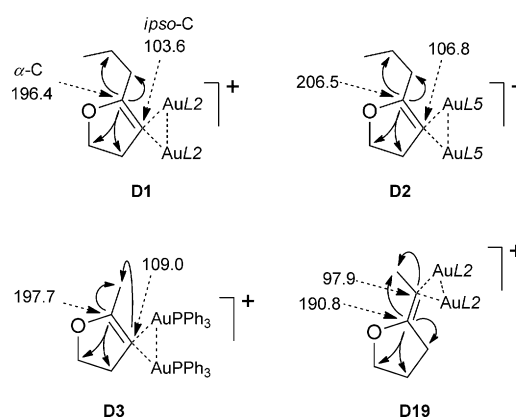


Figure 4. Key HMBC correlations (arrows) and chemical shifts of α - and *ipso*-carbon signals (dashed arrows) in diaurated species **D1–3** and **D19**.

coupling constant was found to be 58–65 Hz, the same as was earlier reported by the group of Fürstner.^[11] It can be concluded, that in contrast to aryl-based diaurated species Ar(AuL)₂⁺, enol ether-derived diaurated species should generally exhibit this signal in NMR spectroscopic analyses. Likely in Ar(AuL)₂⁺ this signal is also not absent, but difficult to recognize because it might be hidden in the aromatic region behind other stronger signals. Another important feature in the ¹³C NMR spectra is the appearance of the α -C atom at relatively low fields at $\delta = 191$ –207 ppm. Interestingly, in HMBC spectra this carbon gives strong cross-peaks to all the hydrogen atoms located up to three bonds away (Figure 4).

In addition to the spectroscopic methods, in one case the structure of diaurated species was fully confirmed by X-ray analysis (**D1**, Figure 5). In the X-ray structure an apparent aurophilic interaction (Au–Au 2.95 Å) is still present despite the large size of the ligand. The C=C (136.3 pm) bond is lengthened and the C–O to the enol ether carbon (134.0 pm) is shortened compared with normal enol ether geometry, in complete accordance with previous observations.^[11]

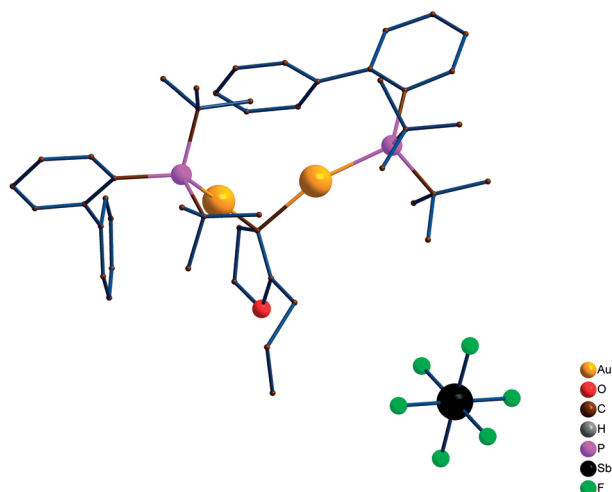
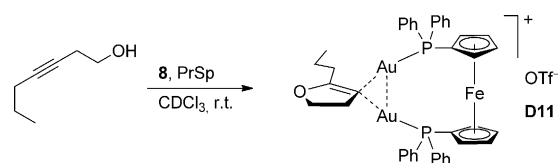


Figure 5. X-ray structure of the diaurated complex **D1**.

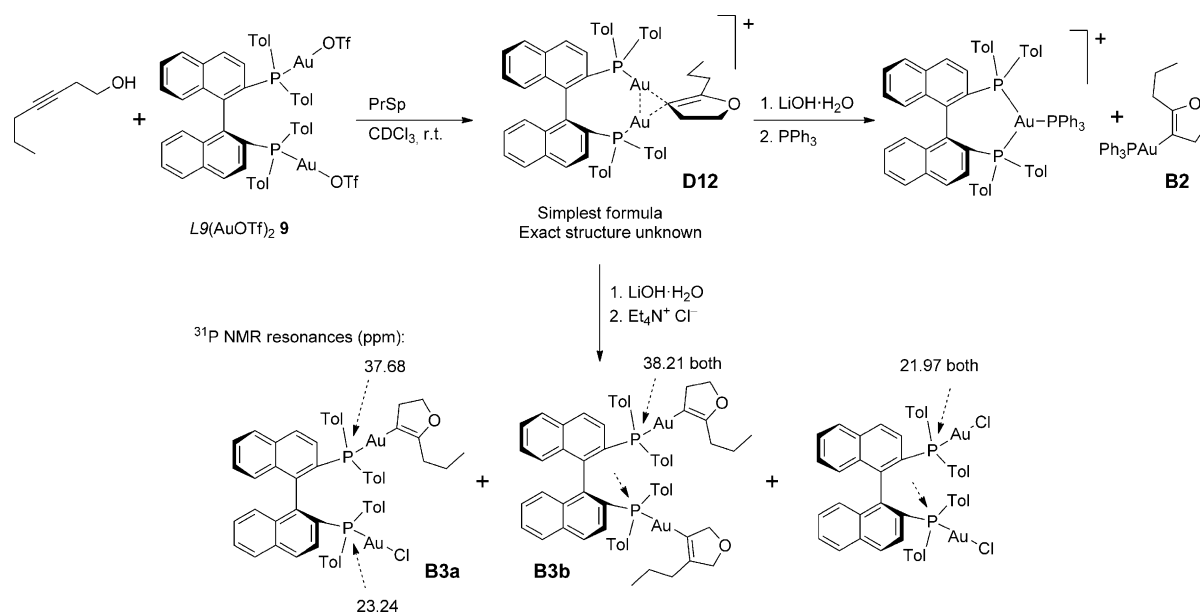
Formation of diaurated species from binuclear catalysts: Besides the mononuclear catalysts, we also examined three binuclear ones (**8–10**) in reaction with 3-heptyn-1-ol under standard conditions. Theoretically, from a binuclear gold catalyst one may expect formation of a cyclic diaurated species. This was indeed found to be true in the case of catalyst **8** giving cyclic diaurated species **D11**, whose composition was established by NMR spectroscopy showing a single set of signals of the enol ether core, a single phosphorus resonance and a single molecular ion peak at 1059.11573 in the ESI-HRMS spectrum (Scheme 4).

In contrast to catalyst **8**, binuclear catalysts **9** and **10** displayed some peculiarities that deserve special attention. Thus, diaurated species obtained from **9** exhibited a very complicated inconclusive ^1H NMR spectrum. No informa-



Scheme 4. Formation of the dppf-derived diaurated species **D11**.

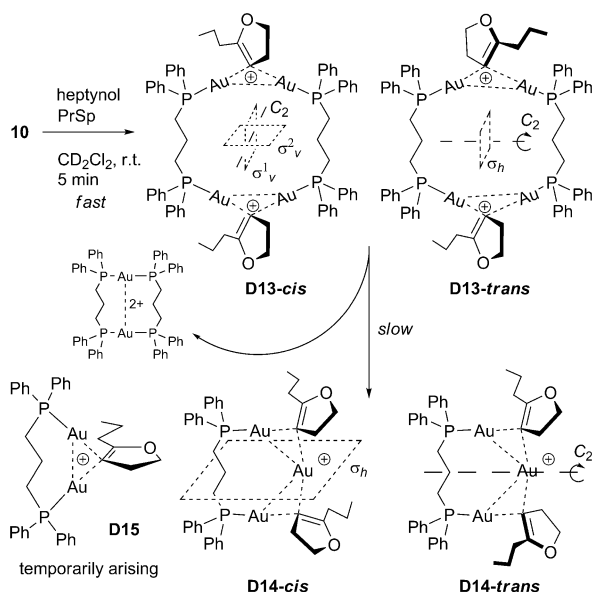
tion could be obtained also from ^{31}P NMR spectroscopy, which showed a number of weak broad resonances. This precluded us from establishing the exact composition of this material. However, ESI-HRMS analysis of the reaction mixture exhibited a signal at m/z 1183.27406, which is consistent with the presence of diaurated species **D12** with the molecular composition as shown in Scheme 5; their monomeric monocationic composition was evident from the isotope pattern. However, it cannot be excluded that this is a result of the HRMS conditions and that in the normal reaction mixture at room temperature, oligomeric diaurated species of irregular or unknown structure might also be present. Therefore, although a species with the exact structure as shown for **D12** might exist, we may not confirm if this is the only possible component in the mixture. Anyway, whatever the exact structure is, the conclusion that this substance has to consist of diaurated units follows from the experimental observations performed on this material in situ (Scheme 5). We found that it reacted with excess PPh_3 to give a clear mixture of PPh_3 -derived vinyl gold **B2** and (*S*)-Tol-BINAP- AuPPh_3^+ as a byproduct.¹⁴ In another experiment, it was treated with $\text{Et}_4\text{N}^+\text{Cl}^-$. NMR spectra of the resulting mixture clearly indicated formation of two kinds of vinyl gold species (assigned to **B3a** and **B3b**) and the corresponding (*S*)-Tol-BINAP(AuCl)₂ complex. This also proved that the initial chaotic spectrum for the diaurated species with the



Scheme 5. Observation of diaurated species **D12** with unknown structure and subsequent transformations to confirm the diaurated nature of the compound. Key phosphorus resonances are shown (dashed arrows).

simplest structure **D12** is not the sign of decomposition or some undesired process, but indicates the unusual complexity of the system, which cannot be conveniently analyzed by room-temperature NMR spectroscopy.

In case of catalyst **10**, interesting chemistry was also observed. The diaurated species generated from 3-heptyn-1-ol, the proton sponge, and the catalyst in CD_2Cl_2 rather unexpectedly displayed two triplets for the CH_2O units. In the ^{31}P NMR spectrum, two clear resonances at $\delta=32.4$ and 30.3 ppm were observed. The H,H-COSY spectrum indicated that the CH_2O triplets belong to two different enol ether units. Even more surprisingly, monitoring the reaction mixture revealed the evolution of this diaurated species; in the ^{31}P NMR spectrum, the two initial resonances gradually disappeared and four new signals arose at $\delta=41.4$, 35.9 , 35.7 , and 32.0 ppm, respectively. With a longer reaction time, the signal at $\delta=32.0$ ppm also disappeared so that at the end only the three signals remained. At this point, the ^1H NMR spectrum showed the CH_2O units as two multiplets, indicative of an asymmetric environment. The resonance at $\delta=41.4$ ppm was assigned to $[\text{dpppAu}]_2^{2+}$, which exists as dimeric dication. Accordingly, the two remaining signals were therefore assigned to new gold complexes. These interesting observations are explained as follows (Scheme 6). Initial observation of the two enol ether residues and the two phosphorus resonances indicates that the dimeric diaurated species **D13** is formed, which naturally exists as a mixture of two geometric isomers, giving duplication of spectra. Due to symmetry reasons, each isomer exhibits a single phosphorus resonance and a single CH_2O triplet (homotopic groups). With time, this compound expels a $[\text{dpppAu}]_2^{2+}$ unit and gives rise to a triaurated species **D14**, which features a sandwich-type complexed gold and exists also as a pair of geometric *cis/trans* isomers. Due to the lack of a symmetry plane passing through each enol ether ring, the CH_2O protons are now diastereotopic and give more complicated pat-

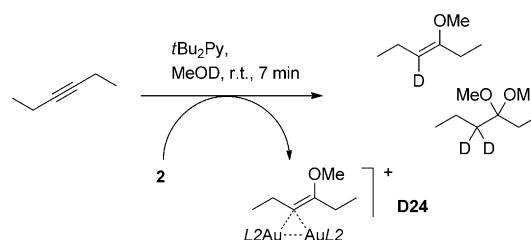


Scheme 6. Evolution of $(\text{dppp})\text{Au}_2^{2+}$ -derived diaurated species.

terns, whereas in the ^{31}P NMR spectrum, each isomer exhibits a single resonance due to the equivalence of both phosphorus atoms in each isomer. The remaining signal at $\delta=32.0$ ppm was tentatively assigned to monomeric diaurated species **D15** temporarily arising in the reaction mixture. These conclusions are supported by ESI-HRMS of the reaction mixture, which exhibits the following ions: m/z 1225.21283 (**D14**), 917.16416 (**D15**), and 609.153 for $[\text{dpppAu}]_2^{2+}$. The isotope pattern of the ion at m/z 917.16416 corresponded exclusively to a single charged cation. Unfortunately, the formation of dimeric dicationic species **D13** could not be confirmed by ESI-HRMS, but their existence follows from the aforementioned features of the NMR spectra.

Synthesis of diaurated species from intermolecular hydroalkoxylation:

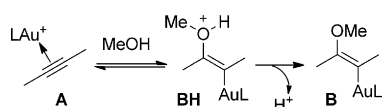
The possibility to synthesize diaurated species from simple internal alkynes and alcohols in an intermolecular manner was also briefly investigated. Thus, when 3-hexyne was treated with complex **1** or **2**, the proton sponge or *t*Bu₂Py, and an excess of MeOH in CDCl_3 no reaction with the organic substrate was observed (aurated oxonium ion was the only product). But when methanol was used as a solvent, diaurated species **D24** could be quickly generated, as evidenced by the appearance of the corresponding signals in the NMR spectra (Scheme 7). However, conversion of **2**



Scheme 7. Formation of diaurated species **D24** from hexyne, MeOH, and complex **2** in presence of *t*Bu₂Py.

to **D24** reached only about a 60% maximum, with the remainder of material being the unbound form of the catalyst. Further monitoring of the reaction mixture after a prolonged time revealed a decrease in diaurated species as consumption of 3-hexyne progressed. This implies that **D24** is not entirely stable under the reaction conditions, eventually slowly turning back to the free catalyst when 3-hexyne is no longer available.

The ability of the reaction to occur only in the presence of a huge excess of an alcohol (taken as a solvent) underscores the high reversibility of the primary interaction between the alcohol and an alkyne π -complex, which is now intermolecular and more strongly shifted to the left compared with the intramolecular process in alkynols, slowing down the overall process. The same phenomenon explains the aforementioned reactivity series for alkynols (Scheme 8).



Scheme 8. Reversibility of the initial interaction between an alcohol and an alkyne π -complex.

Use of aurated oxonium salts and gold hydroxide as gold sources:

Besides the LAu^+/PrSp combination, we also considered the possibility to use aurated oxonium salts as precursors for diaurated species. Recently diaurated oxonium salts $(\text{LAu})_2\text{OH}^+$ have been described.^[15,16] These compounds can be viewed as being constructed from two LAu^+ electrophilic units and one basic OH^- unit, which represents a gold/base 2:1 stoichiometry that is exactly required for the synthesis of diaurated species. Accordingly, one might anticipate the direct synthesis of diaurated species without using additional base, according to Equation (1) in Scheme 9. This



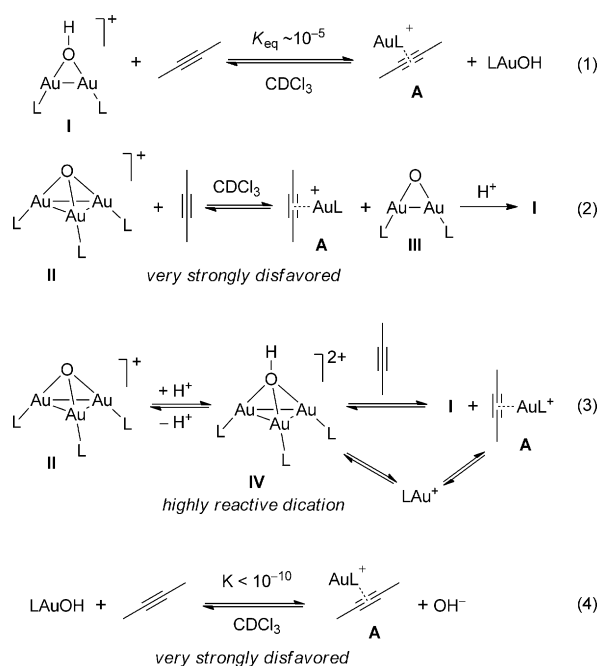
Scheme 9. Reactions of alkynols with oxonium salts (hypothetical balanced equations, see main text for the experimental results).

possibility was verified and was found to be true. Indeed, $(\text{L}2\text{Au})_2\text{OH}^+$ was smoothly converted to diaurated species **D1** upon simple treatment with heptynol. However, the process was again accompanied with competitive enol ether formation so that the overall result is similar to the case of the cat. **2**/PrSp combination.

Correspondingly, triaurated oxonium salts would be expected to react with an alkynol to give a mixture of vinyl gold and diaurated species according to Equation (2) in Scheme 9. Surprisingly, $(\text{Ph}_3\text{PAu})_3\text{O}^+$ reacted only very sluggishly with heptynol to give the diaurated species and Ph_3PAuCl as the only gold products.^[17] Notably, if $(\text{Ph}_3\text{PAu})_3\text{O}^+$ was allowed to react with heptynol in the presence of proton sponge salt PrSpH^+ , diaurated species **D4** was immediately formed according to general Equation (3) in Scheme 9.

Finally, gold hydroxides LAuOH , a new type of useful gold compounds, can be envisaged as potential precursors for direct vinyl gold synthesis, avoiding diaurated species formation, according to Equation (4) in Scheme 9. However, treatment of $\text{L}2\text{AuOH}$ with heptynol in C_6D_6 demonstrated that this is hardly applicable in practice; monitoring the reaction mixture at room temperature revealed gold alkoxide $\text{L}2\text{AuOR}$ formation as the only process. At elevated temperatures, some quantity of vinyl gold could be generated, but the process was largely accompanied by decomposition and therefore cannot be considered of practical value.

The different reactivity of these oxo-compounds is in line with their different ability to undergo ligand exchange with an alkyne to generate alkyne π -complex **A**. The formation of this common active intermediate of gold-catalyzed hydroalkoxylation is the initial step of the whole process. Naturally, the more stable the gold compound is towards the ligand exchange, the less reactive it is. Thus, the $(\text{LAu})_2\text{OH}^+$ **I** species appears to be the most active because it is able to interact already with weak nucleophiles to give reversibly LAuNu^+ and LAuOH , which was already demonstrated in our previous work. According to our ligand strength series,^[15] the K_{eq} for reaction of $(\text{LAu})_2\text{OH}^+$ with an alkyne is expected to be approximately 10^{-4} to 10^{-5} . This value appears to be high enough to trigger fast formation of diaurated species ([Eq. (1)] in Scheme 10). In contrast to **I**,



Scheme 10. Initial steps in reaction of aurated oxonium salts and LAuOH with an alkyne. L = phosphine ligand.

$(\text{LAu})_3\text{O}^+$ **II** appears to be a more stable complex with the charge stabilized on all three gold units and being additionally stabilized with more aurophilic interactions (three vs. one in **I**). Not surprisingly, the extremely low reactivity of **II** alone is explained by its virtual inability to interact with an alkyne to give **A**. Indeed, the aurophilic interactions would be broken and currently non-existing $(\text{LAu})_2\text{O}$ **III** would be formed in such a process ([Eq. (2)] in Scheme 10). This also explains why $(\text{LAu})_3\text{O}^+$ would be inefficient as a catalyst for a catalytic process.^[18] However, the reactivity of **II** gets drastically increased in the presence of an acidic promoter. This acceleration effect may be explained in two ways. First, the acid would allow a fast and irreversible protonation of **III** to give **I**, pushing the initially disfavored equilibrium to the right ([Eq. (2)] in Scheme 10). Second, the acid would

allow protonation of **II** itself to reversibly form a hypothetical dication **IV** as intermediate or transition state ([Eq. (3)] in Scheme 10). This species should be highly reactive towards even weak nucleophiles such as alkyne, making the formation of **A** easy. Of these two hypotheses, the former is less feasible because if the formation of **III** would be possible at all, it would definitely not hesitate to deprotonate any other molecules in solution (H_2O , CDCl_3 , alkynol) that are already acidic enough.^[19] So there would be no need to use any additional stronger proton source to enhance the reactivity of gold. Rather, the latter hypothesis gains strong support from the fact, that $(\text{LAu})_3\text{O}^+$ can be aurated to form the isolable dicationic $(\text{LAu})_4\text{O}^{2+}$, as was established by Schmidbaur and co-workers almost 20 years ago.^[20] It can be concluded, that despite being cationic, cation **II** still has the ability to add electrophiles and undergo electrophilic substitution at oxygen through these reactive dicationic adducts.^[21] Therefore, we conclude that protonation of $(\text{Ph}_3\text{PAu})_3\text{O}^+$ to form **IV** is indeed necessary prior to formation of the active species **A**.^[22,23] This was previously not recognized. Being formed, dication **IV** would either undergo ligand exchange to give **A** or would dissociate spontaneously to active gold electrophile LAu^+ eventually also leading to **A**.

Similarly as was described for **II**, the extremely low reactivity of gold hydroxide LAuOH in forming vinyl gold species is also explained by its inability to form **A** in the corresponding ligand-exchange reaction ([Eq. (4)] in Scheme 8). As can be understood from our ligand strength series,^[15] the equilibrium between LAuOH and an alkyne can be estimated to be far beyond 10^{-10} , virtually making alkyne activation impossible. Naturally, an alkyne is unable to displace OH^- from gold! Likewise it was described for **II**, LAuOH also requires an acidic promoter to initiate the reaction (being a strong base it will react with H^+ to release the active LAu^+ catalyst and H_2O).

Conclusion

We have demonstrated that enol ether-derived diaurated species can be directly obtained from cationic gold(I) catalysts and alkynols by using a proton sponge as a base or by using diaurated oxonium salt $(\text{LAu})_2\text{OH}^+$ as the sole reactant. Other oxo compounds of gold $(\text{LAu})_3\text{O}^+$ and LAuOH were found to be almost inactive towards alkynols, which was explained by their inability to interact with the $\text{C}\equiv\text{C}$ bond due to increased stability of these complexes towards nucleophilic attack. This study demonstrates that the formation of diaurated species is generally not precluded even by bulky ligands at gold. This has led to the development of a practical general route for the synthesis of diaurated species in situ or in an individual state. The described synthesis occurs in catalytically relevant manner, that is, it must follow the same mechanism as shown in Scheme 1, but the catalytic turnover is blocked by trapping active protons. This suggests the involvement of diaurated species also in a standard catalytic hydroalkoxylation process, which was

indeed proven by direct observation of the species in situ during catalytic runs.^[24] Extensive studies on the role of these species as catalytic intermediates in gold catalysis are underway in our laboratory.

Experimental Section

General: Since the exact outcome of the competition between auration/protodeauration was a priori not known, the following syntheses were performed under NMR control. All manipulations were performed without the use of an inert atmosphere.

Synthesis of **D1:** In one shot, complex **2** (78.9 mg, 0.102 mmol, 2.00 equiv) was added to a solution of 3-heptynol-1 (17.07 mg, 0.152 mmol, 2.98 equiv) and the proton sponge (15.1 mg, 0.0706 mmol, 1.38 equiv) in CDCl_3 (1.4 mL), with the reaction flask being shaken by hand. A white crystalline precipitate appeared soon ($\text{PrSpH}^+\cdot\text{SbF}_6^-$). After being shaken for 1 min, a part of the solution was transferred into an NMR tube. ^1H and ^{31}P NMR analysis revealed complete consumption of the starting complex and formation of diaurated species as a sole gold-containing product. The molar ratio of the components in the reaction mixture at this moment was enol ether/**D1**/heptynol/ $\text{PrSp} = 1:1.08:1.22:0.44$. TLC analysis indicated the presence of unreacted heptynol and the remainder of the material simply stayed on the starting line (petroleum ether/ EtOAc , 2:1). Since the starting heptynol and proton sponge were still available in the mixture, the content of the NMR tube was combined with the rest of the material and an additional amount of **2** (24.9 mg 0.032 mmol, 0.63 equiv) was added and the mixture was analyzed again after 5 min. ^1H and ^{31}P NMR analysis now indicated a ratio enol ether/**D1**/heptynol/ $\text{PrSp} = 1:1.17:0.49:0.10$. At this moment, the reaction mixture was filtered to separate most of the $\text{PrSpH}^+\cdot\text{SbF}_6^-$ from the system (the filter cake was washed with CDCl_3). Since the final product will be obtained by crystallization from benzene, the rest of proton sponge salt has to be neutralized because it is also insoluble in benzene. For this purpose, freshly powdered $\text{LiOH}\cdot\text{H}_2\text{O}$ (43 mg) was added to the clear filtrate and the suspension was ultrasonicated for 3 min (Note: NMR analysis indicated that still some quantity of PrSpH^+ was present in solution and more $\text{LiOH}\cdot\text{H}_2\text{O}$ powder (56 mg) was added). At this moment, NMR indicated complete disappearance of PrSpH^+ . Then, the suspension was filtered through celite and the filter cake washed with CH_2Cl_2 . The clear filtrate was transferred to a weighted receiver flask and evaporated in vacuo until dry (the volatile enol ether also disappeared at this stage). The residue was redissolved in a minimum volume of CH_2Cl_2 and layered with benzene; tiny crystal needles soon appeared. As most of the material had crystallized, the mixture was concentrated to further remove CH_2Cl_2 and a fresh portion of benzene (about 1 mL) was added. The final product is insoluble in benzene and the supernatant solution was easily removed by filtration performed by using a Pasteur pipette with a piece of cotton at the end. The crystalline material in the flask was washed twice with benzene and dried in vacuo to yield the diaurated species (87.2 mg, 90%) as very small white needles. NMR analysis confirmed that the compound crystallized as benzene solvate (1 molecule of benzene per 1 molecule of the cation). These crystals were unsuitable for X-ray analysis; the benzene-free material obtained by crystallization from CH_2Cl_2 /pentane was also unsuitable. Finally, we found that the compound was sparingly soluble in methanol and simple crystallization from this solvent provided very good crystals for X-ray analysis, containing no encapsulated solvent molecules. ^1H NMR (400 MHz, CDCl_3): $\delta = 7.87\text{--}7.93$ (m, 2H), 7.48–7.52 (m, 4H), 7.32–7.43 (m, 6H), 7.26 (d, 2H), 7.08–7.16 (m, 4H), 4.20 (t, $J = 9.3$ Hz, 2H), 2.28 (m, 2H), 1.67 (t, $J = 9.3$ Hz, 2H), 1.74 (overlapped sextet, $J = 7.4$ Hz, 2H), 1.51 (d, $J = 15.3$ Hz, 18H), 1.32 ppm (d, $J = 15.2$ Hz, 18H), 0.88 (t, $J = 7.4$ Hz, 3H); ^{31}P NMR (162 MHz, CDCl_3): $\delta = 63.94$ ppm; ^{13}C NMR (100 MHz, CDCl_3): $\delta = 196.4$ (t, $J = 2.9$ Hz), 149.0 (d, $J = 14.6$ Hz), 142.7 (d, $J = 5.9$ Hz), 134.47, 133.9 (d, $J = 7.3$ Hz), 130.9, 130.1, 129.6, 128.4, 127.9, 127.1 (d, $J = 5.9$ Hz), 125.2 (d, $J = 39.5$ Hz), 103.6 (t, $J = 60$ Hz), 74.4, 38.01 (d, $J = 22.7$ Hz), 37.97 (d, $J = 21.2$ Hz), 36.3, 35.9, 31.5 (d, $J = 7.3$ Hz), 30.7 (d, $J = 6.6$ Hz),

22.6, 14.2 ppm; HRMS (ESI) m/z calcd for $C_{47}H_{65}Au_2OP_2^+$: 1101.3836 [M^+]; found 1101.3832.

Note: Later we found that $PrSpH^+ \cdot SbF_6^-$ in chloroform solutions is much more readily neutralized by freshly powdered K_2CO_3 (by shaking the reaction mixture for 10 seconds, without ultrasound). This does not apply however for CH_2Cl_2 , in which $PrSpH^+ \cdot SbF_6^-$ is much more soluble. Also, the rate of neutralization is dependent on the amount or residual water in solution; it occurs more sluggishly in a highly dry (freshly opened) $CDCl_3$.

Synthesis of D2: Since the corresponding fast-forming oxonium species ($L5Au$) $_3O^+$ is not soluble in $CDCl_3$, thus preventing the formation of diaurated species, this synthesis should be performed in CH_2Cl_2 . In one shot, complex **5** (81.8 mg, 0.0715 mmol, 2.00 equiv) was added to a solution of 3-heptynol-1 (8.03 mg, 0.0706 mmol, 1.97 equiv) and the proton sponge (12 mg, 0.0561 mmol, 1.57 equiv) in CD_2Cl_2 (0.7 mL), with the reaction flask being shaken by hand. The resulting solution was filtered by using cotton and a Pasteur pipette (to remove traces of Ag_2O , coming from Ag^+ impurity in the catalyst) and transferred into an NMR tube. 1H and ^{31}P NMR analysis revealed complete consumption of the starting complex and formation of diaurated species as a sole gold-containing product. The molar ratio of the components in the reaction mixture at this moment was enol ether/**D2**/heptynol = 0.59:1:0.60. Then, freshly powdered K_2CO_3 was added and the reaction mixture was shaken and analyzed by NMR from time to time to observe sluggish neutralization of $PrSpH^+$. This way approximately 80% of the proton sponge was neutralized. Since we planned to obtain the final product by crystallization from MeOH, we hypothesized that minor quantities of $PrSpH^+$ would not cause problems. Also we knew that this diaurated species will slowly decompose if excess of base is present in solution. Therefore, without waiting for complete neutralization the suspension was filtered through celite (the filter cake was washed with CH_2Cl_2) and the clear filtrate was transferred to a weighted receiver flask and evaporated in vacuo until almost dry (the diaurated species had crystallized already during the time of evaporation). The wet residue (containing tiny crystal needles) was mixed with methanol and allowed to stay in the cold for about 30 min. The supernatant solution was easily removed by filtration performed by using a Pasteur pipette with a piece of cotton at the end, the crystals washed with cold MeOH and dried in vacuo to yield diaurated species (34.9 mg, 47%) as white needles. The material additionally obtained from the mother liquor was of bad quality and therefore was disregarded. Surprisingly, the compound was found to be insoluble in $CDCl_3$. 1H NMR (400 MHz, CD_2Cl_2): δ = 8.20 (s, 6H), 7.98 (d, J = 12.4 Hz, 12H), 4.77 (t, J = 9.1 Hz, 2H), 2.97 (t, J = 9.1 Hz, 2H), 2.82 (t, J = 7.4 Hz, 2H), 1.74 (sextet, J = 7.4 Hz, 2H), 0.91 ppm (t, J = 7.4 Hz, 3H); ^{31}P NMR (162 MHz, CD_2Cl_2): δ = 40.77 ppm; ^{19}F NMR (376 MHz, CD_2Cl_2): δ = -63.69 ppm; ^{13}C NMR (100 MHz, CD_2Cl_2): δ = 206.5 (t, J = 4 Hz), 134.3 (d, J = 16 Hz), 134.0 (dq, J_P = 12 Hz, J^F = 35 Hz), 130.2 (d, J = 55.6 Hz), 128.0, 122.7 (d, J^F = 273 Hz), 106.8 (t, J = 66 Hz), 77.7, 36.8, 24.0, 13.9.

Synthesis of D3: Complex **1** (58.5 mg, 0.0795 mmol, 2.00 equiv) was added in one shot to a solution of 3-pentynol-1 (11.5 mg, 0.137 mmol, 3.4 equiv) and the proton sponge (16.5 mg, 0.0771 mmol, 1.9 equiv) in $CDCl_3$ (1.4 mL), with the reaction flask being shaken by hand. A white crystalline precipitate soon appeared ($PrSpH^+ \cdot SbF_6^-$). After being shaken for 1 min, part of the solution was transferred into an NMR tube. 1H and ^{31}P NMR analysis revealed complete consumption of the starting complex and formation of diaurated species as a sole gold-containing product. The mole ratio of the components in the reaction mixture at this moment was enol ether/**D3**/pentynol/ $PrSp$ = 0.67:1:1.03:0.43. Since the starting pentynol and proton sponge were still available in the mixture, the content of the NMR tube was combined with the rest of the material and additional **1** (28.7 mg) was added and the mixture analyzed again after 5 min; however, that was still not enough and more **1** (5.07 mg) was added. At this moment the reaction mixture was filtered to separate most of $PrSpH^+ \cdot SbF_6^-$ from the system (the filter cake was washed with $CDCl_3$). Freshly powdered K_2CO_3 (19 mg) was added to the clear filtrate and the suspension was briefly shaken (the crystals changed their appearance almost instantly) and then ultrasonicated for 5 more seconds. NMR analysis indicated complete disappearance of $PrSpH^+$ and even that

traces of $(Ph_3PAu)_3O^+$ formed, so even this short ultrasonication was not necessary. Then the suspension was filtered through celite and the filter cake washed with CH_2Cl_2 directly to a weighted receiver flask and evaporated in vacuo until dry (volatile enol ether also disappeared at this stage). As judged by NMR spectroscopy, the oily residue was already quite pure diaurated species, the mole ratio of the components in the mixture was diaurated/pentynol/ $PrSp$ = 1:0.09:0.20 (which could be \approx 94% mass of pure material). The subsequent crystallization of the material proved more difficult than in other cases. Attempted crystallization from CH_2Cl_2 /pentane was unsuccessful (the concentrated oily residue remained uncrystallized even if cooled to $-30^\circ C$). The use of CH_2Cl_2 /MeOH proved more successful: the product crystallized soon as a solid powder. Obviously, crystal growth rate is rather slow. Nevertheless, the pure product was obtained as creamy, very small crystals after several attempts of crystallizations from CH_2Cl_2 /MeOH. Cold MeOH should be always used because of the moderate solubility of the product. Bigger crystals arose from slow evaporation of the mother liquor. The product is well soluble in CH_2Cl_2 , chloroform, sparingly soluble in MeOH. With benzene it forms an insoluble oil (so crystallization from benzene is practically impossible). 1H NMR (400 MHz, $CDCl_3$): δ = 7.46–7.55 (m, 6H), 7.36–7.42 (m, 24H), 4.69 (t, J = 9.1 Hz, 2H), 2.87 (t, J = 9.1 Hz, 2H), 2.52 ppm (s, 3H); ^{31}P NMR (162 MHz, $CDCl_3$): δ = 37.07 ppm; ^{13}C NMR (100 MHz, $CDCl_3$): δ = 197.7 (t, J = 4 Hz), 133.9 (d, J = 13.9 Hz), 132.2, 129.6 (d, J = 11.7 Hz), 128.7 (d, J = 57.1 Hz), 109.0 (t, J = 65 Hz), 76.0, 37.5, 20.2 ppm.

Synthesis of D5: Complex **2** (70.0 mg, 0.0907 mmol, 2.00 equiv) was added in one shot to a solution of 3-pentynol-1 (7.79 mg, 0.0926 mmol, 2.04 equiv) and a proton sponge (10.2 mg, 0.0477 mmol, 1.05 equiv) in $CDCl_3$ (0.7 mL), with shaking in hand. A white crystalline precipitate soon appeared ($PrSpH^+ \cdot SbF_6^-$). At this moment, the reaction mixture was filtered to separate the most of $PrSpH^+ \cdot SbF_6^-$ from the system (the filter cake was washed with $CDCl_3$). 1H and ^{31}P NMR spectroscopic analyses revealed complete consumption of the starting complex and formation of diaurated species as a sole gold-containing product. The molar ratio of the components in the reaction mixture at this moment was enol ether/**D5**/pentynol/ $PrSp$ = 0.98:1:0.02:0.06, indicating that the initial amounts of the reagents were chosen well and no corrections were required. Then freshly powdered K_2CO_3 (20 mg) was added for complete neutralization of the remaining $PrSpH^+$. The suspension was filtered through celite (the filter cake was washed with CH_2Cl_2) and the clear filtrate was transferred to a weighted receiver flask and evaporated in vacuo until almost dry. The residue was layered with methanol and allowed to remain at room temperature for 30 min and then cooled for about 30 min. Crystallization occurred smoothly and the cold supernatant solution was easily removed by using filtration performed with a Pasteur pipette with a piece of cotton at the end. The crystals were washed with cold MeOH and dried in vacuo to yield diaurated species (52 mg, 88%) as white needles. The compound was characterized by 1H , and ^{31}P NMR spectra. 1H NMR (400 MHz, $CDCl_3$): δ = 7.88–7.92 (m, 2H), 7.48–7.52 (m, 4H), 7.31–7.39 (m, 6H), 7.21 (d, 2H), 7.10–7.13 (m, 4H), 4.21 (t, J = 9.1 Hz, 2H), 1.98 (s, 3H), 1.74 (t, J = 9.1 Hz, 2H), 1.52 (d, J = 15.3 Hz, 18H), 1.32 (d, J = 15.2 Hz, 18H); ^{31}P NMR (162 MHz, $CDCl_3$): δ = 63.91 ppm; HRMS (ESI): m/z calcd for $C_{45}H_{61}Au_2OP_2^+$: 1073.3523 [M^+]; found 1073.3531.

Synthesis of D19: Complex **2** (39.0 mg, 50.5 μ mol) was added in one shot to a solution of 4-hexynol-1 (3.2 mg, 32.6 μ mol), the proton sponge (5.93 mg, 27.7 μ mol) in $CDCl_3$ (0.6 mL), with the reaction flask being shaken by hand. A white crystalline precipitate soon appeared ($PrSpH^+ \cdot SbF_6^-$). After 2 min, the supernatant solution was filtered into an NMR tube by using a piece of cotton and a Pasteur pipette. NMR examination revealed complete formation of diaurated species. The molar ratio of the components in the reaction mixture at this moment was 5-*exo* diaurated/6-*endo* diaurated/5-*exo* enol ether/6-*endo* enol ether/hexynol/ $PrSp$ = 1:0.08:0.06:0.07:0.07:0.05. From this spectrum it became clear that the initial amounts of the reagents were chosen well and no corrections were required. Next, the reaction mixture was treated with freshly powdered K_2CO_3 (ca. 15 mg) to achieve complete neutralization of $PrSpH^+$. Then the suspension was filtered through celite directly into a weighted receiver flask (the filter cake washed with CH_2Cl_2). The solution was evaporat-

ed in vacuo until dry (the volatile enol ethers also disappeared at this stage). The residue was diluted with few drops of CH_2Cl_2 and layered with benzene. Crystallization did occur, but the precipitate was too difficult to separate from the supernatant solution, therefore crystallization was performed with methanol (about 1 mL) at -30°C . The product was washed with cold methanol (-30 to -60°C). The solid residue was dried in vacuo to yield diaurated species (23 mg, 69%) as white needles. From the mother liquor, a mixture of 5-*exo* diaurated/6-*endo* diaurated species (1:0.13) could be obtained (6.5 mg). $^1\text{H NMR}$ (400 MHz, CDCl_3): δ = 7.87–7.91 (m, 2H), 7.45–7.50 (m, 4H), 7.25–7.38 (m, 6H), 7.08–7.17 (m, 6H), 4.46 (t, J = 6.7 Hz, 2H), 2.71 (t, J = 7.3 Hz, 2H), 2.04 (app pent, 2H), 1.49 (d, J = 15.2 Hz, 18H), 1.32 (d, J = 15.2 Hz, 18H), 1.05 ppm (s, 3H); $^{31}\text{P NMR}$ (162 MHz, CDCl_3): δ = 63.66; $^{13}\text{C NMR}$ (100 MHz, CDCl_3): δ = 190.8 (t, J = 3.3 Hz), 149.3 (d, J = 14.6 Hz), 142.6 (d, J = 5.9 Hz), 134.4, 133.8 (d, J = 8.0 Hz), 130.7, 129.5, 129.2, 128.4, 128.3, 128.1, 126.9 (d, J = 6.6 Hz), 125.4 (d, J = 38.8 Hz), 97.9 (t, J = 58 Hz), 73.8, 38.4 (d, J = 22.0 Hz), 38.3 (d, J = 20.5 Hz), 36.7, 31.5 (d, J = 7.3 Hz), 30.8 (d, J = 6.6 Hz), 24.5, 22.5; HRMS (ESI): m/z calcd for $\text{C}_{46}\text{H}_{63}\text{Au}_2\text{OP}_2^+$: 1087.3680 [M^+]; found 1087.3682.

Synthesis of D22: Complex **2** (24.0 mg, 31.1 μmol , 2.00 equiv) was added in one shot to a solution of 5-octynol-1 (2.22 mg, 17.6 μmol), the proton sponge (3.55 mg, 16.7 μmol , 1.07 equiv) in CDCl_3 (0.6 mL), with the reaction flask being shaken by hand. A white crystalline precipitate appeared soon ($\text{PrSpH}^+ \text{SbF}_6^-$). Because of insufficient rate of the 6-*exo* cyclization, the resulting rate of diaurated species formation is slow, therefore at this moment only oxonium salt (L_2Au) OH^+ was generated. After shaking for 1 min, the solution was filtered into an NMR tube using a piece of cotton and a Pasteur pipette. The reaction mixture was heated at 40°C for 30 min. After this time, NMR examination revealed complete consumption of octynol and formation of diaurated species, but the oxonium salt was still present. Therefore, more octynol (about 1 mg) was added and the reaction mixture was brought to a condition when only small traces of oxonium salt were present. Then, the reaction mixture was filtered once again and treated with freshly powdered K_2CO_3 (about 20 mg). NMR examination showed complete neutralization of PrSpH^+ . At this moment the reaction mixture was filtered through celite into a weighted receiver flask and evaporated in vacuo until dry (volatile enol ethers also disappeared at this stage). Then MeOH (about 0.8 mL) was added to the residue and the solution was kept at -30°C for 30 min. The product precipitated as a white solid. The supernatant solution was removed by using a Pasteur pipette with cotton. The solid was washed with small portions of cold (-30 to -60°C) MeOH and dried in vacuo to afford the first crop of the title compound as a white solid, 9.3 mg (44%). $^1\text{H NMR}$ (400 MHz, CDCl_3): δ = 7.88–7.92 (m, 2H), 7.44–7.48 (m, 4H), 7.29–7.39 (m, 6H), 7.03–7.17 (m, 6H), 4.32 (t, J = 6.0 Hz, 2H), 2.49 (t, J = 6.8 Hz, 2H), 1.95 (app. pent, 2H), 1.71 (app. pent, 2H), 1.51–1.58 (m, 2H), 1.469 (d, J = 15.2 Hz, 18H), 1.35 (d, J = 15.3 Hz, 18H), 0.60 (t, J = 7.4 Hz, 3H) ppm; $^{31}\text{P NMR}$ (162 MHz, CDCl_3): δ = 64.51 ppm; HRMS (ESI): m/z calcd for $\text{C}_{48}\text{H}_{67}\text{Au}_2\text{OP}_2^+$: 1115.3993 [M^+]; found 1115.3995.

Acknowledgements

We thank Dr. M. Ströbele for the X-ray analyses, Dr. D. Wistuba for HRMS analyses, Dr. K. Eichele and the Institut für Anorganische Chemie for allowing us to use their NMR spectrometer.

- [1] For reviews on gold catalysis, see: a) A. Corma, A. Leyva-Pérez, M. J. Sabater, *Chem. Rev.* **2011**, *111*, 1657–1712; b) M. Bandini, *Chem. Soc. Rev.* **2011**, *40*, 1358–1367; c) T. C. Boorman, I. Larrosa, *Chem. Soc. Rev.* **2011**, *40*, 1910–1925; d) A. S. K. Hashmi, M. Bührle, *Aldrichimica Acta* **2010**, *43*, 27–33; e) N. D. Shapiro, F. D. Toste, *Synlett* **2010**, 675–691; f) S. Sengupta, X. Shi, *ChemCatChem* **2010**, *2*, 609–619; g) N. Bongers, N. Krause, *Angew. Chem.* **2008**, *120*, 2208–2211; *Angew. Chem. Int. Ed.* **2008**, *47*, 2178–2181; h) D. J.

- Gorin, B. D. Sherry, F. D. Toste, *Chem. Rev.* **2008**, *108*, 3351–3378; i) E. Jiménez-Núñez, A. M. Echavarren, *Chem. Rev.* **2008**, *108*, 3326–3350; j) Z. Li, C. Brouwer, C. He, *Chem. Rev.* **2008**, *108*, 3239–3265; k) A. Arcadi, *Chem. Rev.* **2008**, *108*, 3266–3325; l) J. Muzart, *Tetrahedron* **2008**, *64*, 5815–5849; m) M. Rudolph, A. S. K. Hashmi, *Chem. Soc. Rev.* **2012**, *41*, 2448–2462; n) H. C. Shen, *Tetrahedron* **2008**, *64*, 7847–7870; o) R. A. Widenhoefer, *Chem. Eur. J.* **2008**, *14*, 5382–5391; p) D. J. Gorin, F. D. Toste, *Nature* **2007**, *446*, 395–403; q) A. Fürstner, P. W. Davies, *Angew. Chem.* **2007**, *119*, 3478–3519; *Angew. Chem. Int. Ed.* **2007**, *46*, 3410–3449; r) E. Jiménez-Núñez, A. M. Echavarren, *Chem. Commun.* **2007**, 333–346; s) A. S. K. Hashmi, *Chem. Rev.* **2007**, *107*, 3180–3211; t) A. S. K. Hashmi, G. J. Hutchings, *Angew. Chem.* **2006**, *118*, 8064–8105; *Angew. Chem. Int. Ed.* **2006**, *45*, 7896–7936.
- [2] a) A. S. K. Hashmi, *Angew. Chem.* **2010**, *122*, 5360–5369; *Angew. Chem. Int. Ed.* **2010**, *49*, 5232–5241; b) L.-P. Liu, G. B. Hammond, *Chem. Soc. Rev.* **2012**, *41*, 3129–3139.
- [3] a) M. Pernpointner, A. S. K. Hashmi, *J. Chem. Theory Comput.* **2009**, *5*, 2717–2725; b) M. Lein, M. Rudolph, S. K. Hashmi, P. Schwerdtfeger, *Organometallics* **2010**, *29*, 2206–2210.
- [4] a) C. M. Krauter, A. S. K. Hashmi, M. Pernpointner, *ChemCatChem* **2010**, *2*, 1226–1230; b) G. Mazzone, N. Russo, E. Sicilia, *Organometallics* **2012**, *31*, 3074–3080.
- [5] A. N. Nesmeyanov, E. G. Perevalova, K. I. Grandberg, D. A. Leme-novskii, T. V. Baukova, O. B. Afanassova, *J. Organomet. Chem.* **1974**, *65*, 131–144.
- [6] a) D. Weber, M. A. Tarselli, M. R. Gagné, *Angew. Chem.* **2009**, *121*, 5843–5846; *Angew. Chem. Int. Ed.* **2009**, *48*, 5733–5736; b) Ag^+ engages in a similar dimetalation reaction to afford the corresponding mixed-metal species with an $\text{Au}\cdots\text{Ag}$ interaction, see: D. Weber, M. R. Gagné, *Org. Lett.* **2009**, *11*, 4962–4965.
- [7] a) A. S. K. Hashmi, I. Braun, P. Nösel, J. Schädlich, M. Wietek, M. Rudolph, F. Rominger, *Angew. Chem.* **2012**, *124*, 4532–4536; *Angew. Chem. Int. Ed.* **2012**, *51*, 4456–4460; b) A. S. K. Hashmi, I. Braun, M. Rudolph, F. Rominger, *Organometallics* **2012**, *31*, 644–661; c) Y. Chen, M. Chen, Y. Liu, *Angew. Chem.* **2012**, *124*, 6285–6290; *Angew. Chem. Int. Ed.* **2012**, *51*, 6181–6186; d) A. S. K. Hashmi, M. Wietek, I. Braun, P. Nösel, L. Jongbloed, M. Rudolph, F. Rominger, *Adv. Synth. Catal.* **2012**, *354*, 555–562.
- [8] a) D. Weber, T. D. Jones, L. L. Adduci, M. R. Gagné, *Angew. Chem.* **2012**, *124*, 2502–2506; *Angew. Chem. Int. Ed.* **2012**, *51*, 2452–2456; b) J. E. Heckler, M. Zeller, A. D. Hunter, T. G. Gray, *Angew. Chem.* **2012**, *124*, 6026–6030; *Angew. Chem. Int. Ed.* **2012**, *51*, 5924–5928.
- [9] T. J. Brown, D. Weber, M. R. Gagné, R. A. Widenhoefer, *J. Am. Chem. Soc.* **2012**, *134*, 9134–9137.
- [10] Quite recently, observation of diaurated species in the gold-catalyzed hydroalkoxylation of 1-phenylpropyne by ESI-MS was reported: J. Roithová, Š. Janková, L. Jašíková, J. Váňa, S. Hybelbauerová, *Angew. Chem.* **2012**, *124*, 8503–8507; *Angew. Chem. Int. Ed.* **2012**, *51*, 8378–8382.
- [11] G. Seidel, C. W. Lehmann, A. Fürstner, *Angew. Chem.* **2010**, *122*, 8644–8648; *Angew. Chem. Int. Ed.* **2010**, *49*, 8466–8470.
- [12] For the use of a base to systematically obtain vinyl gold species from catalysis reactions, see: a) A. S. K. Hashmi, A. M. Schuster, F. Rominger, *Angew. Chem.* **2009**, *121*, 8396–8398; *Angew. Chem. Int. Ed.* **2009**, *48*, 8247–8249; b) A. S. K. Hashmi, T. D. Ramamurthi, F. Rominger, *Adv. Synth. Catal.* **2010**, *352*, 971–975; c) A. S. K. Hashmi, A. M. Schuster, S. Gaillard, L. Cavallo, A. Poater, S. P. Nolan, *Organometallics* **2011**, *30*, 6328–6337; d) A. S. K. Hashmi, *Gold Bull.* **2009**, *42*, 275–279.
- [13] If the reactants are taken in such a ratio that the substrate (alkynol) finishes sooner than all the gold is converted to diaurated species, and excess of PrSp is still available in the mixture, then the remaining gold will be present as aurated oxonium ion (LAu) OH^+ or (LAu) O^+ depending on the catalyst initially used. This oxonium ion is further converted into diaurated species if more substrate is added. If it is present as impurity in a starting gold catalyst, Ag^+ will form a black precipitate.

- [14] Prior to the generation of vinyl gold, the initial PrSpH^+ has to be neutralized to prevent protodeauration, occurring otherwise immediately (LiOH was used as indicated on the Scheme). The identity of **B2** follows from the independent synthesis from **D2**. The complex $(S)\text{-Tol-BINAPAuPPH}_3^+$ is known from ref. [15].
- [15] A. Zhdanko, M. Ströbele, M. E. Maier, *Chem. Eur. J.* **2012**, *18*, 14732–14744.
- [16] S. Gaillard, J. Bosson, R. S. Ramón, P. Nun, A. M. Z. Slawin, S. P. Nolan, *Chem. Eur. J.* **2010**, *16*, 13729–13740.
- [17] A related intramolecular aminoauration of alkenes by $(\text{Ph}_3\text{PAu})_3\text{O}^+$ was reported. This process also required a prolonged reaction time. See: R. L. LaLonde, J. Brenzovich, W. E. D. Benitez, E. Tkatchouk, K. Kelley, W. A. Goddard III, F. D. Toste, *Chem. Sci.* **2010**, *1*, 226–233.
- [18] The inability of $(\text{Ph}_3\text{PAu})_3\text{O}^+$ to give diaurated species nicely demonstrates that any catalytic process with this salt taken as a catalyst will occur sluggishly (or not at all), not because of slow protodeauration, but simply because of inability to form the necessary organogold intermediates.
- [19] Since LAuOH is known to be a strongly basic compound, it is quite sure to assume that if $(\text{LAu})_2\text{O}$ existed it would be even more basic; it would be considered as an organic soluble analogue of K_2O (similarly as LAuOH can be considered as organic soluble analogue of KOH).
- [20] H. Schmidbauer, S. Hofreiter, M. Paul, *Nature* **1995**, *377*, 503–504.
- [21] Similarly, protonation of $(\text{LAu})_2\text{OH}^+$ can be considered in addition to the simple ligand exchange possible with this complex.
- [22] PrSpH^+ naturally is a very weak acid to react with $(\text{Ph}_3\text{PAu})_3\text{O}^+$ alone and the total equilibrium $(\text{Ph}_3\text{PAu})_3\text{O}^+ + 2 \text{PrSpH}^+ + 3 \text{Sol} \leftrightarrow 3 \text{Ph}_3\text{PAu}(\text{Sol})^+ + 2 \text{PrSp} + \text{H}_2\text{O}$ is strongly shifted to the left (rather $(\text{Ph}_3\text{PAu})_3\text{O}^+$ is stoichiometrically obtained by this equation). But there is no doubt that the highly reactive dicationic species **IV** has to be involved in the equilibrium in an undetectable amount. If strong acid is used instead of PrSpH^+ (for example TfOH), $(\text{Ph}_3\text{PAu})_3\text{O}^+$ will simply undergo electrophilic substitution at oxygen to give Ph_3PAuOTf and H_2O as final products. More discussion about mechanisms of formation and interconversion between various aurated oxonium ions, LAuOH and $\text{LAu}(\text{Sol})^+$ was given in ref. [15].
- [23] Although sometimes $(\text{Ph}_3\text{PAu})_3\text{O}^+$ is used alone as a sole catalyst, its activity is naturally much less than the activity of normal cationic $\text{LAu}(\text{Sol})^+$ catalysts. This is evidenced by prolonged reaction times or diminished yields of the catalytic reactions. However, the milder reactivity of $(\text{Ph}_3\text{PAu})_3\text{O}^+$ becomes advantageous in the case of sensitive substrates in which the active $\text{LAu}(\text{Sol})^+$ catalysts caused decomposition or an unselective reaction. This can be understood from the reports of Toste et al. concerning cycloisomerizations of enynes: a) P. H.-Y. Cheong, P. Morganelli, M. R. Luzung, K. N. Houk, F. D. Toste, *J. Am. Chem. Soc.* **2008**, *130*, 4517–4526; b) B. D. Sherry, F. D. Toste, *J. Am. Chem. Soc.* **2004**, *126*, 15978–15979. According to our data, activity of $(\text{Ph}_3\text{PAu})_3\text{O}^+$ can be greatly enhanced (while still maintaining the mild conditions) if it is used in combination with a suitable mild acid (PrSpH^+ and stronger) or another suitable oxophilic electrophile.
- [24] A. Zhdanko, unpublished results.

Received: December 17, 2012
Published online: February 11, 2013

Paper 4

For the Section 6.3.2.

Gold-Catalyzed Hydroalkoxylation

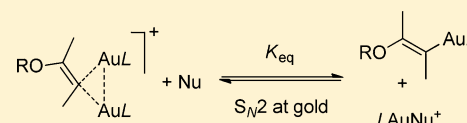
Quantitative Evaluation of the Stability of *gem*-Diaurated Species in Reactions with Nucleophiles

Alexander Zhdanko and Martin E. Maier*

Institut für Organische Chemie, Universität Tübingen, Auf der Morgenstelle 18, 72076 Tübingen, Germany

Supporting Information

ABSTRACT: The reactivity of diaurated species toward nucleophiles was investigated. The reaction yields vinyl gold species and is described as simple S_N2 ligand exchange at gold. Using suitably strong nucleophiles, equilibrium constants were determined to measure the stability of various diaurated species. On the basis of these equilibrium constants the influence of ligand and the nature of vinyl cores on the stability were analyzed. These results have direct implication for gold catalysis: it was demonstrated that vinyl gold intermediates bind the catalytic LAu^+ species generally stronger than an alkyne (the substrate) by a factor of 10^6 – 10^9 . This demonstrates that the formation of diaurated species from vinyl gold intermediates is thermodynamically favored in a catalytic reaction.



1. INTRODUCTION

Since 2012 the scientific community witnessed a rapid growth of publications in the chemistry of *gem*-diaurated species, important intermediates in gold catalysis.^{1,2} At this time, involvement of this class of compounds has been confirmed for several catalytic processes and their role in gold catalysis is currently a major topic of research.³ In our previous study we provided a convenient route to enol ether derived diaurated species in a catalytically relevant manner.⁴ As part of our study on mechanisms of gold catalysis we report herein on quantitative evaluation of stability of *gem*-diaurated species in reactions with nucleophiles and provide insights into the mechanism of these reactions.

Reversible formation of diaurated species (eq 1) is one of the central processes in the mechanism of catalytic hydroalkoxylation.⁵ This reversible reaction is responsible for the removal of gold from the catalytic cycle because **D** is an inactive intermediate, while **B** is a reactive participant of the living catalytic cycle. However, the position of this equilibrium or even whether it is established at all during the catalytic process has not been investigated. This depends on thermodynamic stability of diaurated species and on the corresponding reaction rates, a subject which has not been looked at so far.

2. RESULTS AND DISCUSSION

Since thermodynamic stability constants of diaurated species **D** (eq 1) were experimentally inaccessible, much useful information was obtained from reactions with nucleophiles (eq 2).

Previously we established a ligand strength series for LAu^+ (MeOH \ll 3-hexyne $<$ MeCN \ll Me₂S $<$ 2,6-lutidine $<$ 4-picoline $<$ DMAP $<$ TMTU $<$ PPh₃) with binding affinities covering \sim 11 orders of magnitude.⁶ Now, using 4-picoline, DMAP, and TMTU as suitably strong nucleophiles we determined equilibrium constants of ligand exchange reactions with a number of enol ether derived diaurated species **D1**–**D16**

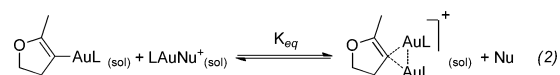


(Table 1; for the ligand abbreviations see Figure 1). The choice of these nucleophiles came from the reaction of the diaurated species with some ligands from the above series. For example, PPh₃ destroyed all diaurated species while Me₂S did not touch them at all. Species **D2**, **D5**, **D6**, **D12**, and **D14**–**D16** were used as SbF₆[−] salts prepared in individual states, and in all other cases the species were obtained from catalysts (Figure 1) and manipulated in situ.⁴ All reactions were performed at constant 26.1 °C temperature, and amounts of equilibrium participants were determined by integration of NMR spectra. A representative example is given in Figure 2. Here the CH₂O signals of the vinyl gold and the diaurated species appear at different chemical shifts and their integrals could be immediately used for the calculation of K_{eq} . The peak at 2.34 ppm contains the methyl group of 4-picoline but also the methyl group of the $L2AuPic^+$ salt and an endocyclic methylene group of vinyl gold complex **B5**. In the case of a fast LAu^+ exchange the molar ratio **B**/**D** was determined from the exact position of the CH₂O peak common for these species. Complete experimental details are given in the Supporting Information. In these ligand exchange reactions the vinyl gold species **B** serves as a ligand and the equilibrium is achieved through the competition of **B** and a nucleophile for the electrophilic LAu^+ center. The results are summarized in Table 1.

Received: January 30, 2013

Published: March 11, 2013



Table 1. Reactions of Diaurated Species with Nucleophiles: Equilibrium Constants

| N | Reaction ^a | K_{eq} | N | Reaction | K_{eq} |
|----|-----------------------|---------------------|----|----------|---------------------|
| 1 | | 2·10 ⁴ | 14 | | 17 |
| 2 | | 52 | 15 | | 11 |
| 3 | | 5.5 | 16 | | 5–6·10 ² |
| 4 | | 1·10 ⁴ | 17 | | 6.6 |
| 5 | | 24 | 18 | | 2.6 |
| 6 | | 2.5 | 19 | | 3·10 ³ |
| 7 | | 3.5·10 ² | 20 | | 2·10 ² |
| 8 | | 2·10 ³ | 21 | | 4.5 |
| 9 | | 36 | 22 | | 7·10 ³ |
| 10 | | 66 | 23 | | 1.6 |
| 11 | | 5.4 | 24 | | 1.9 |
| 12 | | 30 | 25 | | 42 |
| 13 | | 13 | | | |

^aAll reactions in CDCl₃ at 26.1 °C except otherwise noted. Abbreviations: Pic, 4-picoline; DMAP, 4-dimethylaminopyridine; TMTU, tetramethylthiourea ((Me₂N)₂C=S); Lut, 2,6-lutidine.

Substrate Effect on Stability of Diaurated Species.

First of all, these equilibrium constants allow direct comparison of the stability of diaurated species bearing different vinyl cores but having the same ligand or, in other words, establishing the substrate effect on the stability of diaurated species. In order to avoid too much steric influence, it seemed better to study these substrate effects on species bearing nonbulky ligands such as PMe₃ and PPh₃. This way it could be established that changing a propyl to a methyl substituent decreases the stability of PPh₃-based diaurated species by a factor of 2 (compare entries 1 and 4, 2 and 5, and 3 and 6), indicating that with a more electron rich substituent the stability of diaurated species increases. The same trend was found for PMe₃-based diaurated species (compare entries 17 and 18). In contrast, installation of a conjugated π system in the side chain decreases the stability of the diaurated species rather significantly, be it a simple double bond or a phenyl substituent (as evidenced from entries 1 and

7, 1 and 8, and 19 and 20). These effects are rather surprising, since conjugation with a π system should help in stabilization of a positive charge and should increase the stability. Obviously this principle does not apply here and other effects must account for the decrease of stability. We hypothesize that this is due to an increase in the stability of the vinyl gold species, the dissociation product. Indeed, in this case there is also a nicely conjugated π system in vinyl gold (e.g., B3), which gets disturbed with introduction of a second LAu⁺ moiety. This effect might dominate over stabilization in the diaurated species, making them more prone to dissociation, together with a small $-I$ effect of the sp² carbon favoring the same trend. Introduction of an electron-rich substituent (NMe₂) in the aromatic side chain increases the stability (entries 20 and 21), while an electron-withdrawing substituent (CN) decreases the stability dramatically.⁷ Use of an electron-deficient ligand also negatively affects the stability (see below).

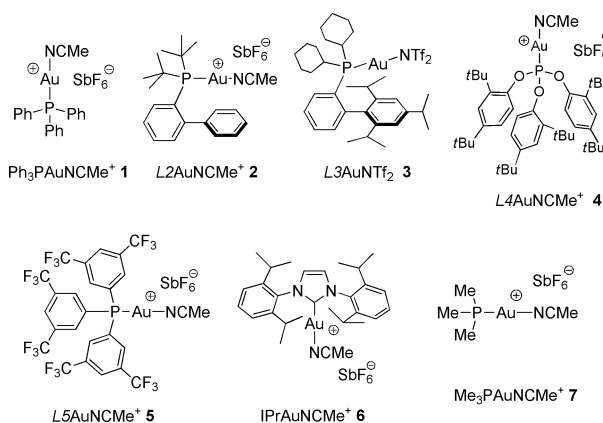


Figure 1. Precursors for diaurated species used in the study and abbreviations of the ligands.

On the basis of this information the following can be concluded about the influence of a substituent at the enol ether core on the stability of diaurated species: (1) electron-rich substituents will increase the stability, while electron-poor substituents decrease it; (2) any conjugation will decrease the stability in comparison to nonconjugated systems.

Ligand Effect on Stability of Diaurated Species.

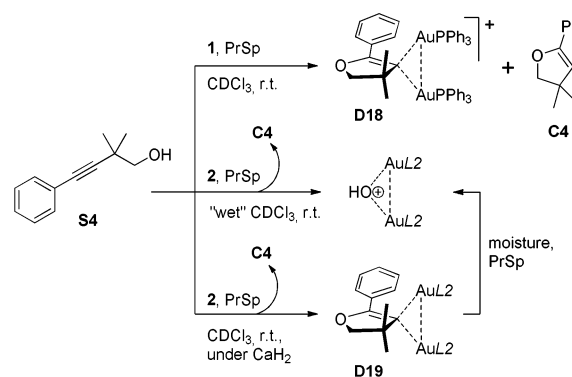
Further, the equilibrium constants disclose ligand effects on the stability of diaurated species. Thus, among the five ligands the most stable diaurated species are formed with PPh_3 and PMe_3 and the stability decreases in the order $\text{PMe}_3 \approx \text{PPh}_3 > \text{L4} \approx \text{L5} \gg \text{L2} > \text{L3}$. According to this series electron-donor phosphines favor the formation of diaurated species; however, in the case of L2 and L3 steric effects obviously predominate and the stability drastically decreases.

Changing the PPh_3 ligand to a more bulky one (L2 , L3) not only generally reduces the stability but also might cause some transpositions in the aforementioned trends of the substrate effects. Thus, in some cases a conjugated π system in the side chain decreases the stability as before (compare Table 1, entries 9 and 11 and 9 and 12), but in others the stability increased (entries 13 and 14). This must be caused by a steric effect which becomes more and more pronounced as the ligand gets larger. Indeed, a free-rotating propyl side chain now brings

more destabilization in the system than the more rigid and flat alkenyl or phenyl group. The same steric effect could cause an increase of stability with the change of a propyl substituent to a smaller methyl group (entries 9 and 10), while in case of the PPh_3 and PMe_3 ligands the opposite was true.

Another good illustration of the impact of steric effects is given by the reaction of sterically hindered alcohol **S4**. Thus, when **S4** was reacted with catalyst **1** and PrSp (Proton Sponge), diaurated species **D18** smoothly formed, but only minor formation of diaurated species was observed with **2** (Scheme 1). Instead, the oxonium salt $(\text{L2Au})_2\text{OH}^+$ was

Scheme 1. Steric Effects Greatly Reduce Stability of Diaurated Species



formed as a major gold product resulting from residual water in the system.⁸ When the reaction was repeated under essentially water-free conditions in the presence of CaH_2 , the new species **D19** could be generated. Not surprisingly, **D19** appears to be highly unstable toward nucleophilic attack and readily reverts back to $(\text{L2Au})_2\text{OH}^+$ upon simple manipulation of the reaction mixture in open air. Obviously, installation of two methyl groups in close proximity to the bulky diaurated core drastically reduced the stability of **D19** in comparison to the less crowded situation for **D18** with the PPh_3 ligand. It appears that in sterically hindered diaurated species the steric effects naturally become more and more important and in many cases may dominate over electronic effects.

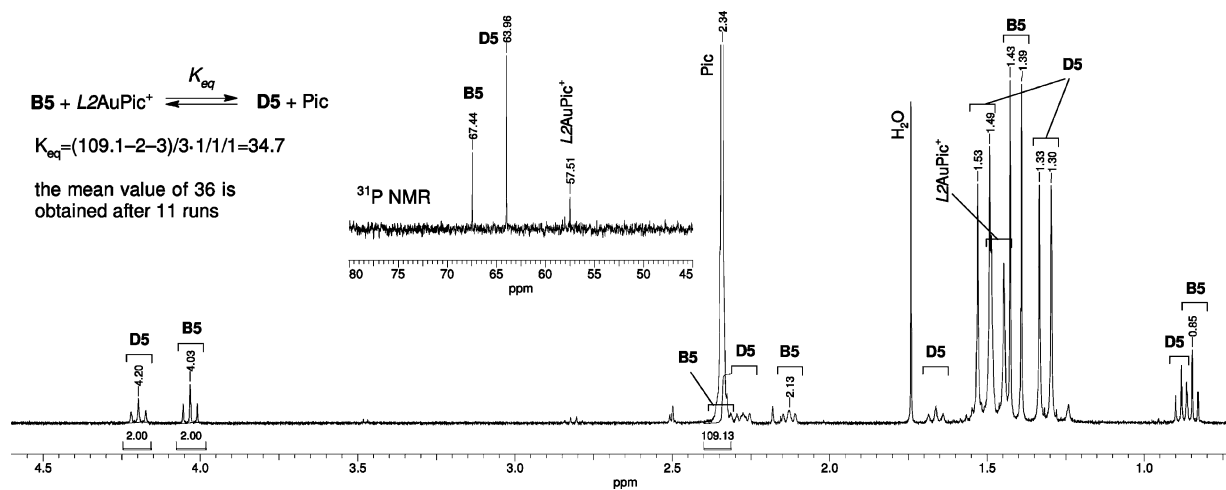
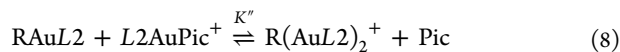
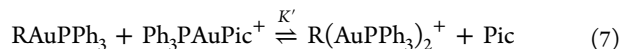
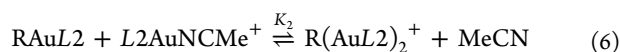
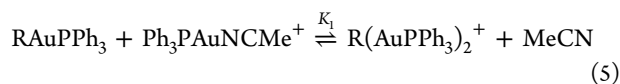
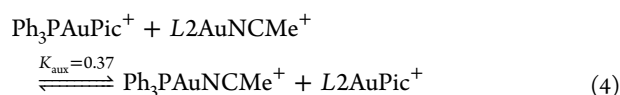
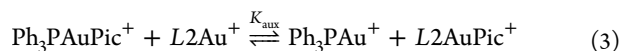


Figure 2. Representative NMR spectrum of the reaction mixture in CDCl_3 for determination of the equilibrium constant for **D5/B5** (entry 9, Table 1).

However, since the affinities of various LAu^+ species for the spectator ligands are also slightly different, rigorous comparison (in terms of thermodynamic stability constants) is not possible without an auxiliary equilibrium constant (3). Such a constant was also experimentally inaccessible. In order to evaluate the ligand effect in a situation closely analogous to catalytic conditions, we determined an auxiliary constant for MeCN (4). With this value it was possible to compare equilibria (5) and (6) theoretically. The ratio of the constants is now related to the experimentally established picoline constants (7) and (8) by the simple expression (9). For example, this way it could be established that diaurated species **D1** is 1500 times more stable than **D5** (in chloroform). That is the impact of the bulky ligand!



$$\frac{K_1}{K_2} = \frac{K'}{K''K_{\text{aux}}} = \frac{2 \times 10^4}{36 \times 0.37} = 1500 \quad (9)$$

Since the auxiliary constant (3) for different LAu^+ can be assumed to be generally around 1, since it is an equilibrium between species of similar nature, direct comparison of equilibria with picoline can be used to roughly compare thermodynamic stabilities of diaurated species bearing different ligands. It can be suggested that PPh_3 -based species should be generally 1000 times stronger than with *L2*. Given the inhibitory effect of diaurated species in catalysis, this constitutes one of the reasons why catalyst **2** is far more efficient than **1** in many reactions in this study and in the literature.⁹

Comparison with the Previously Known Aryl Diaurated Species. Finally, we synthesized one example of the well-known aryl diaurated species **D17** in order to compare the stability of this compound with those of our enol ether derived species.¹⁰ As can be concluded from Table 1, entries 1 and 23, installation of an enol ether moiety in place of an aryl ring increases the stability of diaurated species by a factor of 10000! Thus, the aryl diaurated species Ar(AuL)_2^+ should be generally much less stable than the enol ether derived analogues. Even dimethyl sulfide can be used to cause reversible dissociation of this weak species (entry 25).

Outlook. In our previous report on the coordination chemistry of gold catalysts we established a ligand strength series for a number of ligands covering 11 orders of magnitude.⁶ Now we can supplement the series with our new data on binding affinities of vinyl gold to a LAu^+ unit (Figure 3). Using the intermediate equilibrium constants it could thereby be estimated that enol ether derived vinyl gold binds LAu^+ generally 10^6 – 10^9 times more strongly than the alkyne

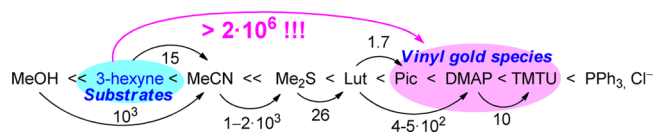
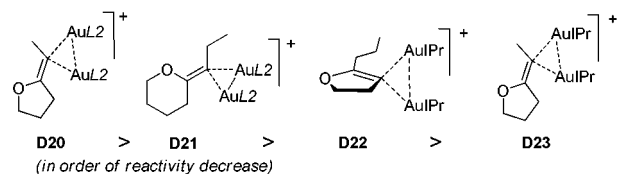


Figure 3. General ligand strength series showing thermodynamic binding affinities of the key catalytic intermediates to a LAu^+ unit. Some key equilibrium constants are given for ligand exchange at L2Au^+ .

substrate! Obviously vinyl gold species represent the strongest binding partners among all species in the whole hydroalkoxylation reaction mixture, and this binding to a LAu^+ unit is remarkably strong. It can be also suggested that the corresponding alkene derived diaurated species should be generally weaker than the corresponding enol ether derived analogues by 2–3 orders of magnitude.

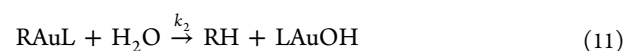
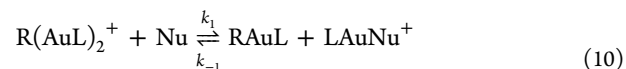
Kinetic Aspects. Unfortunately, the determination of equilibrium constants in reactions with nucleophiles was not possible in a number of cases due to kinetic reasons (slow reaction). For example, an equilibrium of **D5** with 2,6-lutidine is not established even after 2 h reaction time. Some other examples are given in Scheme 2. Thus, diaurated species **D20**–

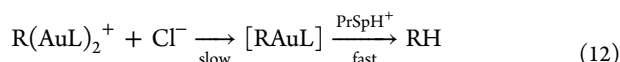
Scheme 2. Slowly Reacting Diaurated Species



| initial concentrations (CDCl_3 , r.t.) | conversion | k , $\text{L}\cdot\text{mmol}^{-1}\cdot\text{h}^{-1}$ |
|---|----------------|---|
| D20 (3.0 mM), Pic (144 mM, 48 equiv) | 50% in 1 h | |
| D20 , TMTU, PrSpH^+ (see text) ^a | 90% in 0.47 h | 3.02 |
| D21 (2.5 mM), $\text{Et}_4\text{N}^+\text{Cl}^-$ (5.5 mM, 2.2 equiv) | 100% in <5 min | |
| D21 (2.5 mM), Pic (160 mM, 64 equiv) | 19% in 40 min | |
| D21 (2.94 mM), TMTU (7.23 mM, 2.5 equiv) ^a | 85% in 1.3 h | 0.27 |
| D22 (1.3 mM), TMTU (6.6 mM, 5 equiv) | 90% in 2 h | 0.2 |
| D23 (1.8 mM), $\text{Et}_4\text{N}^+\text{Cl}^-$ (8.5 mM, 4.7 equiv) | 66% in 4 h | 0.03 |
| D23 (2.2 mM), Pic (22 mM, 10 equiv) | 61% in 46 h | |

D23 reacted with picoline slowly within hours. Reactions with stronger nucleophiles (TMTU and $\text{Et}_4\text{N}^+\text{Cl}^-$) occurred considerably more quickly. However, in the case of **D23** reaction even with Cl^- (a strong and unhindered nucleophile) is slow (66% conversion in 4 h), which is unprecedented for diaurated species. In all these slow cases liberation of vinyl gold is accompanied by subsequent slow protodeauration, taking place at the cost of water in the system (11), so that equilibrium constants (10) cannot be determined. In contrast, all vinyl gold products generated from **D20**–**D23** are kinetically reactive, like all other vinyl gold species from Table 1, reacting immediately already with the weak acid $\text{PrSpH}^+\text{OTf}^-$. Thus, addition of $\text{PrSpH}^+\text{OTf}^-$ to the mixture of **D23** and $\text{Et}_4\text{N}^+\text{Cl}^-$ immediately removes all vinyl gold but cannot speed up decomposition of diaurated species themselves (12). This further proves the kinetic inertness of this species.



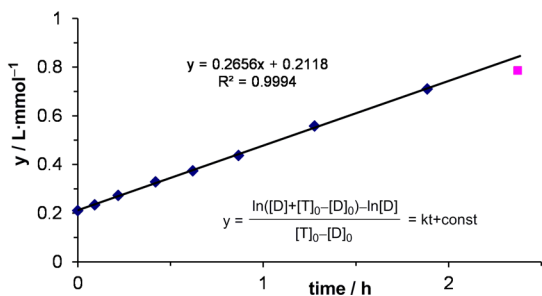
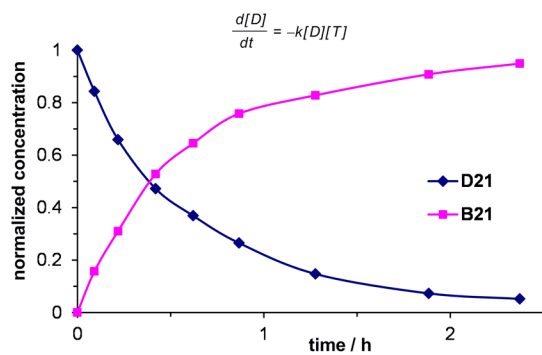
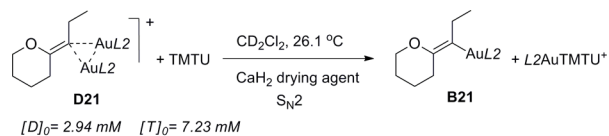


The aforementioned examples point out that diaurated species derived from the sterically hindered IPr ligand are the most kinetically inert among all other diaurated species in this study (despite the fact that they should be the least stable thermodynamically). The reactivity also depends on the vinyl core (Scheme 2). Thus, 5-*endo* and 6-*endo* diaurated species are generally more reactive than 5-*exo* or 6-*exo* species. There are also ligand effects on the reactivity. Thus, PPh₃-derived diaurated species are the most kinetically reactive (but at the same time thermodynamically stable), which is evident from the fact that R(AuPPh₃)₂⁺/RAuPPh₃ mixtures always exhibit a single set of sharp signals in proton NMR spectra, indicating fast exchange of the Ph₃PAu⁺ unit.¹¹ A similar situation is observed for DTBP and L5 based species, but the rate of exchange is less, which is evident from the broader shape of the signals. In the case of L2 and L3, the corresponding R(AuL)₂⁺/RAuL mixtures always exhibited separate sets of signals, indicating a slow mode of LAu⁺ exchange (despite the fact that these diaurated species are thermodynamically less stable).

Slow reactions of D20 and D21 with TMTU were used to conveniently study the reaction kinetics and reaction mechanism.

Thus, the kinetics of reaction of D21 with TMTU was investigated in CD₂Cl₂ under water-free conditions in the presence of CaH₂ (Scheme 3). In a completely closed and dry system the appearing vinyl gold species B21 remained stable during the entire course of the reaction. Correspondingly, the reaction system was free of any side processes, including protodeauration. The reaction cleanly displayed general

Scheme 3. Second-Order Kinetics of Reaction of D21 with TMTU



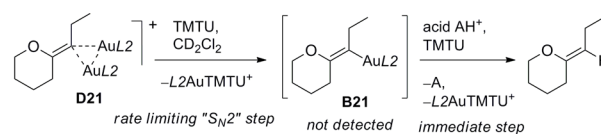
second-order kinetics with the rate constant $k = 0.27 \text{ L}\cdot\text{mmol}^{-1}\cdot\text{h}^{-1}$, as evidenced from the linear graph

$$y = \frac{\ln([\text{D}]_0 + [\text{T}]_0 - [\text{D}]_0) - \ln[\text{D}]}{[\text{T}]_0 - [\text{D}]_0} = kt + \text{const}$$

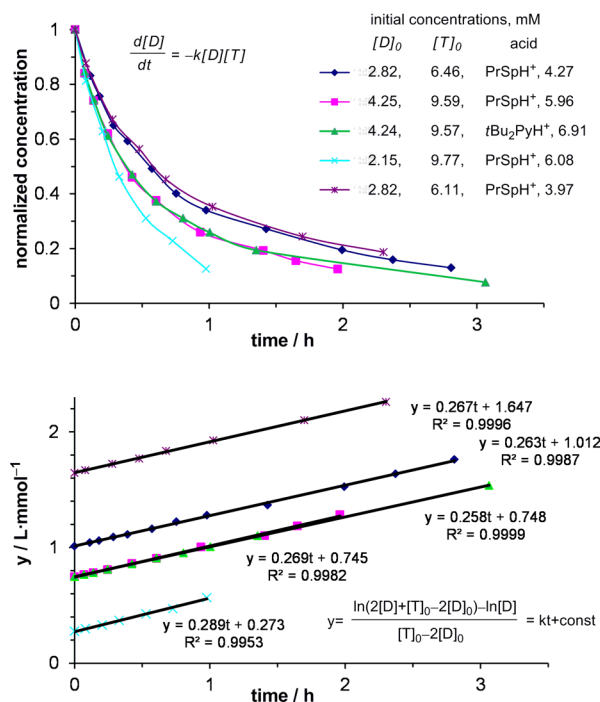
where $[\text{D}]_0$ and $[\text{T}]_0$ are starting concentrations of the reactants (derivation of this equation is given in the Supporting Information). Importantly, the reverse reaction did not have any impact because the equilibrium theoretically could be prognosticated to be reached only at >99% conversion.¹² Thus, the entire process can be accurately described as an irreversible one-way reaction (Scheme 3).

To further demonstrate that the reaction is not influenced by the reverse process and does not involve predissociation of D21 to free vinyl gold species B21, the reaction kinetics were performed in the presence of acid additives at various concentrations (Scheme 4). In comparison with the previous

Scheme 4. Second-Order Kinetics of Reaction of D21 with TMTU in the Presence of an Acid Additive



Overall reaction stoichiometry:



case here one should consider the expenditure of an additional 1 equiv of TMTU to immediately bind the gold liberated upon protodeauration of the vinyl gold intermediate. The whole reaction sequence now consists of slow liberation of the vinyl gold species B21 and subsequent fast protodeauration with formation of additional L2AuTMTU⁺. In complete accordance with our expectations, the reaction nicely followed general second-order kinetics. Importantly, the kinetics was independent not only on the acid concentration but also on the acid

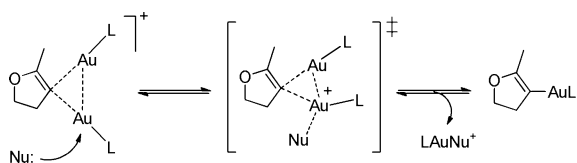
strength (two differently strong acids were used: $\text{PrSpH}^+\text{OTf}^-$ and $t\text{Bu}_2\text{PyH}^+\text{OTf}^-$), which is consistent with the rate-limiting vinyl gold formation step. The rate constant $k = 0.27 \pm 0.01 \text{ L mmol}^{-1} \text{ h}^{-1}$ determined in this series is equal to that obtained in the previous experiment above, which further demonstrates the independence of the reaction of any acid.

Analogously the rate constant $k = 3.0 \text{ L mmol}^{-1} \text{ h}^{-1}$ for reaction of **D20** with TMTU was found. Therefore, **D20** reacts with TMTU 11 times more quickly than **D21**, which reflects the easier accessibility of gold in **D20** toward nucleophilic attack. This can be associated with both the reduced steric hindrance (methyl substituent vs ethyl) and the higher rigidity and flat character of the five-membered ring in comparison to the six-membered ring.

These experiments unambiguously point to an associative $\text{S}_{\text{N}}2$ mechanism for the reaction of diaurated species with nucleophiles. In order to establish the thermodynamic parameters of this reaction, we performed a series of experiments at various temperatures (-10.2 , -4.1 , 4.9 , 15 , 26 , and 36.9 °C). From this, the Arrhenius activation energy E_{A} for the reaction of **D21** with TMTU was found to be 60.1 kJ mol^{-1} . Analysis of the Eyring equation gave the following activation parameters for the reaction: $\Delta H^{\ddagger} = 57.7 \text{ kJ mol}^{-1}$ and $\Delta S^{\ddagger} = -73.6 \text{ J mol}^{-1} \text{ K}^{-1}$. The negative value of ΔS^{\ddagger} is consistent with an associative process.

That reaction of diaurated species with nucleophiles occurs as an associative process additionally follows from a number of observations. We mentioned that the equilibrium in the reaction of **D5** with Lut is established much more slowly than with Pic. This fact unambiguously points to an associative $\text{S}_{\text{N}}2$ mechanism for the reaction. Indeed, if the reaction followed a dissociative $\text{S}_{\text{N}}1$ -like route, the dependence of the overall reaction rate on the nature of the nucleophile would not be so pronounced (if at all).¹³ Similar nucleophile effects are revealed in reactions of Scheme 2 and the aforementioned comparisons of $\text{R}(\text{AuL})_2^+/\text{RAuL}$ exchange rates. Indeed, if the reaction followed a dissociative $\text{S}_{\text{N}}1$ mechanism, the least stable **L2** and **L3** derived diaurated species should dissociate more easily and undergo fast exchange, which is not the case. It therefore can be generally accepted that the reaction of diaurated species with nucleophiles occurs via an associative $\text{S}_{\text{N}}2$ nucleophilic substitution at gold (Scheme 5). It is known that gold complexes undergo ligand exchange by an associative $\text{S}_{\text{N}}2$ mechanism, and our experiments established that diaurated species are not an exception.¹⁴

Scheme 5. $\text{S}_{\text{N}}2$ Mechanism of the Reaction of Diaurated Species with Nucleophiles



3. CONCLUSION

In summary, we have investigated the reactivity of diaurated species toward nucleophiles and determined the corresponding equilibrium constants. On the basis of these constants, the influence of various structural factors on the stability of diaurated species was analyzed. Thus, electron-donor substituents at the α -carbon atom of the enol ether core increase

stability, as do electron donor ligands at gold. Any conjugation of the enol ether residue with a simple double bond or an aryl residue will decrease the stability. Steric factors also play a crucial role in the stability of diaurated species and can readily dominate over the electronic factors. Thus, diaurated species derived from the very bulky ligands **L2**, **L3**, and **IPr** will be considerably less stable than the PPh_3 - or PMe_3 -derived analogues. Additionally, we have found that the rate of reaction with nucleophiles drastically depends on steric factors. While diaurated species bearing small or nonrigid ligands such as PMe_3 , PPh_3 , **L4**, and **L5** always reacted quickly with suitably strong nucleophiles, some species bearing very bulky ligands reacted very sluggishly, even if the reaction was thermodynamically favored. This is a consequence of the mechanism of the reaction, which was found to occur as an associative $\text{S}_{\text{N}}2$ process.

The results presented herein have direct implications for gold catalysis, because they demonstrate that the formation of diaurated species from vinyl gold intermediates generally is thermodynamically very favored but will strongly depend on the catalyst and substrate used. Also, the kinetic reactivity of diaurated species can vary significantly depending on the steric accessibility of gold: sterically hindered diaurated species are less reactive and at the same time less stable than their less hindered analogues.

It can be also concluded that formation/dissociation of diaurated species in a catalytic cycle should be considered as an associative $\text{S}_{\text{N}}2$ process with any suitable molecule acting as a nucleophile (solvent, substrate, product, water, MeCN, etc.).

■ ASSOCIATED CONTENT

Supporting Information

Text, tables, and figures giving complete experimental procedures and detailed NMR spectra. This material is available free of charge via the Internet at <http://pubs.acs.org>.

■ AUTHOR INFORMATION

Corresponding Author

*E-mail for M.E.M.: martin.e.maier@uni-tuebingen.de.

Notes

The authors declare no competing financial interest.

■ ACKNOWLEDGMENTS

We thank Dr. K. Eichele and Institut für Anorganische Chemie for allowing us to use their NMR spectrometer, Dr. D. Wistuba for HRMS analysis, and Dr. M. Kramer for the assistance with the various temperature experiments. Financial support by the state of Baden-Württemberg is gratefully acknowledged.

■ REFERENCES

- General reviews about gold catalysis: (a) Rudolph, M.; Hashmi, A. S. K. *Chem. Soc. Rev.* **2012**, *41*, 2448–2462. (b) Corma, A.; Leyva-Peréz, A.; Sabater, M. J. *Chem. Rev.* **2011**, *111*, 1657–1712. (c) Bandini, M. *Chem. Soc. Rev.* **2011**, *40*, 1358–1367. (d) Boorman, T. C.; Larrosa, I. *Chem. Soc. Rev.* **2011**, *40*, 1910–1925. (e) Hashmi, A. S. K.; Bührle, M. *Aldrichim. Acta* **2010**, *43*, 27–33. (f) Shapiro, N. D.; Toste, F. D. *Synlett* **2010**, 675–691. (g) Sengupta, S.; Shi, X. *ChemCatChem* **2010**, *2*, 609–619. (h) Bongers, N.; Krause, N. *Angew. Chem., Int. Ed.* **2008**, *47*, 2178–2181. (i) Gorin, D. J.; Sherry, B. D.; Toste, F. D. *Chem. Rev.* **2008**, *108*, 3351–3378. (j) Jiménez-Núñez, E.; Echavarren, A. M. *Chem. Rev.* **2008**, *108*, 3326–3350. (k) Li, Z.; Brouwer, C.; He, C. *Chem. Rev.* **2008**, *108*, 3239–3265. (l) Arcadi, A. *Chem. Rev.* **2008**, *108*, 3266–3325. (m) Muzart, J. *Tetrahedron* **2008**,

64, 5815–5849. (n) Shen, H. C. *Tetrahedron* **2008**, *64*, 7847–7870. (o) Widenhoefer, R. A. *Chem. Eur. J.* **2008**, *14*, 5382–5391. (p) Gorin, D. J.; Toste, F. D. *Nature* **2007**, *446*, 395–403. (q) Fürstner, A.; Davies, P. W. *Angew. Chem., Int. Ed.* **2007**, *46*, 3410–3449. (r) Jiménez-Núñez, E.; Echavarren, A. M. *Chem. Commun.* **2007**, 333–346. (s) Hashmi, A. S. K. *Chem. Rev.* **2007**, *107*, 3180–3211. (t) Hashmi, A. S. K.; Hutchings, G. J. *Angew. Chem., Int. Ed.* **2006**, *45*, 7896–7936.

(2) Important reviews about catalytic intermediates in gold catalysis: (a) Hashmi, A. S. K. *Angew. Chem.* **2010**, *122*, 5360–5369; *Angew. Chem., Int. Ed.* **2010**, *49*, 5232–5241. (b) Liu, L.-P.; Hammond, G. B. *Chem. Soc. Rev.* **2012**, *41*, 3129–3139.

(3) (a) Weber, D.; Tarselli, M. A.; Gagné, M. R. *Angew. Chem., Int. Ed.* **2009**, *48*, 5733–5736. (b) Hashmi, A. S. K.; Braun, I.; Nösel, P.; Schädlich, J.; Wieteck, M.; Rudolph, M.; Rominger, F. *Angew. Chem., Int. Ed.* **2012**, *51*, 4456–4460. (c) Hashmi, A. S. K.; Braun, I.; Rudolph, M.; Rominger, F. *Organometallics* **2012**, *31*, 644–661. (d) Chen, Y.; Chen, M.; Liu, Y. *Angew. Chem., Int. Ed.* **2012**, *51*, 6181–6186. (e) Hashmi, A. S. K.; Wieteck, M.; Braun, I.; Nösel, P.; Jongbloed, L.; Rudolph, M.; Rominger, F. *Adv. Synth. Catal.* **2012**, *354*, 555–562. (f) Brown, T. J.; Weber, D.; Gagné, M. R.; Widenhoefer, R. A. *J. Am. Chem. Soc.* **2012**, *134*, 9134–9137. (g) Weber, D.; Jones, T. D.; Adduci, L. L.; Gagné, M. R. *Angew. Chem., Int. Ed.* **2012**, *51*, 2452–2456. (h) Heckler, J. E.; Zeller, M.; Hunter, A. D.; Gray, T. G. *Angew. Chem., Int. Ed.* **2012**, *51*, 5924–5928. (i) Hashmi, A. S. K.; Wieteck, M.; Braun, I.; Rudolph, M.; Rominger, F. *Angew. Chem., Int. Ed.* **2012**, *51*, 10633–10637. (j) Hansmann, M. M.; Rudolph, M.; Rominger, F.; Hashmi, A. S. K. *Angew. Chem., Int. Ed.* **2013**, *52*, 2593–2598. (k) For a recent highlight about *gem*-diaurated species, see: Gómez-Suárez, A.; Nolan, S. P. *Angew. Chem., Int. Ed.* **2012**, *51*, 8156–8159.

(4) Zhdanko, A.; Maier, M. E. *Chem. Eur. J.* **2013**, DOI: 10.1002/chem.201204491.

(5) Seidel, G.; Lehmann, C. W.; Fürstner, A. *Angew. Chem., Int. Ed.* **2010**, *49*, 8466–8470. See also ref 3f.

(6) Zhdanko, A.; Ströbele, M.; Maier, M. E. *Chem. Eur. J.* **2012**, *18*, 14732–14744.

(7) The corresponding equilibrium constant for the CN-containing species could not be determined, because the species already decomposed upon addition of K₂CO₃ during preparation of the reaction mixture for determination of the equilibrium constant (see the Supporting Information). This fact points to the high instability of the species.

(8) Complexes L₂AuNu⁺ bearing a weak ligand (e.g., MeCN) are known to react with PrSp and H₂O to displace the Nu: 2 L₂AuNu⁺ + PrSp + H₂O → (L₂Au)₂OH⁺ + PrSpH⁺ + Nu.⁶ Nu should be weaker than Me₂S for this reaction to occur.

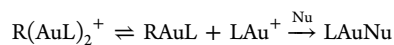
(9) The superiority of catalyst **2** over **1** can be seen in the following examples: (a) Nieto-Oberhuber, C.; López, S.; Echavarren, A. M. *J. Am. Chem. Soc.* **2005**, *127*, 6178–6179. (b) Nieto-Oberhuber, C.; Muñoz, M. P.; López, S.; Jiménez-Núñez, E.; Nevado, C.; Herrero-Gómez, E.; Raducan, M.; Echavarren, A. M. *Chem. Eur. J.* **2006**, *12*, 1677–1693; **2008**, *14*, 5096 (corrigendum). (c) Aponick, A.; Li, C.-Y.; Palmes, J. A. *Org. Lett.* **2009**, *11*, 121–124. (d) Barabé, F.; Bétournay, G.; Bellavance, G.; Barriault, L. *Org. Lett.* **2009**, *11*, 4236–4238.

(10) Nesmeyanov, A. N.; Perevalova, E. G.; Grandberg, K. I.; Lemenovskii, D. A.; Baukova, T. V.; Afanassova, O. B. *J. Organomet. Chem.* **1974**, *65*, 131–144.

(11) The same fast exchange was previously observed in Ar(AuPPh₃)₂⁺/ArAuPPh₃ systems.^{3g}

(12) The prognosis for the equilibrium is described in the Supporting Information.

(13) Assume a fast dissociation preequilibrium with the subsequent reaction with a nucleophile:



The difference in reactivity of Pic and Lut with LAu⁺ unit is not so high as to cause such a dramatic difference in the reactivity of **D5**. The equilibrium constant for the exchange L₂AuLut⁺/Pic is 1.7 and is established immediately,⁶ indicating that any LAu⁺ would react almost

equally quickly with both Pic and Lut. Therefore, if the reaction of **D5** with Pic and Lut followed this stepwise dissociative pathway, it would have a closely comparable reaction rate.

(14) (a) Brown, T. J.; Dickens, M. G.; Widenhoefer, R. A. *Chem. Commun.* **2009**, 6451–6453. (b) Brown, T. J.; Dickens, M. G.; Widenhoefer, R. A. *J. Am. Chem. Soc.* **2009**, *131*, 6350–6351. (c) Zhu, Y.; Day, C. S.; Jones, A. C. *Organometallics* **2012**, *31*, 7332–7335.

Paper 5

For the Section 6.3.2.

Gold-Catalyzed Hydroalkoxylation

Reaction Mechanisms

The Mechanism of Gold(I)-Catalyzed Hydroalkoxylation of Alkynes: An Extensive Experimental Study

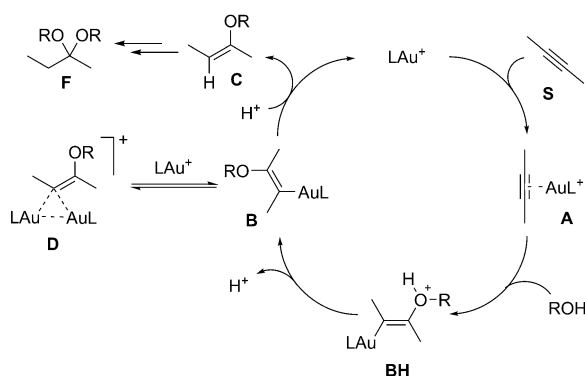
Alexander Zhdanko* and Martin E. Maier*[a]

Abstract: An extensive experimental study of the mechanism of gold(I)-catalyzed hydroalkoxylation of internal alkynes has been conducted by using NMR spectroscopy. This study was focused on the organogold intermediates, observations of actual catalytic intermediates in situ, and the reaction kinetics that are involved in this reaction. Based on the experimental results, a complete mechanistic picture was es-

tablished, including on- and off-cycle processes that explain the role of diaurated species. We have shown that gold-catalyzed hydroalkoxylation of internal alkynes is a reaction that requires only one gold atom for the catalytic cycle, disproving a recent hypothesis regarding the involvement of cooperative gold catalysis.

Introduction

The hydroalkoxylation of alkynes catalyzed by cationic gold(I) complexes was first described 15 years ago,^[1,2] and has long been considered to occur through four key steps (Scheme 1).



Scheme 1. Gold-catalyzed hydroalkoxylation and concurrent formation of *gem*-diaurated species **D**.

The first step is complexation of the gold catalyst to the substrate to form π complex **A**. Upon complexation, the substrate becomes activated towards nucleophilic attack by an alcohol (either inter- or intramolecularly). Nucleophilic attack leads to the formation of the vinyl gold complex, **B**, with the liberation

of a proton. Following this, protodeauration occurs to give enol ether **C**. Further transformation of **C** into acetal **F** is considered to be a classical proton-catalyzed process. A number of π complexes (**A**) have already been described;^[3] however, the properties of vinyl gold species **B** have never been investigated experimentally. The closest analogue to this structure was described by Hashmi and co-workers in 2009.^[4] Further information was provided by experimental model studies on vinyl gold species not bearing a heteroatom at the double bond. In particular, protodeauration was found to be a highly stereoselective process, occurring with retention of the configuration at the double bond.^[5] In addition to this experimental evidence, there have been a number of theoretical studies on the mechanism of this reaction.^[6] However, no experimental research focusing on the actual catalytic intermediates has been carried out; only the catalytic process as a whole has been reported so far.^[7] Some theoretical studies continue to support *syn*-alcohol addition, introducing even more ambiguity into the mechanistic picture.

In 2010 it was reported, by Fürstner et al., that enol-ether derived vinyl gold species **B** is very aurophilic and can readily form *gem*-diaurated species **D** by attracting a second LAu^+ unit.^[8,9] In a previous study, we provided a convenient route to enol-ether derived diaurated species **D** and confirmed the hypothesis of Fürstner et al.^[10] Our previous study provided access to the relevant catalytic intermediates, allowing in-depth research on the role of **D** within the catalytic cycle. Herein, we provide a detailed NMR investigation into the mechanism of gold-catalyzed hydroalkoxylation. The aim of this investigation was to gain insight into each of the elementary steps in the catalytic cycle.

[a] A. Zhdanko, Prof. Dr. M. E. Maier
Institut für Organische Chemie, Universität Tübingen
Auf der Morgenstelle 18, 72076 Tübingen (Germany)
Fax: (+49) 7071-295137
E-mail: vinceero@gmail.com
martin.e.maier@uni-tuebingen.de

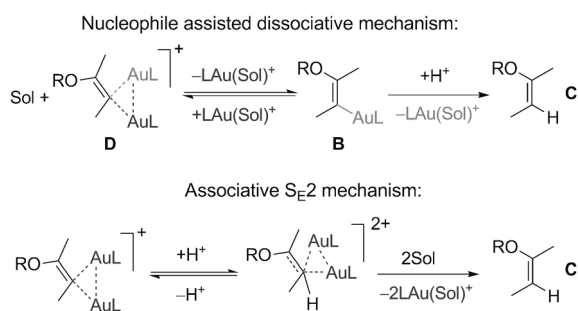
Supporting information for this article is available on the WWW under <http://dx.doi.org/10.1002/chem.201303795>.

Results and Discussion

The mechanism of protonolysis of diaurated species

Originally, diaurated species **D** was proposed as an off-cycle intermediate.^[8] However, to fully understand the mechanism of hydroalkoxylation, it is necessary to understand whether **D** continues to contribute to the overall process, or if the gold center gets trapped as species **D**. Therefore, we have studied the possibility that **D** can undergo protodeauration.

There are two possibilities that have to be considered (Scheme 2). Firstly, a nucleophile-assisted dissociative pathway, in which **D** first forms vinyl gold species **B**, which undergoes



Scheme 2. Preliminary consideration of the possible protonolysis pathways of the diaurated species.

subsequent protodeauration to finally liberate the product and the catalyst. Secondly, one might also envision the reaction to occur as a direct S_E2 process. However, in a different example, Gagne and Wiedenhofer have already reported that an S_E2 process does not operate.^[9f] Because the S_E2 process for the gold exchange at diaurated species cannot be completely ruled out,^[11] we have investigated the possibility of protodeauration to resolve any ambiguities.

To establish the correct mechanism, we studied the reaction of **D2** and **D1** (Figure 1) with acids ($t\text{Bu}_2\text{PyH}^+$, $\text{TfOH}\cdot(\text{Me}_2\text{N})_2\text{CO}$) under several conditions. We found that protonolysis is greatly

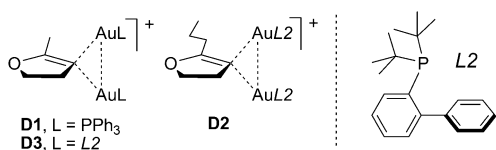
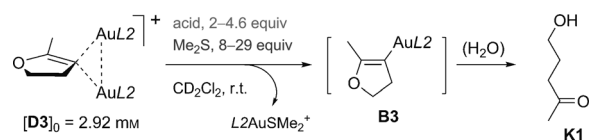
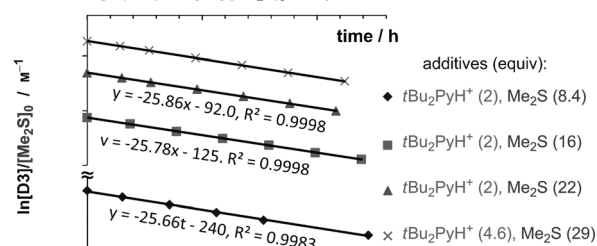


Figure 1. The diaurated species used in protonolysis studies.

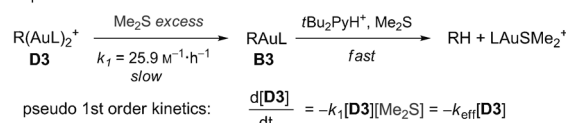
enhanced in the presence of a suitable nucleophile, unambiguously suggesting that the nucleophile-assisted dissociative mechanism is operating (see the Supporting Information). To confirm this mechanism, we conducted a series of kinetic experiments. Species **D3** was reacted with $t\text{Bu}_2\text{PyH}^+\text{OTf}^-$ in CD_2Cl_2 , in the presence of various amounts of Me_2S (8–29 equivalents), as shown in Scheme 3. The reaction was moni-



first order graphs $y = \ln[\text{D3}]/[\text{Me}_2\text{S}]_0 = -k_1t + \text{const}$:



Explanation:



Scheme 3. Kinetics of the nucleophile-assisted protodeauration of **D3**.

tored by NMR spectroscopy (the CH_2O signal was used for quantitative determination of **D3**). As expected, the reaction followed pseudo-first-order kinetics. The rate of the reaction is independent of the concentration of the acid, indicating that the reaction does not occur as a direct S_E2 process, but rather as a stepwise process through initial formation of the vinyl gold species **B3** as the rate-limiting step (Scheme 3). Importantly, fast protodeauration ensures that an equilibrium between **D3** and **B3** is never established. Therefore, in this case, the conversion of diaurated species **D3** into vinyl gold species **B3** can be considered as an irreversible rate-limiting step.

These findings unambiguously indicate that protodeauration of the diaurated species cannot occur through the direct reaction with an acid as a S_E2 process, but must occur by means of a nucleophile-assisted dissociative process that involves the formation of free vinyl gold species **B**. This finding is in accordance with conclusions by Gagne et al.^[9f]

Protonolysis of enol-ether derived vinyl gold

Our attention was then turned to the reactivity of vinyl gold species **B** towards acids. During this study we realized that this type of vinyl gold species is more susceptible to protodeauration than any other vinyl gold species described in the literature.^[12] Most of the vinyl gold species encountered in this study undergo protodeauration immediately even by using PrSpH^+ (1,8-bis(dimethylamino)naphthalene salt) in CDCl_3 or MeOD . More interestingly, these species also undergo protodeauration immediately in methanol. However, strong electron-withdrawing groups slow down this process significantly. Conjugation with the π system of an alkene or phenyl ring also slows down protodeauration.

To quantitatively describe the structural effects of the substrate and ligand on the protodeauration, we studied the reac-

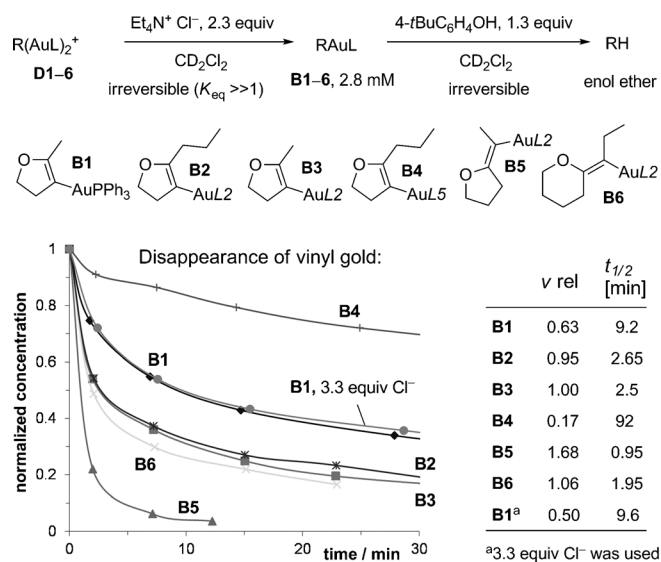
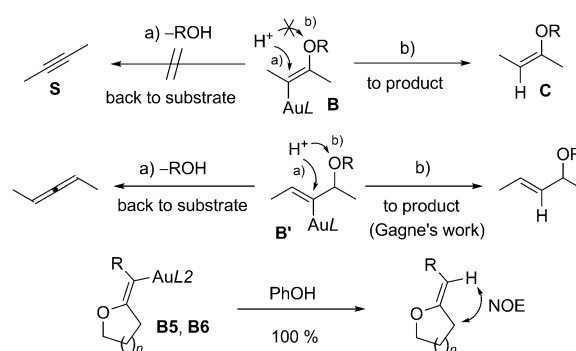


Figure 2. Protonolysis of vinyl gold species B1–6 by 4-*tert*-butylphenol.

tions of vinyl gold species B1–B6 (generated in situ) with 4-*tert*-butylphenol, which is a suitably strong acid (Figure 2). Unfortunately, rigorous quantitative comparison of the rate of protodeauration was not possible because none of the reactions displayed general second-order kinetics. This is explained by the formation of molecular aggregates between free phenol and its phenoxide product, accounting for the autoretardation of the reaction.^[13] Nevertheless, some quantitative information could be obtained; we estimated the relative initial rates and vinyl gold species half-life periods (measured from 0–50% conversion) and found that the rate of protodeauration increases in the presence of electron-donating ligands. Also, it is likely that steric interactions play no (or an insignificant) role in this reaction. Thus, protodeauration of vinyl gold species B3, bearing bulky ligand L2, reaches 50% conversion almost four times faster than B1 (bearing a PPh₃ ligand), and 37 times faster than B4 (bearing electron-deficient ligand L5; see Scheme 5 for structure). Furthermore, because the reaction was insensitive to an excess of Et₄N⁺ Cl[−], it can be concluded that protodeauration does not require any precoordination to the gold center and starts upon interaction of the double bond with the proton source.

An important aspect of protodeauration, established by these experiments, is the stereo- and regioselectivity of the process. The protodeauration can be concluded to be a one-way reaction, towards product C, because the alkyne substrate, S, cannot be reformed during the protodeauration reaction (Scheme 4). This behavior is opposite to that of vinyl gold species B', an intermediate in the gold-catalyzed hydroalkoxylation of allenes.^[9f] This difference in behavior is due to the strong mesomeric effect of oxygen, making the carbon atom the only possible site for protonation in B, but not in B'. Also, the protodeauration of B5 and B6 occurred with complete retention of configuration, as revealed by the NOESY spectra of the corre-



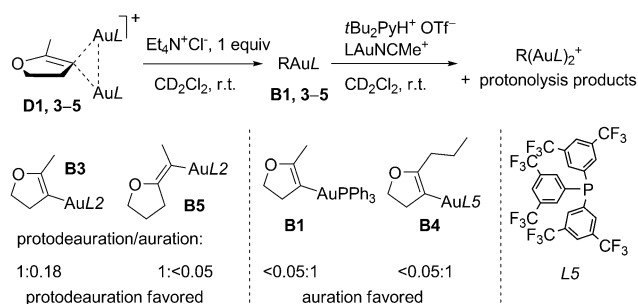
Scheme 4. Stereo- and regioselective protodeauration of vinyl gold species B as opposed to B'.

sponding enol-ether products. This result is in accordance with another model study.^[14]

Competitive experiments on protodeauration or auration of the vinyl gold species

Diaurated species are reluctant to undergo protonolysis, therefore, it can be concluded that fast product formation in gold-catalyzed hydroalkoxylation can only occur by protodeauration from the vinyl gold intermediate. However, this protodeauration process is in competition with the formation of a diaurated species. Therefore, it is important to understand the dependence of this competition on the structural parameters of the vinyl gold species.

To address this issue, we conducted competitive studies on the protodeauration or auration of vinyl gold intermediates. For this purpose, diaurated species D1, D3, D4, and D5 were treated with Et₄N⁺ Cl[−] (1 equivalent) to quantitatively generate the corresponding vinyl gold species in situ. These species were then treated with a solution of *t*Bu₂PyH⁺ and the LAuNC-Me⁺ SbF₆[−]. The results strongly depend on the ligand attached to the gold center (Scheme 5). When the bulky L2-containing species was used protodeauration was favored, whereas when PPh₃ and L5 ligands were used the formation of a diaurated species was favored. These results directly correlate with the stability of diaurated species and the trends in the protodeauration of vinyl gold species.^[15] Based on this result, it can be



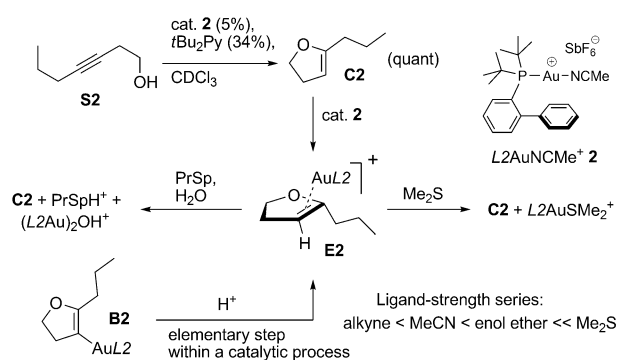
Scheme 5. Competitive protodeauration/auration of vinyl gold species.

concluded that sterically hindered electron-rich ligands (L2) will favor protodeauration over the formation of **D**. For other ligands (PPh₃, L5), formation of **D** is favored.

π -enol-ether gold complexes as intermediates

Enol-ether product **C** is a component in the system even if it is eventually transformed into an acetal, therefore, it is necessary to consider its complexation to the gold catalyst. The corresponding complexes **E** have been independently reported by A. Jones et al.^[16] During our investigation, we discovered that if catalytic hydroalkoxylation is performed under buffered conditions (using 2,6-di-*tert*-butylpyridine, *t*Bu₂Py, as an additive), the targeted synthesis of enol ethers becomes possible. Under these conditions, we were able to observe π complexes of enol ethers with gold centers.

Thus, when 3-heptynol, **S2**, was treated with catalyst **2** (L2AuNCMe⁺ SbF₆⁻, 5%) in the presence of *t*Bu₂Py (34%), in CDCl₃, cyclization occurred immediately (within 5 min), providing enol ether **C2** in quantitative yield (in situ). At the end of this reaction, the gold catalyst was predominantly present as a new π -enol-ether complex **E2** which was characterized in situ and exhibited typical spectroscopic values for a complex of this type, analogous to the literature data (Scheme 6).^[16] The



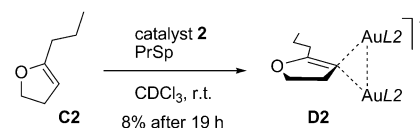
Scheme 6. π -enol-ether complex **E2** and its stability. PrSp = proton sponge (1,8-bis(dimethylamino)naphthalene).

uncomplexed and complexed enol ether showed two clear separate signal sets, indicating slow mode of L Au(C2)⁺/C2 ligand exchange in CDCl₃. However, in methanol this exchange becomes a fast equilibrium [Eq. (1)], as evidenced by a single doublet for the *t*Bu groups. Ligand-exchange reactions characterize the enol ether as a weak ligand for gold(I) centers, taking an intermediate position between MeCN and Me₂S, in accordance with the literature data.^[16]



Since **E** exists as an individual compound, it is reasonable to postulate that the addition of a proton to the vinyl gold species is a necessary step in the mechanism of catalytic hydroalkoxylation (Scheme 6).

However, **E** is a cationic complex that could be susceptible to deprotonation, resulting in the formation of vinyl gold species **B**. Therefore, it is important to determine whether the formation of **E** from **B** is reversible under catalytic conditions. For this purpose, we attempted the auration of enol ether **C2** under basic conditions. Treatment of **C2** with catalyst **2** and a proton sponge, in CDCl₃, did afford diaurated species **D2** as the only product, but in low yield (8%, in situ) after 19 h at room temperature (Scheme 7). On the one hand, this result



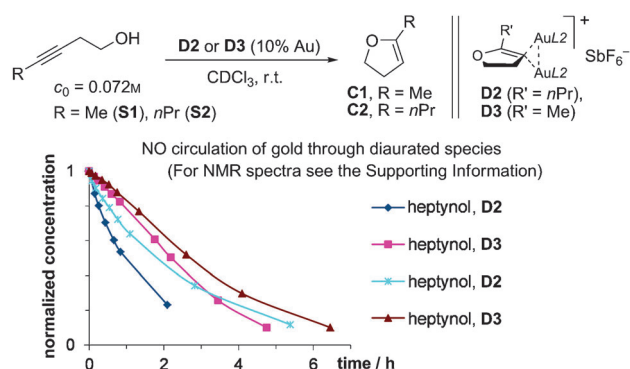
Scheme 7. Direct auration of enol ether **C2**.

proved that the direct auration of enol ethers, a hitherto unprecedented process, is possible.^[17] However, because this process occurred so slowly, even under basic conditions, it would be virtually impossible under the weakly acidic conditions of catalytic hydroalkoxylation. Therefore, proton addition to the vinyl gold species to provide **E** can be considered as an irreversible process within the catalytic cycle, whereas release of **C** from **E** is an ordinary reversible ligand-exchange process at the gold center.

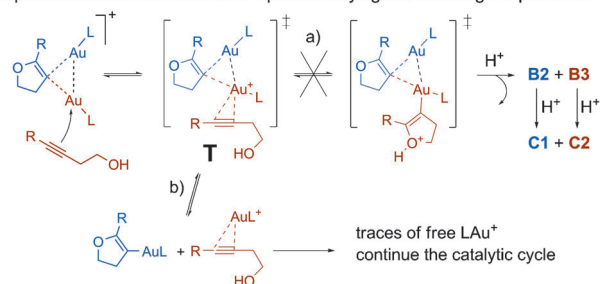
Catalytic performance of diaurated species in the hydroalkoxylation reaction

Diaurated species are unable to undergo direct protonolysis, therefore, it is important to ascertain whether there are other ways in which they might contribute to the catalytic process. To investigate this subject, we performed four experiments by using two substrates and two diaurated species (10 mol% Au; see Scheme 8). We found that in both cross-experiments no circulation of gold was observed through the diaurated species. The fact that the diaurated species remained completely unreacted indicated that the catalytic activity was due to the turnover of traces of free LAu⁺ species, and that these species performed so many catalytic cycles that the substrate had completely reacted before the diaurated species could be renewed. Furthermore, this observation suggests that tricoordinate gold complexes, L Au(B)(Alkyne)⁺ (**T**), do not trigger hydroalkoxylation, but are only transition states in the S_N2 ligand-exchange processes, otherwise the diaurated species would be renewed (see below for further corroboration). Hence, we have demonstrated that the diaurated species themselves are not active catalysts and are only able to communicate with the catalytic cycle through the ligand-exchange pathway. This finding implies that in processes that have used diaurated species as catalysts, these species were not acting as direct catalysts, but instead through dissociation.^[18] Accordingly, the less stable **D2** was more active because it can dissociate more easily than **D3**.

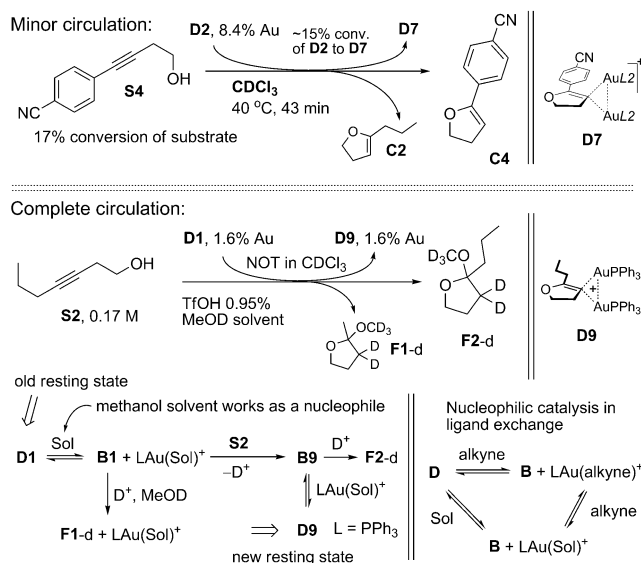
In addition, we observed circulation through diaurated species in other experiments. Thus, partial circulation was ob-



Upon interaction with diaurated species only ligand exchange is possible:



Scheme 8. Absence of gold circulation in catalysis by diaurated species D.



Scheme 9. Observation of gold circulation in catalysis by diaurated species.

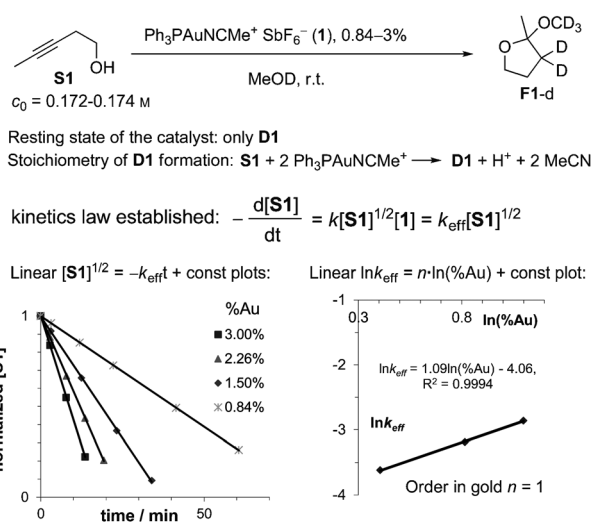
served when a less-reactive alcohol **S4** was used (Scheme 9). Formation of **D7** is possible owing to preferential protodeauration of electron-rich **B2** compared with that of the vinyl gold species bearing an electron-withdrawing group (EWG). This reaction liberates $L2Au(Sol)^+$, which eventually ends up in the new diaurated species **D7**. Fast circulation (leading to complete and immediate renewal of the diaurated species) was observed in the cyclization of **S2**, catalyzed by **D1**/TfOH in MeOD (Scheme 9). Again, no circulation was observed for the same reaction in $CDCl_3$ (despite the overall catalytic reaction taking

place smoothly). This observation demonstrates nucleophilic catalysis by the solvent, consisting of speeding up the circulation of the gold species through establishing additional fast-working ligand-exchange equilibria that do not affect the global equilibrium. This kind of nucleophilic catalysis, by a weakly nucleophilic solvent or indifferent third nucleophile, is frequently observed in ligand exchange at gold centers.

Direct observation of catalytic intermediates in situ

To get a complete understanding of the mechanism of gold-catalyzed hydroalkoxylation, we conducted kinetic studies by using NMR spectroscopy. In each experiment we monitored the disappearance of the substrate with time, the presence of organic intermediate products, and the development of the final products. Besides this, particular attention was given to the observation of catalytic organogold intermediates (resting states) in situ. Complete tables, diagrams, explanations, and spectra are given in the Supporting Information.

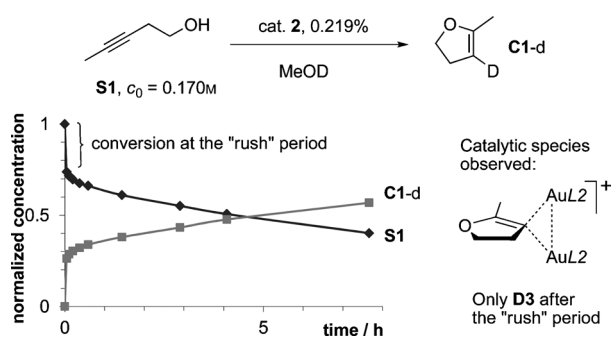
Initially, catalytic hydroalkoxylation of 3-pentyn-1-ol (**S1**), in CD_3OD , in the presence of catalyst **1** ($Ph_3PAuNCMe^+ SbF_6^-$) was investigated (Scheme 10).^[19] This reaction is characterized



Scheme 10. Cyclization of **S1** catalyzed by **1**.

by immediate and complete formation of diaurated species **D1**, as observed by NMR spectroscopy. According to the reaction stoichiometry, formation of **D1** is accompanied by the formation of the same amount of a strong acid ($HSbF_6$). This acid further catalyzed the transformation of the enol ether so that only a negligible amount ($<0.4\%$) of the enol ether is detectable. The overall reaction was found to be half-order in substrate and first-order in gold (see below).

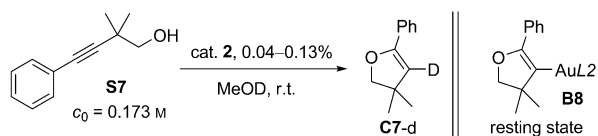
In contrast, when using the more bulky catalyst **2**, we found that diaurated species **D3** does not form as quickly as when catalyst **1** was used.^[20] Rather, **D3** accumulates relatively slowly (within few minutes) and eventually becomes predominant, resulting in the appearance of a characteristic "rush" period and the L-shape curve of the kinetic plot shown in Scheme 11. The



Scheme 11. Observation of the "rush" period.

shape of this curve is readily explained; the reaction starts very fast, but the gold species inevitably starts to form the diaurated species, resulting in significant slowing of the reaction. Indeed, an experiment with 0.15% catalyst loading allowed us to observe accumulation of **D3**, during an extended period of time, and to register the signals of $L2Au(Sol)^+$ and **B3** disappearing at the end of the rush period. Therefore, it can be suggested that formation of the diaurated species accounts for catalyst deactivation. This problem is not encountered at higher loadings of **2**. When more gold catalyst is present, it is possible that the reaction can reach completion during the very fast rush period, before any **D3** can accumulate.^[21] However, after the rush period (when formation of diaurated species is complete) the system establishes half-order kinetics for the rest of conversion (see below).

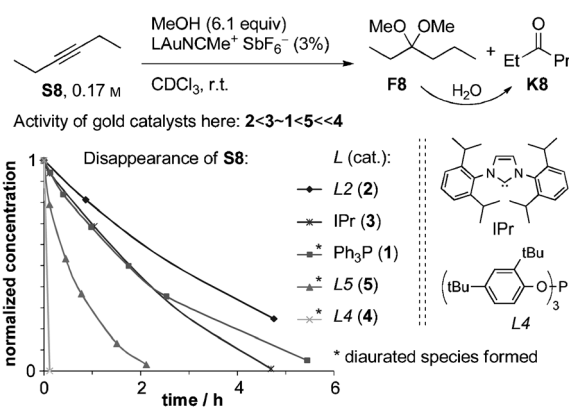
Catalyst **2** (less likely to form the diaurated species) is more active than **1** for the cyclization of **S1**. Therefore, we investigated whether the pure vinyl gold species could be observed if the formation of the diaurated species is completely suppressed. Recalling that sterically hindered alcohol **S7** forms extremely unstable diaurated species with catalyst **2**,^[15] we used this substrate for the reactions with catalyst **2**. We performed catalytic runs at different catalyst loadings (0.04–0.13 mol%) and in all cases the gold catalyst rested as a single compound, which was unambiguously proven to be vinyl gold species **B8** by comparison with an authentic sample prepared in situ under noncatalytic conditions (Scheme 12). This finding is the



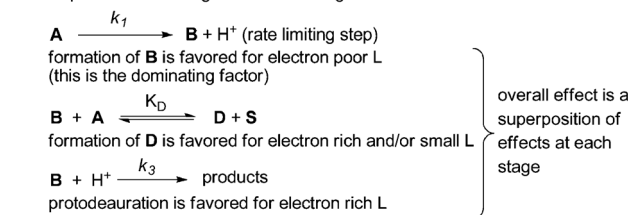
Scheme 12. Direct observation of vinyl gold species.

first direct evidence of the intermediacy of a vinyl gold species in a catalytic alkyne hydroalkoxylation process. Next, we established that the reaction is drastically accelerated by acid, proving protodeauration to be the rate-limiting step of this process.

Similarly, we investigated an intermolecular hydroalkoxylation of hex-3-yne **S8**, a more challenging reaction type, in the



Scheme 13. Hydroalkoxylation of hexyne **S8**.



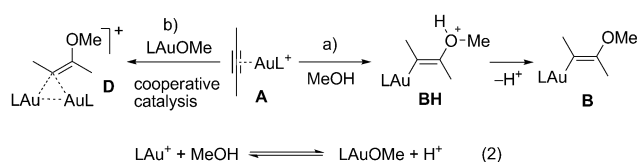
Scheme 13. Hydroalkoxylation of hexyne **S8**.

presence of various catalysts in $CDCl_3$ (Scheme 13). This study indicated that bulky electron-rich catalysts **2** and **3** did not form diaurated species at all, whereas more electron-deficient and less-crowded catalysts (**1**, **4**, and **5**) readily formed the corresponding diaurated species. Therefore, in this case, the reaction is much more efficiently catalyzed by electron-deficient catalysts, even though the catalysis might be accompanied by the formation of the corresponding diaurated species.

The above experiments demonstrated that the formation of a diaurated species is, generally, not obligatory for gold catalysis and the formation of this species can vary broadly (from 0 to 100%). Secondly, and very importantly, thorough monitoring of resting states should be performed to allow unambiguous conclusions to be made.

Probing the early stages of the catalytic cycle

Our experimental data has provided a clear understanding of the mechanism of gold-catalyzed hydroalkoxylation, starting from the formation of the vinyl gold species. All that remained was to define what happens before the formation of this species, at the early stages of the catalytic cycle. It is well known that alkynes form a π complex **A** which is a reasonable proposal for the first step of the catalytic process.^[22] However, exactly how **A** transforms into the vinyl gold species continues to be a subject of debate. According to one model, π complex **A** reacts directly with an alcohol to give cationic addition product **BH**, which immediately expels a proton to give vinyl gold species **B** (Scheme 14, route a).^[6] The only experimental study that investigated the viability of this hypothesis was conducted in the gas phase under strictly bimolecular collisions. Under these conditions, formation of the C–O bond was found to be impossible.^[23] A number of theoretical studies have been pub-



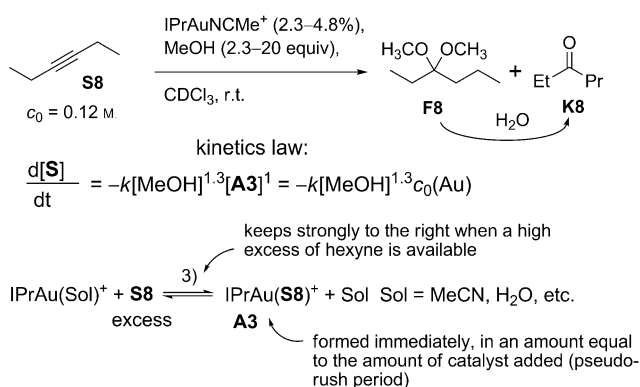
Scheme 14. Current viewpoints to account for the C–O bond-forming event.

lished, concluding that alcohol addition to π complex **A** must be thermodynamically disfavored and that the subsequent proton transfer can only occur in the presence of neighboring molecules in the condensed phase.^[6] Recently, a new hypothesis based on theoretical calculations was proposed.^[24] This hypothesis suggested that diaurated species could form by the direct reaction of two gold-containing species, cationic π complex **A** and a neutral molecule of gold methoxide L2AuOMe (cooperative catalysis, Scheme 14, route b). However, L2AuOMe must arise from a reversible reaction of the gold catalyst with methanol (Scheme 14, [Eq. (2)]). This reaction is highly disfavored because L2AuOMe is a highly basic compound that may not exist under the weakly acidic conditions that are typical for gold-catalyzed hydroalkoxylation.^[25]

In order to resolve the above ambiguities, we relied on kinetic experiments. We hypothesized that information about the early stages of the catalytic cycle may only be obtained if formation of the vinyl gold species becomes the rate-limiting step and the formation of any diaurated species is suppressed. These two conditions were applied in a series of experiments described below.

Catalysis by $\text{IPrAuNCMe}^+ \text{SbF}_6^-$

The reaction of hex-3-yne with MeOH, catalyzed by $\text{IPrAuNCMe}^+ \text{SbF}_6^-$ (IPr = 1,3-bis(2,6-diisopropylphenyl)-1,3-dihydro-2H-imidazol-2-ylidene), in CDCl_3 or CD_2Cl_2 , exhibited zero-order dependence in substrate, but first-order in gold (Scheme 15). The examination of the reaction mixtures by NMR spectroscopy revealed complete formation of $\text{IPrAu}(\text{hex})^+$ (hex = hex-3-yne) **A3**, the concentration of which remains constant during the conversion and eventually converts into

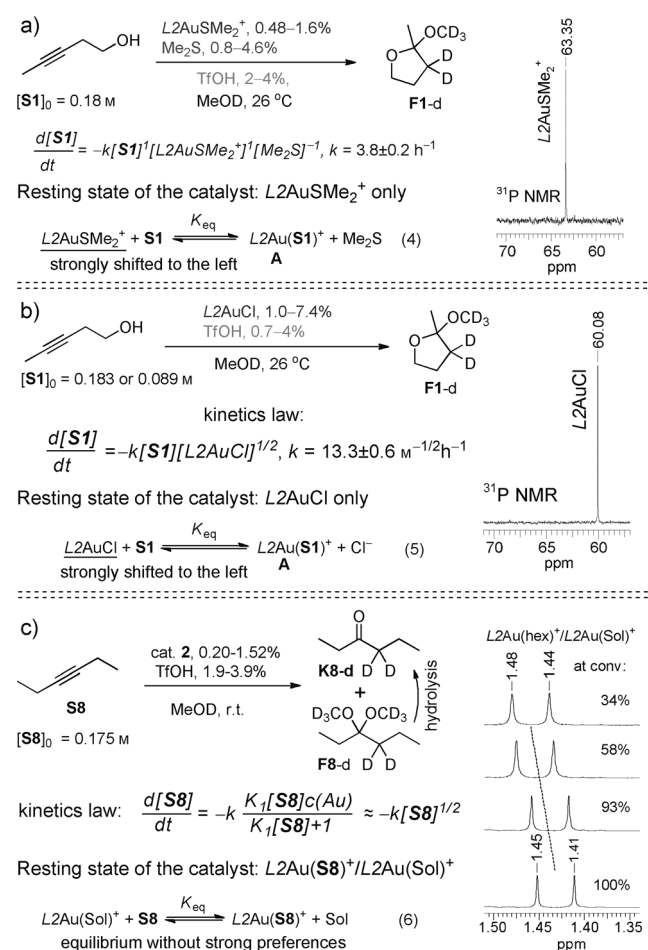


Scheme 15. Addition of methanol to 3-hexyne.

$\text{IPrAu}(\text{Sol})^+$ (Sol = solvent, MeCN, H_2O , etc.). This result is significant because it demonstrates that, **A3** is the necessary intermediate. Also, because **A3** is formed quantitatively, the first-order dependence with respect to the gold center also means that the reaction is first-order in **A3**. Finally, quantitative formation of **A3** indicates that the ligand-exchange equilibrium (Scheme 15) remains strongly to the right during most of the conversion. This finding explains why the reaction is zero-order in substrate; on reaching saturation the change in concentration of the substrate does not lead to a substantial change in the concentration of **A3**. However, closer to the end of reaction the concentration of **A3** will not be equal to the concentration of Au and the reaction will deviate from the zero-order law. Interestingly, the reaction exhibited 1.3-order kinetics in MeOH, the reason for which will be discussed below.

The role of the ligand-exchange equilibrium

In order to confirm that **A** (the necessary starting point of hydroalkoxylation) arises as the result of the ligand-exchange equilibrium with a L2AuX species and **S**, we studied the chemical kinetics of a number of reactions (Scheme 16). The resting state of the catalysts was monitored in each case by NMR spectroscopy. Thus, the reaction catalyzed by a L2AuSM_2^+ /



Scheme 16. Reaction kinetics and resting states.

Me₂S system (see Scheme 16 a), exhibited first-order kinetics in **S1**, first-order kinetics in gold species, minus first-order kinetics in Me₂S, and had L2AuSMe₂⁺ as a resting state. The reaction catalyzed by L2AuCl (see Scheme 16 b), exhibited first-order kinetics in **S1**, half-order kinetics in gold species, and had L2AuCl as a resting state. In these cases, the ligand-exchange equilibria (Scheme 16, [Eq. (4 and 5)]) are strongly on the side of the resting states.

The intermolecular reaction catalyzed by **2** (see Scheme 16 c) exhibited pseudo-half-order kinetics in substrate and first-order kinetics in gold.^[26] In each experiment, the ¹H NMR spectrum of catalyst **2** exhibited a single doublet, the chemical shift of which gradually changed from 1.46 to 1.43 ppm (corresponding to the pure catalyst in methanol). This observation indicates that the catalyst existed as a L2Au(hex)⁺/L2Au(Sol)⁺ mixture undergoing fast ligand exchange. As the reaction progresses to completion, only L2Au(Sol)⁺ remains and the spectroscopic values of the free catalyst are restored.^[27] In this case, the ligand-exchange equilibrium (Scheme 16, [Eq. (6)]) does not favor any side strongly.

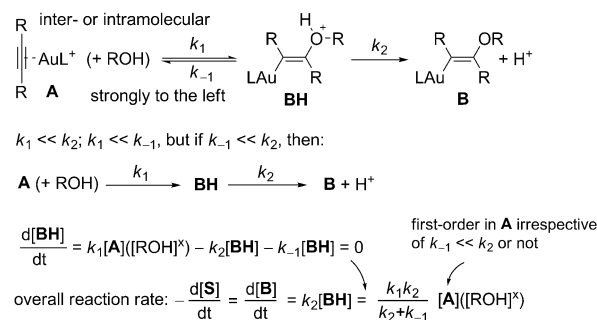
All reactions were independent from acid, to establish that protodeauration is not the rate-limiting step in these cases. The kinetics laws were theoretically derived based on the assumption that the necessary intermediate **A** must arise as a result of the corresponding ligand-exchange equilibrium. Also, the material balance of the system was taken into account. The theoretically derived rate laws (Figure 3) were in accordance with experimentally observed laws, confirming the following: 1) The hydroalkoxylation is only possible from **A**; 2) The reaction will follow first-order kinetics with respect to **A**, but the order of the reaction with respect to the catalyst and substrate **S** may vary, depending on the functional dependence $[A] = f(S, c(Au))$ being operative; 3) Hypothetical tricoordinate complexes LAu(N)(Alkyne)⁺ are only intermediates (or transition states) of S_N2 ligand-exchange processes and productive hydroalkoxylation is not triggered in this state; 4) Simple ligand-exchange equilibria (known to be very fast processes for the coordination of gold)^[28] are established.

This result fully supports the original model (Scheme 14 a), and the cooperative catalysis mechanism (Scheme 14 b) is con-

tradicted by our experimental study.^[29] The cooperative catalysis mechanism is contradictory to all of our kinetic observations (it would require second-order kinetics with respect to the gold species, which was never observed). Also, the cooperative catalysis mechanism is contradictory to the direct observation of vinyl gold species in situ (Scheme 12). Furthermore, the presence of an acid promoter would diminish the equilibrium shown in [Eq. (2)] (Scheme 14), and negatively affect the reaction. For the reactions carried out in this section no acid dependence was observed. However, in many cases, the reaction can be greatly accelerated in the presence of additional acid in comparison with the use of a gold catalyst alone.

The transformation of gold-alkyne complex **A** into vinyl gold species **B**: the role of hydrogen bonding

Although the results of the above experiments excluded the possibility of a cooperative catalysis pathway, these experiments did not reveal exactly how **A** was transformed into vinyl gold species **B**. However, we have shown that the catalytic reaction occurs because of the availability of **A** and that the reaction must proceed via **B** (and not **D**). Therefore, we propose the involvement of **BH**, resulting from pure *anti*-addition (Scheme 17). This elusive intermediate cannot be observed directly and remains hypothetical. However, based on the current knowledge of related species, we are able to predict the



Scheme 17. The transformation of **A** into **B**.

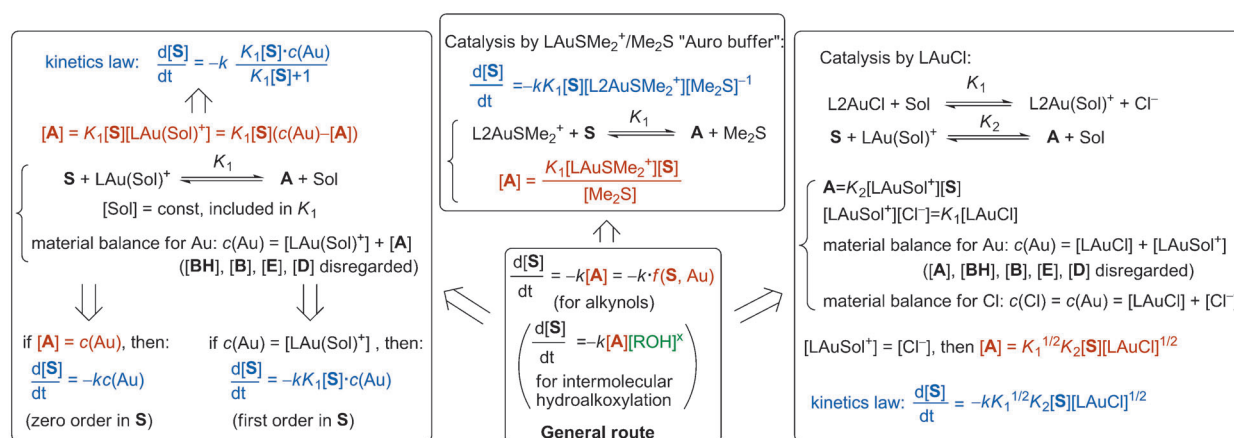
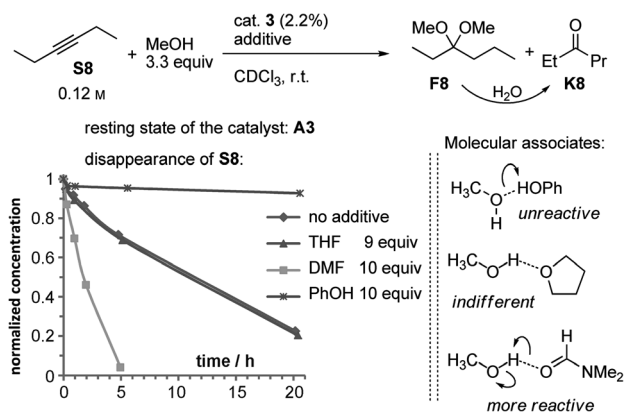


Figure 3. The first-order dependence in **[A]** is the common root of the kinetics laws shown.

properties of **BH**. Thus, it is well known, that any species of the type $\text{LAu-C}\equiv\text{C-X}$ and LAu-C-C-X are prone to elimination, resulting in the parent alkyne or alkene (depending on the quality of X as a leaving group).^[30] Also, the inability of hydroalkoxylation to proceed in the gas phase, under conditions of bimolecular collisions,^[23] is in agreement with proton transfer from **BH** only being possible in solution phase, as was suggested by earlier computational studies.^[6] It can be concluded that the formation of **BH** (the C–O bond forming event) must be a highly reversible endothermic process (always $k_1 \ll k_{-1}$). Furthermore, we are able to conclude that proton loss by **BH** is irreversible. This follows from the experimental observations and considerations discussed above and in Scheme 4.

However, two important aspects remain unclear with regard to the **A** into **B** transformation: 1) The importance of the hydrogen bonding involving ROH, as suggested by the computational study; 2) The elimination of H^+ is considered to be a very fast step (k_2 is large), therefore, it becomes unclear whether the whole sequence, from **A** to **B**, should be considered as a combination of one reversible step and a second irreversible step (if $k_{-1} \approx k_2$), or as a sequence of two irreversible steps (if $k_{-1} \ll k_2$). Remarkably, all of the experiments described above do not provide an answer. Regardless of the real situation, both considerations result in the same kinetics, that is, first-order kinetics with respect to **A** (Scheme 17).

To begin to answer these questions, we studied the effect of various hydrogen-bond donors (PhOH) and acceptors (THF, DMF) in the reaction of hexyne **S8** in CDCl_3 (Scheme 18). A dra-

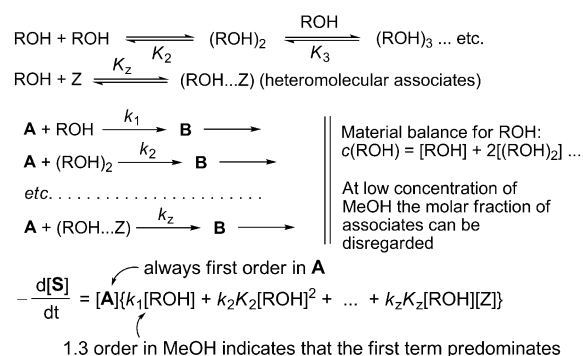


Scheme 18. Effect of hydrogen-bond donors and acceptors.

matic increase in the reaction rate was seen in the presence of DMF (10 equivalents), whereas phenol slowed down the reaction. Given the fact that DMF and PhOH behave as chemically inert additives, not influencing the formation and reactivity of gold–acetylene complex **A3** and not giving rise to any new products, the changes in the reaction rate are, presumably, due to their influence on the reactivity of MeOH through hydrogen bonding.^[31] This influence can be explained by the formation of molecular aggregates with variable reactivity towards **A3**. It can be concluded that the association of MeOH to a strong hydrogen-bond acceptor (DMF) increases the nucleo-

philicity of the oxygen atom, activating methanol for addition (at the same time enhancing deprotonation of **BH**), whereas association with a strong hydrogen-bond donor (PhOH) has the opposite effect. THF did not exhibit any substantial effect, despite having the ability to form hydrogen bonds. This indicates that the strength of the hydrogen-bond effect depends on the “quality” of an associated molecule as hydrogen-bond donor or acceptor. Together with the average 1.3-order kinetics in methanol that was previously established for this reaction, this fact suggests that hydrogen bonding with ether or alcohol has a weak influence on the reaction kinetics.

The hydrogen-bond effect can be interpreted, with regards to chemical kinetics, as shown in Scheme 19. Thus, considering the formation of homo- and heteromolecular species that are



Scheme 19. An interpretation of hydrogen-bond effects by chemical kinetics.

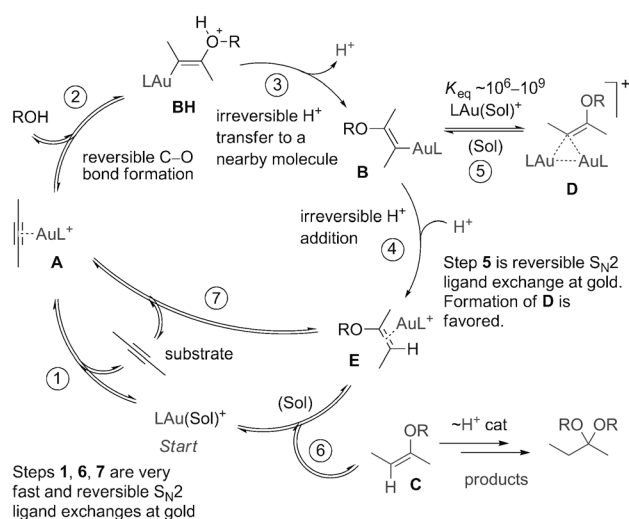
in equilibrium with each other (K_2, K_3, \dots, K_z), each of them is reactive towards **A** (k_1, k_2, \dots, k_z) and the rate law appears as a polynomial equation. According to this treatment, if the formation of these associated species was really necessary for a simple reaction with MeOH, very strong dependence on the concentration of MeOH would be observed because the molar fraction of the associated species depends on the concentration of MeOH in the order ≥ 2 , which at low concentrations of MeOH will lead to at least second-order kinetics in methanol.

The chemical shift of the OH proton in solvents such as CDCl_3 or CD_2Cl_2 strongly depends on the concentration of the alcohol, a direct consequence of the formation of molecular associates. That effect is the same as that observed in our earlier experiments: $\delta(\text{OH})$ changes from 1.37 to 3.25 ppm as the amount of MeOH increases from 2.3 to 20 equivalents (Scheme 15). Evidently, the molar fraction of the molecular associates increased significantly, whereas the average order in MeOH was 1.3, which is close to 1. This indicates that the overall effect of hydrogen bonding between MeOH molecules is not strong and the reaction system still behaves as if it was simply a bimolecular reaction with a free molecule of MeOH in the solvent. This experimental finding is in contrast with the earlier computational study, which suggested that the association of the alcohol is crucial. Our experiments have established that hydrogen bonding is not obligatory for simple MeOH addition to take place. However, the reactivity of MeOH can be

changed significantly in the presence of a third additive (or a co-solvent), which forms strong molecular associates with different reactivity (and also changes the $\delta(\text{OH})$ chemical shift). From a practical point of view it is worth noting the strong positive effect of DMF, which can be used as a solvent or co-solvent. However, this advantage can be invalidated by DMF's basicity, which can negatively affect an acid-dependent reaction (see below).

Generalized mechanistic picture

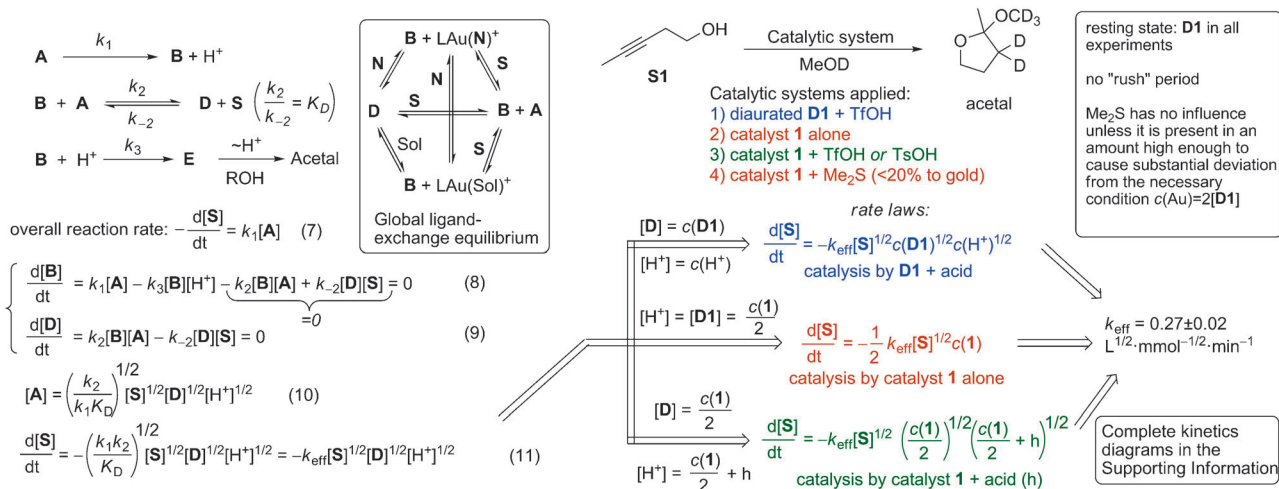
Based on the experimental evidence, a complete mechanistic picture of the catalytic process can be assembled (Scheme 20). From this mechanism all experimentally observed kinetics laws are derived. The kinetics of the reactions characterized by rate-limiting formation of vinyl gold species **B** and no formation of



Scheme 20. The mechanism of the gold-catalyzed hydroalkoxylation of alkynes.

diaurated species are derived from $v = -k[\text{A}]$, in which $[\text{A}] = f(\text{S}, c(\text{Au}))$ by using the ligand-exchange equilibrium and material balance that is shown in Figure 3.

The kinetics of the reaction accompanied by formation of a diaurated species requires a more sophisticated treatment because three key steps need to be considered; the formation of vinyl gold species **B** (k_1), the formation of diaurated species **D** (k_2/k_{-2}), and protodeauration (k_3) (Scheme 21). The (k_2/k_{-2}) equilibrium is part of global ligand-exchange equilibrium. However, in contrast with the other equilibria discussed, this equilibrium is dependent on the concentration of vinyl gold species **B**, which itself depends on the rate of protodeauration (k_3) and, hence, from the acidity of the system. In turn, because the formation of **D** is accompanied by the formation of an equal amount of acid, the acidity of the system actually depends on **D**. It is clear that all parts of the system become highly interrelated. Still, the behavior of a catalytic system that results in immediate and complete formation of **D** is amenable to easy analysis. Thus, by using the steady-state approximation shown in [Eq. (8)] (Scheme 21), for **B** (always present in undetectable amounts) and the steady-state approximation shown in [Eq. (9)] (Scheme 21), for **D** (always present, contains all of the gold in the system), the expression for **A** shown in [Eq. (10)] (Scheme 21), can be calculated.^[32] Putting this expression into the overall reaction rate ([Eq. (7)], Scheme 21), results in the rate law shown in [Eq. (11)] (Scheme 21).^[33] According to this law the reaction kinetics are characterized as being half-order in substrate, half-order in **D** and half-order in acid. The following important consequences are drawn from this working law: 1) If the formation of **D** is complete, the reaction will always depend on acidity, regardless of whether protodeauration is the rate-limiting step of the catalytic cycle or not; 2) The reaction does not depend on the presence of any indifferent nucleophile (**N**), unless it causes significant deviations from the necessary condition for the material balance $c(\text{Au}) = 2[\text{D}]$, which would become $c(\text{Au}) = 2[\text{D}] + [\text{LAu}(\text{N})^+]$; 3) The reaction follows this law regardless of how the catalytic system is created, either from the catalyst alone (giving rise to 0.5 equiv-



Scheme 21. Reaction kinetics at immediate and complete formation of the diaurated species.

alents of H^+ and 0.5 equivalents of **D** per 1 equivalent of gold catalyst), or from the catalyst and acid or from **D** and acid. 4) Proton delivery, from **BH** to **E**, does not occur intramolecularly through a chain of alcohol molecules clustered around **BH** by hydrogen bonding (as suggested by an earlier computational study^[6]). Rather, the proton from **BH** is removed, becoming free in solution, and then proton addition to **B** occurs to give **E** as an independent intermolecular event.

These principles were demonstrated by the reaction of pentynol **S1** in methanol using various catalytic systems. We experimentally determined that this reaction can be described by the rate laws shown in Scheme 21, originating from the general rate law [Eq. (11)] containing $k_{\text{eff}} = 0.27 \pm 0.02 \text{ L}^{1/2} \text{ mmol}^{-1/2} \text{ min}^{-1}$, irrespective of the catalytic system. In particular, first-order kinetics with respect to the gold species is established by catalyst **1** alone, leading to the rate law shown in Scheme 10. According to the tolerance of the system to an indifferent nucleophile, the kinetic profile is insensitive to small amounts of Me_2S .

If a reaction is characterized by the partial formation of **D**, the reaction kinetics cannot easily be analyzed because the steady-state approximation cannot be applied to either of the resting states of the catalyst. This situation takes place in reactions with a rush period (a kinetic effect caused by accumulation of diaurated species with time, Scheme 11) or for a reaction, in which partial formation of **D** is caused by a relatively low K_D value, with the result that the actual concentrations of the equilibrium participants do not allow the equilibrium system to stay entirely on the side of species **D**, whereas the equilibrium K_D is established at any time. In the latter case the catalyst will rest in at least two resting states and will follow a kinetic profile that fits between the kinetic profile at complete formation of **D** and the kinetic profile at complete formation of the other resting states. These principles are exemplified by the following experimental observations. The reaction of pentynol **S1** in MeCN follows first-order kinetics with respect to the substrate, despite being accompanied by the formation of **D3** (14% maximum). This means that the catalytic system has resting states (major: L2AuNCMe^+ and minor: **D3**) that are close in ratio to that of $\text{L2AuNCMe}^+/\text{MeCN}_{(\text{sol})}$, which is an auro buffer (see above, Figure 2). For example, the reaction of **S4** in MeOD follows the order in substrate between half- and first-order because of significant, but not complete, formation of **D7**. These cases are considered in more detail in the Supporting Information.

Conclusion

Based on experimental observations, a complete mechanism for gold-catalyzed hydroalkoxylation was constructed (Scheme 20). The reaction starts with reversible coordination of the alkyne at the gold center, forming π complex **A** (within the global ligand-exchange equilibrium among all possible LAu(N)^+ complexes).^[34] The binding affinity of alkynes is generally low and is weaker than MeCN. The π complex **A** then undergoes reversible *anti*-addition of an alcohol to form **BH**. This equilibrium is strongly shifted to the left because **BH** is a good

substrate for 1,2-elimination, the reverse process. However, **BH** is also a highly acidic species that can partake in rapid proton transfer to a nearby molecule. Therefore, some of the extremely elusive short-lived **BH** molecules will succeed in the transformation into vinyl gold species **B**. The difficulty of the alcohol addition to **A**, which will eventually form **B**, is the reason for the reaction rate order: intermolecular $< 6\text{-exo-dig} \ll 5\text{-endo-dig}$. Intermolecular hydroalkoxylation is, therefore, the most challenging, typically requiring excess alcohol. Neutral hydrogen-bond acceptors facilitate, whereas hydrogen-bond donors inhibit, the transformation of **A** into **B**. Electron-poor ligands increase the electrophilicity of **A**, greatly enhancing the transformation of **A** into **B**. The formation of **B** is irreversible, providing a fundamental basis for the reaction to proceed until no alkyne is left in the mixture. Vinyl gold species **B** is also a highly reactive species; it can competitively undergo protonolysis or auration to give π complex **E** or diaurated species **D**, respectively. Formation of **E** is a necessary step in the process, whereas formation of **D** is a drawback for the whole catalytic cycle. Although formation of **D** is reversible, it is strongly favored thermodynamically; **B** binds the catalytic LAu^+ species more strongly than an alkyne (the substrate) by a factor of $10^6\text{--}10^9$.^[15] Furthermore, **D** is completely unable to undergo direct protodeauration. Therefore, any gold centers that are trapped in this species are simply unable to take part in the catalytic cycle. Hence, **D** is viewed as an off-cycle inert complex, participating in the global ligand-exchange equilibrium in the same way as any other LAu(N)^+ complex. Destruction of **D** by using an indifferent nucleophile (**N**) will further inhibit the overall catalytic reaction. The application of very bulky ligands at the gold center, branched substrates, and acidic promoters can totally eliminate the formation of **D**. To complete the catalytic cycle, the resulting enol ether gold complex **E** will quickly undergo ligand exchange with any nucleophile (including the substrate) to finally liberate enol ether product **C**. The latter will stay as such or will be transformed into the corresponding acetal by means of a classical acid-catalyzed process, depending on the acidity of the reaction mixture. It is important to highlight that the formation of **D** is accompanied by the liberation of an equal amount of a super acid, which can drastically change the outcome of the initial gold-catalyzed process by speeding up additional acid-catalyzed processes (desired or undesired). Catalytic systems that are not accompanied by the formation of **D** will be less acidic than the systems with a high concentration of **D** (**B** quickly undergoes protodeauration so there will be no significant accumulation of H^+ , unless **D** is formed). As a consequence, the outcome of a gold-catalyzed reaction in the presence of various ligands (for example, PPh_3 or **L2**) can differ because of the level of acidity developed in the mixture, a reason that is not directly related to the gold catalysis itself.

With regard to the problem of the formation of diaurated species, we have shown that gold catalysis would be even more powerful if there was not an intrinsic property of gold centers to form this idle species. In perspective, new catalysts could be designed to result in increased reaction rates, productivity, and scope for gold catalysis. For example, the inability to

form diaurated species could be the reason for the exceptionally high efficiency of the catalyst recently reported by Hashmi et al.^[35]

Acknowledgements

Financial support by the state of Baden-Württemberg is gratefully acknowledged. We thank Dr. K. Eichele and the Institut für Anorganische Chemie for allowing us to use their NMR spectrometer.

Keywords: catalysis · gold · hydroalkoxylation · reaction mechanisms

- [1] a) J. H. Teles, S. Brode, M. Chabanas, *Angew. Chem.* **1998**, *110*, 1475; *Angew. Chem. Int. Ed.* **1998**, *37*, 1415; b) For a review, see: N. Huguet, A. M. Echavarren in *Hydrofunctionalization, Top. Organomet. Chem.* (Eds.: V. P. Ananikov, M. Tanaka), Springer, Heidelberg, **2013**, *43*, 291.
- [2] For general reviews on gold catalysis, see: a) M. Rudolph, A. S. K. Hashmi, *Chem. Soc. Rev.* **2012**, *41*, 2448; b) A. Corma, A. Leyva-Peréz, M. J. Sabater, *Chem. Rev.* **2011**, *111*, 1657; c) M. Bandini, *Chem. Soc. Rev.* **2011**, *40*, 1358; d) T. C. Boorman, I. Larrosa, *Chem. Soc. Rev.* **2011**, *40*, 1910; e) A. S. K. Hashmi, M. Bührle, *Aldrichimica Acta* **2010**, *43*, 27; f) N. D. Shapiro, F. D. Toste, *Synlett* **2010**, 675; g) S. Sengupta, X. Shi, *ChemCatChem* **2010**, *2*, 609; h) N. Bongers, N. Krause, *Angew. Chem.* **2008**, *120*, 2208; *Angew. Chem. Int. Ed.* **2008**, *47*, 2178; i) D. J. Gorin, B. D. Sherry, F. D. Toste, *Chem. Rev.* **2008**, *108*, 3351; j) E. Jiménez-Núñez, A. M. Echavarren, *Chem. Rev.* **2008**, *108*, 3326; k) Z. Li, C. Brouwer, C. He, *Chem. Rev.* **2008**, *108*, 3239; l) A. Arcadi, *Chem. Rev.* **2008**, *108*, 3266; m) J. Muzart, *Tetrahedron* **2008**, *64*, 5815; n) H. C. Shen, *Tetrahedron* **2008**, *64*, 7847; o) R. A. Widenhoefer, *Chem. Eur. J.* **2008**, *14*, 5382; p) D. J. Gorin, F. D. Toste, *Nature* **2007**, *446*, 395; q) A. Fürstner, P. W. Davies, *Angew. Chem.* **2007**, *119*, 3478; *Angew. Chem. Int. Ed.* **2007**, *46*, 3410; r) E. Jiménez-Núñez, A. M. Echavarren, *Chem. Commun.* **2007**, 333; s) A. S. K. Hashmi, *Chem. Rev.* **2007**, *107*, 3180; t) A. S. K. Hashmi, G. J. Hutchings, *Angew. Chem.* **2006**, *118*, 8064; *Angew. Chem. Int. Ed.* **2006**, *45*, 7896.
- [3] a) T. J. Brown, R. A. Widenhoefer, *J. Organomet. Chem.* **2011**, *696*, 1216; b) T. J. Brown, M. G. Dickens, R. A. Widenhoefer, *Chem. Commun.* **2009**, 6451; c) T. J. Brown, R. A. Widenhoefer, *Organometallics* **2011**, *30*, 6003; d) N. D. Shapiro, F. D. Toste, *Proc. Natl. Acad. Sci. USA* **2008**, *105*, 2779; e) S. Flügge, A. Anoop, R. Goddard, W. Thiel, A. Fürstner, *Chem. Eur. J.* **2009**, *15*, 8558; f) J. A. Akana, K. X. Bhattacharyya, P. Müller, J. P. Sadighi, *J. Am. Chem. Soc.* **2007**, *129*, 7736.
- [4] A. S. K. Hashmi, A. Schuster, F. Rominger, *Angew. Chem.* **2009**, *121*, 8396; *Angew. Chem. Int. Ed.* **2009**, *48*, 8247.
- [5] A. S. K. Hashmi, T. D. Ramamurthi, F. Rominger, *J. Organomet. Chem.* **2009**, *694*, 592.
- [6] a) M. Pernpointner, A. S. K. Hashmi, *J. Chem. Theory Comput.* **2009**, *5*, 2717; b) C. M. Krauter, A. S. K. Hashmi, M. Pernpointner, *ChemCatChem* **2010**, *2*, 1226; c) M. Lein, M. Rudolph, S. K. Hashmi, P. Schwerdtfeger, *Organometallics* **2010**, *29*, 2206; d) G. Mazzone, N. Russo, E. Sicilia, *Organometallics* **2012**, *31*, 3074.
- [7] For important reviews about catalytic intermediates in gold catalysis, see: a) A. S. K. Hashmi, *Angew. Chem.* **2010**, *122*, 5360; *Angew. Chem. Int. Ed.* **2010**, *49*, 5232; b) L.-P. Liu, G. B. Hammond, *Chem. Soc. Rev.* **2012**, *41*, 3129.
- [8] G. Seidel, C. W. Lehmann, A. Fürstner, *Angew. Chem.* **2010**, *122*, 8644; *Angew. Chem. Int. Ed.* **2010**, *49*, 8466.
- [9] Diaurated species are encountered in other gold-catalyzed processes, see: a) D. Weber, M. A. Tarselli, M. R. Gagne, *Angew. Chem.* **2009**, *121*, 5843; *Angew. Chem. Int. Ed.* **2009**, *48*, 5733; b) A. S. K. Hashmi, I. Braun, P. Nösel, J. Schädlich, M. Wietek, M. Rudolph, F. Rominger, *Angew. Chem.* **2012**, *124*, 4532; *Angew. Chem. Int. Ed.* **2012**, *51*, 4456; c) A. S. K. Hashmi, I. Braun, M. Rudolph, F. Rominger, *Organometallics* **2012**, *31*, 644; d) Y. Chen, M. Chen, Y. Liu, *Angew. Chem.* **2012**, *124*, 6285; *Angew. Chem. Int. Ed.* **2012**, *51*, 6181; e) A. S. K. Hashmi, M. Wietek, I. Braun, P. Nösel, L. Jongbloed, M. Rudolph, F. Rominger, *Adv. Synth. Catal.* **2012**, *354*, 555; f) T. J. Brown, D. Weber, M. R. Gagne, R. A. Widenhoefer, *J. Am. Chem. Soc.* **2012**, *134*, 9134; g) D. Weber, T. D. Jones, L. L. Adduci, M. R. Gagne, *Angew. Chem.* **2012**, *124*, 2502; *Angew. Chem. Int. Ed.* **2012**, *51*, 2452; h) J. E. Heckler, M. Zeller, A. D. Hunter, T. G. Gray, *Angew. Chem.* **2012**, *124*, 6026; *Angew. Chem. Int. Ed.* **2012**, *51*, 5924; i) M. M. Hansmann, M. Rudolph, F. Rominger, A. S. K. Hashmi, *Angew. Chem.* **2013**, *125*, 2653; *Angew. Chem. Int. Ed.* **2013**, *52*, 2593; j) For a recent highlight regarding gem-diaurated species, see: A. Gómez-Suárez, S. P. Nolan, *Angew. Chem.* **2012**, *124*, 8278; *Angew. Chem. Int. Ed.* **2012**, *51*, 8156.
- [10] A. Zhdanko, M. E. Maier, *Chem. Eur. J.* **2013**, *19*, 3932.
- [11] A. Zhdanko, M. E. Maier, unpublished results.
- [12] K. E. Roth, S. A. Blum, *Organometallics* **2010**, *29*, 1712.
- [13] The influence of phenoxide on the reactivity of the parent phenol is a well-known phenomenon, see: a) M. F. Nielsen, O. Hammerich, *Acta Chem. Scand.* **1989**, *43*, 269; b) S. E. Denmark, R. C. Weintraub, N. D. Gould, *J. Am. Chem. Soc.* **2012**, *134*, 13415.
- [14] Vinyl gold is also assumed to react with other electrophiles with retention of configuration, see: M. Yu, G. Zhang, L. Zhang, *Org. Lett.* **2007**, *9*, 2147; b) M. S. Hadfield, A.-L. Lee, *Org. Lett.* **2010**, *12*, 484; c) A. Buzas, F. Gagosz, *Org. Lett.* **2006**, *8*, 515.
- [15] The stability of diaurated species, depending on the enol-ether core and the ligand at the gold center, has been quantitatively evaluated, see: A. Zhdanko, M. E. Maier, *Organometallics* **2013**, *32*, 2000.
- [16] a) Y. Zhu, C. S. Day, A. C. Jones, *Organometallics* **2012**, *31*, 7332; b) A single complex with 2,3-dimethoxybuta-1,3-diene was reported, see: R. A. Sanguramath, T. N. Hooper, C. P. Butts, M. Green, J. E. McGrady, C. A. Russell, *Angew. Chem.* **2011**, *123*, 7734; *Angew. Chem. Int. Ed.* **2011**, *50*, 7592.
- [17] See the Supporting Information for more details and explanation of this result. We suppose that deprotonation of an enol-ether π complex by a strong base to give a vinyl gold species should be successful, but only under strictly water-free and nucleophile-free conditions excluding any ligand exchange.
- [18] a) see ref 9b; b) A. S. K. Hashmi, T. Lauterbach, P. Nösel, M. H. Vilhelmsen, M. Rudolph, F. Rominger, *Chem. Eur. J.* **2013**, *19*, 1058.
- [19] For the cyclization of homopropargylic alcohols, see: V. Belting, N. Krause, *Org. Lett.* **2006**, *8*, 4489.
- [20] In an initial study, we found that the presence of 0.2% of allenic alcohol 2,3-pentadien-1-ol as an impurity was responsible for formation of extra species and influenced the whole kinetics. This finding is described in the Supporting Information. In this case, the substrate has to be essentially free of any allene.
- [21] This scenario is likely for very reactive substrates. Examples of such reactions can be found in the Supporting Information.
- [22] For a review regarding gold complexes with π systems, see: H. Schmidbauer, A. Schier, *Organometallics* **2010**, *29*, 2.
- [23] J. Roithová, J. Hrusák, D. Schröder, H. Schwarz, *Inorg. Chim. Acta* **2005**, *358*, 4287.
- [24] J. Roithová, Š. Janková, L. Jašíková, J. Váňa, S. Hybelbauerová, *Angew. Chem.* **2012**, *124*, 8503; *Angew. Chem. Int. Ed.* **2012**, *51*, 8378.
- [25] A. Zhdanko, M. Ströbele, M. E. Maier, *Chem. Eur. J.* **2012**, *18*, 14732.
- [26] Indeed, mathematical modeling indicated that the integrated form of the fractional rate law may behave similarly to the integrated form of the half-order law within an extended range of conversions (from 0 to $\approx 80\%$), but without knowledge of k_1 , K_1 , and K_2 such a demonstration is of no probative force.
- [27] Free catalyst **2** exists in methanol as a $L_2AuNCMe^+/L_2Au(MeOD)^+$ mixture with $\delta P = 58.00$, therefore, the free form is abbreviated as $L_2Au(Sol)^+$.
- [28] a) R. E. M. Brooner, T. J. Brown, R. A. Widenhoefer, *Chem. Eur. J.* **2013**, *19*, 8276; b) Y. Tang, B. Yu, *RSC Adv.* **2012**, *2*, 12686; c) See ref. [24].
- [29] However, we acknowledge that cooperative catalysis does take place in gold-catalyzed hydrophenoxylation reactions, demonstrating the difference in these mechanisms, see: Y. Oonishi, A. Gómez-Suárez, A. R. Martin, S. P. Nolan, *Angew. Chem.* **2013**, *125*, 9949; *Angew. Chem. Int. Ed.* **2013**, *52*, 9767.
- [30] a) R. L. LaLonde, W. E. Brenzovich, Jr., D. Benitez, E. Tkatchouk, K. Kelley, W. A. Goddard III, F. D. Toste, *Chem. Sci.* **2010**, *1*, 226; b) A. S. K. Hashmi, A. M. Schuster, S. Gaillard, L. Cavallo, A. Poater, S. P. Nolan, *Organometal-*

- lics* **2011**, *30*, 6328; c) A. S. K. Hashmi, W. Yang, Y. Yu, M. M. Hansmann, M. Rudolph, F. Rominger, *Angew. Chem.* **2013**, *125*, 1368; *Angew. Chem. Int. Ed.* **2013**, *52*, 1329; d) see reference [3f]; e) see reference. [9f].
- [31] The Supporting Information contains more subtle details about what exactly is observed. Control experiments to prove that DMF behaved as a hydrogen-bond acceptor and not as a nucleophile reactive with **A3** were also performed.
- [32] Steady-state approximation for **D**, in this case, is equivalent to the equilibrium approximation for the process.
- [33] The same law is derived if the concentration of **B** is expressed through **A**, **D**, and **S** and H^+ is put into expression for the rate of protodeauration.
- [34] All ligand-exchange steps at gold appear to be fast and the corresponding equilibria are established throughout the entire process. The high reactivity of LAu^+ resembles that of H^+ , so LAu^+ can be called the "magic proton", in accordance with the isolobal principle: H. G. Raubenheimer, H. Schmidbaur, *Organometallics* **2012**, *31*, 2507.
- [35] M. C. Blanco Jaimes, C. R. N. Böhlring, J. M. Serrano-Becerra, A. S. K. Hashmi, *Angew. Chem.* **2013**, *125*, 8121; *Angew. Chem. Int. Ed.* **2013**, *52*, 7963.

Received: September 27, 2013
 Revised: November 25, 2013
 Published online on January 8, 2014

Paper 6

For the Section 6.2.1.

Spirocyclization

Gold(I)-, Palladium(II)-, Platinum(II)-, and Mercury(II)-Catalysed Spirocyclization of 1,3-Enynediols: Reaction Scope

Alexander Zhdanko*^[a] and Martin E. Maier*^[a]

Keywords: Spiro compounds / Enynes / Acetals / Cyclization / Oxygen heterocycles / Homogeneous catalysis

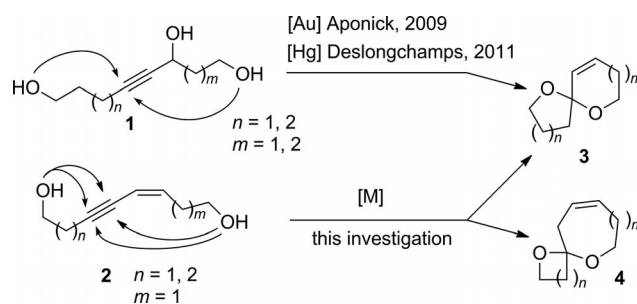
The spirocyclization of different 1,3-enynediols was investigated. The reaction was only efficient for the synthesis of [5,6]-spiroacetals. In this case, the reaction was characterized by almost quantitative yields, short reaction times, and low catalyst loadings (0.5–1 %). When the synthesis of [6,6]-spiroacetals was attempted, the reaction suffered from poor regioselectivity and a higher propensity of the intermediate dienol ethers to decompose under the acidic conditions, and it became no longer viable. But it is possible to generate the

dienol ethers cleanly under milder conditions as a mixture of regioisomers. This striking difference in reaction efficiency was explained by the unstable dienol ethers cyclizing more quickly to give [5,6]-spiroacetals than to give [6,6]-spiroacetals. In this study, the successful application of a new cationic palladium pincer complex for electrophilic alkyne activation at room temperature has been demonstrated for the first time.

Introduction

The spiroketal unit is frequently found in natural products of various types, including insect pheromones and polyether antibiotics.^[1] Prominent and recent examples include the spongistatins/altohyrtins.^[2] Some of them, like avermectin A_{1a},^[3] salinomycin,^[4] and okadaic acid,^[5] have a double bond in one of the rings. A double bond can be an important functional group for the introduction of additional substituents into a spiroketal substructure. During investigations towards the total synthesis of natural products in our laboratory, the question arose as to whether monounsaturated spiroketal structures can be synthesized by a transition-metal-catalysed double cyclization of 1,3-enyne diols.^[6] A similar cyclization of propargylic triols was reported by Aponick,^[7] and later extended by Deslongchamps^[8] (Scheme 1). In these cases, the double bond is formed by the elimination of water during the spirocyclization.

Our approach would be a good alternative for the synthesis of this type of structure because the starting materials are easily available by Sonogashira coupling between terminal alkynes and *cis*-vinyl bromides under mild conditions. It is also well known that transition-metal-catalysed addition to internal alkynes suffers from poor regioselectivity; the addition can occur at either atom of the triple bond, resulting in a mixture of products.^[9–11] Spirocyclization is



Scheme 1. Routes to unsaturated spiroacetals. The arrows indicate the formal cyclization modes.

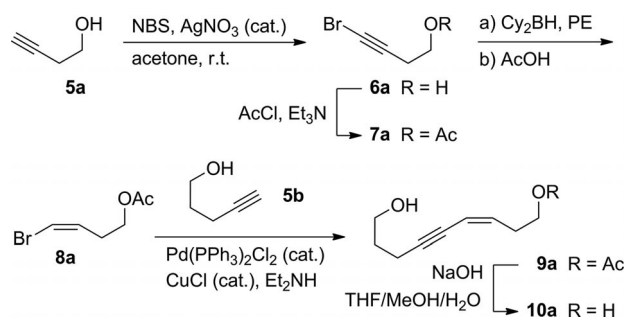
not an exception.^[12] In our case, this would lead to two possible regioisomers, **3** and **4** (Scheme 1). Therefore, we investigated whether the regioselectivity is controlled, and to what extent, by the double bond. The double bond might have a purely electronic effect, but it may also have conformational effects, since the two hydroxy groups at the left and right sides of the alkyne have different approaches to the reaction centre.

Results and Discussion

Starting enynediols **10a–10i** were obtained in a straightforward manner by the general strategy shown in Scheme 2. The five-step sequence is illustrated with the preparation of enynediol **10a**. Thus, (*Z*)-vinyl bromide **8a** was obtained from alkynol **5a** by converting it into the corresponding bromoalkyne^[13] (i.e., **6a**), followed by protection of the hydroxy function, subsequent hydroboration with dicyclohexylborane,^[14] and acidic work-up.^[15] As protecting groups, acetate, tetrahydropyranyl (THP), and *tert*-butyldi-

[a] Institut für Organische Chemie, Universität Tübingen, Auf der Morgenstelle 18, 72076 Tübingen, Germany
E-mail: vinceero@gmail.com
martin.e.maier@uni-tuebingen.de
http://www.uni-tuebingen.de/uni/com/welcome.htm
Supporting information for this article is available on the WWW under <http://dx.doi.org/10.1002/ejoc.201402029>.

methylsilyl (TBS) were used. Vinyl bromide **8a** was then subjected to Sonogashira coupling^[16] with alkynol **5b** to give enyne **9a**. Final deprotection delivered enynediol **10a**.



Scheme 2. General approach to starting enynediols **10** used in this study; NBS = *N*-bromosuccinimide.

Figure 1 shows the (*Z*)-vinyl bromides (i.e., **8a–8d**) that were prepared and used in this study. In addition, aryl iodide^[17] **8e** also served as a substrate for the Sonogashira coupling reaction.

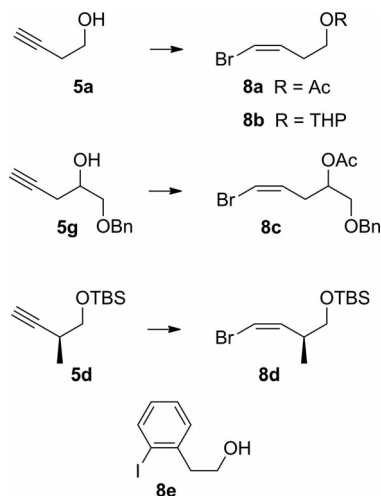


Figure 1. (*Z*)-Vinyl bromides **8a–8e** prepared according to Scheme 2.

The yields for the individual steps leading to the vinyl bromides are listed in Table 1. As can be seen, the yields were generally high. In case of the homoallylic acetates (i.e., **8a**, **8c**) a small amount (4–8%) of the corresponding (*E*)-isomer was also present. This can be explained by intramolecular addition of the acetate to the vinylborane, bond rotation, and *anti* elimination (see Supporting Information). The isomerization could be avoided by using the

Table 1. Yields for the transformation of alkynols **5a**, **5d**, and **5g** into (*Z*)-vinyl bromides **8a–8f**.

| Vinyl bromide | Bromination product (yield [%]) | Protection product (yield [%]) | R | Hydroboration yield [%] |
|---------------|---------------------------------|--------------------------------|-----|-------------------------|
| 8a | 6a (88) | 7a (96) | Ac | 83 |
| 8b | 6a (88) | 7b (99) | THP | 80 |
| 8c | 6c (99) | 7c (98) | | 97 |
| 8d | 6d (95) | | | 91 |

THP protecting group instead. Alkynol **5g**^[18] and protected alkynol **5d**^[19] were prepared as described in the literature.

The alkynols that were used for the cross-coupling reaction are shown in Figure 2. Compound **5a** was bought, whereas alkynols **5b**,^[20] **5c**,^[21] **5d**,^[19] **5e**, and **5f**^[22] were prepared according to the literature.

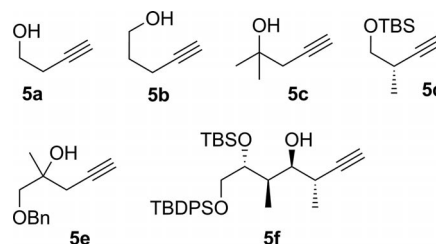


Figure 2. Alkynols used for the Sonogashira coupling with (*Z*)-vinyl bromides. TBDPS = *tert*-butyldiphenylsilyl.

Classical conditions were used for the coupling reaction, i.e., catalytic amounts of Pd(PPh₃)₂Cl₂ (0.6 mol-%) and CuI (1.2 mol-%) in a mixture of THF and diethylamine. The yields ranged from 77 to 90%. Subsequently, the protecting group was removed under appropriate conditions (NaOH in THF/MeOH/H₂O for acetate, HCl in MeOH for THP and TBS).

Enynediols **10** that were prepared for this study are shown in Figure 3. They can be divided into enynediols with either two or three carbon atoms on the alkyne terminus. On the side of the alkene, there are always two carbon atoms between the alkene and the hydroxy terminus.

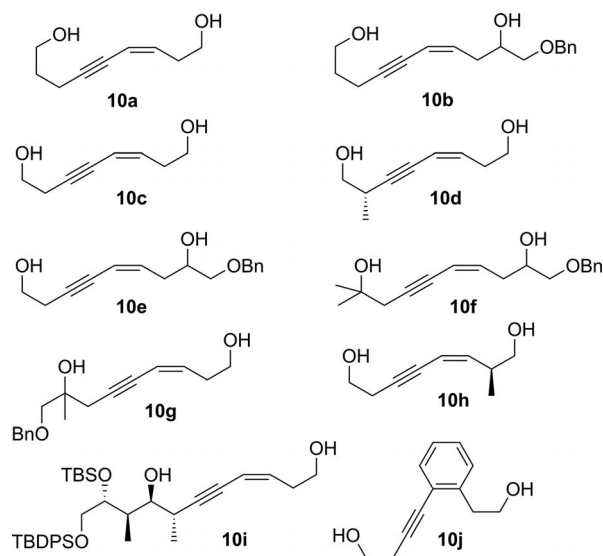


Figure 3. Enynediols **10a–10i** prepared in this study.

The yields for the individual steps leading to the enynediols are listed in Table 2. Both the coupling and the deprotection steps proceeded in good yield.

Table 2. Yields for the preparation of enynediols **10a–10i** by Sonogashira coupling and deprotection.

| Alkynol | Vinyl bromide | Coupling yield [%] | Deprotection yield [%] | Enynediol |
|-----------|---------------|--------------------|------------------------|------------|
| 5b | 8a | 80 | 99 | 10a |
| 5b | 8c | 77 | 99 | 10b |
| 5a | 8b | 79 | 71 | 10c |
| 5d | 8d | 79 | 81 | 10d |
| 5a | 8c | 89 | 99 | 10e |
| 5c | 8c | 68 | 99 | 10f |
| 5e | 8c | 79 | 99 | 10g |
| 5a | 8d | 90 | 91 | 10h |
| 5f | 8a | 87 | 90 | 10i |
| 5a | 8e | 70 | | 10j |

With the substrates in hand, we began our studies with the spiroketalization of diols **10a** and **10b**, with the aim of synthesizing 1,7-dioxaspiro[5.5]-undec-4-ene ring systems **3** ([6,6]-acetals). This is probably the most important olefin-containing spiroketal structure found in natural products.

Some of the catalysts used in this study are shown in Figure 4. This includes Zeise's dimer, new pincer complex **11**, and gold(I) complex^[23] **12**.

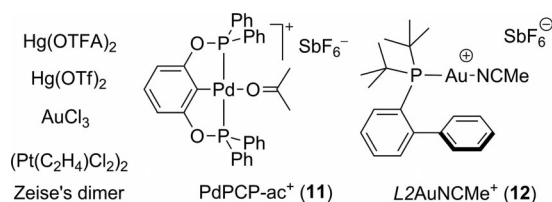
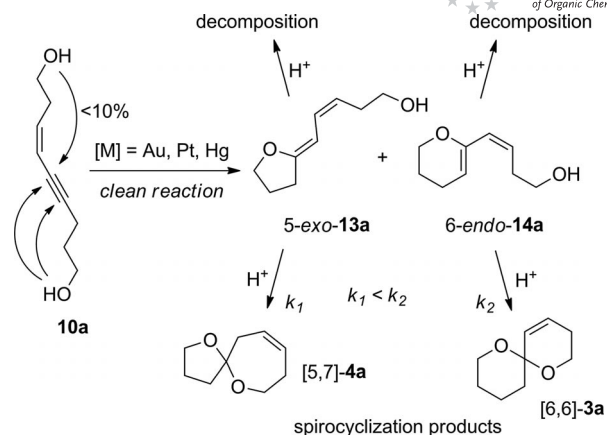


Figure 4. Catalysts for the spirocyclization.

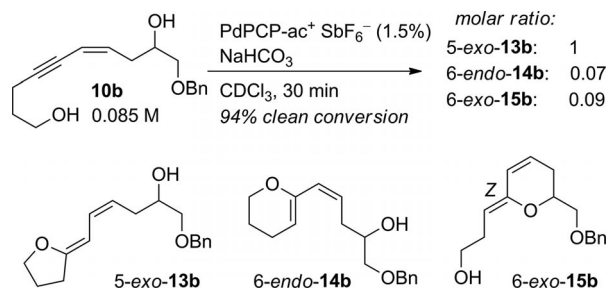
But using various gold, platinum, and mercury catalysts in different solvents, we could not achieve an efficient synthesis of the desired [6,6]-acetals.^[24,25] This screening is discussed in more detail in the Supporting Information. Our results show that the failure to synthesize [6,6]-acetals is associated with the poor regioselectivity of the first cyclization event, and decomposition of the intermediate dienol ethers competing with the second cyclization event, as exemplified in Scheme 3. It is possible to cleanly generate the dienol ethers (e.g., **13a** and **14a**) as a mixture of regioisomers under less acidic conditions in situ, but the higher level of acidity required for the second cyclization causes unavoidable competitive decomposition, making the spiroacetals isolable only in a low yield. We think that the decomposition of **13a** and **14a** is facilitated by the additional unsaturation, which makes them more vulnerable towards competitive side-reactions (carbocation is more stable, lives longer, and becomes more susceptible to intermolecular processes such as cationic polymerization and/or Diels–Alder reactions). Such processes should decrease the level of unsaturation, which is indeed observed in the ¹H NMR spectra.^[26] This is supported also by the fact that a saturated analogue (non-3-yne-1,9-diol) gave no decomposition in Au-, Pd-, and Pt-catalysed reactions, even when the reaction mixture was left overnight.^[27]



Scheme 3. Competitive spirocyclization and decomposition of dienol ether intermediates.

Obviously, the conjugated double bond in **2** has little or no impact on the regioselectivity of the alcohol addition to the triple bond (the reaction remains unselective). This is somewhat surprising: the hydroxy group coming from the alkene substituent (alkenol hydroxy group) and being apparently well preorganized for cyclization generally appeared to be the least reactive, so ca. 90% of the cyclization originated from the saturated side (alkynol hydroxy group). It appears that the rule about the preference for 5-*exo* over 6-*exo* cyclization is valid also here.^[28]

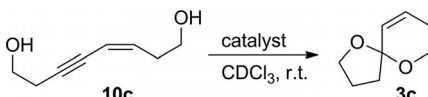
Besides Au, Pt, and Hg catalysts, we tried to solve the regioselectivity problem by using a Pd catalyst. Since the Pd(MeCN)₂Cl₂-catalysed reaction was found to be inefficient, we supposed that cationic palladium pincer complexes might work better. Prompted by the fact that complexes of this kind have been already used for the electrophilic activation of alkenes, but not of alkynes,^[29] we synthesized a new catalyst, PdPCP-ac⁺ SbF₆⁻ (Figure 1, available in two easy steps), and investigated its ability to catalyse the spirocyclization. To our delight, this catalyst appeared to be very active, giving a mixture of dienol ethers. However, this catalyst favours the 5-*exo* product with high selectivity (ca. 90%, determined in situ by NMR spectroscopy). This makes the reaction synthetically valuable, but again unsuitable for [6,6]-spiroacetal synthesis (Scheme 4). The successful application of this well-defined

Scheme 4. Pd pincer catalyst **11** provided 5-*exo* dienol ether **13b** most selectively.

catalyst in this reaction opens new perspectives for the chemistry of alkynes that could become complementary to modern gold catalysis.

Having failed to achieve the synthesis of [6,6]-acetals, we continued to search for another type of unsaturated spiroacetal system that could be formed more efficiently. We found that the cyclization of (3*Z*)-oct-3-en-5-yne-1,8-diol **10c** occurred cleanly to give the corresponding [5,6]-spiroacetal (i.e., **3c**; Table 3). The reaction is applicable to a wide range of differently substituted diols, and occurs equally well in CH₂Cl₂, CHCl₃, THF, and MeOH in the presence of different Au, Pd, Pt, and Hg catalysts. Generally, the reaction is fastest in CH₂Cl₂ or CHCl₃, solvents that neither solvate H⁺ nor coordinate to a catalyst. The overall process is characterized by short reaction times, and the initial monocyclization products are detectable by TLC as reaction intermediates that eventually completely disappear. For example, the cyclization of model substrate **10c** in the presence of various catalysts was monitored by NMR spectroscopy, and a quantitative in situ yield of the corresponding spiroacetal product (i.e., **3c**) was achieved within 4 min (Table 3, entries 1–4). The less active Hg(OTFA)₂ catalyst (OTFA = trifluoroacetate) also gave a quantitative yield, but the reaction was slower (Table 3, entry 5). The reaction catalysed by gold catalyst *L*2AuNCMe⁺ (**12**; Figure 4) was slower in methanol than in CDCl₃ (Table 3, entries 1 and 6).

Table 3. Efficient formation (in situ) of spiroacetal **3c** with various catalysts.



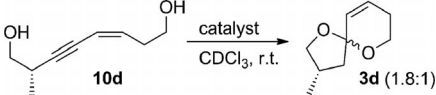
| Entry | Catalyst | Amount [mol-%] | Time [min] | Yield of 3c [%] |
|------------------|---|----------------|------------|------------------------|
| 1 | <i>L</i> 2AuNCMe ⁺ SbF ₆ ⁻ (12) | 0.8 | 4 | 99 |
| 2 | Ph ₃ PAuNCMe ⁺ SbF ₆ ⁻ | 1.0 | 4 | 99 |
| 3 | Zeise's dimer | 1.1 | 4 | 99 |
| 4 | PdPCP-ac ⁺ SbF ₆ ⁻ (11) | 0.7 | 4 | 99 |
| 5 | Hg(OTFA) ₂ | 4.1 | 26 | 99 |
| 6 ^[a] | <i>L</i> 2AuNCMe ⁺ SbF ₆ ⁻ (12) | 0.8 | 18 | 95 |

[a] Reaction in CD₃OD.

Similarly, reaction of a chiral substrate **10d** led to the formation of spirocycle **3d** as a thermodynamic mixture of diastereomers (Table 4, entries 1–3). Notably, catalysis by PdPCP-ac⁺ (**11**) was rather slow in methanol (Table 4, entry 3).^[30] The parent spiroacetal **3c** is known in the literature. Originally, it was prepared from the saturated spiroacetal by bromination and elimination.^[31] In another route, a dihydrofuran with an alkenol side-chain was subjected to proton-catalysed acetalization.^[32] While natural products with a double bond in a pyran ring of a spiroacetal are rare, derivatives of compounds **3c** have been used as synthetic intermediates en route to bis-spiroacetals.^[33]

Some preparative examples are given in Table 5. Generally, these reactions gave the spiroacetals in high yield with virtually no decomposition. When the starting enyne-

Table 4. Efficient formation (in situ) of spiroacetal **3d** with various catalysts.



| Entry | Catalyst | Amount [mol-%] | Time [min] | Yield of 3d [%] |
|------------------|---|----------------|------------|------------------------|
| 1 | <i>L</i> 2AuNCMe ⁺ SbF ₆ ⁻ (12) | 0.8 | 7 | 95 |
| 2 | PdPCP-ac ⁺ SbF ₆ ⁻ (11) | 1.0 | 10 | 95 |
| 3 ^[a] | PdPCP-ac ⁺ SbF ₆ ⁻ (11) | 4.6 | 7 | 25 ^[b] |

[a] Reaction in CD₃OD. [b] 95% after reaction overnight.

diol contained a chiral centre, the spiroacetal products were obtained as thermodynamic mixtures of epimers at the acetal carbon. Thus, some substrates provided mixtures of both epimers (Table 5, entries 8, 9, and 11), while all other substrates provided a single isomer, due to the strong control from the side-chain, which favours an equatorial position in the ring (Table 5, entries 1–6, and 8). From a practical point of view, all the catalysts gave equally good yields. Interestingly, AuCl₃, which could not be used in the previous reaction at all, now appears to be one of the most active catalysts! The catalyst loading could be further reduced to 0.1 mol-% without the addition of an extra acidic promoter (see Supporting Information).^[34] However, for preparative purposes, we recommend a catalyst loading of 0.2–1 mol-%, and a substrate concentration of >0.1 M.

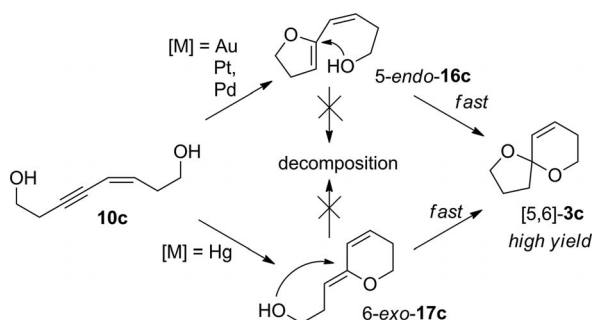
From our experiments, it follows that the striking efficacy of [5,6]-**3c** formation over [6,6]-**3a** or [5,7]-**4a** relies on the faster cyclization of the intermediate monocyclization products, Scheme 5. As we will show later,^[35] formation of the [5,6]-**3c** spiroacetal occurs via either 5-*endo*-**16c** dienol ether (for Au, Pd, and Pt) or 6-*exo*-**17c** ether (for Hg), and both of these intermediates appear to ring-close to form the second cycle faster than do the previously described examples 5-*exo*-**13a** and 6-*endo*-**14a** (Scheme 3).^[36] This difference is explained as follows: 5-*endo* enol ether **16c** suffers from some ring strain because of the deviation from the 120° angle for both sp² carbons, and this strain is released upon the second cyclization. 6-*exo* Enol ether **16c** does not suffer from this strain, but then formation of a five-membered ring occurs, which is faster than six- or seven-membered ring formation to give [6,6]-**3a** or [5,7]-**4a**. This further supports our viewpoint that the inability of 5-*exo*-**13a** and 6-*endo*-**14a** to cyclize quickly enough makes them more susceptible to decomposition, which may become a major process, while 5-*endo*-**16c** and 6-*exo*-**17c** avoid decomposition due to a fast cyclization to give more stable spiroacetal [5,6]-**3c** (Scheme 5). It can be also pointed out that due to the “harsher” conditions required for the cyclization of 5-*exo*-**13a** and 6-*endo*-**14a**, their [6,6]-**3a** or [5,7]-**4a** products may open reversibly and decompose as a result of such an equilibration.

Although these explanations are quite clear, it was rather surprising to find that simply shortening the substrate by

Table 5. Spirocyclization of (3*Z*)-oct-3-en-5-yne-1,8-diols. Preparative examples.

| Entry | Substrate | Solvent | Catalyst | Catalyst loading [mol-%] | Time | Product | Yield [%] |
|-------|------------|---|-----------------------|--------------------------|-----------|-----------|-------------------|
| 1 | | CH ₂ Cl ₂ | Hg(OTFA) ₂ | 1.0 | 24 h | | 92 |
| 2 | 10e | CH ₂ Cl ₂ | L2AuNCMe ⁺ | 0.5 | 10–15 min | 3e | 93 |
| 3 | 10e | CH ₂ Cl ₂ | PdPCP-ac ⁺ | 0.8 | 10–15 min | 3e | 90 |
| 4 | 10e | THF/MeCN (15:1) | Hg(OTf) ₂ | 1.5 | 12 min | 3e | 93 |
| 5 | 10e | CH ₂ Cl ₂ /traces of MeCN | AuCl ₃ | 0.5 | 10 min | 3e | 90 |
| 6 | | CH ₂ Cl ₂ /MeCN (50:1) | Hg(OTf) ₂ | 0.5 | 10–15 min | | 90 |
| 7 | 10f | CH ₂ Cl ₂ | L2AuNCMe ⁺ | 0.8 | 10 min | 3f | 92 |
| 8 | | CH ₂ Cl ₂ /MeCN (50:1) | Hg(OTf) ₂ | 0.5 | 5 min | | 83 ^[a] |
| 9 | | CH ₂ Cl ₂ | L2AuNCMe ⁺ | 0.4 | 4 min | | 83 ^[b] |
| 10 | | CH ₂ Cl ₂ | L2AuNCMe ⁺ | 0.4 | 10 min | | 95 |
| 11 | | CDCl ₃ | L2AuNCMe ⁺ | 1.0 | 10 min | | 94 |

[a] The yield is lower because of the presence of a *trans*-alkene impurity (ca. 10%) in the starting substrate. [b] Volatile compound.



Scheme 5. Fast ring closure saves dienol ether intermediates from decomposition.

just one methylene unit may dramatically change the situation so that a low-yielding and unselective reaction becomes an efficient process.

Conclusions

In conclusion, we investigated gold(I)-, palladium(II)-, platinum(II)-, and mercury(II)-catalysed spirocyclizations of 1,3-enynediols **10**, and found that the reaction is only efficient for the synthesis of [5,6]-spiroacetals. The failure to efficiently provide [6,6]-spiroacetals is due to both the

poor regioselectivity of the first cyclization event, and the high propensity of the dienol ether intermediates (i.e., 5-*exo*-**13a** and 6-*endo*-**14a**) to decomposition under acidic conditions (which is necessary to complete the spirocyclization sequence). But it is possible to generate dienol ethers 5-*exo*-**13a** and 6-*endo*-**14a** cleanly under milder conditions in situ as a mixture of regioisomers. In contrast, enol ethers 5-*endo*-**16c** or 6-*exo*-**17c** are much more difficult to generate in situ, because of their higher propensity to undergo the second ring closure.

Thus, spirocyclization of (3*Z*)-oct-3-en-5-yne-1,8-diols is a very convenient new route to unsaturated [5,6]-spiroacetals. The starting materials are easily available in high yield by Sonogashira coupling of two subunits. The yields of the [5,6]-spiroacetals are close to quantitative, and are achievable with a broad range of Au, Pd, Pt, and Hg electrophilic catalysts used at low catalyst loadings (<1 mol-%). The reaction provides a thermodynamic mixture of epimers at the acetal carbon, and the reaction product is therefore influenced by the side-chain substituents.

Experimental Section

4-Bromobut-3-yn-1-ol (6a): Silver nitrate (0.6 g, 6 mol-%) was added to a solution of but-3-yn-1-ol (4.20 g, 60 mmol) in acetone (60 mL).

Then NBS (11.0 g, 1.03 equiv.) was added in portions. The reaction was exothermic, and the reaction flask was cooled in a water bath. After the addition of NBS, the reaction mixture was stirred at room temperature for 1 h (TLC control: EtOAc/petroleum ether, 1:1 or 1:2). The resulting milky solution was concentrated in vacuo, then diethyl ether (50 mL) was added, and the mixture was washed with water (60 mL). The aqueous phase was extracted with diethyl ether (2 × 30 mL). The combined organic phases were washed with saturated NaCl solution, dried with MgSO₄, filtered, and concentrated. The residue was purified by chromatography on a silica column (13 × 3 cm) to give bromoalkyne **6a** (7.9 g, 88%) as a colourless liquid. The ¹H NMR spectroscopic data were in accordance with the literature.^[13]

1-(Benzyloxy)-5-bromopent-4-yn-2-ol (6c): Silver nitrate (0.199 g, 3 mol-%) was added to a solution of **5g** (7.61 g, 39.0 mmol) in acetone (40 mL). Then NBS (7.15 g, 1.03 equiv.) was added in portions. The reaction was exothermic, and the reaction flask was cooled in a water bath. After the addition of NBS, the reaction mixture was stirred at room temperature for 1 h (TLC control: EtOAc/petroleum ether, 1:1 or 1:2). The resulting milky solution was concentrated in vacuo, then diethyl ether (20 mL) was added, and the mixture was washed with water (20 mL). The aqueous phase was extracted with diethyl ether (2 × 10 mL). The combined organic phases were washed with saturated NaCl solution, dried with MgSO₄, filtered, and concentrated. The residue was purified by chromatography on a silica column to give bromoalkyne **6c** (10.6 g, 99%) as a colourless oil. ¹H NMR (400 MHz, CDCl₃): δ = 2.45 (d, 1 H, OH), 2.47 (d, *J* = 6.1 Hz, 2 H, CH₂), 3.48 (dd, *J* = 6.4, 9.4 Hz, 1 H, CH₂), 3.59 (dd, *J* = 4.1, 9.4 Hz, 1 H, CH₂), 3.92–3.99 (m, 1 H, CH), 4.56 (s, 2 H, CH₂), 7.28–7.38 (m, 5 H, Ph) ppm. ¹³C NMR (100 MHz, CDCl₃): δ = 24.7 (CH₂), 40.3 (quat.), 68.7, 72.7, 73.4, 76.1 (quat.), 127.7, 127.8, 128.5, 137.7 (quat.) ppm.

{[(2S)-4-Bromo-2-methylbut-3-ynyl]oxy}(tert-butyl)dimethylsilane (6d): Silver nitrate (0.061 g, 3.5 mol-%) and NBS (1.91 g, 1.05 equiv.) were added to a solution of alkyne **5d** (2.02 g, 10.2 mmol) in acetone (10 mL), and the mixture was stirred at room temperature for 1 h (TLC control: petroleum ether/Et₂O, 40:1). The resulting milky solution was concentrated in vacuo, then diethyl ether (20 mL) was added, and the mixture was washed with water (20 mL). The aqueous phase was extracted with diethyl ether (2 × 10 mL). The combined organic phases were washed with saturated NaCl solution, dried with MgSO₄, filtered, and concentrated. The residue was purified by flash chromatography to give bromoalkyne **6d** (2.69 g, 95%) as a colourless liquid. *R_f* (petroleum ether/Et₂O, 40:1): 0.66. ¹H NMR (400 MHz, CDCl₃): δ = 0.05 (s, 6 H), 0.89 (s, 9 H), 1.15 (d, *J* = 6.9 Hz, 3 H), 2.58 (app. sext, 1 H), 3.46 (dd, *J* = 9.7, 7.6 Hz, 1 H), 3.65 (dd, *J* = 9.7, 5.9 Hz, 1 H) ppm. ¹³C NMR (100 MHz, CDCl₃): δ = -5.4, -5.3, 16.9, 18.3, 25.8, 30.3, 39.1, 66.9, 82.4 ppm.

4-Bromobut-3-ynyl Acetate (7a): Et₃N (9.5 mL, 1.3 equiv.) was added to a solution of 4-bromobut-3-yn-1-ol (**6a**; 6.11 g, 52.6 mmol) and AcCl (4.3 mL, 1.15 equiv.) in EtOAc (30 mL) at 0 °C. A white precipitate formed immediately. An additional small amount of AcCl (0.1 mL) was added to reach full conversion (TLC control: petroleum ether/EtOAc, 2:1). The precipitate was removed by filtration and washed with Et₂O. The filtrate was concentrated in vacuo, and the residue was purified by flash chromatography (Et₂O/petroleum ether, 1:1) on a short column to give **7a** (9.64 g, 96%) as a colourless oil. *R_f* (petroleum ether/Et₂O, 5:1): 0.37. ¹H NMR (400 MHz, CDCl₃): δ = 2.07 (s, 1 H, CH₃), 2.54 (t, *J* = 6.7 Hz, 2 H, CH₂), 4.14 (t, *J* = 6.7 Hz, 2 H, CH₂) ppm.

2-[(4-Bromobut-3-yn-1-yl)oxy]tetrahydro-2H-pyran (7b): pTsOH·H₂O (23 mg) was added to a solution of 4-bromobut-3-yn-1-ol (**6a**;

1.811 g, 12.2 mmol) and dihydropyran (1.33 mL) in CH₂Cl₂ (10 mL). An exothermic reaction soon started. The solution was cooled in a water bath. When the reaction was complete (ca. 30 min, TLC control: petroleum ether/EtOAc, 2:1), the reaction mixture was quenched with Et₃N (0.02 mL), and the solvents evaporated to dryness in vacuo. The crude compound **7b** was used for the hydroboration without further purification.

1-[(Benzyloxy)methyl]-4-bromobut-3-ynyl Acetate (7c): AcCl (3.3 mL, 1.2 equiv.) was added to a solution of crude 1-(benzyloxy)-5-bromopent-4-yn-2-ol (**6c**; 10.5 g, 39.0 mmol) in Et₂O (60 mL) and petroleum ether (40 mL). The solution was cooled to -10 °C, and Et₃N (7.6 mL, 1.4 equiv.) was added. Initially, a thick, heavy oil precipitated. The flask was shaken, and the temperature was allowed to rise, whereupon the oil slowly disappeared, and a solid precipitate formed. At this stage, the reaction mixture was stirred for a few min at room temperature. If necessary, additional AcCl and Et₃N can be added to achieve complete conversion of the alcohol into the ester (TLC control: petroleum ether/EtOAc, 2:1). When complete conversion was achieved, the reaction mixture (with precipitate) was directly passed through a short column of silica gel (1.5 × 3.5 cm), which was further eluted with petroleum ether/Et₂O, 3:1. The fractions containing the acetate were evaporated to give pure acetate (11.89 g, 98%) as a yellow oil. The combination petroleum ether/Et₂O is probably not the best solvent for the filtration, because of the precipitation of polar components as an oil that must be crystallized by scratching with a spatula, but it allows very easy separation of the product when the reaction is finished and no oil is left (no need to extract, wash and purify). ¹H NMR (400 MHz, CDCl₃): δ = 2.08 (s, 1 H, CH₃), 2.57 (dd, *J* = 5.6, 16.8 Hz, 1 H, CH₂), 2.63 (dd, *J* = 6.6, 16.8 Hz, 1 H, CH₂), 3.60 (dd, *J* = 4.6, 10.4 Hz, 1 H, CH₂), 3.64 (dd, *J* = 5.1, 10.4 Hz, 1 H, CH₂), 4.52 (d, *J* = 12.2 Hz, 1 H, CH₂Ph), 4.58 (dd, *J* = 12.2 Hz, 1 H, CH₂Ph), 5.06 (app. quint, 1 H, CH), 7.26–7.37 (m, 5 H, Ph) ppm. ¹³C NMR (100 MHz, CDCl₃): δ = 21.1 (CH₃), 22.0 (CH₂), 40.4 (quat.), 69.4, 70.3, 73.3, 75.3 (quat.), 127.6, 127.8, 128.4, 137.7 (quat.), 170.3 ppm.

Dicyclohexylborane: A three-necked round-bottomed flask equipped with a magnetic stirrer, a gas inlet, and a thermometer was flushed with nitrogen, and cyclohexene (5.8 mL, 4.70 g, 57.7 mmol, 2.4 equiv.) and absolute Et₂O (15 mL) were added. The flask was immersed in an ice–water bath. At +10 °C, borane dimethyl sulfide complex (2.65 mL, 27.9 mmol, 1.15 equiv.) was added in one portion by syringe to the stirred mixture. The flask was partially removed from the bath to prevent further cooling, but to keep the temperature around +10 °C. The reaction mixture was stirred in this position until a precipitate began to form (ca. 5 min). The reaction was exothermic. Then the reaction mixture was allowed to stir without cooling for ca. 20 min (during this time, the mixture may reach room temperature; moreover, a lot of precipitate was already formed).

(3Z)-4-Bromobut-3-enyl Acetate (8a): The slurry of dicyclohexylborane in Et₂O prepared as described above was cooled again to +15 °C. Starting from this temperature, a solution of bromoalkyne **7a** (4.66 g, 24.3 mmol, 1 equiv.) in petroleum ether (15 mL) was added from a dropping funnel. The reaction was exothermic, and it started to occur actively in the region of 17–22 °C. The rate of addition and depth of immersion of the reaction flask in the cooling bath can be regulated so as to keep the temperature within this region. The initially formed precipitate dissolved. Following this regime, the exothermic phase of the reaction lasted ca. 5 min. After the addition was complete, and when most of the precipitate had dissolved, the cooling bath was removed, and the temperature was

allowed to rise to ca. 25–27 °C. The mixture was stirred for some 10 min to form an almost clear solution (higher temperatures were avoided). Then the solution was cooled back to ca. 20 °C, and acetic acid (1.5 mL, 1.1 equiv.) was added by pipette. The solution was stirred for ca. 5 min (this step was only slightly exothermic). Then ethanolamine (H₂NCH₂CH₂OH; 3.16 mL, 2.3 equiv.) was added by pipette at ca. 20 °C, and the mixture was stirred for another 30 min. Eventually, a sticky crystalline precipitate formed. Then the reaction mixture (with the precipitate) was passed through a short column of flash silica gel (1.5 × 3.5 cm), and further eluted with petroleum ether/Et₂O, 4:1. The filtrate was evaporated to give the crude vinyl bromide (3.9 g, 83%) as a sufficiently pure yellow oil. Alternatively, purification by flash column chromatography (petroleum ether/Et₂O, 5:1) can be performed. *R*_f (petroleum ether/Et₂O, 5:1): 0.37. ¹H NMR (400 MHz, CDCl₃): δ = 6.28 (dt, *J* = 7.1, 1.3 Hz, 1 H), 6.12 (app. q, *J* = 7.1 Hz, 1 H), 4.13 (t, *J* = 6.6 Hz, 2 H), 2.54 (app. dq, 2 H), 2.05 (s, 3 H) ppm. HRMS (ESI): calcd. for C₆H₉BrO₂ [M + Na]⁺ 214.96781; found 214.96795.

2-[(4-Bromobut-3-yn-1-yl)oxy]tetrahydro-2H-pyran (8b): This compound was prepared by a similar method to that described for **8a**. Thus, dicyclohexylborane was prepared from cyclohexene (2.30 g, 2.84 mL, 28.0 mmol, 2.3 equiv.) and borane dimethyl sulfide complex (1.27 mL, 13.4 mmol) in Et₂O (10 mL). A solution of crude bromoalkyne **7b** (2.84 g, 12.2 mmol) in petroleum ether (10 mL) was added to the resulting suspension. Flash chromatography (pentane/Et₂O, 10:1) gave alkenyl bromide **8b** (2.27 g, 80% over two steps) as a colourless oil. *R*_f (petroleum ether/Et₂O, 5:1): 0.4. ¹H NMR (400 MHz, CDCl₃): δ = 1.47–1.61 (m, 4 H), 1.68–1.73 (m, 1 H), 1.77–1.85 (m, 1 H), 2.46–2.52 (m, 2 H), 3.48 (dt, *J* = 6.6, 9.6 Hz, 1 H, CH₂), 3.48–3.53 (m, 1 H), 3.78 (dt, *J* = 6.8, 9.6 Hz, 1 H, CH₂), 3.85 (ddd, *J* = 3.3, 7.8, 11.1 Hz, 1 H), 4.60 (dd, *J* = 2.8, 4.3 Hz, 1 H, OCHO), 6.19 (app. q, *J* = 6–7 Hz, 1 H, =CH), 6.23 (d, *J* = 7.1 Hz, 1 H, =CH) ppm. ¹³C NMR (100 MHz, CDCl₃): δ = 19.5, 25.4, 30.5, 30.6, 62.3, 65.4, 98.7, 109.2, 131.7 ppm. HRMS (ESI): calcd. for C₉H₁₅BrO₂ [M + Na]⁺ 257.01476; found 257.01469.

(3Z)-1-[(Benzyloxy)methyl]-4-bromobut-3-enyl Acetate (8c): This compound was prepared by a similar method to that described for **8a**, starting from cyclohexene (6.15 g, 4.99 g, 60.7 mmol, 2.3 equiv.) and borane dimethyl sulfide complex (2.76 mL, 29.1 mmol, 1.1 equiv.) in Et₂O (25 mL), and bromoalkyne **7c** (8.21 g, 26.4 mmol, 1 equiv.) in petroleum ether (25 mL). Flash chromatography (petroleum ether/Et₂O, 4:1) gave alkenyl bromide **8c** (7.85 g, 95%) as a colourless oil. *R*_f (petroleum ether/Et₂O, 4:1): 0.4. ¹H NMR (400 MHz, CDCl₃): δ = 2.06 (s, 1 H, CH₃), 2.56 (dt, *J* = 1.5, 6.9 Hz, 2 H, CH₂), 3.52 (dd, *J* = 4.6, 10.5 Hz, 1 H, CH₂), 3.55 (dd, *J* = 5.6, 10.5 Hz, 1 H, CH₂), 4.51 (d, *J* = 12.1 Hz, 1 H, CH₂), 4.58 (dd, *J* = 12.1 Hz, 1 H, CH₂), 5.14 (app. quint, 1 H, CH), 6.09 (q, *J* = 7.1 Hz, 1 H, =CH), 6.26 (dt, *J* = 1.5, 7.1 Hz, 1 H, =CH), 7.26–7.36 (m, 5 H, Ph) ppm. ¹³C NMR (100 MHz, CDCl₃): δ = 21.1 (CH₃), 31.6 (CH₂), 70.5, 71.1, 73.2, 110.6 (=CH), 127.6 (Ph), 127.7 (Ph), 128.4 (Ph), 129.7 (=CH), 137.9 (Ph_{quat}), 170.5 ppm. HRMS (ESI): calcd. for C₁₄H₁₇BrO₃ [M + Na]⁺ 335.02533; found 335.02540.

[[2S,3Z)-4-Bromo-2-methylbut-3-enyl]oxy}tert-butyl]dimethylsilane (8d): This compound was prepared by a similar method to that described for **8a**, starting from cyclohexene (2.36 mL, 23.3 mmol, 2.4 equiv.) and borane dimethyl sulfide complex (1.06 mL, 11.2 mmol, 1.15 equiv.) in Et₂O (7 mL), and bromoalkyne **6d** (2.692, 9.7 mmol, 1 equiv.) in petroleum ether (10 mL). Flash chromatography (petroleum ether/Et₂O, 4:1) gave alkenyl bromide

8d (2.33 g, 91%) as a colourless oil. ¹H NMR (400 MHz, CDCl₃): δ = 0.04 (s, 6 H), 0.88 (s, 9 H), 1.01 (d, *J* = 6.9 Hz, 3 H), 2.79–2.89 (m, 1 H), 3.47 (dd, *J* = 9.8, 5.7 Hz, 1 H), 3.53 (dd, *J* = 9.8, 6.3 Hz, 1 H), 5.95 (dd, *J* = 8.9, 6.9 Hz, 1 H), 6.14 (d, *J* = 7.1 Hz, 1 H) ppm. ¹³C NMR (100 MHz, CDCl₃): δ = -5.4, 15.9, 18.3, 25.9, 37.5, 66.4, 107.3, 137.6 ppm.

(Z)-9-Hydroxynon-3-en-5-yn-1-yl Acetate (9a): THF (19 mL) and diethylamine (5 mL) were added to alkenyl bromide **8a** (2.46 g, 12.7 mmol) and pentynol (**5b**; 1.18 g, 14.03 mmol, 1.1 equiv.) under a nitrogen atmosphere. The mixture was stirred to dissolve the starting materials. Then Pd(PPh₃)₂Cl₂ (55 mg, 0.6%) and CuI (30 mg, 1.2%) were added, the flask was closed, and the nitrogen flow was disconnected. The reaction mixture was stirred for 24 h at room temperature (TLC control: petroleum ether/EtOAc, 2:1). The white precipitate was removed by filtration and washed with portions of EtOAc, the filtrate was evaporated in vacuo, and the residue was purified by flash chromatography (petroleum ether/EtOAc, 2:1→1:1) to give **9a** (1.99 g, 80%) as a slightly orange oil. *R*_f (petroleum ether/EtOAc, 1:1): 0.38. ¹H NMR (400 MHz, CDCl₃): δ = 1.74 (br. s, 1 H, OH), 1.78 (ap. quint., *J* = 6.6 Hz, 2 H, 8-H), 2.04 (s, 3 H, CH₃), 2.46 (dt, *J* = 2.0, 6.9 Hz, 2 H, 7-H), 2.60 (ap. dq, *J* = 1.2, 6.9 Hz, 2 H, 2-H), 3.76 (t, *J* = 6.1 Hz, 2 H, 9-H), 4.12 (t, *J* = 6.9 Hz, 2 H, 1-H), 5.54 (br. d, *J* = 10.7 Hz, 1 H, 4-H), 5.81 (dt, *J* = 7.1, 10.7 Hz, 1 H, 3-H) ppm. ¹³C NMR (100 MHz, CDCl₃): δ = 16.0 (C-7), 21.0 (CH₃), 29.5, 31.3, 61.5 (C-9), 63.1 (C-1), 77.3, 94.5, 112.1, 137.0, 171.2 ppm. HRMS (ESI): calcd. for C₁₁H₁₆O₃ [M + Na]⁺ 219.09917; found 219.09920.

(Z)-1-(Benzyloxy)-10-hydroxydec-4-en-6-yn-2-yl Acetate (9b): Benzene (16 mL) and diethylamine (4.2 mL, 2.97 g, 40.6 mmol, 3 equiv.) were added to alkenyl bromide **8c** (4.21 g, 13.5 mmol) and pentynol (1.20 g, 14.3 mmol, 1.1 equiv.) under a nitrogen atmosphere. The mixture was stirred to dissolve the starting materials. After that, Pd(PPh₃)₂Cl₂ (57 mg, 0.6%) and CuI (43 mg, 1.7%) were added, the flask was closed, and the nitrogen flow was disconnected. The reaction mixture was stirred for 5 h at room temperature (TLC control: petroleum ether/EtOAc, 2:1; the reaction was slightly exothermic, the initial light solution darkened, and a precipitate formed). After that, the precipitate was removed by filtration and washed with portions of EtOAc, the filtrate was evaporated in vacuo, and the residue was purified by flash chromatography (petroleum ether/EtOAc, 2:1→1:1) to give **9b** (3.28 g, 77%) as a slightly orange oil. The yield was higher if pure substrate was used. The use of 5 equiv. of Et₂NH instead of 3 equiv. is recommended. *R*_f (petroleum ether/EtOAc, 1:1): 0.40. ¹H NMR (400 MHz, CDCl₃): δ = 1.75 (quint., *J* = 6.6 Hz, 2 H), 2.06 (s, 1 H, CH₃), 2.44 (dt, *J* = 2.0, 6.8 Hz, 2 H, CH₂), 2.57–2.69 [m (ddt), 2 H, CH₂], 3.53 (d, *J* = 5.1 Hz, 2 H, CH₂), 3.73 (t, *J* = 6.3 Hz, 2 H, CH₂), 4.50 (d, *J* = 12.2 Hz, 1 H, CH₂), 4.58 (dd, *J* = 12.2 Hz, 1 H, CH₂), 5.12 [tt (almost quint), 1 H, CH], 5.53 (br. d, *J* = 10.7 Hz, 1 H, =CH), 5.81 (dt, *J* = 7.3, 10.7 Hz, 1 H, =CH), 7.26–7.36 (m, 5 H, Ph) ppm. ¹³C NMR (100 MHz, CDCl₃): δ = 16.0, 21.2 (CH₃), 31.2, 31.5, 61.4, 70.6, 71.9, 73.2, 77.4, 94.6, 112.6 (=CH), 127.6 (Ph), 127.7 (Ph), 128.4 (Ph), 136.2 (=CH), 138.0 (Ph_{quat}), 170.7 ppm. HRMS (ESI): calcd. for C₁₉H₂₄O₄ [M + Na]⁺ 339.15668; found 339.15662.

(Z)-8-[(Tetrahydro-2H-pyran-2-yl)oxy]oct-5-en-3-yn-1-ol (9c): This compound was prepared similarly to **9b** starting from alkenyl bromide **8b** (0.224 g, 0.952 mmol), butynol **5a** (78 mg, 1.11 mmol), diethylamine (0.5 mL, 0.354 g, 4.84 mmol), toluene (1 mL), Pd(PPh₃)₂Cl₂ (4.2 mg), and CuI (3.2 mg). The residue was purified by flash chromatography (petroleum ether/EtOAc, 2:1→1:1) to give enynol **9c** (0.475 g, 79%) as a slightly yellow oil. *R*_f (petroleum ether/EtOAc, 1:1): 0.39. ¹H NMR (400 MHz, CDCl₃): δ = 1.49–

1.61 (m, 4 H), 1.66–1.73 (m, 1 H), 1.78–1.86 (m, 1 H), 2.04 (t, $J = 6.4$ Hz, 2 H), 2.54–2.64 (m, 4 H), 3.46–3.52 (m, 2 H), 3.71–3.88 (m, 4 H), 4.61 (dd, $J = 3.0, 3.0$ Hz, 1 H), 5.52 (br. d, $J = 10.9$ Hz, 1 H), 5.94 (dt, $J = 7.3, 10.6$ Hz, 1 H) ppm. ^{13}C NMR (100 MHz, CDCl_3): $\delta = 19.5, 24.0, 25.4, 30.6, 61.2, 62.3, 66.1, 79.1, 91.1, 98.6, 110.8$ (=CH), 139.4 (=CH) ppm. HRMS (ESI): calcd. for $\text{C}_{13}\text{H}_{20}\text{O}_3$ $[\text{M} + \text{Na}]^+$ 247.13047; found 247.13041.

(3Z,7S)-8-{{tert-butyl(dimethyl)silyloxy}-7-methyloct-3-en-5-ynyl Acetate (9d): This compound was prepared from alkenyl bromide **8a** (0.169 g, 0.876 mmol), alkyne **5d** (191 mg, 1.1 equiv.), diethylamine (2 mL), $\text{Pd}(\text{PPh}_3)_2\text{Cl}_2$ (6.1 mg), and CuI (3.3 mg). The residue was purified by flash chromatography (petroleum ether/EtOAc, 15:1→10:1) to give enynol **9d** (0.215 g, 79%) as a slightly yellow oil. R_f (petroleum ether/EtOAc, 10:1): 0.42. ^1H NMR (400 MHz, CDCl_3): $\delta = 0.05$ (s, 6 H, CH_3), 0.89 (s, 9 H), 1.18 (d, $J = 6.8$ Hz, 3 H), 2.04 (s, 3 H), 2.61 (app. q, 2 H), 2.67–2.76 (m, 1 H), 3.47 (dd, $J = 9.4, 7.5$ Hz, 1 H), 3.68 (dd, $J = 9.4, 5.7$ Hz, 1 H), 4.11 (t, $J = 6.7$ Hz, 2 H), 5.55 (d, $J = 10.7$ Hz, 1 H), 5.81 (dt, $J = 7.2, 10.8$ Hz, 1 H) ppm. ^{13}C NMR (100 MHz, CDCl_3): $\delta = -5.3, 17.4, 18.3, 21.0, 25.9, 29.5, 29.9, 63.2, 67.2, 77.5, 97.4, 112.0, 137.1, 171.0$ ppm.

(Z)-1-(Benzyloxy)-9-hydroxynon-4-en-6-yn-2-yl Acetate (9e): This compound was prepared similarly to **9b** starting from alkenyl bromide **8c** (0.626 g, 2.0 mmol), butynol (**5a**; 0.154 g, 2.20 mmol, 1.1 equiv.), benzene (2.4 mL), and diethylamine (1 mL, 0.71 g, 9.67 mmol, 4.8 equiv.). The mixture was stirred to dissolve the starting materials. After that, $\text{Pd}(\text{PPh}_3)_2\text{Cl}_2$ (8.4 mg, 0.6 mol-%) and CuI (6.6 mg, 1.7 mol-%) were added, the reaction flask was closed, and the nitrogen flow was disconnected. The components of the catalytic system soon dissolved to give a yellow-green solution. The reaction mixture was stirred overnight at room temperature (TLC control: petroleum ether/EtOAc, 2:1; almost complete conversion was observed already after 2.5 h, when a precipitate was formed). After that, the precipitate was removed by filtration and washed with portions of EtOAc, the filtrate was evaporated on a rotary evaporator, and the residue was purified by flash chromatography (petroleum ether/EtOAc, 2:1→1:1) to give enynol **9e** (0.535 g, 89%) as a slightly yellow oil. R_f (petroleum ether/EtOAc, 1:1): 0.41. ^1H NMR (400 MHz, CDCl_3): $\delta = 2.06$ (s, 1 H, CH_3), 2.28 (t, 1 H, OH), 2.58 (dt, $J = 2.0, 6.1$ Hz, 2 H, CH_2), 2.65 (t, $J = 7.3$ Hz, 2 H, CH_2), 3.53 (d, $J = 5.1$ Hz, 2 H, CH_2), 3.70 (q, $J = 6.1$ Hz, 2 H, CH_2), 4.52 (d, $J = 12.2$ Hz, 1 H, CH_2), 4.58 (dd, $J = 12.2$ Hz, 1 H, CH_2), 5.10 (app. quint, 1 H, CH), 5.55 (br. d, $J = 10.7$ Hz, 1 H, =CH), 5.81 (dt, $J = 7.6, 10.7$ Hz, 1 H, =CH), 7.26–7.36 (m, 5 H, Ph) ppm. ^{13}C NMR (100 MHz, CDCl_3): $\delta = 21.2$ (CH_3), 24.0, 31.5, 61.1, 70.4, 71.9, 73.2, 78.6, 92.0, 112.4 (=CH), 127.6 (Ph), 127.7 (Ph), 128.4 (Ph), 136.7 (=CH), 137.9 (Ph_{quat}), 170.8 ppm. HRMS (ESI): calcd. for $\text{C}_{18}\text{H}_{22}\text{O}_4$ $[\text{M} + \text{Na}]^+$ 325.14103; found 325.14109.

(Z)-1-(Benzyloxy)-9-hydroxy-9-methyldec-4-en-6-yn-2-yl Acetate (9f): Prepared from alkenyl bromide **8c** (0.313 g, 1.0 mmol), 2-methylpent-4-yn-2-ol **5c** (78 mg, 0.79 mmol), diethylamine (0.5 mL, 354 mg, 4.8 mmol), THF (1.3 mL), $\text{Pd}(\text{PPh}_3)_2\text{Cl}_2$ (4.9 mg), and CuI (2.7 mg). The residue was purified by flash chromatography (petroleum ether/EtOAc, 2:1→1:1) to give enynol **9f** (0.178 g, 68%) as a slightly yellow oil. R_f (petroleum ether/EtOAc, 2:1): 0.25. ^1H NMR (400 MHz, CDCl_3): $\delta = 1.30$ (s, 6 H, CH_3), 2.05 (s, 3 H, CH_3), 2.12 (br. s, 1 H, OH), 2.50 (d, $J = 1.8$ Hz, 2 H, CH_2), 2.66 (app. t, $J = 7.3$ Hz, 2 H, CH_2), 3.51 (dd, $J = 4.8, 10.6$ Hz, 1 H, CH_2), 3.55 (dd, $J = 5.3, 10.6$ Hz, 1 H, CH_2), 4.50 (s, $J = 12.1$ Hz, 1 H, CH_2), 4.56 (s, $J = 12.1$ Hz, 1 H, CH_2), 5.10 (tt, $J = 5.1, 6.3$ Hz, 1 H, CH), 5.57 (br. d, $J = 10.9$ Hz, 1 H, =CH), 5.82 (dt, $J = 7.6, 10.9$ Hz, 1 H, =CH), 7.26–7.36 (m, 5 H, Ph) ppm. ^{13}C NMR (100 MHz, CDCl_3): $\delta = 21.2$ (CH_3CO), 28.70 (CH_3), 28.73 (CH_3), 31.7, 35.2, 70.0, 70.5,

71.8, 73.2, 79.6, 91.7, 112.4 (=CH), 127.6 (Ph), 127.7 (Ph), 128.4 (Ph), 136.8 (Ph_{quat}), 138.0 (=CH), 170.7 ppm.

(3Z)-9-(Benzyloxy)-8-hydroxy-8-methylnon-3-en-5-ynyl Acetate (9g): Prepared from alkenyl bromide **8a** (0.255 g, 1.14 equiv.), alkynol **5e** (238 mg, 1.16 mmol), diethylamine (2 mL), $\text{Pd}(\text{PPh}_3)_2\text{Cl}_2$ (8.1 mg), and CuI (4.4 mg). The residue was purified by flash chromatography (petroleum ether/EtOAc, 4:1→2:1) to give enynol **9g** (0.289 g, 79%) as a slightly yellow oil. R_f (petroleum ether/EtOAc, 2:1): 0.38. ^1H NMR (400 MHz, CDCl_3): $\delta = 1.29$ (s, 3 H, CH_3), 2.03 (s, 3 H), 2.53–2.63 (m, 5 H), 3.37 (d, $J = 9.0$ Hz, 1 H), 3.49 (d, $J = 9.0$ Hz, 1 H), 4.10 (t, $J = 6.7$ Hz, 2 H), 4.58 (s, 2 H), 5.55 (d, $J = 10.6$ Hz, 1 H), 5.83 (dt, $J = 10.6, 7.3$ Hz, 1 H), 7.27–7.36 (m, 5 H) ppm. ^{13}C NMR (100 MHz, CDCl_3): $\delta = 20.9, 23.7, 29.6, 30.6, 63.1, 71.8, 73.5, 75.9, 79.0, 91.3, 112.0, 127.6, 127.7, 128.4, 137.5, 171.1$ ppm.

(5Z,7S)-8-{{tert-Butyl(dimethyl)silyloxy}-7-methyloct-5-en-3-yn-1-ol (9h): Prepared from alkenyl bromide **8d** (0.319 g, 1.14 mmol), alkynol **5a** (88 mg, 1.1 equiv.), diethylamine (2 mL), $\text{Pd}(\text{PPh}_3)_2\text{Cl}_2$ (8.1 mg), and CuI (4.5 mg). The residue was purified by flash chromatography (petroleum ether/EtOAc, 4:1) to give enynol **9h** (0.276 g, 90%) as a slightly yellow oil. R_f (petroleum ether/EtOAc, 4:1): 0.33. ^1H NMR (400 MHz, CDCl_3): $\delta = 0.04$ (s, 3 H, CH_3), 0.04 (s, 3 H, CH_3), 0.88 (s, 9 H), 1.00 (d, $J = 6.8$ Hz, 3 H), 1.84 (br., 1 H), 2.59 (dt, $J = 6.1, 2.0$ Hz, 2 H), 2.85–2.96 (m, 1 H), 3.45 (dd, $J = 6.6, 9.9$ Hz, 1 H), 3.51 (dd, $J = 6.1, 9.9$ Hz, 1 H), 3.73 (t, $J = 6.4$ Hz, 2 H), 5.44 (d, $J = 11.4$ Hz, 1 H), 5.69 (dd, $J = 10.4, 9.9$ Hz, 1 H) ppm. ^{13}C NMR (100 MHz, CDCl_3): $\delta = -5.37, -5.31, 16.5, 18.4, 24.0, 25.9, 37.7, 61.2, 67.3, 79.5, 90.2, 109.1, 146.0$ ppm.

Acetate 9i: Prepared from alkenyl bromide **8a** (14.3 mg, 1.2 equiv.), alkynol **5f** (32.4 mg, 0.0617 mmol), diethylamine (0.5 mL), $\text{Pd}(\text{PPh}_3)_2\text{Cl}_2$ (0.5 mg), and CuI (0.3 mg). The residue was purified by flash chromatography (petroleum ether/EtOAc, 10:1) to give enynol **9i** (39.3 mg, 87%) as a slightly yellow oil. R_f (petroleum ether/EtOAc, 4:1): 0.55. ^1H NMR (400 MHz, CDCl_3): $\delta = -0.19$ (s, 3 H, CH_3), -0.03 (s, 3 H), 0.78 (s, 9 H), 1.00 (d, $J = 7.3$ Hz, 3 H), 1.03 (s, 9 H), 1.19 (d, $J = 7.1$ Hz, 3 H), 2.04 (s, 3 H), 2.14–2.19 (m, 1 H), 2.65 (app. q, 2 H), 2.73–2.83 (m, 1 H), 3.51–4.13 (m, 7 H), 5.62 (d, $J = 10.9$ Hz, 1 H), 5.82 (dt, $J = 10.8, 7.1$ Hz, 1 H), 7.37–7.44 (m, 6 H), 7.62–7.66 (m, 4 H) ppm. ^{13}C NMR (100 MHz, CDCl_3): $\delta = -5.2, -4.7, 10.2, 17.6, 17.8, 19.2, 21.0, 25.7, 26.8, 29.6, 31.3, 34.6, 63.3, 64.3, 73.8, 77.7, 98.0, 112.4, 127.8, 129.9, 133.2, 135.48, 135.53, 137.0, 177.8$ ppm.

General Procedure for the Synthesis of Diols 10 from Acetates 9: Typically, methanol (0.4 mL) and water (1 mL) were added to a solution of acetate (1 mmol) in THF (2 mL). Solid NaOH or KOH (1.5–2 equiv.) was then added to this mixture with stirring. The resulting biphasic mixture was stirred at room temperature. The reaction was normally finished within 2 h, but it can be left to stir overnight. When TLC (petroleum ether/EtOAc, 1:1) showed complete conversion, the mixture was diluted with diethyl ether and water. The organic phase was separated, washed with a small amount of saturated NaCl solution, and dried with Na_2SO_4 . After filtration, the solvent was evaporated, and the residue was purified by chromatography to give the diols as sticky oils in quantitative yields.

(Z)-Non-3-en-5-yne-1,9-diol (10a): This diol was prepared from acetate **9a** in quantitative yield as a colourless oil. R_f (EtOAc): 0.32. ^1H NMR (400 MHz, CDCl_3): $\delta = 1.78$ (ap. quint., $J = 6.5$ Hz, 2 H, 8-H), 2.09 (br. s, 1 H, OH), 2.46 (dt, $J = 2.0, 6.9$ Hz, 2 H, 7-H), 2.55 (ap. dq, $J = 1.2, 6.4$ Hz, 2 H, 2-H), 3.68 (t, $J = 6.9$ Hz, 2 H, 1-H), 3.76 (t, $J = 6.1$ Hz, 2 H, 9-H), 5.56 (br. d, $J = 10.7$ Hz, 1 H, 4-H), 5.85 (dt, $J = 7.4, 10.7$ Hz, 1 H, 3-H) ppm. ^{13}C NMR

(100 MHz, CDCl₃): δ = 16.1 (C-7), 31.2, 33.6, 61.6, 61.8, 77.6, 94.2, 112.0, 138.1 ppm.

(Z)-10-(Benzyloxy)dec-6-en-4-yne-1,9-diol (10b): Prepared from acetate **9b** in quantitative yield as a colourless oil. R_f (EtOAc): 0.5. ¹H NMR (400 MHz, CDCl₃): δ = 1.76 (quint., J = 6.6 Hz, 2 H, CH₂), 2.44 (dt, J = 6.8, 2.0 Hz, 2 H, CH₂), 2.50 (t, J = 7.0 Hz, 2 H, CH₂), 3.39 (dd, J = 7.3, 9.6 Hz, 1 H, CH₂), 3.52 (dd, J = 3.5, 9.6 Hz, 1 H, CH₂), 3.73 (t, J = 6.2 Hz, 2 H, CH₂), 3.92 (app. dq, 1 H, CH), 4.56 (s, 2 H, CH₂), 5.55 (br. d, J = 10.7 Hz, 1 H, =CH), 5.90 (dt, J = 7.4, 10.7 Hz, 1 H, =CH), 7.27–7.37 (m, 5 H, Ph) ppm.

(Z)-9-(Benzyloxy)non-5-en-3-yne-1,8-diol (10c): Prepared from acetate **9c** (0.245 g, 0.810 mmol), dissolved in THF (1.5 mL) and MeOH (0.3 mL). Compound **10c** (0.211 g, 99%) was obtained as a colourless oil. R_f (EtOAc): 0.54. ¹H NMR (400 MHz, CDCl₃): δ = 2.14 (br. s, 2 H, OH), 2.51 [m (app. t), 2 H, CH₂], 2.57 (dt, J = 2.0, 6.1 Hz, 2 H, CH₂), 3.39 (dd, J = 7.3, 9.6 Hz, 1 H, CH₂), 3.52 (dd, J = 3.5, 9.6 Hz, 1 H, CH₂), 3.70 (q, J = 6.1 Hz, 2 H, CH₂), 3.92 (app. dq, 1 H, CH), 4.55 (s, 2 H, CH₂), 5.57 (br. d, J = 10.7 Hz, 1 H, =CH), 5.94 (dt, J = 7.6, 10.7 Hz, 1 H, =CH), 7.27–7.37 (m, 5 H, Ph) ppm. ¹³C NMR (100 MHz, CDCl₃): δ = 23.9, 34.0, 61.1, 70.0, 73.4, 73.9, 79.0, 91.7, 111.8 (=CH), 127.7 (Ph), 127.8 (Ph), 128.5 (Ph), 137.9 (Ph_{quat}), 138.2 (=CH) ppm. HRMS (ESI): calcd. for C₁₆H₂₀O₃ [M + Na]⁺ 283.13047; found 283.13034.

(Z)-1-(Benzyloxy)-9-methyldec-4-en-6-yne-2,9-diol (10f): Prepared from acetate **9f** in quantitative yield as a colourless oil. ¹H NMR (400 MHz, CDCl₃): δ = 1.29 (s, 6 H, CH₃), 2.19 (br. s, 2 H, OH), 2.50 (s, 2 H, 8-H), 2.51 (t, J = 7.1 Hz, 2 H, 3-H), 3.39 (dd, J = 7.3, 9.6 Hz, 1 H, 1-H), 3.51 (dd, J = 3.5, 9.6 Hz, 1 H, 1-H), 3.92 (app. dq, J = 3.5, 7.1 Hz, 1 H, 2-H), 4.55 (s, 2 H, CH₂Ph), 5.57 (br. d, J = 10.9 Hz, 1 H, 5-H), 5.94 (dt, J = 7.6, 10.9 Hz, 1 H, 4-H), 7.26–7.36 (m, 5 H, Ph) ppm. ¹³C NMR (100 MHz, CDCl₃): δ = 28.7, 34.1, 35.2, 70.0, 70.1, 73.4, 73.9, 79.9, 91.5, 111.8 (=CH), 127.7 (Ph), 127.8 (Ph), 128.4 (Ph), 137.9 (Ph_{quat}), 138.1 (=CH) ppm. HRMS (ESI): calcd. for C₁₈H₂₄O₃ [M + Na]⁺ 311.16178; found 311.16195.

(Z)-9-(Benzyloxy)-8-methylnon-3-en-5-yne-1,8-diol (10g): Prepared from acetate **9g** (0.270 g, 0.853 mmol) in THF (1.2 mL), MeOH (0.2 mL), KOH (76 mg, 1.6 equiv.), and H₂O (0.8 mL) according to the general procedure. Compound **10g** (0.225 g, 99%) was obtained as a colourless oil. R_f (petroleum ether/EtOAc, 1:1): 0.27. ¹H NMR (400 MHz, CDCl₃): δ = 1.29 (s, 3 H, CH₃), 2.53 (app. q, 2 H, CH₂), 2.62 (s, 2 H, CH₂), 3.38 (d, J = 9.1 Hz, 1 H, CH₂), 3.49 (d, J = 9.1 Hz, 1 H, CH₂), 3.68 (t, J = 6.3 Hz, 1 H, CH₂), 4.58 (s, 2 H, CH₂), 5.57 (br. d, J = 10.6 Hz, 1 H, =CH), 5.89 (dt, J = 7.3, 10.6 Hz, 1 H, =CH), 7.27–7.37 (m, 5 H, Ph) ppm. ¹³C NMR (100 MHz, CDCl₃): δ = 23.7, 30.5, 33.6, 61.8, 71.9, 73.4, 76.0, 79.4, 91.0, 112.0 (=CH), 127.6 (Ph), 127.7 (Ph), 128.4 (Ph), 138.0 (Ph_{quat}), 138.6 (=CH) ppm. HRMS (ESI): calcd. for C₁₇H₂₂O₃ [M + Na]⁺ 297.14612; found 297.14603.

(7S,8S,9R,10R,Z)-10-[(tert-Butyldimethylsilyloxy]-11-[(tert-butyl-diphenylsilyloxy]-7,9-dimethylundec-3-en-5-yne-1,8-diol (10i): Prepared from acetate **9i**. Compound **10i** (32 mg, 90%) was obtained as a colourless oil. R_f (petroleum ether/EtOAc, 2:1): 0.45. ¹H NMR (400 MHz, CDCl₃): δ = -0.20 (s, 3 H, SiCH₃), -0.04 (s, 3 H, SiCH₃), 0.79 (s, 9 H), 1.00 (d, J = 7.4 Hz, 3 H, CH₃), 1.03 (s, 9 H), 1.18 (d, J = 6.9 Hz, 3 H, CH₃), 1.72 (br. s, 2 H, OH), 2.17 (app. br. q, 1 H, CH), 2.50 (s, 2 H, CH₂), 2.58 (q, J = 6.6 Hz, 2 H, CH₂), 2.76 (app. quint., 1 H, CH), 3.58 (dd, J = 9.4, 14.2 Hz, 1 H, CH₂), 3.71 (t, J = 6.4 Hz, 2 H, CH₂), 3.71–3.77 (overlapped m, 2 H, CH), 3.93 (d, J = 1.5, 8.7 Hz, 1 H, CH), 5.65 (br. d, J = 10.7 Hz, 1 H, =CH), 5.89 (dt, J = 7.5, 10.7 Hz, 1 H, =CH), 7.35–7.46 (m, 6 H, Ph), 7.64 (app. t, 4 H, Ph) ppm. ¹³C NMR (100 MHz, CDCl₃): δ

= -5.2, -4.7, 10.2, 17.5, 17.8, 19.1, 25.7, 26.8, 31.2, 33.7, 34.4, 61.9, 64.2, 74.0, 77.7, 78.4, 97.6, 112.4 (=CH), 127.77 (Ph), 127.80 (Ph), 129.83 (Ph), 129.86 (Ph), 133.06 (Ph), 133.06 (Ph_{quat}), 133.22 (Ph_{quat}), 135.48 (Ph), 135.52 (Ph), 138.21 (=CH) ppm. HRMS (ESI): calcd. for C₃₅H₅₄O₄Si₂ [M + Na]⁺ 617.34528; found 617.34561.

General Procedure for the Synthesis of Diols 10 from Alkoxytetrahydro-2H-pyrans 9 or tert-Butyldimethylsilyl Ethers 9: Deprotection of THP acetals or tert-butyldimethylsilyl ethers **9** can be carried out in MeOH (0.4–0.5 M) in the presence of a few drops of concd. HCl (about 2 drops for 3 mL of MeOH) at room temperature in high yield (ca. 90%). Reactions were monitored by TLC (petroleum ether/EtOAc, 1:1), and aqueous HCl was used in such amounts that the reactions were complete within 5–30 min. The HCl was neutralized by adding Et₃N (about 4 drops for 3 mL of MeOH), and then the mixture was concentrated in vacuo. The residue was purified by flash chromatography (petroleum ether/EtOAc, 1:1 to 0:1) to give enynediols **10**.

(Z)-Oct-3-en-5-yne-1,8-diol (10c): Prepared from **9c** (0.289 g, 1.29 mmol) in MeOH (3 mL), and concd. aqueous HCl (2 drops). The reaction time was 20 min. The acid was quenched with Et₃N (4 drops). Diol **10c** (0.126 g, 71%) was obtained as a colourless oil. R_f (EtOAc): 0.3. ¹H NMR (400 MHz, CDCl₃): δ = 1.63 (br., 1 H), 2.19 (t, 1 H), 2.54–2.62 (m, 4 H), 3.70–3.77 (m, 4 H), 5.60 (dt, J = 10.7, 2.2, 1.3 Hz, 1 H), 5.92 (dt, J = 10.7, 7.5 Hz, 1 H) ppm.

(S,Z)-7-Methyloct-3-en-5-yne-1,8-diol (10d): MeOH (0.5 mL) and concd. aqueous HCl (0.02 mL) were added to a solution of **9d** (0.2 g, 0.64 mmol) in THF (1 mL). The reaction mixture was stirred at room temperature for 30 min to achieve complete removal of the TBS group (TLC petroleum ether/EtOAc, 1:1). Then H₂O (0.5 mL) and NaOH (52 mg) were added to the reaction mixture. The reaction mixture was stirred further at room temperature until the acetate had been completely saponified. The mixture was diluted with diethyl ether and water. The organic phase was separated, washed with a small amount of saturated NaCl solution, and dried with Na₂SO₄. After filtration, the solvent was evaporated, and the residue was purified by chromatography (petroleum ether/EtOAc, 1:1→1:2) to give diol **10d** (79 mg, 81%) as a colourless oil. R_f (EtOAc): 0.44. ¹H NMR (400 MHz, CDCl₃): δ = 1.19 (d, J = 7.1 Hz, 3 H, 9-H), 1.54 (br. s, 1 H, OH), 2.10 (br. s, 1 H, OH), 2.56 (ddt, J = 1.2, 6.8, 7.3 Hz, 2 H, 2-H), 2.77–2.86 (m, 1 H, 7-H), 3.53 (dd, J = 10.1, 7.2 Hz, 1 H, 8-H), 3.61 (dd, J = 10.1, 5.3 Hz, 1 H, 8-H), 3.73 (t, J = 6.1 Hz, 2 H, 1-H), 5.61 (br. d, J = 10.7 Hz, 1 H, 4-H), 5.92 (dt, J = 7.4, 10.7 Hz, 1 H, 3-H) ppm. ¹³C NMR (100 MHz, CDCl₃): δ = 16.9, 30.3, 33.5, 61.8, 67.0, 78.9, 96.4, 112.0, 138.8 ppm.

(S,Z)-2-Methyloct-3-en-5-yne-1,8-diol (10h): Prepared from silyl ether **9h** (0.276 g, 1.02 mmol) in MeOH (3 mL), and concd. aqueous HCl (2 drops). The acid was quenched with Et₃N. Diol **10h** (0.140 g, 91%) was obtained as a colourless oil. R_f (EtOAc): 0.44. ¹H NMR (400 MHz, CDCl₃): δ = 1.00 (d, J = 6.8 Hz, 3 H), 1.72 (t, 1 H), 2.35 (t, 1 H), 2.59 (t, 2 H), 2.97–3.06 (m, 1 H), 3.41–3.49 (m, 1 H), 3.55–3.61 (m, 1 H), 3.74 (app. q, 2 H), 5.56 (d, J = 10.6 Hz, 1 H), 5.68 (dd, 1 H) ppm. ¹³C NMR (100 MHz, CDCl₃): δ = 16.2, 24.0, 37.7, 61.2, 67.6, 79.2, 91.4, 110.7, 145.3 ppm.

4-[2-(2-Hydroxyethyl)phenyl]but-3-yn-1-ol (10j): Prepared from aryl iodide **8e** (0.347 g, 1.4 mmol), alkynol **5a** (108 mg, 1.1 equiv.), diethylamine (2 mL), Pd(PPh₃)₂Cl₂ (7.1 mg), and CuI (3.8 mg). The residue was purified by flash chromatography (EtOAc) to give enynol **10j** (0.186 g, 70%) as a slightly yellow oil. R_f (EtOAc): 0.25. ¹H NMR (400 MHz, CDCl₃): δ = 2.42 (br., 1 H), 2.67 (t, J = 5.9 Hz, 2 H), 3.04 (t, J = 6.8 Hz, 2 H), 3.07 (br., 1 H), 3.80 (br., 2 H), 3.86

(t, $J = 6.7$ Hz, 2 H), 7.13–7.24 (m, 3 H), 7.38 (d, $J = 8.3$ Hz, 1 H) ppm. ^{13}C NMR (100 MHz, CDCl_3): $\delta = 22.9, 38.0, 61.1, 63.4, 80.9, 91.1, 123.5, 126.4, 128.1, 129.4, 131.9, 140.7$ ppm.

General Procedure. [5,6]-Spiroacetals 3 from Enynediols 10: Enynediol **10** was dissolved in CH_2Cl_2 or another solvent, and the catalyst was added, either as a solid or in solution (in CH_2Cl_2 or MeCN or a mixture of these two solvents). The progress of reaction was monitored by TLC, and when the conversion was complete, the reaction was quenched by the addition of Et_3N (about 1 drop per 0.1 mmol of substrate). The mixture was directly loaded onto a small silica column and further eluted with petroleum ether/EtOAc, 4:1 (or pentane/ Et_2O , 4:1 for volatile compounds) to give spiroacetal **3**.

7-[(Benzyloxy)methyl]-1,6-dioxaspiro[4.5]dec-9-ene (3e)

Method A: A solution of **10e** (26.5 mg, 0.102 mmol) in CH_2Cl_2 (1 mL) containing $\text{Hg}(\text{O}_2\text{CCF}_3)_2$ (0.47 mg, 1 mol-%) was stirred for 24 h at room temperature. Et_3N was added, the mixture was concentrated in vacuo, and the residue was purified by flash chromatography to give spiroacetal **3e** (24.4 mg, 92%) as a colourless oil.

Method B: A solution of **10e** (50.7 mg, 0.195 mmol) in CH_2Cl_2 (1.3 mL) containing $L_2\text{AuNCMe}^+ \text{SbF}_6^-$ (0.75 mg, 0.975 μmol , 0.5 mol-%) was stirred for 10–15 min at room temperature. Et_3N was added, the mixture was concentrated in vacuo, and the residue was purified by flash chromatography to give spiroacetal **3e** (47.2 mg, 93%).

Method C: A solution of **10e** (43.0 mg, 0.165 mmol) in CH_2Cl_2 (1.4 mL) containing $[\text{PdPCP-ac}]^+ \text{SbF}_6^-$ (1.16 mg, 0.132 μmol , 0.8 mol-%) was stirred for 10–15 min at room temperature. Et_3N was added, the mixture was concentrated in vacuo, and the residue was purified by flash chromatography to give spiroacetal **3e** (38.7 mg, 90%).

Method D: A solution of **10e** (32.1 mg, 0.123 mmol) in THF (1.1 mL) and acetonitrile (0.074 mL) containing $\text{Hg}(\text{O}_2\text{CCF}_3)_2$ (0.85 mg, 1.5 mol-%) was stirred for 10–15 min at room temperature. Et_3N was added, the mixture was concentrated in vacuo, and the residue was purified by flash chromatography to give spiroacetal **3e** (38.7 mg, 90%). R_f (petroleum ether/EtOAc, 4:1): 0.5. ^1H NMR (400 MHz, CDCl_3): $\delta = 1.82$ (ddd, $J = 12.1, 9.3, 8.3$ Hz, 1 H), 1.89–1.98 (m, 2 H), 2.01–2.19 (m, 3 H), 3.51 (dd, $J = 10.4, 4.6$ Hz, 1 H), 3.51 (dd, $J = 10.4, 5.6$ Hz, 1 H), 3.89–3.99 (m, 2 H), 4.14–4.20 (m, 1 H), 4.58 (d, $J = 12.1$ Hz, 1 H), 4.60 (d, $J = 12.1$ Hz, 1 H), 5.63 (ddd, $J = 9.9, 2.7, 1.5$ Hz, 1 H), 5.99 (ddd, $J = 9.9, 5.6, 2.2$ Hz, 1 H), 7.26–7.34 (m, 5 H) ppm. ^{13}C NMR (100 MHz, CDCl_3): $\delta = 24.6, 26.9, 37.4, 67.3, 67.7, 72.6, 73.1, 103.5, 127.5, 127.6, 128.3, 128.5, 138.5$ ppm.

7-[(Benzyloxy)methyl]-2,2-dimethyl-1,6-dioxaspiro[4.5]dec-9-ene (3f)

Method A: A solution of **10f** (28.8 mg, 0.100 mmol) in a mixture of CH_2Cl_2 (1.0 mL) and acetonitrile (0.02 mL) containing mercury(II) trifluoromethanesulfonate $[\text{Hg}(\text{OTf})_2]$ (0.25 mg, 0.5 μmol , 0.5 mol-%) was stirred for 10–15 min at room temperature. Et_3N was added, the mixture was concentrated in vacuo, and the residue was purified by flash chromatography to give spiroacetal **3f** (25.9 mg, 90%).

Method B: A solution of **10f** (23.7 mg, 0.082 mmol) in CH_2Cl_2 (1.0 mL) containing $L_2\text{AuNCMe}^+ \text{SbF}_6^-$ (0.51 mg, 0.656 μmol , 0.8 mol-%) was stirred for 10 min at room temperature. Et_3N was added, the mixture was concentrated in vacuo, and the residue was purified by flash chromatography to give spiroacetal **3f** (21.8 mg, 92%). R_f (petroleum ether/EtOAc, 4:1): 0.5. ^1H NMR (400 MHz,

CDCl_3): $\delta = 1.23$ (m, 3 H), 1.38 (m, 3 H), 1.80 (m, 1 H), 1.89–1.97 (m, 2 H), 2.02–2.17 (m, 3 H), 3.50 (dd, $J = 10.5, 4.5$ Hz, 1 H), 3.57 (dd, $J = 10.5, 5.6$ Hz, 1 H), 4.20–4.26 (m, 1 H), 4.56 (d, $J = 12.4$ Hz, 1 H), 4.61 (d, $J = 12.4$ Hz, 1 H), 5.60 (d, $J = 9.9$ Hz, 1 H), 5.95 (ddd, $J = 9.9, 5.6, 2.0$ Hz, 1 H), 7.23–7.33 (m, 5 H) ppm. ^{13}C NMR (100 MHz, CDCl_3): $\delta = 26.9, 29.1, 30.3, 37.3, 38.1, 66.9, 72.7, 73.1, 82.3, 103.7, 127.4, 127.5, 128.2, 129.0, 138.5$ ppm.

2-[(Benzyloxy)methyl]-2-methyl-1,6-dioxaspiro[4.5]dec-9-ene (3g): A solution of **10g** (32.5 mg, 0.118 mmol) in a mixture of CH_2Cl_2 (1.2 mL) and acetonitrile (0.024 mL) containing mercury(II) trifluoromethanesulfonate $[\text{Hg}(\text{OTf})_2]$ (0.29 mg, 0.59 μmol , 0.5 mol-%) was stirred for 5 min at room temperature. Et_3N was added, the mixture was concentrated in vacuo, and the residue was purified by flash chromatography to give spiroacetal **3g** (27.0 mg, 83%) as a mixture of epimers (1:1.1 mol ratio). R_f (petroleum ether/EtOAc, 4:1): 0.5. ^1H NMR (400 MHz, CDCl_3): $\delta = 1.29$ (s, minor, 3 H), 1.35 (s, major, 3 H), 1.72–2.03 (m, 4 H), 2.06–2.18 (m, 1 H), 2.19–2.31 (m, 1 H), 3.29 (d, $J = 9.5$ Hz, major, 1 H), 3.34 (d, $J = 9.5$ Hz, major, 1 H), 3.43 (d, $J = 9.1$ Hz, minor, 1 H), 3.48 (d, $J = 9.1$ Hz, minor, 1 H), 3.69 (dd, $J = 11.2, 6.1$ Hz, minor, 1 H), 3.75 (dd, $J = 11.2, 6.1$ Hz, major, 1 H), 3.93 (ddd, $J = 11.6, 11.6, 3.8$ Hz, minor, 1 H), 4.01 (ddd, $J = 11.6, 11.6, 3.7$ Hz, major, 1 H), 4.53 (d, $J = 12.1$ Hz, major, 1 H), 4.57 (d, $J = 12.1$ Hz, major, 1 H), 4.57 (d, $J = 12.1$ Hz, minor, 1 H), 4.61 (d, $J = 12.1$ Hz, minor, 1 H), 5.60 (d, major, minor, 1 H), 5.96–6.00 (m, major, minor, 1 H), 7.24–7.36 (m, 5 H) ppm. ^{13}C NMR (100 MHz, CDCl_3): $\delta = 24.5, 26.1, 33.6, 33.9, 37.3, 38.4, 58.46, 57.51, 73.41, 76.8, 78.2, 83.8, 83.9, 103.0, 103.2, 127.4, 128.3, 128.5, 128.2, 128.3, 128.78, 128.83, 128.87, 129.03, 138.7, 138.7$ ppm.

(8S)-8-Methyl-1,6-dioxaspiro[4.5]dec-9-ene (3h): A solution of **10h** (32.7 mg, 0.212 mmol) in CH_2Cl_2 (0.8 mL) containing $L_2\text{AuNCMe}^+ \text{SbF}_6^-$ (0.655 mg, 0.848 μmol , 0.4 mol-%) was stirred for 4 min at room temperature. Et_3N was added, the mixture was concentrated in vacuo, and the residue was purified by flash chromatography to give spiroacetal **3h** (27.1 mg, 83%) as a mixture of epimers (2:1 mol ratio). R_f (petroleum ether/EtOAc, 4:1): 0.5. ^1H NMR (400 MHz, CDCl_3): $\delta = 0.89$ (d, $J = 7.1$ Hz, major, 3 H), 1.05 (d, $J = 7.1$ Hz, minor, 3 H), 1.76–1.84 (m, major, minor, 1 H), 1.88–2.18 (m, major, minor, 3.3 H), 2.33–2.43 (m, major, 1 H), 3.43–3.51 (m, major, minor, 1 H), 3.67 (ddd, $J = 11.1, 5.7, 1.4$ Hz, major, 1 H), 3.87–4.00 (m, major, minor, 2 H), 4.04 (dd, $J = 11.4, 3.8$ Hz, minor, 1 H), 5.53–5.59 (m, major, minor, 1 H), 5.82 (ddd, $J = 10.0, 1.6, 1.5$ Hz, major, 1 H), 5.95 (ddd, $J = 10.0, 5.2, 1.3$ Hz, major, 1 H) ppm. ^{13}C NMR (100 MHz, CDCl_3): $\delta = 15.8$ (major), 17.7 (minor), 24.5 (minor), 24.6 (major), 28.8 (minor), 29.0 (major), 37.4 (major, minor), 65.2 (minor), 65.8 (major), 67.4 (major), 67.5 (minor), 102.5 (major), 102.6 (minor), 127.2 (minor), 127.4 (major), 134.5 (minor), 135.5 (major) ppm.

4,5-Dihydro-3H-spiro[furan-2,1'-isochroman] (3j): A solution of **10j** (20.1 mg, 0.212 mmol) in CH_2Cl_2 (0.8 mL) containing $L_2\text{AuNCMe}^+ \text{SbF}_6^-$ (0.4 mol-%) was stirred for 10 min at room temperature. Et_3N was added, the mixture was concentrated in vacuo, and the residue was purified by flash chromatography to give spiroacetal **3j** (19.1 mg, 95%) as a colourless oil. R_f (petroleum ether/EtOAc, 4:1): 0.56. ^1H NMR (400 MHz, CDCl_3): $\delta = 2.04$ –2.17 (m, 1 H), 2.18–2.34 (m, 3 H), 2.60 (ddd, $J = 16.0, 2.5, 2.4$ Hz, 1 H), 3.03 (ddd, $J = 16.0, 12.1, 5.8$ Hz, 1 H), 3.90 (ddd, $J = 11.1, 5.8, 1.8$ Hz, 1 H), 4.01–4.13 (m, 3 H), 7.07–7.11 (m, 1 H), 7.18–7.29 (m, 3 H) ppm. ^{13}C NMR (100 MHz, CDCl_3): $\delta = 25.1, 28.8, 39.5, 59.5, 68.0, 105.6, 126.4, 127.7, 128.4, 135.2, 136.3$ ppm.

(5R)-2,2,3,3,9,9-Hexamethyl-5-[(1R)-1-[(2S,3S)-3-methyl-1,6-dioxaspiro[4.5]dec-9-en-2-yl]ethyl]-8,8-diphenyl-4,7-dioxo-3,8-disila-

decane (3i): A solution of **10i** (13.6 mg, 0.0313 mmol) in CH₂Cl₂ (0.3 mL) containing L₂AuNCMe⁺ SbF₆⁻ (0.242 mg, 0.313 μmol, 1.0 mol-%) was stirred for 10 min at room temperature. Et₃N was added, the mixture was concentrated in vacuo, and the residue was purified by flash chromatography to give spiroacetal **3i** (12.8 mg, 94%) as a mixture of epimers (0.56:0.44 mol ratio). R_f (petroleum ether/Et₂O, 10:1): 0.41 and 0.49. ¹H NMR (400 MHz, CDCl₃): δ = -0.04 (s, minor, 3 H), -0.03 (s, major, 3 H), 0.04 (s, major, 3 H), 0.08 (s, minor, 3 H), 0.80 (d, minor, 3 H), 0.84 (d, major, 3 H), 0.88 (s, major, 9 H), 0.89 (s, minor, 9 H), 0.98 (d, major, 3 H), 1.04 (d, minor, 3 H), 1.04 (s, major, minor, 9 H), 1.47 (dd, *J* = 12.1, 11.9 Hz, major, 1 H), 1.63 (dd, *J* = 12.9, 6.8 Hz, minor, 1 H), 1.73–1.89 (m, 2 H), 1.95–2.13 (m), 2.16–2.26 (m, major, minor, 1 H), 2.30–2.40 (m, major, H), 3.61–3.87 (m, 6 H), 5.53 (d, 1 H), 5.86–5.93 (m, 1 H), 7.33–7.41 (m, 6 H), 7.66–7.70 (m, 4 H) ppm. ¹³C NMR (100 MHz, CDCl₃): δ = -5.1, -5.0, -4.1, -4.0, 8.5, 9.4, 16.7, 17.7, 18.10, 18.13, 19.25, 24.4, 24.5, 25.9, 26.0, 26.89, 26.92, 34.8, 36.1, 38.8, 39.3, 46.4, 47.0, 58.4, 59.5, 66.5, 66.6, 75.5, 75.7, 84.0, 86.3, 101.4, 102.4, 127.2, 127.5, 128.1, 129.4, 129.5, 129.6, 133.7, 133.8, 133.84, 133.9, 135.70, 135.73, 135.77, 135.79 ppm.

Supporting Information (see footnote on the first page of this article): Synthesis of some starting materials, synthesis of pincer complex **11**, description of unselective cyclization reactions with enynediol **10b**, description of in situ NMR experiments, copies of ¹H and ¹³C NMR spectra of key intermediates and final products.

Acknowledgments

Financial support by the German Federate State of Baden-Württemberg is greatly acknowledged. The authors thank Dr. D. Wistuba (Univ. Tübingen) for HRMS analysis.

- [1] For some reviews, see: a) J. E. Aho, P. M. Pihko, T. K. Rissa, *Chem. Rev.* **2005**, *105*, 4406–4440; b) H. Kiyota, *Top. Heterocycl. Chem.* **2006**, *5*, 65–95.
- [2] I. Paterson, A. D. Findlay, *Aust. J. Chem.* **2009**, *62*, 624–638.
- [3] a) T. W. Miller, L. Chaiet, D. J. Cole, L. J. Cole, J. E. Flor, R. T. Goegelman, V. P. Gullo, H. Joshua, A. J. Kempf, W. R. Krellwitz, R. L. Monaghan, R. E. Ormond, K. E. Wilson, G. Albers-Schönberg, I. Putter, *Antimicrob. Agents Chemother.* **1979**, *15*, 368–371; b) G. Albers-Schönberg, B. H. Arison, J. C. Chabala, A. W. Douglas, P. Eskola, M. H. Fisher, A. Lusi, H. Mrozik, J. L. Smith, R. L. Tolman, *J. Am. Chem. Soc.* **1981**, *103*, 4216–4221.
- [4] a) Isolation: Y. Miyazaki, M. Shibuya, H. Sugawara, O. Kawaguchi, C. Hirose, J. Nagatsu, S. Esumi, *J. Antibiot.* **1974**, *27*, 814–821; b) X-ray structure: H. Kinashi, N. Otake, H. Yonehara, S. Sato, Y. Saito, *Tetrahedron Lett.* **1973**, *14*, 4955–4958; c) total synthesis: P. J. Kocienski, R. C. D. Brown, A. Pommier, M. Procter, B. Schmidt, *J. Chem. Soc. Perkin Trans. 1* **1998**, 9–39.
- [5] K. Tachibana, P. J. Scheuer, Y. Tsukitani, H. Kikuchi, D. Van Engen, J. Clardy, Y. Gopichand, F. J. Schmitz, *J. Am. Chem. Soc.* **1981**, *103*, 2469–2471.
- [6] For a general review about transition-metal-catalysed nucleophilic addition to C–C triple bonds, see: F. Alonso, I. P. Beletskaya, M. Yus, *Chem. Rev.* **2004**, *104*, 3079–3160.
- [7] A. Aponick, C.-Y. Li, J. A. Palmes, *Org. Lett.* **2009**, *11*, 121–124.
- [8] K. Ravindar, M. Sridhar Reddy, P. Deslongchamps, *Org. Lett.* **2011**, *13*, 3178–3181.
- [9] For examples catalysed by gold(I), see: a) J. H. Teles, S. Brode, M. Chabanas, *Angew. Chem. Int. Ed.* **1998**, *37*, 1415–1418; *Angew. Chem.* **1998**, *110*, 1475–1478; b) E. Mizushima, K. Sato, T. Hayashi, M. Tanaka, *Angew. Chem. Int. Ed.* **2002**, *41*, 4563–4565; *Angew. Chem.* **2002**, *114*, 4745–4747; c) P. Roembke, H. Schmidbaur, S. Cronje, H. Raubenheimer, *J. Mol. Catal. A* **2004**, *212*, 35–42; by gold(III): d) Y. Fukuda, K. Utimoto, *J. Org. Chem.* **1991**, *56*, 3729–3731; e) A. S. K. Hashmi, L. Schwarz, J.-H. Choi, T. M. Frost, *Angew. Chem. Int. Ed.* **2000**, *39*, 2285–2288; *Angew. Chem.* **2000**, *112*, 2382–2385.
- [10] For examples catalysed by platinum(II), see: a) P. W. Jennings, J. W. Hartman, W. C. Hiscox, *Inorg. Chim. Acta* **1994**, *222*, 317–322; b) Y. Kataoka, O. Matsumoto, K. Tani, *Organometallics* **1996**, *15*, 5246–5249; c) J. W. Hartman, L. Sperry, *Tetrahedron Lett.* **2004**, *45*, 3787–3788.
- [11] For examples catalysed by palladium(II), see: K. Imi, K. Imai, K. Utimoto, *Tetrahedron Lett.* **1987**, *28*, 3127–3130.
- [12] a) B. Liu, J. K. De Brabander, *Org. Lett.* **2006**, *8*, 4907–4910; b) M. C. B. Jaimes, C. R. N. Böhlring, J. M. Serrano-Becerra, A. S. K. Hashmi, *Angew. Chem. Int. Ed.* **2013**, *52*, 7963–7966; *Angew. Chem.* **2013**, *125*, 8121–8124.
- [13] a) J. M. Montierth, D. R. DeMario, M. J. Kurth, N. E. Schore, *Tetrahedron* **1998**, *54*, 11741–11748; b) S. Melnes, A. Bayer, O. R. Gautun, *Tetrahedron* **2012**, *68*, 8463–8471.
- [14] A. Abiko, *Org. Synth.* **2002**, *79*, 103–108; A. Abiko, *Org. Synth., Coll.* **2004**, *10*, 273–275.
- [15] H. C. Brown, C. D. Blue, D. J. Nelson, N. G. Bhat, *J. Org. Chem.* **1989**, *54*, 6064–6067.
- [16] For recent reviews, see: a) R. Chinchilla, C. Najera, *Chem. Rev.* **2007**, *107*, 874–922; b) R. R. Tykwinski, *Angew. Chem. Int. Ed.* **2003**, *42*, 1566–1568; *Angew. Chem.* **2003**, *115*, 1604–1606.
- [17] a) R. M. Acheson, G. C. M. Lee, *J. Chem. Soc. Perkin Trans. 1* **1987**, 2321–2332; b) A. Minatti, S. L. Buchwald, *Org. Lett.* **2008**, *10*, 2721–2724.
- [18] a) Y. Ichikawa, M. Isobe, D. Bai, T. Goto, *Tetrahedron* **1987**, *43*, 4737–4748; b) L. Ye, L. Cui, G. Zhang, L. Zhang, *J. Am. Chem. Soc.* **2010**, *132*, 3258–3259.
- [19] C. Rink, V. Navickas, M. E. Maier, *Org. Lett.* **2011**, *13*, 2334–2337.
- [20] E. R. H. Jones, G. Eglinton, M. C. Whiting, *Org. Synth.* **1953**, *33*, 68; E. R. H. Jones, G. Eglinton, M. C. Whiting, *Org. Synth., Coll.* **1963**, *4*, 755–757.
- [21] Y. Q. Tu, A. Hübener, H. Zhang, C. J. Moore, M. T. Fletcher, P. Hayes, K. Dettner, W. Francke, C. S. P. McErlean, W. Kitching, *Synthesis* **2000**, 1956–1978.
- [22] V. Navickas, C. Rink, M. E. Maier, *Synlett* **2011**, 191–194.
- [23] C. Nieto-Oberhuber, M. P. Muñoz, S. López, E. Jiménez-Núñez, C. Nevado, E. Herrero-Gómez, M. Raducan, A. M. Echavarren, *Chem. Eur. J.* **2006**, *12*, 1677–1693.
- [24] For catalysis by Zeise's dimer, see: W. Hiscox, P. W. Jennings, *Organometallics* **1990**, *9*, 1997–1999.
- [25] For catalysis by Hg(OTf)₂, see: a) M. Nishizawa, M. Skwarczynski, H. Imagawa, T. Sugihara, *Chem. Lett.* **2002**, 12; b) H. Imagawa, T. Kurisaki, M. Nishizawa, *Org. Lett.* **2004**, *6*, 3679–3681.
- [26] Decomposition was evident from the ¹H NMR spectrum: an increase was seen in the multiplets in the regions 3–4.5 and 1–2 ppm, while the unsaturated region 5–6 ppm was left clear.
- [27] It was claimed that the mercury-catalysed cyclization of non-3-yne-1,9-diol gave the corresponding saturated [6,6]-spiroacetal as a single product.^[8] However, in our hands, treatment of this substrate with Hg(OTf)₂ in either CDCl₃ or MeCN (under identical conditions) gave a mixture of regioisomers. Secondly, in relation to the same ref.^[8] we would like to comment that Hg(OTf)₂ is so active that there is no need to use 10 mol-% catalyst loading, as was done in that work. An amount of 1 mol-% or less is enough. It appears that this toxic but cheap compound is also a useful catalyst for the activation of C–C triple bonds and, as it may be used in very small amounts, it may indeed find practical applications in Synthesis despite its toxicity.
- [28] J. E. Baldwin, *J. Chem. Soc., Chem. Commun.* **1976**, 734–741.
- [29] a) F. E. Michael, B. M. Cochran, *J. Am. Chem. Soc.* **2006**, *128*, 4246–4247; b) N. Selander, K. J. Szabó, *Chem. Rev.* **2010**, *111*,

- 2048–2076; c) R. Chinchilla, C. Nájera, *Chem. Rev.* **2014**, DOI: 10.1021/cr400133p.
- [30] The catalysis by PdPCP⁺ is slow in methanol because the ligand-exchange equilibrium PdPCP-MeOH⁺ + alkyne \rightleftharpoons PdPCP-alkyne⁺ + MeOH is strongly on the left, so alkyne coordination is suppressed. More mechanistic details will be published separately.
- [31] E. N. Lawson, W. Kitching, C. H. L. Kennard, K. A. Byriel, *J. Org. Chem.* **1993**, *58*, 2501–2508.
- [32] P. Kocienski, S. Wadman, K. Cooper, *J. Am. Chem. Soc.* **1989**, *111*, 2363–2365.
- [33] For a review of such spiroacetals, generated by intramolecular hydrogen abstraction, see: J. Sperry, Y.-C. W. Liu, M. A. Brimble, *Org. Biomol. Chem.* **2010**, *8*, 29–38.
- [34] A control experiment with **10e** (0.1 M in CH₂Cl₂) indicated that cyclization of enynediols is not catalysed by Brønsted acid alone (3% TfOH, room temp., 1 d gave 0% conversion). However, a Brønsted acid (H⁺) is required for a) the turnover of a transition metal catalyst, because it is necessary for protodemetalation of organometallic intermediates; b) the transformation of the dienol ether into the final spiroacetal. When a transition metal catalyst is used alone, the necessary Brønsted acid arises naturally in the catalytic cycle. It is clear that lowering the catalyst loading can be compensated by the addition of external Brønsted acid to speed up the overall process.
- [35] A. Zhdanko, M. E. Maier, unpublished results. We note here that 6-*exo*-**17c** is not a product of the direct and selective 6-*exo*-cyclization, but the product of rearrangement of a vinyl mercury intermediate with subsequent transformations.
- [36] The difference in reactivity of both 5-*endo*-**16c** and 6-*exo*-**17c** compared with 5-*exo*-**13a** and 6-*endo*-**14a** is very pronounced. Thus, a mixture 5-*exo*-**13a** and 6-*endo*-**14a** is reliably obtained even under unbuffered catalytic conditions (simple use of active Pd, Au, or Pt catalysts, as mentioned). The generation of 5-*endo*-**16c** or 6-*exo*-**17c**, on the other hand, is very challenging, and requires buffered conditions (use of a weak base like *t*Bu₂Py), otherwise they are all transformed into the final spiroacetals within minutes.

Received: February 7, 2014
Published Online: April 17, 2014

Paper 7

For the Section 6.3.5.

Gold-Catalyzed Hydroamination

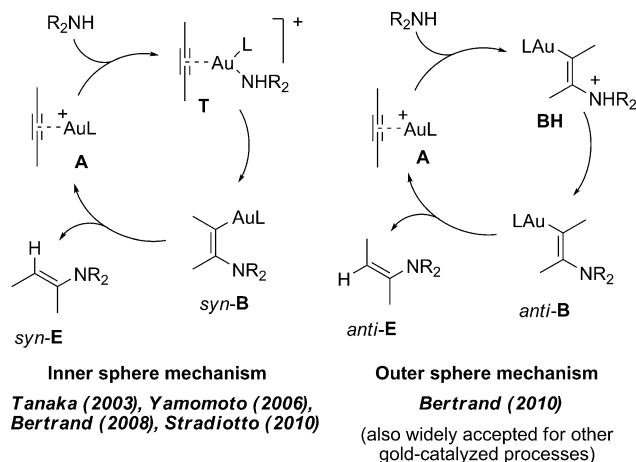
Gold Catalysis

Mechanistic Study of Gold(I)-Catalyzed Hydroamination of Alkynes: Outer or Inner Sphere Mechanism?*

Alexander Zhdanko* and Martin E. Maier*

Abstract: An experimental mechanistic study of the gold(I)-catalyzed hydroamination shows the formation of conformationally flexible auro-iminium salts **Au-Im**, which originate from the protonation of a vinyl gold species. Rotation around the C–Au bond is the reason for the loss of stereospecificity of protodeauration, which explains the stereochemical result of the Stradiotto reaction. The ambiguity about inner or outer sphere mechanism is thus resolved in favor of the outer sphere mechanism.

Gold(I)-catalyzed hydroamination of alkynes is an important synthetic tool for the functionalization of C≡C bonds.^[1] Like some other processes in gold catalysis, it was already described in 1987,^[2] but did not receive much attention until around 2000, when the interest in gold catalysis started to rise. Nowadays, the scope of gold(I)-catalyzed hydroamination of alkynes is not limited to the synthesis of imine or enamine structures by the formal addition of various N–H reagents onto the C≡C bond.^[3,4] Rather, a number of complex cascade reactions were reported, using this addition as one step within a complicated multistep process.^[5] However, the hydroamination reaction often requires harsh conditions, which limits its scope. Last but not least, the development of the method is also limited because of the lack of understanding of the reaction mechanism. In several studies gold–amine complexes [LAu(amine)]⁺ were identified as reaction intermediates. This fact, together with the stereoselective formation of *syn-E* in the intermolecular reaction described by Stradiotto and co-workers, was considered as sufficient evidence for the inner sphere mechanism (Scheme 1).^[3a,6] However, ionic organo–gold complexes formed upon intramolecular *5-endo-dig* and *5-exo-dig* addition of a tertiary amine moiety described by Bertrand and co-workers^[7] as well as a single vinyl–gold complex described by Hashmi and co-workers,^[8] provided evidence for the outer sphere mechanism. It should be stressed, that according to the current understanding of protodeauration, the outer sphere mechanism should lead to the product of *anti*-addition (*anti-E*), which is in contradiction to the formation of *syn-E* described by Stradiotto and co-



Scheme 1. Short representation of inner and outer sphere mechanism proposed for the hydroamination of alkynes.

workers.^[3a] As it stands, there is still an unresolved ambiguity: should the reaction generally be considered as proceeding through an inner or outer sphere mechanism (Scheme 1)?

As part of our studies on mechanisms of gold catalysis,^[9] we report herein an experimental NMR investigation of the mechanism of the gold(I)-catalyzed hydroamination of alkynes. We describe the key organo–gold intermediates originating from catalysts [Ph₃PAuNCMe]⁺ SbF₆[−] (**1**) and [L₂AuNCMe]⁺ SbF₆[−] (**2**) (L₂ = *o*-(di-*tert*-butylphosphino)bi-phenyl) as well as the chemistry of gold complexes relevant to the process, leading to a consensus: the gold(I)-catalyzed hydroamination reaction is best described by the outer sphere mechanism, whereas the inner sphere mechanism cannot be accepted anymore as an explanation.

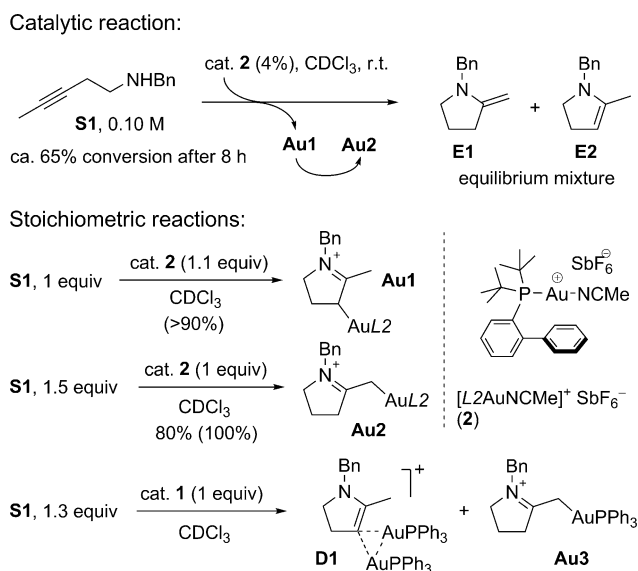
The addition of catalyst **2** (4 mol%) to alkyne-amine **S1** in CDCl₃ led to a sluggish catalytic reaction. Monitoring by ¹H NMR spectroscopy showed the immediate formation of two organo–gold species **Au1** and **Au2**, but after a few minutes only **Au2** remained (Scheme 2). After 8 h 60–70% conversion of **S1** was achieved, giving a mixture of enamines **E1/E2** as the main product.^[10] In a stoichiometric study, 1.5 equiv of **S1** reacted with 1 equiv of **2** in CDCl₃ instantly giving complex **Au2** which was isolated in its individual state (80% yield, 100% yield in situ) and fully characterized by NMR spectroscopy and X-ray analysis. However, reaction of a slight excess of **2** with **S1** led to the immediate formation of **Au1** (> 90% in situ). Reaction of the sterically less hindered catalyst **1** led to a mixture of diaurated species **D1** and **Au3**.

Complexes **Au1–Au3** are depicted as auro-iminium salts and not as gold enamine π-complexes. This structure assignment and understanding of bonding follows from the NMR

[*] Dipl.-Chem. A. Zhdanko, Prof. Dr. M. E. Maier
 Institut für Organische Chemie, Universität Tübingen
 Auf der Morgenstelle 18, 72076 Tübingen (Germany)
 E-mail: Vinceero@gmail.com
 martin.e.maier@uni-tuebingen.de

[**] Financial support by the State of Baden-Württemberg is gratefully acknowledged. We thank Dr. K. Eichele and the Institut für Anorganische Chemie for allowing us to use their NMR spectrometer.

Supporting information for this article is available on the WWW under <http://dx.doi.org/10.1002/anie.201402557>.



Scheme 2. Reactions of amine **S1** with catalysts **1** and **2**.

spectra in solution and X-ray analysis. The ^1H NMR spectrum of pure **Au2** in CD_2Cl_2 at room temperature contains simple signals (including the doublet at 1.91 ppm, $J_{\text{P}} = 8.9$ Hz of the CH_2Au group), but at low temperature the spectrum shows a complicated pattern (Figure 1). Structural parameters determined from the solid structure of **Au2** are between the typical values for known gold–enol ether complexes and gold–ene-1,1-diamine complexes (Figures 2 and 3).^[11] This unambiguously characterizes the alkyl enamine **E1** as a ligand with a high degree of slippage when coordinated to gold.

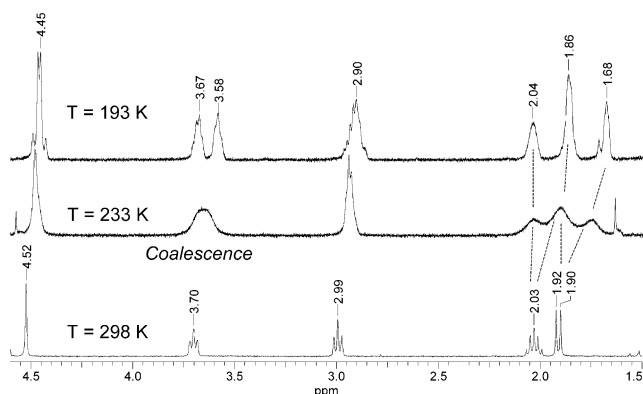


Figure 1. ^1H NMR spectra of **Au2** at various temperatures in CD_2Cl_2 .

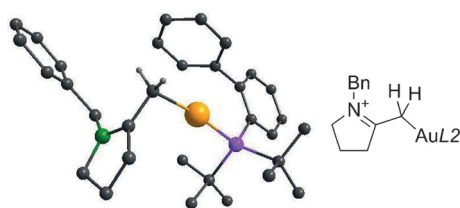


Figure 2. Structure of the **Au2** cation in the solid state. All hydrogens are omitted except for the CH_2Au fragment.

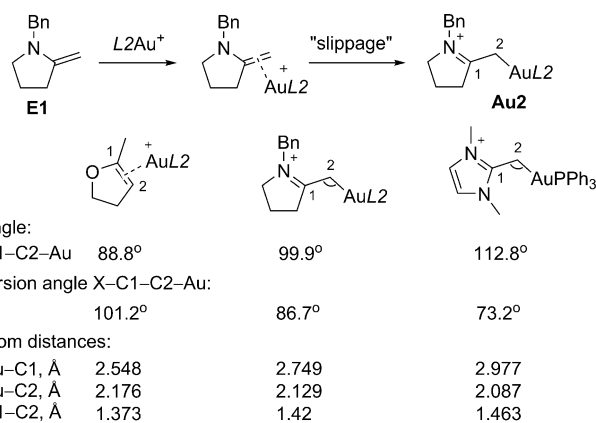
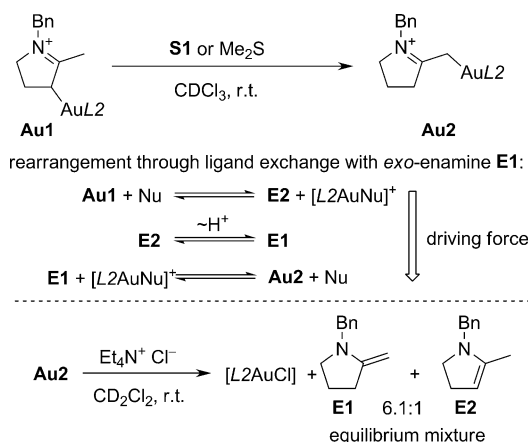


Figure 3. Slippage mechanism and structure comparison of representative gold–enol ether,^[11a] gold–enamine, and gold–ene-1,1-diamine complexes.^[11b]

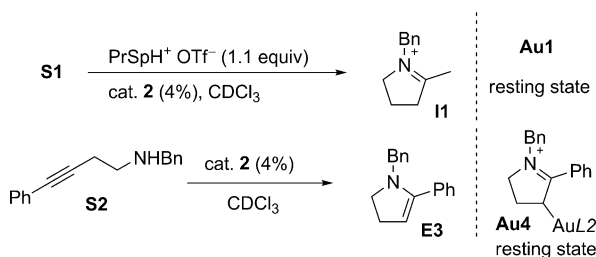
Correspondingly, **Au2** exhibits a high degree of η^1 -coordination mode to gold and a predominant loss of the double-bond character of the C1–C2 bond; this enables easy rotation around this bond and therefore **Au2** should rather be considered an alpha auro-iminium salt than a π -alkene complex. This property is the key to understand the stereochemical outcome of alkyne hydroamination reactions (see below).

In order to conclude about the role of auro-iminium salts in the hydroamination mechanism, the origin of these species has to be established. First, the chemistry of **Au1** and **Au2** was studied. The addition of free **S1** to a solution of **Au1** led to the rapid rearrangement of **Au1**, thereby forming **Au2** (with concomitant slow catalytic reaction). The same occurs upon addition of a moderately strong nucleophile (Me_2S) to **Au1**. However, the addition of Cl^- as a strong nucleophile either to **Au1** or **Au2** led to complete liberation of $[\text{L2AuCl}]$ and the formation of free enamines **E1/E2** as an equilibrium mixture (Scheme 3). It becomes clear that the rearrangement of **Au1** to **Au2** is simply a ligand exchange with free **E1**, giving the thermodynamically more stable **Au2**. This process can be considered as catalytic in enamine (or another nucleophile).



Scheme 3. Reaction of auro-iminium salts with nucleophiles.

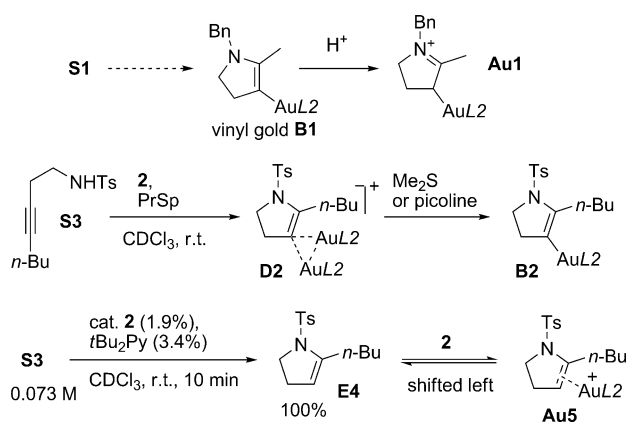
To confirm that **Au2** arises as a product of ligand exchange and not as a direct participant of the catalytic cycle, we performed the hydroamination of **S1** in the presence of an acid (1,8-bis(dimethylamino)naphthalene triflate salt, PrSpH⁺OTf⁻). Under these conditions the formed enamines are immediately protonated, giving iminium salt **I1** as a single final product (Scheme 4).^[12] Because of the negligible con-



Scheme 4. Observation of resting states.

centration of free enamine at all times, the rearrangement of **Au1** to **Au2** should be suppressed. Indeed, gold was exclusively present as **Au1** (directly evidenced from NMR spectra). This confirms that **Au1** is the primary organo-gold intermediate, originating from pure 5-endo-dig cyclization, and that **Au2** is a thermodynamically more stable isomer originating from ligand exchange with free **E1**. In addition, the application of phenyl-substituted alkyne-amine **S2** leads to single enamine **E3**. Accordingly, the single auro-iminium salt **Au4** was observed as a resting state (Scheme 4).

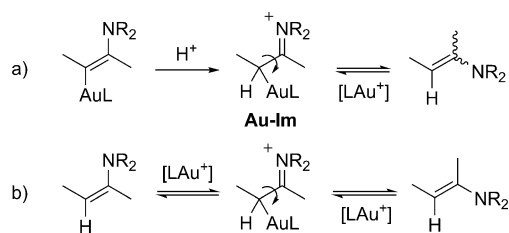
In the next step the mechanism of the formation of the auro-iminium salt was analyzed. Since the 5-endo-dig cyclization cannot be triggered by a proton, we hypothesized that the auro-iminium salt **Au1** forms as a result of the protonation of vinyl-gold complex **B1**, which itself is undetectable because of its very high affinity to protonation (Scheme 5). Indeed, attempts to deprotonate **Au2** to generate *exo*-vinyl-gold failed, suggesting that this species is highly basic (and definitely more basic than simple enamines). To confirm the vinyl-gold complex as an essential organo-gold intermediate, we studied substrate **S3** having a sulfonamide functionality to



Scheme 5. Origin of auro-iminium. Confirmation of the intermediacy of vinyl-gold.

reduce the basicity of the relevant species. When **S3** was treated with 1,8-bis(dimethylamino)naphthalene (PrSp) and catalyst **2**, the diaurated species **D2** was generated as the single organo-gold product. Upon treatment with K₂CO₃, Me₂S, or picoline, **D2** readily gives rise to **B2** (Scheme 5). In addition, diaurated species were found in the aforementioned reaction of **S1** with catalyst **1** (**D1**, Scheme 2). Even though **B1** or **B2** cannot be directly observed under normal catalytic conditions, the formation of the diaurated species confirms that vinyl-gold indeed has to be an intermediate of the hydroamination process, because diaurated species are known to be the product of trapping vinyl-gold intermediates with an LAu⁺ unit.^[13,9] Correspondingly, the auro-iminium salt is considered to be the product of protonation of the vinyl-gold species.

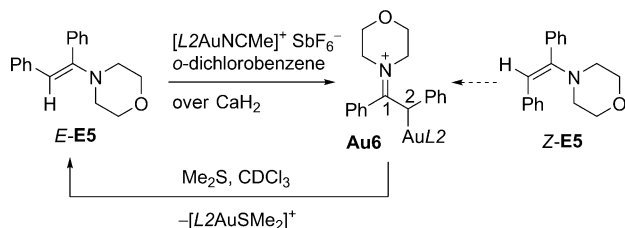
After the work of Bertrand and co-workers,^[7] these observations further confirm the outer sphere mechanism at least for intramolecular gold-catalyzed hydroamination reactions since the formation of vinyl-gold complex **B** as an essential intermediate is simply not possible by an inner sphere mechanism. However, there is no reason to assume the mechanism to be different for the intermolecular version.^[14] So far, the stereochemical outcome of the intermolecular hydroamination reaction as described by Stradiotto and co-workers^[3a] was the only experimental evidence which was seemingly inconsistent with the outer sphere mechanism. However, from now on with the knowledge of the nature of auro-iminium salts, it is possible to correctly explain these experimental results also with regard to this mechanism. Thus, even though the *anti*-addition of an amine onto a gold-alkyne complex would lead to vinyl-gold in a stereospecific manner, this stereochemical information is completely lost upon formation of the conformationally flexible auro-iminium salt **Au-Im**, which makes the overall protodeauration process no longer stereospecific, unlike it is generally considered for other vinyl-gold species (Scheme 6a). It is clear, that via **Au-Im**, gold will also catalyze the isomerization of one geometrical isomer of an enamine into another until the thermodynamic equilibrium is reached, regardless of the exact stereochemical outcome of the ligand exchange itself (Scheme 6b).^[15] Likewise, the isomerization of enamines will additionally occur through the classical protonation/deprotonation pathway promoted by traces of Brønsted acid in the reaction mixture. In literature, the *E*-enamine is known to be thermodynamically more stable than the *Z*-enamine, and this simple fact explains the selective formation of *E*-enamine in the reaction described by Stradiotto and co-workers.^[16] The



Scheme 6. a) Loss of stereoselectivity due to protodeauration and b) isomerization of enamines through auro-iminium salt **Au-Im**.

overall stereochemical outcome of the reaction is thus determined solely by the thermodynamics of the final enamines. With this explanation, the consensus is reached that gold-catalyzed hydroamination reactions should be described by the outer sphere mechanism, same as other hydrofunctionalization reactions of alkynes.^[17]

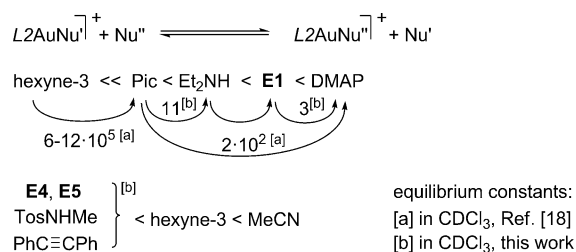
To confirm this conclusion experimentally, we generated auro-iminium salt **Au6** from the corresponding *E*-**E5**. The ¹H NMR spectrum of **Au6** exhibits a similar temperature dependence as was described above for **Au2**, confirming the rotation around the C1–C2 bond (see the Supporting Information). Addition of Me₂S to a solution of **Au6** regenerates *E*-**E5** with > 95% stereoselectivity, Scheme 7.



Scheme 7. Preparation of an enriched sample of **Au6** and its conversion back to *E*-**E5**.

The fast rotation of the C1–C2 bond in **Au6** implies that the formation of this compound is independent of the initial geometric configuration of the double bond at the enamine. Therefore, the same compound would be formed from the corresponding *Z*-isomer of **E5**. This argument together with the stereoselective regeneration of *E*-**E5** from **Au6** confirms the mechanism of enamine isomerization which is proposed in Scheme 6 and that our explanation of the stereochemical outcome of the intermolecular hydroamination reaction is consistent with the outer sphere mechanism.

To gain a deeper understanding of the course of the hydroamination process, we determined the binding affinity of the L₂Au⁺ unit to representative neutral compounds using the ligand exchange with auxiliary nucleophiles with known binding affinities (Scheme 8).^[18] From the ligand strength series it is clear that simple alkyl amines and alkyl enamines would be ≳ 10⁵ stronger ligands than the alkyne substrate. Not surprisingly, [LAu(amine)]⁺ complexes were previously as well as in our research observed as resting states. It appears that the ligand exchange equilibrium strongly disfavors the formation of the activated gold–alkyne complex **A**. This is the principal reason why hydroamination reactions often require



Scheme 8. Binding affinity scale for L₂Au⁺ (pic = 4-picoline).

elevated temperature. However, the situation improves significantly when amide substrates with a reduced binding affinity to gold are used. For example, the reaction of **S3** takes only a few minutes (or less), whereas the reaction of **S1** requires many hours (Schemes 5 and 2). The same accounts for the reactivity series established by Tanaka and co-workers (anilines with electron-deficient substituents react faster).^[3b]

In summary, the gold-catalyzed hydroamination reaction is described by the outer sphere mechanism which is also the case for other hydrofunctionalization reactions of alkynes. The process includes the formation of gold–enamine complexes as intermediates. These complexes exhibit a loss of the double bond character, which enables an easy rotation around the C–CAu bond, and therefore they are viewed as auro-iminium salts. Because of the rotation, the liberation of an enamine from the auro-iminium salt upon ligand exchange is not stereospecific. This is responsible for the fact that the protodeauration of enamine-derived vinyl–gold complexes **B** is not stereospecific, thereby constituting the fundamental difference from other protodeaurations known to occur with retention of the configuration at the double bond.^[19] Via intermediate auro-iminium salts, gold will also catalyze the isomerization of one geometrical isomer of an enamine into the other until the thermodynamical equilibrium is reached. Furthermore, the positional rearrangement of the enamine double bond can occur as a Brønsted-acid-catalyzed process. It can be concluded, that the gold-catalyzed hydroamination reaction yields enamines as a thermodynamically controlled mixture of isomers and can only be selective if the dominant isomer is considerably more stable than the other. The overall mechanism of the gold-catalyzed hydroamination reaction appears to be similar to hydroamination reactions catalyzed by other transition metals (e.g. palladium(II)^[20] and iridium(III)^[21]).

Received: February 18, 2014

Revised: April 7, 2014

Published online: June 12, 2014

Keywords: gold catalysis · hydroamination · reaction mechanisms

- [1] For general reviews about the hydroamination reaction of multiple bonds, see: a) T. E. Müller, M. Beller, *Chem. Rev.* **1998**, *98*, 675–703; b) T. E. Müller, K. C. Hultsch, M. Yus, F. Foubelo, M. Tada, *Chem. Rev.* **2008**, *108*, 3795–3892; c) R. A. Widenhoefer, X. Han, *Eur. J. Org. Chem.* **2006**, 4555–4563.
- [2] a) Y. Fukuda, K. Utimoto, H. Nozaki, *Heterocycles* **1987**, *25*, 297–300; b) Y. Fukuda, K. Utimoto, *Synthesis* **1991**, 975–978.
- [3] a) K. D. Hesp, M. Stradiotto, *J. Am. Chem. Soc.* **2010**, *132*, 18026–18029; b) E. Mizushima, T. Hayashi, M. Tanaka, *Org. Lett.* **2003**, *5*, 3349–3352; c) J.-E. Kang, H.-B. Kim, J.-W. Lee, S. Shin, *Org. Lett.* **2006**, *8*, 3537–3540; d) S. L. Crawley, R. L. Funk, *Org. Lett.* **2006**, *8*, 3995–3998; e) Y. Zhang, J. P. Donahue, C.-J. Li, *Org. Lett.* **2007**, *9*, 627–630; f) L.-A. Schaper, X. Wei, S. J. Hock, A. Pöthig, K. Öfele, M. Cokoja, W. A. Herrmann, F. E. Kühn, *Organometallics* **2013**, *32*, 3376–3384; g) V. Lavallo, J. H. Wright, F. S. Tham, S. Quinlivan, *Angew. Chem.* **2013**, *125*, 3254–3258; *Angew. Chem. Int. Ed.* **2013**, *52*, 3172–3176.

- [4] Addition of hydrazine: R. Kinjo, B. Donnadieu, G. Bertrand, *Angew. Chem.* **2011**, *123*, 5674–5677; *Angew. Chem. Int. Ed.* **2011**, *50*, 5560–5563.
- [5] a) H. Wu, Y. P. He, L. Z. Gong, *Adv. Synth. Catal.* **2012**, *354*, 975–980; b) Y.-P. He, H. Wu, D.-F. Chen, J. Yu, L.-Z. Gong, *Chem. Eur. J.* **2013**, *19*, 5232–5237; c) S. Fleischer, S. Werkmeister, S. Zhou, K. Junge, M. Beller, *Chem. Eur. J.* **2012**, *18*, 9005–9010; d) X.-Y. Liu, C.-M. Che, *Org. Lett.* **2009**, *11*, 4204–4207; e) P. P. Sharp, M. G. Banwell, J. Renner, K. Lohmann, A. C. Willis, *Org. Lett.* **2013**, *15*, 2616–2619; f) X. Chen, H. Chen, X. Ji, H. Jiang, Z.-J. Yao, H. Liu, *Org. Lett.* **2013**, *15*, 1846–1849; g) J. Han, B. Xu, G. B. Hammond, *Org. Lett.* **2011**, *13*, 3450–3453; h) J. Han, B. Xu, G. B. Hammond, *J. Am. Chem. Soc.* **2010**, *132*, 916; i) X. Wang, Z. Yao, S. Dong, F. Wei, H. Wang, Z. Xu, *Org. Lett.* **2013**, *15*, 2234–2237; j) X. Wang, S. Dong, Z. Yao, L. Feng, P. Daka, H. Wang, Z. Xu, *Org. Lett.* **2014**, *16*, 22–25.
- [6] a) V. Lavallo, G. D. Frey, B. Donnadieu, M. Soleilhavoup, G. Bertrand, *Angew. Chem.* **2008**, *120*, 5302–5306; *Angew. Chem. Int. Ed.* **2008**, *47*, 5224–5228; b) N. Nishina, Y. Yamamoto, *Angew. Chem.* **2006**, *118*, 3392–3395; *Angew. Chem. Int. Ed.* **2006**, *45*, 3314–3317.
- [7] X. Zeng, R. Kinjo, B. Donnadieu, G. Bertrand, *Angew. Chem.* **2010**, *122*, 954–957; *Angew. Chem. Int. Ed.* **2010**, *49*, 942–945.
- [8] A. S. K. Hashmi, T. D. Ramamurthi, F. Rominger, *Adv. Synth. Catal.* **2010**, *352*, 971–975.
- [9] a) A. Zhdanko, M. E. Maier, *Chem. Eur. J.* **2013**, *19*, 3932–3942; b) A. Zhdanko, M. E. Maier, *Organometallics* **2013**, *32*, 2000–2006; c) A. Zhdanko, M. E. Maier, *Chem. Eur. J.* **2014**, *20*, 1918–1930.
- [10] The ratio of enamines cannot be accurately established due to the broad signals in the spectrum, which are presumably caused by the fast isomerization rate. However, the ratio was easily measured in another experiment performed at a lower concentration (Scheme 3). Isomerization of *endo*-enamine to *exo*-enamine is catalyzed by acid but not by gold, as proven in the Supporting Information.
- [11] a) For enol ether complexes, see: Y. Zhu, C. S. Day, A. C. Jones, *Organometallics* **2012**, *31*, 7332–7335; b) For ene-1,1-diamine complexes, see: A. Fürstner, M. Alcarazo, R. Goddard, C. W. Lehmann, *Angew. Chem.* **2008**, *120*, 3254–3258; *Angew. Chem. Int. Ed.* **2008**, *47*, 3210–3214.
- [12] In contrast to the enamine, **S1** is predominantly not protonated in the presence of PrSpH⁺. In the presence of a stronger acid (*t*Bu₂PyH⁺) both, enamine and **S1**, are protonated and the reaction is even slower because of the deactivation of the amine as a nucleophile.
- [13] a) D. Weber, M. A. Tarselli, M. R. Gagne, *Angew. Chem.* **2009**, *121*, 5843–5846; *Angew. Chem. Int. Ed.* **2009**, *48*, 5733–5736; b) G. Seidel, C. W. Lehmann, A. Fürstner, *Angew. Chem.* **2010**, *122*, 8644–8648; *Angew. Chem. Int. Ed.* **2010**, *49*, 8466–8470.
- [14] Being unable to confirm this statement experimentally, we appeal to the fact that both inter- and intramolecular hydroalkoxylation of alkynes occur through the same outer sphere mechanism. Furthermore, it is generally accepted that the addition of a nucleophile onto an activated gold–alkyne complex leads to the *anti*-adduct.
- [15] It is possible that the ligand exchange gives the geometrical isomers of enamines in a ratio different from the ratio of the enamines at thermodynamic equilibrium.
- [16] M. E. Munk, Y. K. Kim, *J. Org. Chem.* **1965**, *30*, 3705–3710.
- [17] The hypothetical tricoordinate species **T** (Scheme 1), the key intermediate of the inner sphere mechanism, is only accepted as intermediate or transition state of a ligand exchange at gold, which is commonly known to proceed through an associative S_N2 mechanism. See: a) T. J. Brown, M. G. Dickens, R. A. Widenhoefer, *Chem. Commun.* **2009**, 6451–6453; b) T. J. Brown, M. G. Dickens, R. A. Widenhoefer, *J. Am. Chem. Soc.* **2009**, *131*, 6350–6351.
- [18] A. Zhdanko, M. Ströbele, M. E. Maier, *Chem. Eur. J.* **2012**, *18*, 14732–14744.
- [19] A. S. K. Hashmi, *Angew. Chem.* **2010**, *122*, 5360–5369; *Angew. Chem. Int. Ed.* **2010**, *49*, 5232–5241.
- [20] a) T. E. Müller, M. Grosche, E. Herdtweck, A.-K. Pleier, E. Walter, Y.-K. Yan, *Organometallics* **2000**, *19*, 170–183; b) T. E. Müller, M. Berger, M. Grosche, E. Herdtweck, F. P. Schmidtchen, *Organometallics* **2001**, *20*, 4384–4393.
- [21] X. Li, A. R. Chianese, T. Vogel, R. H. Crabtree, *Org. Lett.* **2005**, *7*, 5437–5440.

Paper 8

For the Section 6.3.3.

Counterion Effects

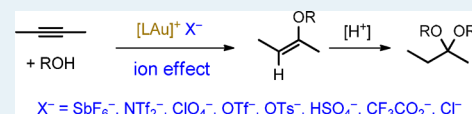
Explanation of Counterion Effects in Gold(I)-Catalyzed Hydroalkoxylation of Alkynes

Alexander Zhdanko* and Martin E. Maier*

Institut für Organische Chemie, Universität Tübingen, Auf der Morgenstelle 18, 72076 Tübingen, Germany

S Supporting Information

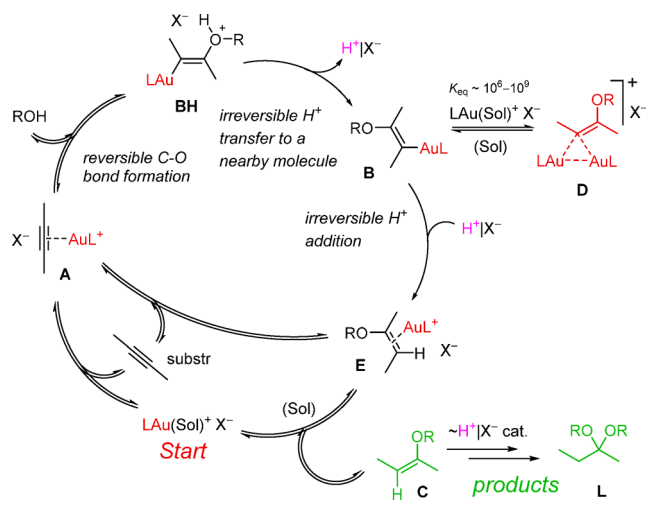
ABSTRACT: Using gold(I)-catalyzed hydroalkoxylation of alkynes as a model reaction with a well-known mechanism, a systematic experimental study was conducted to disclose the influence of the counterion X^- of a gold catalyst $LAuNCMe^+ X^-$ on every step of the catalytic cycle. The overall ion effect is determined as a superposition of several effects, operating on different steps of the reaction mechanism. All effects were explained from a position of hydrogen bonding, coordination chemistry at gold, and affinity for a proton.



KEYWORDS: gold catalysis, hydroalkoxylation, counterion effect, kinetics, reaction mechanism

Hydroalkoxylation of alkynes catalyzed by cationic gold(I) complexes was first described 15 years ago at the dawn of the era of homogeneous gold catalysis.^{1,2} However, only recently has the mechanism of this fundamental reaction been systematically investigated using experimental approaches, yielding a high level of understanding of the process (Scheme 1).³ Thus, the reaction starts from reversible *anti* addition of an

Scheme 1. Mechanism of Gold-Catalyzed Hydroalkoxylation



alcohol onto alkyne gold π -complex **A** to form a highly unstable adduct **BH** that quickly undergoes proton transfer to give vinyl gold **B**. Subsequently, **B** undergoes protonation by the previously released acid to form enol ether π -complex **E** that participates in global ligand exchange equilibrium, releasing product **C**. Competitively, **B** undergoes reversible addition of a second LAu^+ unit to form diaurated species **D**. Depending on the level of acidity in the system, **C** may stay as the end product or further transform into acetal **L** by means of a classical

Brønsted acid catalysis. All cationic species are accompanied by a counterion X^- .

Cationic gold(I) complexes of general composition $[LAu(Sol)]^+ X^-$ are the most frequently used type of catalysts for gold-mediated transformations of alkynes. They are typically applied with various anions (most often $X^- = SbF_6^-, NTf_2^-,$ and OTf^-). The dependence of a reaction from the counterion (the counterion effect) is well-documented in many papers on gold catalysis methodology, but the mechanism by which the anion actually influences the process is still largely unknown.⁴ An impressive example, highlighting the importance of a counterion, has been reported by Toste and co-workers. They showed that high enantioselectivity in gold-catalyzed reactions can be simply achieved using a catalyst with a chiral counterion.⁵ Specific investigations into the counterion effects are scarce and mostly based on theoretical methods.⁶ A nuclear magnetic resonance (NMR) investigation revealed that the prevalent position of a counterion within ion pairs is dependent on the ligands at gold.^{7,8} This finding suggests that the strength of the ion effect may be dependent on the ligand at gold. In particular, the counterion effect has never been explained properly for hydroalkoxylation.^{1b} Herein, using gold(I)-catalyzed hydroalkoxylation of alkynes as a model reaction with a well-established mechanism, we provide a systematic experimental study to disclose the role of counterion X^- on every step of the reaction mechanism.

To understand the ion effect, we conducted kinetic studies by NMR. In every such experiment, we monitored the disappearance of the substrate with time, the presence of organic intermediates, and the development of final products. Besides this, particular attention was given to observations of catalytic organogold intermediates (resting states) *in situ* during the whole process. Because of space limitations, complete

Received: April 4, 2014

Revised: July 9, 2014

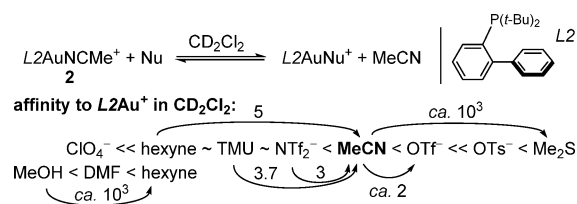
Published: July 10, 2014

tables, diagrams, explanations at a more narrow level, and spectra are given in the Supporting Information.

Gold-catalyzed hydroalkoxylation can be performed in a wide range of solvents: aprotic ones (CH_2Cl_2 , toluene, and dioxane) or an alcohol (MeOH). The occurrence and strength of the ion effect will thus depend on the nature of the solvent. We performed the whole study in CD_2Cl_2 because ion pair effects are quite pronounced in this solvent because of its weak solvation ability.⁹ At the same time, ionic components are sufficiently soluble in this solvent. Thereafter, we performed a control study in CD_3OD to demonstrate that all ion effects disappear in this highly polar solvent with strong solvation ability. As starting materials for the preparation of catalytic systems, we used $[\text{Ph}_3\text{PAuNCMe}]^+ \text{SbF}_6^-$ (catalyst 1) and $[\text{L2AuNCMe}]^+ \text{SbF}_6^-$ (catalyst 2) [$\text{L2} = o$ -(di-*tert*-butylphosphino)-biphenyl].

Prior to discussion of the ion effects, we studied simple ligand exchange and proton exchange processes. This was done as in our previous publication on coordination chemistry.¹⁰ Thus, we performed reactions of 2 with various anions as well as some neutral molecules in CD_2Cl_2 . Upon direct NMR observation, we have built affinity scales for L2Au^+ (Scheme 2).

Scheme 2. Ligand Exchange Equilibria and Affinity Scale in CD_2Cl_2



These experiments are described in the Supporting Information. According to this scheme, anions SbF_6^- and ClO_4^- can be regarded as very little-coordinating to LAu^+ , NTf_2^- and OTf^- as weakly nucleophilic, and OTs^- as a rather nucleophilic anion. Thus, displacement of OTs^- from LAuOTs by an alkyne substrate is difficult, preventing formation of π -alkyne complex **A**, the necessary intermediate of the catalytic cycle. We can conclude that application of a more nucleophilic anion like carboxylate will further prevent formation of **A** (generally in an aprotic solvent like CD_2Cl_2).

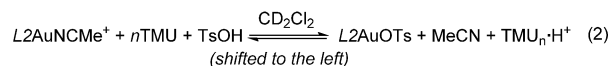
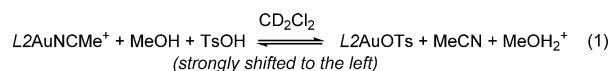
To approximately determine a binding affinity scale to H^+ for our study in CD_2Cl_2 , we conducted experiments with TfOH, the strongest acid available to us in a pure state. As described for benzene and CDCl_3 in the literature,¹¹ simple addition of a small amount TfOH (~ 1 mg) to CD_2Cl_2 upon making an NMR sample caused immediate formation of an emulsion, which is ascribed to protonation of residual water in the solvent. The ^1H and ^{19}F NMR spectra of the emulsion showed several signals. To prepare a clear anhydrous solution of TfOH, a larger amount of the acid (~ 50 mg) was mixed with CD_2Cl_2 (~ 0.8 mL) and allowed to settle. The clear CD_2Cl_2 phase was taken for analysis. An NMR spectrum of this solution showed a single ^{19}F resonance at -76.41 ppm and a single ^1H resonance at 9.21 ppm. Addition of a small amount of $\text{CF}_3\text{CH}_2\text{OH}$ allowed us to establish the ratio of H^+ and OTf^- residues through a combination of ^1H and ^{19}F NMR spectra and to confirm the existence of at least 95% pure, water free TfOH in the initial binary TfOH/ CD_2Cl_2 solution. Presumably, TfOH exists in such a solution as an undissociated molecule, waiting

to protonate anything that would be added. Thus, addition of MeOH to the clear extract immediately gives a heavy emulsion, which is ascribed to the formation of a less soluble $\text{ROH}_2^+ \text{OTf}^-$ salt, forming the new polar liquid phase.

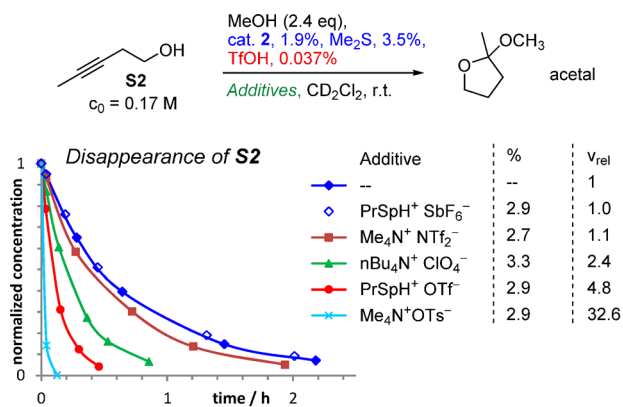
On the other hand, addition of MeOH (6.5 equiv) to a slight emulsion prepared by addition of TfOH (< 1 mg) to an undried CD_2Cl_2 sample (0.5 mL) gives a clear solution. Obviously, the initial polar phase was dissolved with the help of excess MeOH. The ^{19}F resonance in this solution appears at -79.07 ppm, which now corresponds to the OTf^- ion (see the Supporting Information for more details), confirming dissociation of TfOH by MeOH. Because HSbF_6 , HNTf_2 , HClO_4 , and TfOH are all regarded as super acids,¹² they all will protonate an alcohol so the proton will exist in solution as an $\text{ROH}_2^+ \text{X}^-$ oxonium ion pair. In contrast, TsOH was shown not to dissociate in CD_2Cl_2 even in the presence of MeOH. Interestingly, even $[\text{L2AuNCMe}]^+$ does not trigger dissociation of TsOH in the presence of MeOH (neutral $[\text{LAuOTs}]$ would be formed), but partial dissociation occurs in the presence of TMU (tetramethylurea) as a weak base (eqs 1 and 2). The last fact points to the higher strength of $\text{TMU}\cdot\text{H}^+$ versus that of TsOH as an acid in CD_2Cl_2 . The proton affinity scale was built upon these observations (Scheme 3).

Scheme 3. Proton Exchange Equilibria and Affinity Scale in CD_2Cl_2

affinity to H^+ in CD_2Cl_2 : (SbF_6^- , NTf_2^- , ClO_4^- , OTf^-) $<$ MeOH $<$ TMU $<$ OTs^-



The aforementioned basic observations should help us to unambiguously determine the origin of the counterion effect. Because the counterion effect may apply at every step that includes ionic species, the overall effect on the entire reaction may be difficult to understand because of the superposition of the effects. It is therefore important to study the counterion effect under properly selected conditions, excluding the situation with multiple effects. It is convenient first to describe and explain the effects for a reaction in which the transition from **A** to **B** is rate-limiting, because for such a reaction type there is no need to consider diaurated species **D** and protodeauration. A suitable case is the reaction of hexyne **S1** with MeOH catalyzed by 2 ($[\text{L2AuNCMe}]^+ \text{SbF}_6^-$) in CD_2Cl_2 , which was previously shown to fit these requirements.^{3b} Now this reaction was conducted in the presence of various salts and neutral additives (Scheme 4). In all runs, except entries 8 and 9 (OTs^-), gold predominantly existed as $[\text{L2Au}(\text{S1})]^+$ (**A1**) (^{31}P , δ 65.6 ppm) and the reactions exhibited the apparent “half-order” kinetics in substrate. Obviously, all additives in these cases, being very weak ligands, did not lead to substantial changes in the global equilibrium. This circumstance allows us to assign the observed overall effect to a single effect acting exclusively at the stage of alcohol addition on complex **A1**. However, in the two experiments with OTs^- , gold predominantly existed as $[\text{L2AuOTs}]$ (^{31}P , δ 56.6 ppm). This is obviously because of the higher binding affinity of OTs^- for gold, which now shifts the global equilibrium entirely to $[\text{L2AuOTs}]$, establishing an $[\text{L2AuOTs}]/\text{OTs}^-$ auro buffer system. Correspondingly, the kinetics of the reaction entirely

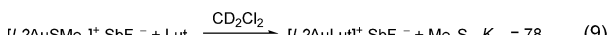
Scheme 6. Ion Effects in CD₂Cl₂

Explanation of the ion effect:

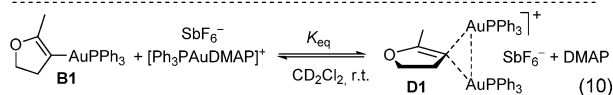


molecule available for hydrogen bonding within the internal ion pair.

To confirm this hypothesis, we conducted a model study to determine if counterions may influence simple ligand exchange equilibria between various [LAuNu]⁺ cationic species. Thus, model equilibria (eqs 9 and 10, in which Lut = 2,6-lutidine) were found to be rather independent, but the equilibrium with dimethylaminoethanol (eq 11) appeared to be obviously dependent on the counterion (Scheme 7). This result nicely

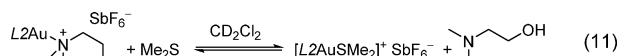
Scheme 7. Ion Effects on Ligand Exchange Equilibria in CD₂Cl₂

no ion effect upon addition of OTf⁻ and OTs⁻



| Additive | K _{eq} |
|---|-----------------|
| no | 59 |
| nBu ₄ N ⁺ ClO ₄ ⁻ (2.2 equiv) | 58.3 |
| Me ₄ N ⁺ OTs ⁻ (3.3 equiv) | 66 |

(No or weak ion effects)

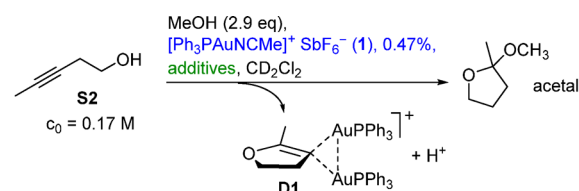


significant ion effect upon addition of OTf⁻ and OTs⁻ (K_{eq} reduces from 5 till 1.6)
stabilization of ion pairs through hydrogen bonding
SbF₆⁻ < OTf⁻ < OTs⁻

demonstrates that simple equilibria should be generally unaffected by the counterion unless some specific interaction becomes possible within the ion pairs. Presumably, the presence of a hydrogen bond donor (OH group) in dimethylaminoethanol does indeed provide substantial stabilization of ion pairs increasingly as the basicity of the counterion increases (eq 11). We can conclude that the equilibrium (eq 5) must also depend on the counterion (although it is always shifted to the left). It becomes clear that the strong counterion

effect in the reaction of Scheme 6 consists of two cumulative effects: enhanced formation of A by stabilization of the A|X⁻ ion pair through hydrogen bonding and, at the same time, enhanced reactivity of the alcohol toward the intramolecular attack (Scheme 6, bottom).

With these explanations in hand, we are ready to explain the ion effects for a more complicated system, a reaction accompanied by the complete formation of diaurated species. A suitable reaction is the cyclization of pentynol S2 catalyzed by 1 ([Ph₃PAuNCMe]⁺ SbF₆⁻) in CD₂Cl₂ in the presence of MeOH. As shown in our previous work, this reaction is characterized by immediate and complete formation of the off-cycle diaurated species D1, correspondingly releasing an equal amount of H⁺.^{3b} The overall reaction is half-order in substrate, half-order in D1, and half-order in H⁺ (being always dependent on acidity regardless of whether protodeauration is the rate-limiting step of the catalytic cycle).^{3b} Therefore, not only the aforementioned ion effects but also the effects associated with the reactivity of H⁺ are expected here. In the work presented here, this reaction was repeated in the presence of various salts and neutral additives (Scheme 8). Rather in contrast with the

Scheme 8. Ion Effects in CD₂Cl₂

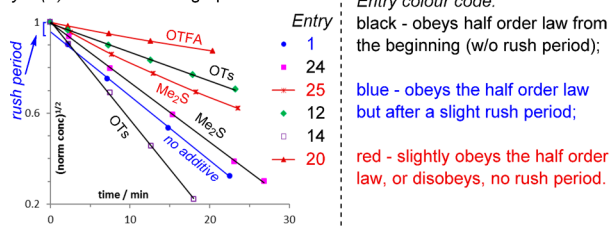
$$\text{Rate law: } \frac{d[S2]}{dt} = -k[S2]^{1/2}[D1]^{1/2}[H^+]^{1/2} = -k_{\text{eff}}[S2]^{1/2} \quad (\text{half order law})$$

Resting state: only D1 in all, except entries 20, 21, 25, 26, 27

D1 + [Ph₃PAuOTFA]⁺ in entries 20, 21

D1 + [Ph₃PAuSMe₂]⁺ in entries 25, 26, 27

y = (S)^{1/2} = -kt + const graphs:



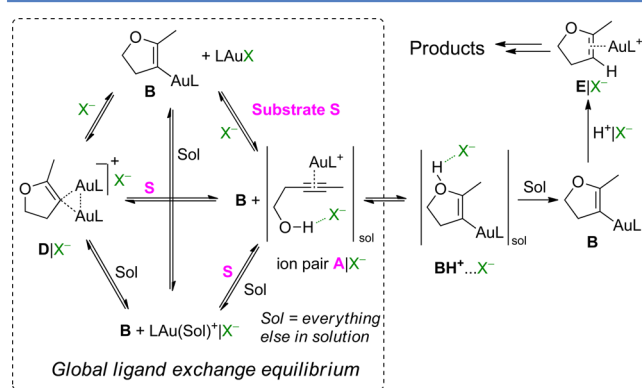
| Additive | % | V _{rel} | Additive | % | V _{rel} |
|----------|---|------------------|----------|----------------------------------|--------------------|
| 1 | no | 1 | 22 | ArCO ₂ H ^a | 0.93 |
| 2 | PrSpH ⁺ SbF ₆ ⁻ | 0.53 | 23 | Me ₂ S | 0.08 |
| 3 | Me ₄ N ⁺ NTf ₂ ⁻ | 0.55 | 24 | " | 0.11 |
| 4 | nBu ₄ N ⁺ ClO ₄ ⁻ | 0.90 | 25 | " | 0.34 |
| 5 | " | 1.16 | 26 | " | 0.57 |
| 6 | " | 2 | 27 | " | 0.8 |
| 7 | " | 2.17 | 28 | MeOH | (3) ^b |
| 8 | PrSpH ⁺ OTf ⁻ | 0.35 | 29 | " | (3.1) ^b |
| 9 | " | 0.4 | 30 | " | (4.1) ^b |
| 10 | " | 0.42 | 31 | " | (7.1) ^b |
| 11 | " | 2.42 | 32 | " | (8.6) ^b |
| 12 | PrSpH ⁺ OTs ⁻ | 0.24 | 33 | " | (12) ^b |
| 13 | " | 0.54 | 34 | TMU | 2 |
| 14 | " | 1.1 | 35 | " | 7.9 |
| 15 | " | 2.07 | 36 | DMF | 2.8 |
| 16 | PrSpH ⁺ OMs ⁻ | 0.2 | 37 | " | 4.1 |
| 17 | " | 0.8 | 38 | PhOH | (7.4) ^c |
| 18 | " | 1.6 | | | |
| 19 | nBu ₄ N ⁺ HSO ₄ ⁻ | 0.9 | | | |
| 20 | PrSpH ⁺ OTFA ⁻ | 0.33 | | | |
| 21 | " | 0.67 | | | |

^a 4-nitrobenzoic acid,

^b total amount of MeOH, equiv

^c amount of PhOH, equiv

previous reactions, weak negative effects were noted here, increasing in the following order: $\text{SbF}_6^- < \text{NTf}_2^- < \text{ClO}_4^- < \text{OTf}^-$ (Scheme 8, entries 1–11). This indicates that the positive ion effect operating at the alcohol addition stage was overridden by some negative effect. The origin of the negative part is definitely not associated with a change in the equilibrium toward **A** [see the global ligand exchange equilibrium in Figure 1 (because, as we know from the previous paragraph, this effect



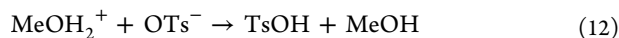
General ion effects:

- 1) hydrogen bonding of ROH to X^- will enhance every equilibrium with alkynol **S** to the side of **A**. Besides that, there is no ion effect on any simple ligand exchange equilibria (not to confuse with binding of LAu^+ by X^- to form LAuX);
- 2) nucleophilicity of X^- enhances formation of LAuX (which should be avoided)
- 3) hydrogen bonding of ROH to X^- will enhance reactivity of **A** towards alcohol addition (valid for intra- and intermolecular alcohol addition);
- 4) solvation of H^+ with X^- will decrease reactivity of acid for protodeauration of **B**. Also any other parallel Brønsted acid catalyzed processes will be affected.

Figure 1. General ion effects.

should also be positive)]. Because the overall process was demonstrated to be always dependent on acidity (the aforementioned half-order in H^+), it is now the only possibility to associate the negative effect with the reduced reactivity of the acid. The predominant acid under these conditions will be an ROH_2^+X^- oxonium ion pair (for $\text{X}^- = \text{SbF}_6^-, \text{NTf}_2^-, \text{ClO}_4^-,$ or OTf^-), or neutral acid in the case of TsOH . In the case of the oxonium ion pair, we suggest that the reactivity of this ion pair should decrease as the affinity of the anion for a proton increases (to form a hydrogen bond). In other words, H^+ is better solvated and less reactive in the presence of a more basic anion. This provides a logical explanation for why the more nucleophilic anions led to retardation of the reaction.

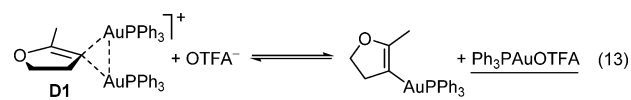
The behavior of OTs^- deserves special consideration (entries 12–15). Thus, if OTs^- is present in a small amount [~ 0.5 equiv to gold (entry 12)], it causes a negative effect. This is associated with quantitative quenching of $\text{MeOH}_2^+\text{X}^-$ pairs to form a neutral molecule of TsOH , which is a weak acid in comparison to $\text{MeOH}_2^+\text{X}^-$ ion pairs (eq 12).



Therefore, as all MeOH_2^+ is titrated, there is no more OTs^- left in solution, and the catalytic system is equivalent to **D1** $\text{SbF}_6^- + \text{TsOH}$ in a 1:1 ratio. Next, if more OTs^- is added, the overall effect becomes positive (entries 13–15). Now an excess of OTs^- is present in solution (together with neutral TsOH).

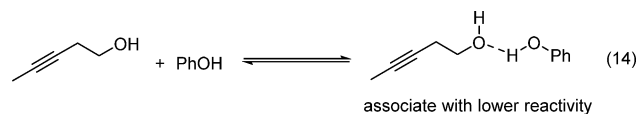
As we already know, OTs^- possesses a huge positive effect, which now overrides the negative effect of the reduced acidity. The same explanations apply for OMs^- and HSO_4^- (entries 16–18 and 19, respectively).

Application of a more basic OTFA^- anion causes a substantial negative effect (entries 20 and 21), which is associated with its higher affinity for both gold and a proton. It binds a proton to form a weak acid TFA , and its high binding affinity for gold inhibits the reaction so that even **D1** is not completely formed, leaving the rest of gold to stay as $\text{Ph}_3\text{PAuOTFA}$ (eq 13). A similar equilibrium accounts for the



decrease in rate upon addition of neutral nucleophile Me_2S [to increasingly form $[\text{Ph}_3\text{PAuSMe}_2]^+$ as the amount of Me_2S increases (entries 23–27)]. We can conclude that highly nucleophilic anions are not beneficial for gold catalysis even though they would exhibit a high level of activation of the alcohol toward addition into the AlX^- ion pair simply because the ligand exchange equilibrium for forming this pair is too small.

Like anions, neutral weak bases TMU and DMF also exhibited a substantial negative effect (entries 34–37). Because they are known to exhibit a positive effect on the alcohol addition step,^{3b} the negative effect associated with their basicity obviously overrides the positive effect. MeOH exhibited no notable effect, which suggests that positive and negative effects were equal (entries 28–33). Addition of a hydrogen bond donor PhOH (entry 38) caused a negative effect, which is associated with alcohol deactivation (eq 14), as demonstrated in our previous study.^{3b}



In summary, the overall effect of an inert additive (be it an ionic salt or a neutral compound) is determined as a superposition of effects, which are different on different steps of the reaction mechanism (Figure 1).

To demonstrate that the aforementioned effects indeed are present within contact ion pairs, we conducted a small study in methanol. In this highly polar solvent, the salts would exist as freely solvated separate ions; therefore, most of the effects must disappear. Indeed, we found that catalytic hydroalkoxylation of **S2** in CD_3OD in the presence of catalyst **I** is not influenced by the presence of any weakly coordinating anions [$\text{SbF}_6^-, \text{NTf}_2^-, \text{ClO}_4^-, \text{OTf}^-$, or OTs^- (Supporting Information)]. However, strong inhibition is observed if the anion possesses a higher affinity for LAu^+ (Cl^-) or H^+ (CF_3CO_2^-). In the case of Cl^- , the catalyst is stoichiometrically transformed into LAuCl and the catalytic reaction becomes strongly inhibited. In the case of CF_3CO_2^- , the catalyst is not inhibited, the diaurated species is still formed, but the whole reaction is inhibited because the active H^+ is bound to form weak acid $\text{CF}_3\text{CO}_2\text{H}$. This result can be easily generalized: weakly coordinating anions of strong acids (at least TsOH and stronger) will have no influence on gold catalysis in methanol, regardless of whether diaurated species are formed. These anions are weakly aurophilic, and

their conjugated acids are equally strong in methanol because of complete dissociation, providing equally efficient protodeauration.

In summary, various counterion effects were established in gold(I)-catalyzed hydroalkoxylation of alkynes. By hydrogen bonding with ROH, the counterion X^- facilitates the transition from **A** to **B** within AlX^- ion pairs in the following order: $SbF_6^- < NTf_2^- < ClO_4^- < OTf^- < OTs^-$. However, the use of anions with a higher affinity for gold should be avoided because they disfavor formation of AlX^- simply by binding gold into $LAuX$ (provided there are no stronger nucleophiles in the system and no diaurated species formed). We suggest OTf^- to be a good compromise for the majority of cases. Counterions X^- reduce the reactivity of H^+ in the following order: $SbF_6^- < NTf_2^- < ClO_4^- < OTf^- < OTs^-$ (reducing the rate of protodeauration). Counterions X^- negligibly influence (if at all) simple ligand exchange equilibria at cationic gold species, unless there is specific interaction arising within the ion pairs or unless the counterion itself binds the metal to form neutral $LAuX$ species. In summary, the overall ion effect is generally determined as a superposition of (at least) the aforementioned elementary effects.

■ ASSOCIATED CONTENT

📄 Supporting Information

Complete experimental procedures and detailed NMR spectra. This material is available free of charge via the Internet at <http://pubs.acs.org>.

■ AUTHOR INFORMATION

Corresponding Authors

*E-mail: vinceero@gmail.com.

*E-mail: martin.e.maier@uni-tuebingen.de.

Notes

The authors declare no competing financial interest.

■ ACKNOWLEDGMENTS

Financial support by the state of Baden-Württemberg is gratefully acknowledged. We thank Dr. K. Eichele and the Institut für Anorganische Chemie for allowing us to use the NMR spectrometer.

■ REFERENCES

(1) (a) Teles, J. H.; Brode, S.; Chabanas, M. *Angew. Chem., Int. Ed.* **1998**, *37*, 1415–1418. (b) For a recent review, see: Huguet, N.; Echavarren, A. M. Gold-Catalyzed O–H Bond Addition to Unsaturated Organic Molecules. In *Hydrofunctionalization, Topics in Organometallic Chemistry*; Ananikov, V. P., Tanaka, M., Eds.; Springer: Berlin, 2013; Vol. 43, pp 291–324. (2) For general reviews on gold catalysis, see: (a) Rudolph, M.; Hashmi, A. S. K. *Chem. Soc. Rev.* **2012**, *41*, 2448–2462. (b) Corma, A.; Leyva-Peréz, A.; Sabater, M. J. *Chem. Rev.* **2011**, *111*, 1657–1712. (c) Bandini, M. *Chem. Soc. Rev.* **2011**, *40*, 1358–1367. (d) Boorman, T. C.; Larrosa, I. *Chem. Soc. Rev.* **2011**, *40*, 1910–1925. (e) Hashmi, A. S. K.; Bührle, M. *Aldrichimica Acta* **2010**, *43*, 27. (f) Shapiro, N. D.; Toste, F. D. *Synlett* **2010**, 675–691. (g) Sengupta, S.; Shi, X. *ChemCatChem* **2010**, *2*, 609–619. (h) Bongers, N.; Krause, N. *Angew. Chem., Int. Ed.* **2008**, *47*, 2178–2181. (i) Gorin, D. J.; Sherry, B. D.; Toste, F. D. *Chem. Rev.* **2008**, *108*, 3351–3378. (j) Jiménez-Núñez, E.; Echavarren, A. M. *Chem. Rev.* **2008**, *108*, 3326–3350. (k) Li, Z.; Brouwer, C.; He, C. *Chem. Rev.* **2008**, *108*, 3239–3265. (l) Arcadi, A. *Chem. Rev.* **2008**, *108*, 3266–3325. (m) Muzart, J. *Tetrahedron* **2008**, *64*, 5815–5849. (n) Shen, H. C. *Tetrahedron* **2008**, *64*, 7847–7870. (o) Widenhoefer, R. A. *Chem.—Eur. J.* **2008**, *14*, 5382–5391.

(p) Gorin, D. J.; Toste, F. D. *Nature* **2007**, *446*, 395. (q) Fürstner, A.; Davies, P. W. *Angew. Chem., Int. Ed.* **2007**, *46*, 3410–3449. (r) Jiménez-Núñez, E.; Echavarren, A. M. *Chem. Commun.* **2007**, 333–346. (s) Hashmi, A. S. K. *Chem. Rev.* **2007**, *107*, 3180–3211. (t) Hashmi, A. S. K.; Hutchings, G. J. *Angew. Chem., Int. Ed.* **2006**, *45*, 7896–7936. (3) (a) Zhdanko, A.; Maier, M. E. *Chem.—Eur. J.* **2013**, *19*, 3932–3942. (b) Zhdanko, A.; Maier, M. E. *Chem.—Eur. J.* **2014**, *20*, 1918–1930. (4) (a) Davies, P. W.; Martin, N. *Org. Lett.* **2009**, *11*, 2293–2296. (b) Gupta, S.; Koley, D.; Ravikumar, K.; Kundu, B. *J. Org. Chem.* **2013**, *78*, 8624. (c) Brouwer, C.; He, C. *Angew. Chem., Int. Ed.* **2006**, *45*, 1744–1747. (d) Schelwies, M.; Dempwolff, A. L.; Rominger, F.; Helmchen, G. *Angew. Chem., Int. Ed.* **2007**, *46*, 5598–5601. (e) Zhang, Z.; Widenhoefer, R. A. *Org. Lett.* **2008**, *10*, 2079–2081. (5) Hamilton, G. L.; Kang, E. J.; Mba, M.; Toste, F. D. *Science* **2007**, *317*, 496–499. (6) (a) Bandini, M.; Bottoni, A.; Chiarucci, M.; Cera, G.; Miscione, G. P. *J. Am. Chem. Soc.* **2012**, *134*, 20690–20700. (b) Xia, Y.; Dudnik, A. S.; Gevorgyan, V.; Li, Y. *J. Am. Chem. Soc.* **2008**, *130*, 6940–6941. (c) Kovács, G.; Ujaque, G.; Lledós, A. *J. Am. Chem. Soc.* **2008**, *130*, 853–864. (7) Zuccaccia, D.; Belpassi, L.; Macchioni, A.; Tarantelli, F. *Eur. J. Inorg. Chem.* **2013**, 4121–4135. (8) (a) Zuccaccia, D.; Belpassi, L.; Tarantelli, F.; Macchioni, A. *J. Am. Chem. Soc.* **2009**, *131*, 3170–3171. (b) Zuccaccia, D.; Belpassi, L.; Rocchigiani, L.; Tarantelli, F.; Macchioni, A. *Inorg. Chem.* **2010**, *49*, 3080–3082. (9) Macchioni, A. *Chem. Rev.* **2005**, *105*, 2039–2074. (10) Zhdanko, A.; Ströbele, M.; Maier, M. E. *Chem.—Eur. J.* **2012**, *18*, 14732–14744. (11) Dang, T. T.; Boeck, F.; Hintermann, L. *J. Org. Chem.* **2011**, *76*, 9353–9361. (12) Kütt, A.; Rodima, T.; Saame, J.; Raamat, E.; Mäemets, V.; Kaljurand, I.; Koppel, I. A.; Garlyauskayte, R. Y.; Yagupolskii, Y. L.; Yagupolskii, L. M.; Bernhardt, E.; Willner, H.; Leito, I. *J. Org. Chem.* **2011**, *76*, 391–395.

Manuscript 9

For the Section 6.3.4.

Silver Effect

Explanation of "Silver Effect" on Gold(I) Catalyzed Hydroalkoxylation of Alkynes

Alexander Zhdanko,* Martin E. Maier*

Institut für Organische Chemie, Universität Tübingen, Auf der Morgenstelle 18, 72076 Tübingen, Germany

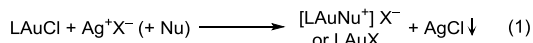
KEYWORDS: gold catalysis, hydroalkoxylation, silver effect, reaction kinetics, reaction mechanism

Supporting Information Placeholder

ABSTRACT: An extensive experimental NMR study of gold catalyzed hydroalkoxylation was conducted to explain the influence of a silver salt additive on the gold catalyzed process (silver effect). Addition of silver salt may have no, a negative or positive effect on gold catalyzed hydroalkoxylation. However, the silver was shown to be essentially innocent (plays no role) with regard to the mechanism of the catalytic process itself. The effect occurs only if silver induces variations of fraction of in-cycle organogold intermediates and H^+ . This is associated with formation of argento vinyl gold species **G** that was proved to be an off-cycle intermediate. This species is formed by trapping vinyl gold **B** with Ag^+ , the same way as diaurated species **D** (another possible off-cycle intermediate) is formed by trapping **B** with LAu^+ . If no **G** is formed, no variations of concentrations of in-cycle participants occur, and, as a consequence, no silver effect takes place. Furthermore, bringing together our results and the topical research of others, we introduced classification of silver effects, to put in order the confusion around interpretation of various erratic effects. The chemical sense of all these silver effects is single: a change (decrease or increase) of the fraction of the non-silver catalytic cycle participants. Ironically, in certain cases a silver effect is not at all "silver" in nature. It can be caused by the absence of MeCN that is secured by the use of $LAuCl/AgX$ system instead of a commercial $LAuNCMe^+X^-$ catalyst. Pertinent examples were discussed in detail. Correct interpretation of silver effects allows conclusion that silver should not be considered as a partner to cooperate with gold. Reactions that are separately catalyzed either by silver or by gold were beyond the scope of this study (for those reactions a "true" silver effect would indeed take place).

1. Introduction

For a long time silver salts AgX have been routinely used to activate gold chloride complexes by halogen abstraction for use in gold catalysis or synthesis of various gold complexes (Eq. 1).¹ Precipitation of $AgCl$ is normally considered stoichiometric and complete. Therefore, for a long time the role of silver in gold catalysis has not been discussed beyond this simple ligand exchange process.

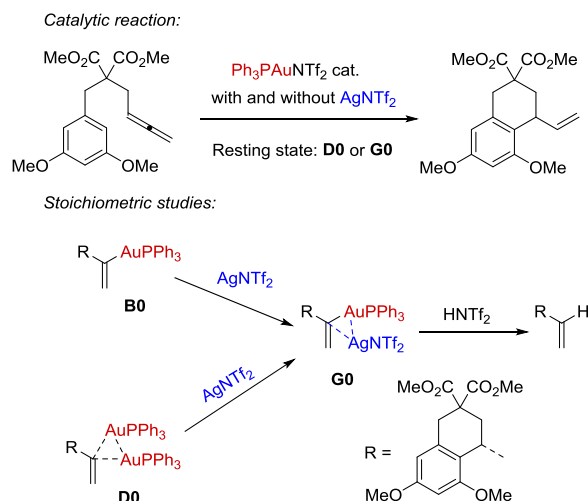


Nu = any molecule or anion with coordination ability to gold,
 $X^- = SbF_6^-, NTf_2^-, OTf^-, \text{etc.}$

However, since recently there has been increased amount of experimental observations suggesting that silver is not totally innocent in gold catalysis. The first mechanistic evidence is observation of mixed Au-Ag intermediates in reaction mixtures, briefly reported by Gagné and Weber in 2009.² They showed that silver is able to react with the key organogold intermediates to generate new bimetallic intermediates (Scheme 1). Diaurated species **D0** and vinyl gold **B0** react with $AgNTf_2$ to give argento vinyl gold **G0**, which was even isolated and characterized by NMR and MS. Unfortunately, no X-ray analysis could be performed and the exact structure remains to be speculative, based on inspection of previously known examples of various Au/Ag bimetallic species.³ This suggests the structure of **G0** must pertain much of the planar vinyl gold character with only side-on coordination of silver, with maintenance of Au-Ag metallophilic interaction. In other words, the 3-center-2-electron interaction which was equal in **D0** now is not equal in **G0** with the C-Au bond dominating the structure.² In accordance with this notion we

will apply the term "argento vinyl gold" to emphasize the predominant vinyl gold vs. vinyl silver character of these species. Furthermore, Gagné and Weber observed **G0** as a resting state of the catalytic reaction, and this remains the only direct evidence of involvement of Au/Ag bimetallic intermediates in gold catalysis. In their case, the reaction was retarded by additions of $AgNTf_2$ (that would be called a "negative silver effect"). Also, no investigation into the role of **G** in reaction mechanism was provided.

Scheme 1. Reactivity of Vinyl Gold and Diaurated Species Toward Ag^+ Observed by Gagné.



An extended work reported in 2012 by Shi et al. demonstrated that the rate (and yield) of many gold catalyzed reactions can be largely influenced by the presence of Ag^+ (in addition to already present gold catalyst).⁴ These observations not only questioned the innocence of silver in gold catalysis, but they even questioned fundamental mechanistic principals of gold catalysis at that time. Therefore, an in depth study is required to clarify the situation. In the following years there have been increased efforts to investigate and explain this "silver effect" in more detail. Notable examples include recent works from the groups of Echavarren,⁵ Hammond and Hu (to be discussed below).⁶ Due to the ambiguous role of silver, several methods for activation of a gold catalyst have been developed that avoid use of silver salts.^{7,8}

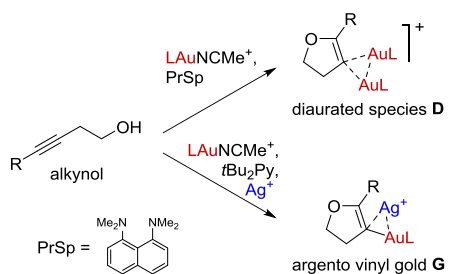
In our laboratory we have been involved in mechanistic investigations of gold catalysis. Recently we have reported extensive experimental studies on gold(I)-catalyzed hydroalkoxylation of alkynes (the mechanism and definitions of species are shown on Scheme 21).⁹ Herein, using this model reaction with a well-established mechanism, we provide a systematic mechanistic experimental study to disclose the origins of the silver effect. Based on our observations and works of others we propose a generalized classification of multiple origins of the silver effect. This would put in order the understanding of erratic results associated with this effect.

2. Results and discussion

In our practice we used silver free gold catalysts $\text{Ph}_3\text{PAuNCMe}^+ \text{SbF}_6^-$ (**1**) and $\text{L}_2\text{AuNCMe}^+ \text{SbF}_6^-$ (**2**, $\text{L}_2 = 2\text{-}(\text{di-}t\text{-butylphosphino})\text{biphenyl}$). For observation of silver effects the reactions were performed in the presence of silver salt AgOTf . MeOD was used as a solvent to ensure complete solubility of the catalytic system and also to eliminate any counterion effect. We found that argento vinyl gold species were involved every time when we observed a silver effect. Therefore, it is necessary to describe properties and reactive pathways of this species prior to discussion and explanation of the effects (Sections 2.1.-2.3.). The silver effect is then explained for a number of catalytic hydroalkoxylation reactions (Sections 2.4.-2.5.). In Section 2.6. we propose a generalized picture of silver effects using the knowledge obtained in our research and that of others.

2.1. Synthesis of Argento Vinyl Gold in Situ and Reactions with Nucleophiles. In 2013 we reported formation of diaurated species **D** using an alkyne, a gold catalyst and a non-nucleophilic base PrSp (1,8-bis(dimethylamino)-naphthalene).¹⁰ Using AgOTf as additional reactant, the same method was initially attempted for the synthesis of the corresponding argento vinyl gold species. However, AgOTf was found to be incompatible with PrSp , causing immediate formation of a black precipitate (reduction of silver). Therefore, $t\text{Bu}_2\text{Py}$ was used as a redox stable base.

Scheme 2. Formation of Diaurated Species D and Argento Vinyl Gold G from Alkyne.

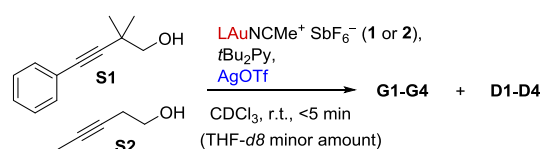


Thus, simple treatment of a concentrated $\text{THF-}d_8$ solution containing a gold catalyst (**1** or **2**) and AgOTf with a CDCl_3 solution containing $t\text{Bu}_2\text{Py}$ and alkyne (**S1** or **S2**) led to immediate quanti-

tative formation of the corresponding organometallic species, accompanied by minor competitive enol ether formation. Argento vinyl gold species **G1** and **G4** were formed exclusively (Table 1, entries 1, 4), while **G2** and **G3** were accompanied yet with a minor formation of the corresponding diaurated species (entries 2, 3). Important requirement for successful formation of argento vinyl gold is that the silver salt should be dissolved prior to the reaction, otherwise formation of **D** and/or gold catalyzed hydroalkoxylation will predominantly occur. But AgOTf is negligibly soluble in CDCl_3 . That is why it was dissolved in a minimum of $\text{THF-}d_8$. Synthesis of **G2-G4** in CDCl_3 occurs under kinetic control, because **D2-D4** are thermodynamically favored (to be discussed below).

We attempted isolation of argento vinyl gold in individual state. But **G4** decomposed upon crystallization attempts. **G1** was stable, albeit it did not provide any crystalline material, at least after brief attempts. Therefore, all characterizations and reactions were performed in solution, using enriched samples prepared in situ.

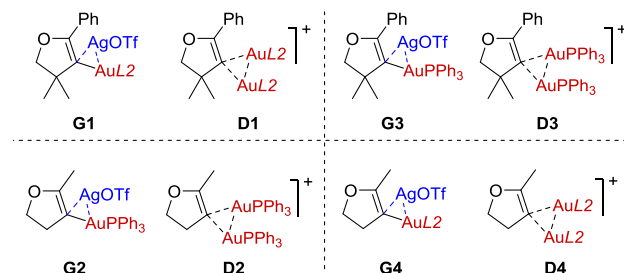
Table 1. Stoichiometric Formation of Argento Vinyl Gold in Situ.



Amounts of reactants (equiv.) and molar ratio of **G:D**

| | Alkyne | Gold ^a | $t\text{Bu}_2\text{Py}$ | AgOTf | G:D |
|---|-----------------|-------------------|-------------------------|----------------|------------|
| 1 | S1 (1.1) | 2 (1.0) | 1.5 | 1.1 | 1:0 |
| 2 | S2 (2.0) | 1 (1.0) | 1.3 | 1.1 | 1:0.1 |
| 3 | S1 (1.1) | 1 (1.0) | 1.6 | 1.1 | 1:0.03 |
| 4 | S2 (1.5) | 2 (1.0) | 2 | 1.4 | 1:0 |

^a1 ($\text{L} = \text{PPh}_3$), 2 ($\text{L} = \text{L}_2 = 2\text{-}(\text{di-}t\text{-butylphosphino})\text{biphenyl}$)



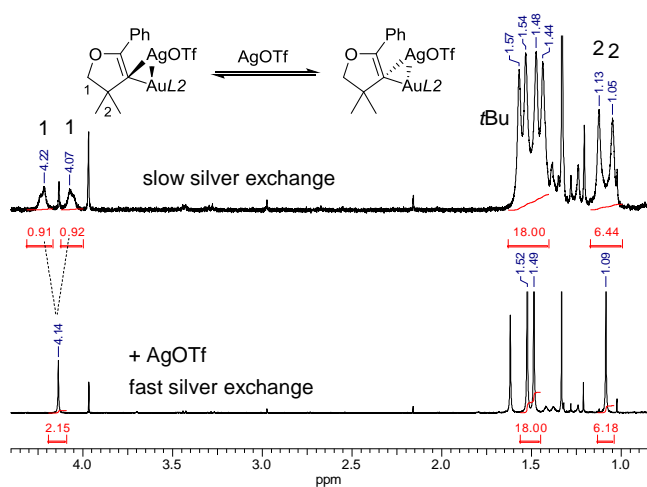
¹H NMR spectra of each of **G1-G4** exhibit simple patterns, despite the molecules being unsymmetrical. A possible reason of the degeneracy of the CH_2 and $\text{C}(\text{CH}_3)_2$ protons is a fast silver exchange, occurring in the presence of a slight excess of AgOTf . This process might occur by a nucleophile assisted dissociative pathway or through a doubly argented intermediate. The last scenario was proposed by Gagné to explain the spectrum of **G0**.² Treatment of **G1** in CDCl_3 with CaH_2 , a routine procedure to dehydrate a solution, led to slight darkening of the suspension. This might be caused by slow reduction of the residual AgOTf by CaH_2 . Surprisingly, under this condition the spectrum of **G1** revealed the unsymmetrical structure. Upon addition of extra AgOTf , the spectrum simplified again (Figure 1). This strongly supports the occurrence of fast silver exchange in the presence of additional Ag^+ .

Complex **G1** was characterized in CDCl_3 solution using ¹H, ³¹P, ¹⁹F, ¹³C and various two dimensional NMR techniques. With the help of $\text{CF}_3\text{CO}_2\text{Me}$ as an internal standard, the overall 1:1:1 ratio of

organic core: Au:Ag could be confirmed by ^1H and ^{19}F NMR spectra.

Observation of the CAu carbon signal in ^{13}C is very intriguing since this signal is often not found. In our case, it could be observed as a doublet at 125.1 ppm, $^2J_{\text{P}} = 93.7$ Hz. The 2J phosphorus coupling through the two bonds of the C–Au–P link appears to be bigger than the 1J coupling through the single C–P bond (36.5 Hz). Also it appears to be comparable to the value typical for vinyl gold (*ca.* 105 Hz) and more distant from the value typical for diaurated species (*ca.* 60 Hz).¹¹ This is in accordance to the planar vinyl gold character being only slightly disturbed by the side-on coordination of silver. The enol ether α -carbon atom appeared at 173.3 ppm as a doublet, $^3J_{\text{P}} = 9.1$ Hz. The coupling to the magnetically active Ag was not observed, presumably because of the fast silver exchange in solution.

Figure 1. Dynamic Behavior of Argento Vinyl Gold in the Presence of AgOTf.

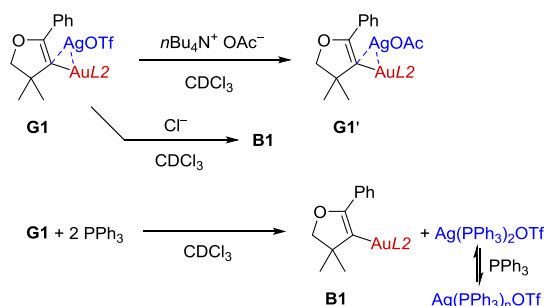


Very intriguing is the binding situation and coordination chemistry at silver. Besides vinyl gold moiety on one side it must have at least one ligand from the other side (at least OTf). To get some insight we conducted NMR titrations of **G1** with various nucleophiles in CDCl_3 (Me_2S , Lut, TMTU, PPh_3 , OAc^- , Cl^-), monitoring ^1H , ^{31}P , ^{19}F NMR spectra after each addition of the nucleophile. No clear picture about the coordination mode of silver could be obtained in most cases. The difficulty was associated with ambiguous interpretation. All reaction mixtures exhibited fast ligand exchange at silver in the NMR time scale, as evidenced by a single set of signals of enol ether core and the ligands. Stoichiometric substitution of the OTf by 1 equiv of OAc^- at **G1** could most convincingly be confirmed by observation of no changes in the ^1H , ^{31}P , ^{19}F NMR spectra of **G1** at >1 equiv of OAc^- (Scheme 3). **G1** was resistant towards detachment of vinyl gold in the presence of excess Me_2S , Lut, or OAc^- . Partial detachment was observed in the presence of 4 equiv TMTU. Stronger nucleophiles PPh_3 and Cl^- caused stoichiometric cleavage of **G1** to form vinyl gold **B1** and $\text{Ag}(\text{PPh}_3)_n^+$ ($n = 2-4$) or AgCl precipitate. No evidence for the alternative cleavage to vinyl silver RAgL and LAuL^+ was obtained, so this pathway appears improbable. Whereas the reaction with Cl^- required 1 equiv of the nucleophile for complete cleavage, the reaction with PPh_3 required 2 equiv PPh_3 . The last fact suggests that **G1** can accept no more than 1 equiv PPh_3 at silver without detachment of the vinyl gold moiety, whereas the second equivalent of PPh_3 causes the cleavage. This finding suggests that the silver in **G1** has a coordination number of two. However, a related gold acetylide derivative $[\text{PhC}\equiv\text{C}(\text{AuPPh}_3)(\text{Ag}(\text{PPh}_3)_2)]^+$ was reported to have a coordination number of three (in solid state).¹² In cases where incomplete

cleavage of **G1** takes place either due to reversible reaction (TMTU) or before the equivalence point (PPh_3 and Cl^-) the enol ether core exhibits a single set of pretty sharp or severely broadened signals, evidencing for fast equilibrium between **G1** and **B1**. This is interpreted as fast vinyl gold exchange at silver.

Based on this NMR data, in the absence of sufficiently strong nucleophiles, OTf^- is suggested to be covalently bound to silver in CDCl_3 solution of **G1**. Rather, in CD_3OD solution **G1** appears to be a cationic complex. This follows from observation of a ^{19}F resonance at the constant -80.1 ppm, the same as AgOTf , $\text{PrSpH}^+ \text{OTf}^-$, TfOH , unambiguously indicating complete dissociation of OTf^- from silver in CD_3OD .

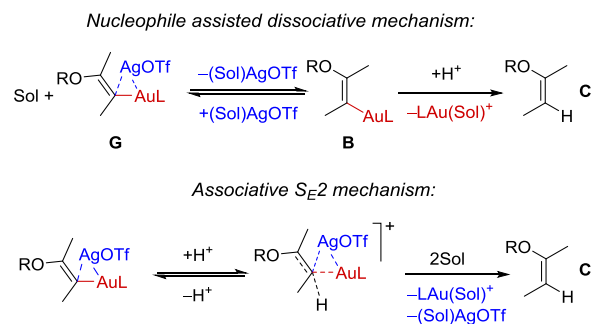
Scheme 3. Stoichiometric Reactions of G1 with Various Nucleophiles (OAc^- , Cl^- and PPh_3).



This all characterizes argento vinyl gold as flexibly reactive species, that would undergo fast silver exchange (in the presence of extra Ag^+), fast ligand exchange at silver (in the presence of extra Nu) and fast vinyl gold exchange at silver (in the presence of extra vinyl gold).

2.2. Mechanism of Protodeauration of Argento Vinyl Gold. In order to understand the role of argento vinyl gold in the catalytic cycle it is necessary to ascertain the mechanism by which it can be protodemetalated, releasing gold and silver back in solution. Similarly as was previously described for diaurated species, also here there is a choice between the nucleophile assisted dissociative mechanism and bimolecular $\text{S}_{\text{E}}2$ mechanism (Scheme 4).

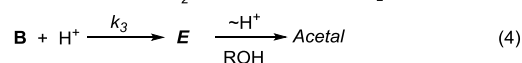
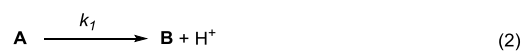
Scheme 4. Possible Mechanisms of Protodemetalation of Argento Vinyl Gold



Preliminary experiments were conducted with argento vinyl gold **G1** generated in situ. Thus, TfOH , $\text{CF}_3\text{CO}_2\text{H}$ and $t\text{Bu}_2\text{PyH}^+ \text{OTf}^-$ all caused instant (<5 min) protodemetalation of this compound in MeOD at room temperature (**G1** was stable towards $t\text{Bu}_2\text{PyH}^+ \text{OTf}^-$ in CDCl_3 though). Reaction with AcOH occurred slower and was found to be inhibited in the presence of additional AgOTf but accelerated in the presence of Me_2S . These results already suggest the nucleophile assisted dissociative mechanism. However, it was difficult to find suitable conditions to allow accurate determination of chemical kinetics that would prove this mechanism more rigorously. Therefore, we turned to a catalytic study instead.

Theoretical analysis of a gold catalyzed hydroalkoxylation in case of complete and immediate formation of argento vinyl gold as a single resting state comes to different results depending on whether it undergoes protodemetalation by nucleophile assisted dissociative mechanism or S_E2 . Analysis of the kinetics with the anticipated nucleophile assisted mechanism is shown in Scheme 5. Using steady state approximation for **B** (always present in undetectable amounts, eq 5) and steady state approximation for **G** (always present in full amount, keeping all the gold of the system, eq 6) one easily comes to the following expression for **B** (eq 7). Putting this into the reaction rate (eq 8) gives the following final expression for the rate law (eq 9). According to this analysis, the reaction should have zero order in substrate, first order in gold, first order in acid and minus first order in silver. Analysis of kinetics in case of S_E2 mechanism is given in the Supporting Information. It leads to zero order in substrate, first order in gold, first order in acid and zero order in silver. Therefore, the order in silver in a catalytic process would be indicative of the actual mechanism of protodemetalation of argento vinyl gold.

Scheme 5. Derivation of the Rate Law for a Catalytic Reaction Having **G** as a Single Resting State.



$$\begin{cases} \frac{d[B]}{dt} = k_1[A] - k_3[B][H^+] - k_2[B][Ag^+] + k_{-2}[G] = 0 \\ \frac{d[G]}{dt} = k_2[B][Ag^+] - k_{-2}[G] = 0 \end{cases} \quad (5)$$

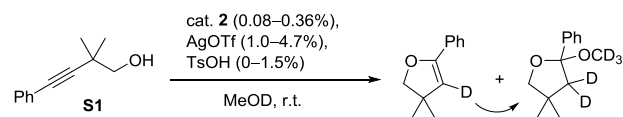
$$[B] = \frac{[G]}{K_{Ag}[Ag^+]} \quad (7)$$

$$\text{overall reaction rate: } -\frac{d[S]}{dt} = k_1[A] = k_3[B][H^+] \quad (8)$$

$$\frac{d[S]}{dt} = -\frac{k_3[G][H^+]}{K_{Ag}[Ag^+]} \quad (9)$$

We determined kinetics of cyclization of **S1** in the presence of various amounts of catalyst **2**, AgOTf and TsOH in CD_3OD (Scheme 6). In each run gold rested as single species **G1**, directly observable by 1H NMR. Protodemetalation of **G1** becomes visible only upon complete consumption of **S1** (the signal of $L_2Au(Sol)^+$ appears). **[S1]** decreased almost linearly with time, therefore zero order in substrate was accepted for further analysis (Supporting Information). The analysis indicated first order in gold, first order in acid and, importantly, *minus first order in silver*. This finding proves protodemetalation of argento vinyl gold to occur by the nucleophile assisted dissociative mechanism. Therefore, argento vinyl gold is considered as an essentially off-cycle intermediate.

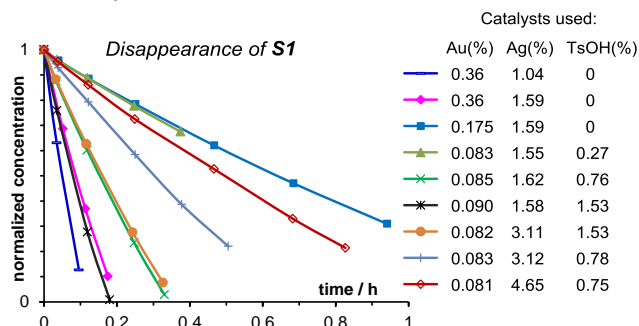
Scheme 6. Kinetics of a Gold Catalyzed Reaction in the Presence of Ag^+ and H^+ .



$$\text{rate law } \frac{d[S1]}{dt} = -k \frac{[G1][H^+]}{[Ag^+]} = -k \frac{c(c+h)}{(a-c)}$$

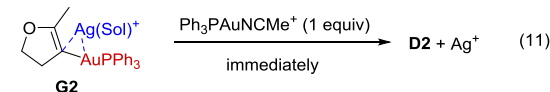
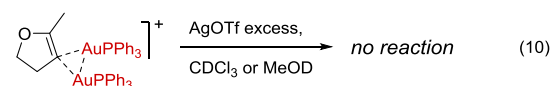
$$\text{resting state: } G1$$

$$\begin{cases} c = c(\text{cat. } 2) \\ a = c(AgOTf) \\ h = c(TsOH) \\ k = (6.4 \pm 0.2) \cdot 10^3 \text{ h}^{-1} \end{cases}$$

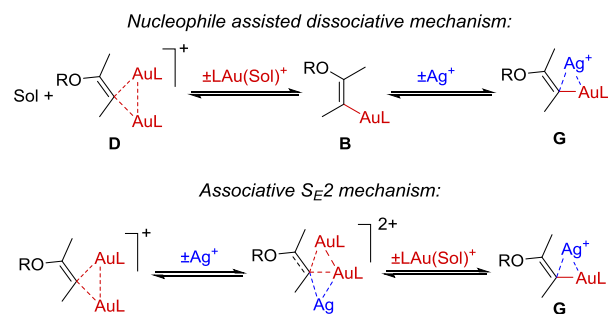


2.3. Reactivity of Silver Salt toward Diaurated Species.

Following the work of Gagné,² we studied transmetalation of diaurated species by silver salts. To our surprise, diaurated species **D2** did not exhibit any appreciable reactivity, giving no argento vinyl gold species (eq 10). Rather, the opposite reaction was found to occur immediately (eq 11). However, the less stable diaurated species **D4** slowly reacted with Ag^+ in methanol affording **G4**. This transformation can be described by two mechanisms: nucleophile assisted dissociative mechanism and bimolecular S_E2 mechanism (Scheme 7). In contrast to protodeauration of diaurated species that occurs only by the nucleophile assisted mechanism, here also S_E2 appear likely (the transition state would be stabilized by multiple metallophilic interactions). It is easy to see that the transmetalation must be considered as a reversible process (if the strong preference of one of the sides is not known beforehand).



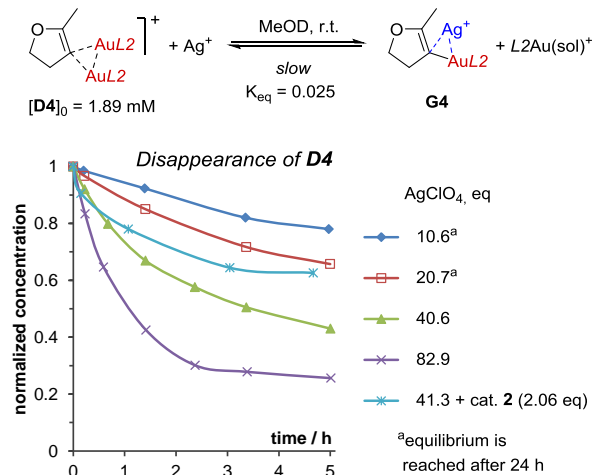
Scheme 7. Possible Mechanisms of Transmetalation of Diaurated Species



We hoped that the slow reaction of **D4** with Ag^+ would give us insight into the actual reaction mechanism. This reaction was performed at a constant initial concentration of **D4** using various amounts of Ag^+ (10 – 80 eq) and catalyst **2** (0 – 2 eq) in MeOD

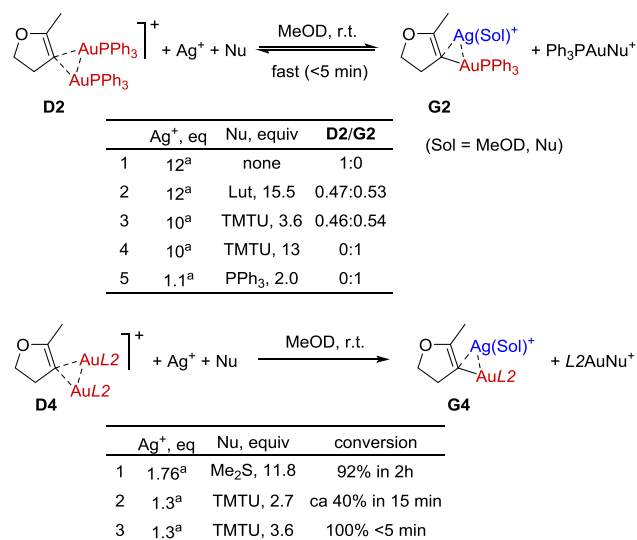
(Scheme 8). Unfortunately, kinetics of this reaction could not be analyzed to differentiate between the two possible mechanisms, because the reaction appeared to be reversible and did not reach 100% conversion even in the presence of 80 eq Ag^+ . But, as a small reward, we were able to determine the equilibrium constant ($K_{\text{eq}} = 0.025 \pm 0.005$). Since **D2** is >1000 more stable than **D4** it is not surprising that **D2** does not show any signs of transmetalation even in the presence of a large excess of a silver salt.¹³

Scheme 8. Slow and Reversible Transmetalation of **D4**.

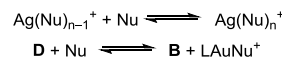


We found that the equilibrium between **D** and **G** can be strongly influenced by addition of a nucleophile (Scheme 9). Thus, using Me_2S , Lut, TMTU, PPh_3 it is possible to entirely shift the equilibrium towards **G** even if it was completely on the side of **D** before the addition of a nucleophile. The main driving force is provided by binding gold to form LAuNu^+ . Clearly, there is the opposite driving force provided by binding silver to form $\text{Ag}(\text{Nu})_n^+$ ($n = 2 - 4$), but it does not play a role, being dominated by gold as indicated by a model study of the binding preferences.¹⁴ The stability of LAuNu^+ increases in the order $\text{Nu} = \text{Me}_2\text{S} < \text{Lut} < \text{TMTU} < \text{PPh}_3$,¹⁵ therefore the ability of a nucleophile to shift the equilibrium between **D** and **G** increases in the same order.

Scheme 9. Influence of a Nucleophile on Transmetalation of Diaurated Species.



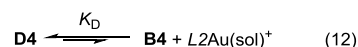
^a Ag^+ exists as an undetermined $\text{Ag}(\text{Nu})_n^+$ ($n = 2 - 4$) or their mixture
 Background equilibriums:



These findings allow the conclusion that not every diaurated species **D** can be transmetalated by silver salts. This appears to be a reversible reaction that obviously depends on thermodynamic stability of **D** and **G**. In most cases **D** would be reluctant to undergo transmetalation, rather the opposite reaction would be favored. In case if **D** is highly destabilized by steric bulk of the LAu , would formation of **G** be more favored (stability of **G** is obviously less sensitive to steric bulk of LAu moiety and enol ether core than that of **D**). Also binding of LAu^+ by additional nucleophile provides a driving force that may shift this equilibrium toward **G** (this may take place under catalytic conditions, see below).

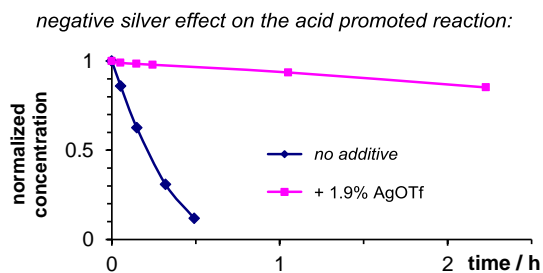
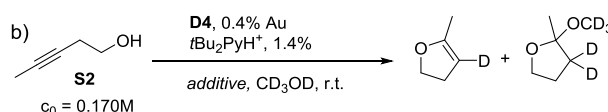
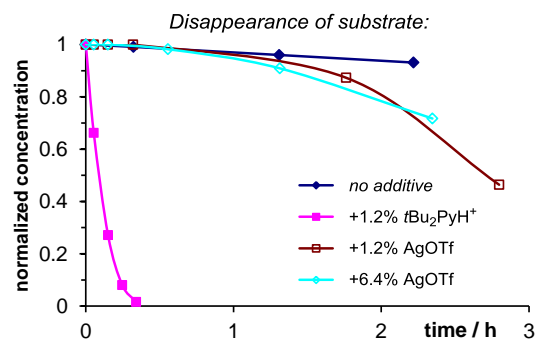
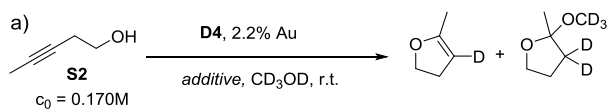
2.4. Influence of Silver and Acid Additives on Catalysis by Diaurated Species. Having briefly investigated the properties of argento vinyl gold we performed a series of catalytic runs to understand the silver effect in gold catalysis. Particular attention was given to observation of catalytic intermediates *in situ* during the whole process. Then, we will straight away explain all the effects using the knowledge of properties of argento vinyl gold and mechanism of gold catalyzed hydroalkoxylation.

First of all we verified catalytic cyclization of 3-pentyn-1-ol using individual diaurated species **D4** as a catalyst (Scheme 10). Without any additives this reaction is known to occur very sluggishly, taking several hours.⁹ However, the reaction gets drastically accelerated in the presence of an acid promoter. NMR examination indicated that diaurated species fully survived during the whole reaction course, being not transformed into $\text{L2Au}(\text{Sol})^+$ to any appreciable amounts. The huge acid effect is clear to understand if one considers material balance of the catalytic system. With catalysis by **D4** the reaction sluggishly proceeds because of the negligible dissociation of **D4** (eq 12, K_{D} is very small). Under these conditions the amounts of all in-cycle intermediates are negligible (including the necessary H^+). Addition of acid as a promoter obviously benefits the catalytic system by increasing active H^+ . In consequence, also the amount of in-cycle intermediates is slightly altered. The overall effect is strongly positive.

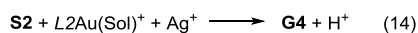


In the presence of AgOTf the reaction is initially retarded but then occurs with acceleration and the overall silver effect is positive (Scheme 10, a). Importantly, NMR examination indicated that **D4** partially transformed into argento vinyl gold **G4**, in accordance with our expectations. Since interaction of silver with **D4** is slow, the strength of the positive effect increases with time, accounting for the rate acceleration. If silver and acid additives are applied together the overall reaction rate is much slower than in the presence of an acid additive alone (Scheme 10, b).

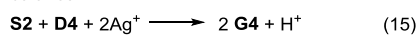
Scheme 10. Silver Effect on a Reaction Catalyzed by Diaurated Species.



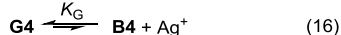
In order to understand this silver effect it is also useful to consider the material balance of the catalytic system. As seen from eqs 13, 14, 15, every equivalent of **D4** that gets transmuted by silver would give rise to 2 equiv. of **G4** and 1 equiv. of H^+ . Both **D4** and **G4** are off-cycle intermediates, but replacement of **D4** by **G4** is accompanied with liberation of H^+ . Moreover, the dissociation constant of **G4** (eq 16, K_G) is bigger than that for **D4**. This makes the overall effect positive.



balance:



dissociation of **G4**:

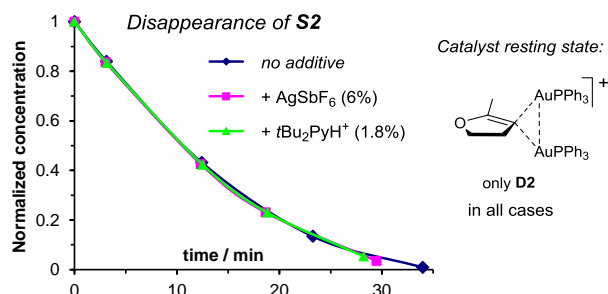
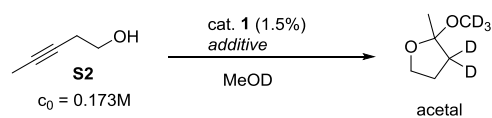


In its turn, the negative silver effect on the acid promoted reaction is explained by shifting the equilibrium (eq 16), decreasing the amount of all in-cycle organogold intermediates.

2.5. Influence of Silver and Acid Additives on Catalysis by Conventional Gold Catalysts. As a next step we investigated the influence of silver on catalysis by conventional gold catalysts. We started from the cyclization of 3-pentyn-1-ol (**S2**) in CD_3OD in the presence of catalyst **1** (Scheme 11). No acid and silver effects were observed since all experiments delivered identical kinetic curves. In the absence of any additives this reaction is characterized by complete formation of **D2** (leaving only undetectable steady state concentrations of other gold species). NMR examination confirmed that the same situation is observed in both experiments with the additives. The absence of an acid effect is explained by the low strength of this acid in comparison to MeOH_2^+ that has been evolved. Indeed, application of 1.5% catalyst **1** results in liberation of 0.75% of a super acid in solution. The presence of additional 1.8% of a weaker acid does not influence the situation in any appreciable way.

Absence of a silver effect is fully consistent with the inability of Ag^+ to influence the distribution of organogold species by changing the resting state from **D2** to **G2** in any appreciable way. In other words, if diaurated species is too stable, the silver effect does not take place.

Scheme 11. Absence of Acid and Silver Effects on Cyclization of S2 in Presence of Catalyst 1.



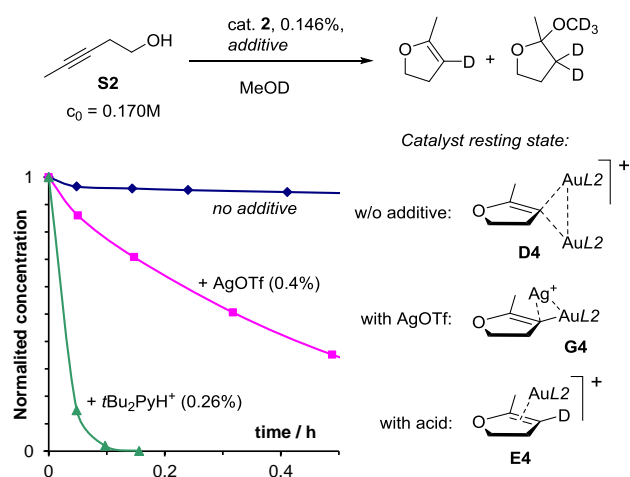
Next we performed a similar study of the cyclization of 3-pentyn-1-ol (**S2**) in CD_3OD in the presence of catalyst **2** (Scheme 12). This reaction is also accompanied by formation of diaurated species **D4** (at low catalyst loading). The reaction exhibited a strong positive silver and acid effect. The acid effect is now explained by the ability of acid to prevent formation of diaurated species, which is ok because **D4** is >1000 less stable than **D2**. This is secured by accelerating the protodeauration step. As a consequence, the amount of in-cycle organogold intermediates is drastically increased, as well as H^+ .

In the presence of Ag^+ the corresponding argento vinyl gold **G4** becomes directly observable by NMR as a single resting state, totally replacing **D4**. Considering the material balance of the catalytic system one comes to conclusion that in the presence of silver we have 1 equiv **G4** and 1 equiv H^+ instead of 1/2 equiv of **D2** and 1/2 equiv of H^+ before (Scheme 13). Secondly, $K_D < K_G$. As a consequence, the gold/silver catalyzed reaction benefits from higher fraction of in-cycle organogold intermediates and higher concentration of H^+ . This adds together to account for the positive silver effect.

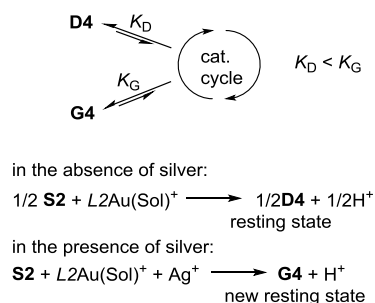
Despite $K_D < K_G$ (**D4** is more stable than **G4**, see Section 2.3.) the catalytic system rests entirely at **G4**. This can be due to kinetics reasons (if **G4** forms faster and is reluctant to equilibrate to **D4**). Also, this does not necessarily contradict the thermodynamics be-

cause additional driving force is certainly provided by binding $L Au^+$ by the reactive substrate, eventually turning both gold and silver into **G4** (eq 14), disfavoring formation of **D4** to some extent. This driving force, however, was unable to cause any changes in resting state in the aforementioned reaction with catalyst **1** (**D2** is simply too much more stable than **G2**).

Scheme 12. Positive Acid and Silver Effects on Cyclization of **S2** in the Presence of Catalyst **2**.

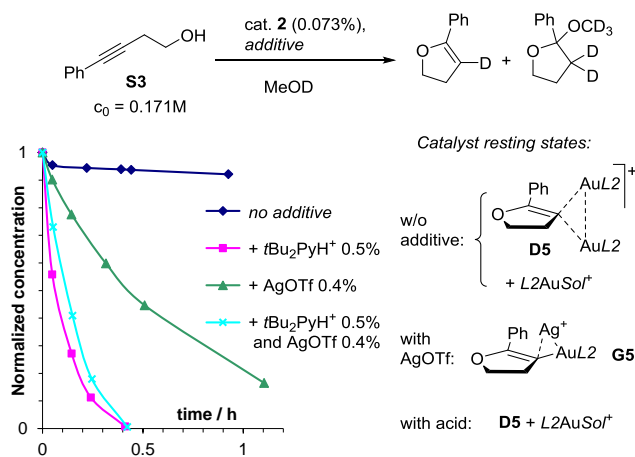


Scheme 13. Changes in the Catalytic System Caused by Addition of Ag^+ .

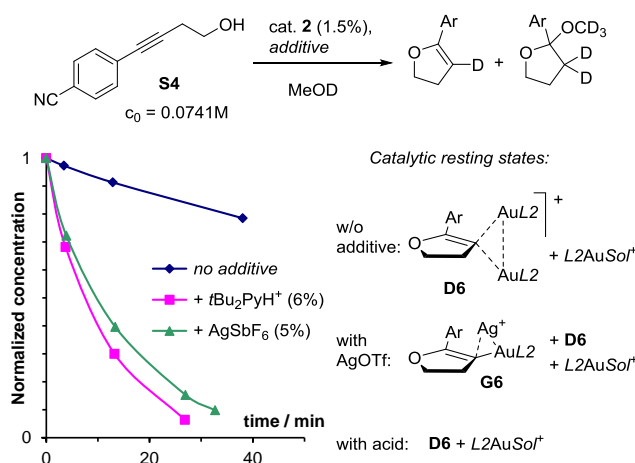


Completely similar explanations can be applied to the positive acid and silver effects that were observed in the cyclizations of 4-phenylbut-3-yn-1-ol (**S3**) and 4-(4-cyanophenyl)-butyn-3-ol-1 (**S4**) in the presence of catalyst **2** (Schemes 14 and 15). In case of **S3** the resting state was entirely changed from **D5** to **G5** upon addition of silver, resembling the situation explained for alcohol **S2** above (Schemes 12 and 13). Only partial changes in resting states were noted in the case of alcohol **S4** (see Supporting Information for more details).

Scheme 14. Positive Acid and Silver Effects on Cyclization of **S3** in the Presence of Catalyst **2**.

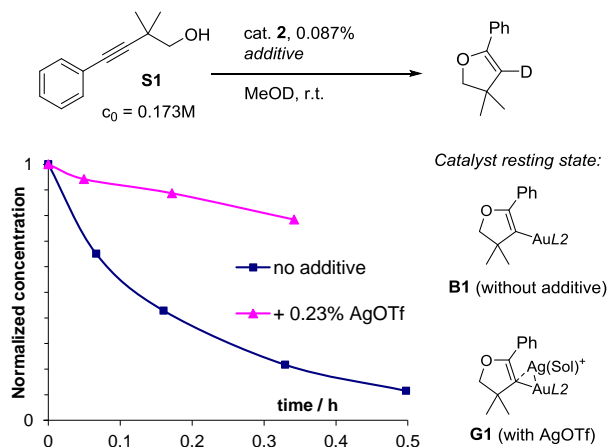


Scheme 15. Positive Acid and Silver Effects on Cyclization of **S4** in the Presence of Catalyst **2**.



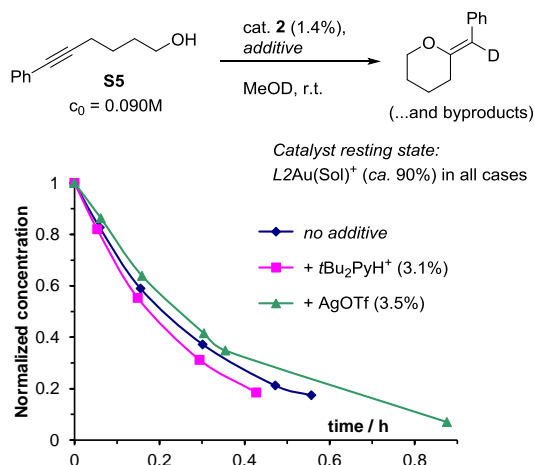
As a further case we examined the reaction of 2,2-dimethyl-4-phenylbut-3-yn-1-ol (**S1**) which is unable to form diaurated species with catalyst **2**. In the absence of any additives this reaction is characterized by complete formation of vinyl gold **B1**, and having protodeauration as the rate limiting step.⁹ Application of silver should bind this vinyl gold into argento vinyl gold. In complete accordance with our expectations, a *negative* silver effect was indeed observed (Scheme 16). As expected, vinyl gold completely disappeared and argento vinyl gold **G1** was instead observed by NMR as the only species. The kinetics of this reaction was analyzed in Section 2.2.

Scheme 16. Negative Silver Effect on the Cyclization of **S1** in the Presence of Catalyst **2**.

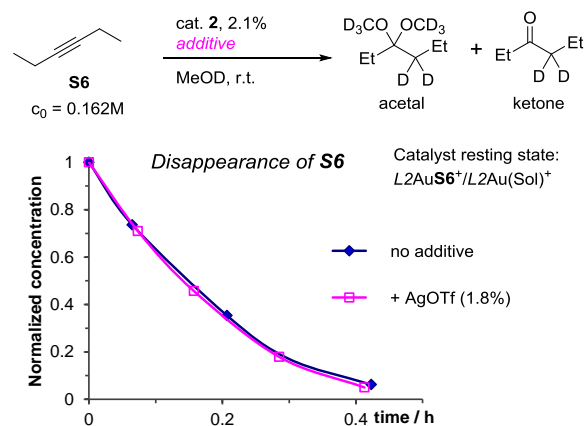


These findings bring us closer to the conclusion that silver effects are caused only by changes in concentrations of in-cycle organogold intermediates and H^+ , associated with formation of a new off-cycle intermediate **G**, and that silver has no direct role in the catalytic cycle itself. One thing remained to be proved: that silver has indeed no influence on the reactivity of a gold acetylene π -complex **A**, the starting point of the catalytic cycle. For this purpose, we conducted reactions where transition from **A** to **B** is rate limiting and formation of any off-cycle intermediate is excluded. The first reaction we looked at in this regard is cyclization of 6-phenylhex-5-yn-1-ol (**S5**) in the presence of catalyst **2** (Scheme 17). In the absence of any additives this reaction is characterized by vinyl gold formation as the rate limiting step and the catalyst being present almost exclusively as $\text{L2Au}(\text{Sol})^+$ (only minor amounts of diaurated species do accumulate). Predictably the reaction has almost no acid and silver effect, which is consistent with all our viewpoints about the mechanism of the entire process. This shows silver has no impact on enhancing vinyl gold formation. This unambiguously proves that silver has no business with the substrate and neither can cooperate with gold. This conclusion is even better confirmed by reaction of hexyne-3 (**S6**) that did not exhibit any detectable silver effect (Scheme 18).

Scheme 17. Lack of Significant Acid and Silver Effects on Cyclization of S5 Catalyzed by 2.

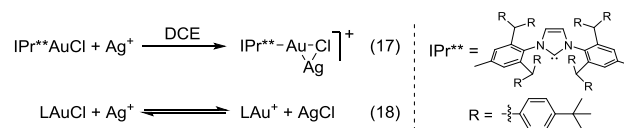


Scheme 18. No Silver Effect on Hydroalkoxylation of S6 Catalyzed by 2.

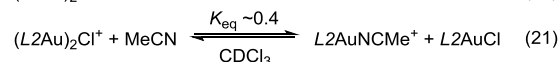
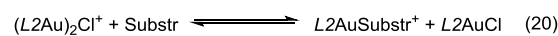
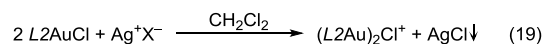


2.6. Classification of Silver Effects. Our research and the topical reports found in literature indicate that silver effect has many origins, but it is not always "silver" in nature (that is, silver is not involved in the catalytic process itself). Therefore, it is convenient to introduce classification of silver effects. Besides our effect being associated with formation of **G**, there are several other effects. After a brief overview it will be possible to make a general conclusion about the nature of a silver effect.

2.6.1. Silver effect associated with incomplete equation 1. In certain conditions the halogen abstraction reaction may not reach completion, leading to other gold complexes instead. In 2012 Straub et al. performed a reaction of a very bulky $\text{IPr}^{**}\text{AuCl}$ with AgSbF_6 under extremely weak nucleophilic conditions and isolated $[\text{IPr}^{**}\text{AuClAg}]^+$, where silver is adjacent to the Au-Cl bond (eq 17).¹⁶ This finding shows that idealistic halogen exchange reaction (eq 18) would be reversible under virtually non-nucleophilic conditions.¹⁴ This complex is considered as the very early intermediate of eq 1.

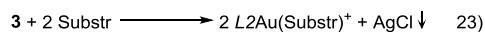
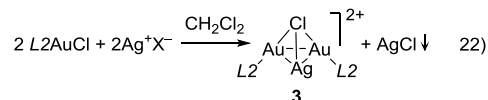


In 2013 Echavarren et al. described formation of bridged chloronium complexes $(\text{LAu})_2\text{Cl}^+$ as products of incomplete halogen abstraction (eq 19).⁵ Since $(\text{LAu})_2\text{Cl}^+$ is a precatalyst that has to react through ligand exchange equilibrium (eq 20), it is clear that the best theoretical performance of 1 equiv of $(\text{LAu})_2\text{Cl}^+$ (with regard to gold) can not be higher than activity of 0.5 equiv of formal LAu^+ . We estimated the equilibrium constant of ligand exchange of $(\text{L2Au})_2\text{Cl}^+$ with MeCN (eq 21) which indicates that $(\text{L2Au})_2\text{Cl}^+$ would be slightly more stable towards reaction with a substrate than L2AuNCMe^+ .



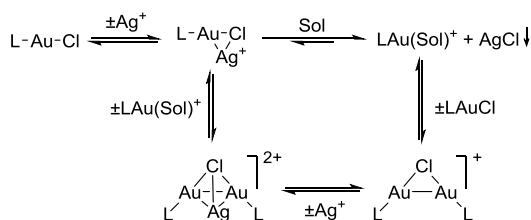
In 2013 yet another complex was identified by Jones et al. as a component of LAuCl/Ag^+ mixtures. They reacted L2AuCl with AgSbF_6 under extremely weak nucleophilic conditions and isolated a mixed silver-gold chloride complex **3** (eq 22).¹⁷ They determined that precipitation of AgCl from LAuCl/Ag^+ 1:1 mixtures is incomplete under nucleophile free conditions at short times and more AgCl precipitates if a nucleophile is added to bind the arising LAu^+

(and thus fulfil the stoichiometry of equation 1). They also noted immediate precipitation of AgCl if a nucleophile (e.g. a substrate) is added to a solution of **3** (eq 23). This fact means that **3** is very unlikely to be formed under real catalytic conditions.



These findings can be combined together to provide an overview of the halogen abstraction reaction, that can be displayed as a series of reversible ligand exchange events (Scheme 19). It can be concluded, that precipitation of AgCl and the presence of a nucleophile (even a weak one, like H₂O, MeCN) or a counterion able to bind gold, are the two driving forces which are simultaneously required for the halogen abstraction to occur stoichiometrically complete. In the absence of an external nucleophile (Sol), the L₂AuCl molecule plays a role as a nucleophile, leading to [LAuClAg]⁺, (LAu)₂Cl⁺ or **3**.

Scheme 19. Pathway of the Halogen Abstraction Reaction as Compiled Using the Knowledge from ref. 5, 16 and 17.



Sol = any molecule or anion able to coordinate to gold

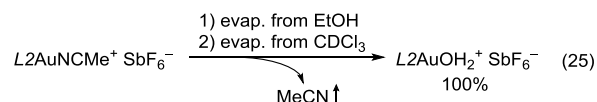
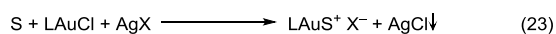
Besides that, yet another factor should be taken into account: simple solubility of the starting AgX salt. This idea came to mind after reading the paper of Echavarren, where they observed incomplete halogen abstraction with AgNTf₂ and AgOTf in CH₂Cl₂.⁵ These salts have coordinating anions; therefore the halogen abstraction should have occurred stoichiometrically according to Eq. 1. However, silver salts AgX typically used for the halogen abstraction are rather insoluble in CH₂Cl₂ or CHCl₃ alone. Presumably, this might be the likely reason for the incomplete reaction: a certain part of AgX may remain in the precipitate. In our own practice, we always dissolved silver salts in a minimum amount of acetone or MeCN prior to halogen abstraction reaction. It never failed under these conditions. In particular L₂AuOTf was synthesized in quantitative yield from L₂AuCl and AgOTf taken in 1:1 ratio.

Without giving it any further investigation, we propose the following condition for reliable and 100% complete halogen abstraction to use in laboratory practice: use the starting silver salt not as a solid, but as a solution in a minimum amount of a *weakly* coordinating solvent (acetone, MeOH, THF or MeCN). Besides providing solubility of the silver salts, these cosolvents provide a nucleophilic medium that accelerates all equilibria (Scheme 19). This ensures immediate and complete reaction strictly according to eq 1, avoiding accumulation of any intermediate complexes like [LAuClAg]⁺, (LAu)₂Cl⁺ or **3**.

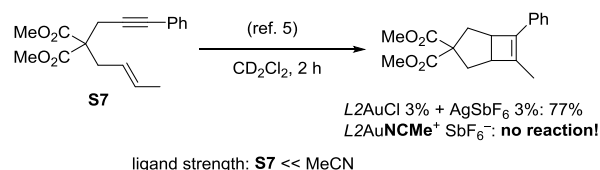
2.6.2. Silver effect associated with reactivation of a gold catalyst, that was poisoned by impurity or celite filtration. It was demonstrated that the reactivity of gold catalysts generated in situ from a L₂AuCl/AgX system can dramatically decrease if they are filtered through celite prior to the reaction.⁴ Since filtration was shown to remove AgCl and Ag⁺ but not gold from the filtrate, it was (wrongly) concluded that silver is crucial for some gold catalyzed reactions. Later, Ham-

mond and Hu nicely explained, that this has nothing to do with silver itself, but poisoning of a gold catalyst by traces of high gold affinity impurities in celite.⁶ They described reactivation of a gold catalyst by using H⁺, Ag⁺ and other Lewis acids as sacrificial electrophiles to bind possible catalyst poisons and set the gold catalyst free. This enabled successful reactions at very low gold catalyst loading. Clearly, such a silver effect has nothing to do with the mechanism of the catalytic transformation itself.

2.6.3. Silver effect wrongly associated with the negative role of MeCN. In connection with the use of a L₂AuCl/AgX system instead of a commercially available family of silver free catalysts L₂AuNCMe⁺ X⁻ we would like to especially stress, that for some substrates the L₂AuCl/AgX system would work more efficiently than L₂AuNCMe⁺, but this is not a silver effect! This might be the effect of absence of MeCN in the system. In fact, many alkynes and alkenes have very weak binding affinity to the catalyst, and for them even MeCN ligand would be a catalyst poison. This is nicely exemplified by *cis*-/*trans*-isomerization of enol ether **C1** (Scheme 20) which is much more efficiently catalyzed by a gold hydrate, a catalyst lacking MeCN.¹⁸ Another example is a reaction of enyne **S7** taken from literature (the authors did not interpret this effect).⁵ We believe the confusing role of MeCN is encountered (but overlooked) in many gold catalyzed reactions of substrates with very low binding affinity to gold. Those reactions would have L₂AuNCMe⁺ as a resting state and, often they would not involve any neutral organogold intermediates in their mechanism. Clear to see, this phenomenon has nothing to do with silver itself. Simply the L₂AuCl/AgX system provides the activated LAuS⁺ (S = substrate) complex more easily (eq 23) than does L₂AuNCMe⁺ (eq 24). The gold hydrate can be quantitatively prepared by rotary evaporation of a commercial L₂AuNCMe⁺ catalyst from EtOH (2 times) and then from CDCl₃ (one time) as exemplified in eq 25. This procedure can be considered as a way to boost a silver-free gold catalyst.



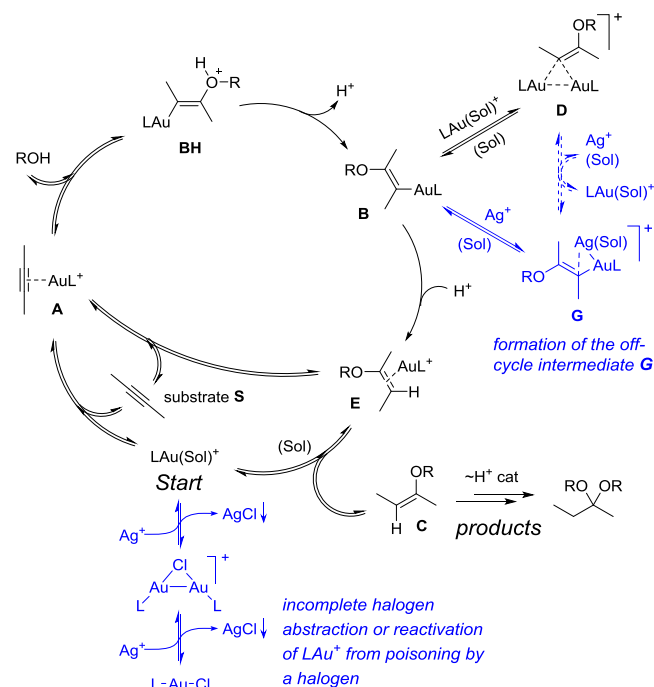
Scheme 20. A Negative Effect of MeCN on a Reaction Rate Should not be Confused With a Silver Effect.



2.7. Outlook. The knowledge obtained in our research (Sections 2.1.-2.5.) and literature (Section 2.6.) adds together to explain the origin of silver effect within the mechanism of gold catalyzed hydroalkoxylation (Scheme 21). This scheme illustrates two main conclusions: 1) Ag⁺ is found to be essentially innocent with regard to the mechanism of the catalytic process; 2) The silver effect (positive or negative) occurs only if silver causes variations of concentrations of in-cycle organogold intermediates and H⁺, which can be

associated either with formation of a new off-cycle intermediate argento vinyl gold **G**, or incomplete halogen abstraction by Ag^+ , or reactivation of a poisoned catalyst by Ag^+ . The steps that cause these variations are shown in blue.

Scheme 21. The Mechanism of Gold(I)-Catalyzed Hydroalkoxylation (in Black) Showing the Steps Responsible for the Silver Effect (in Blue).



3. Conclusion

The chemistry pioneered by Gagné (Scheme 1) was expanded to complete the explanation of the silver effect (Scheme 21). In situ NMR monitoring of gold catalyzed hydroalkoxylation in the presence of a silver salt revealed formation of argento vinyl gold **G** in all cases when a silver effect took place.

Stoichiometric studies indicated argento vinyl gold to be a reactive species, undergoing in the presence of Ag^+ , Nu or vinyl gold **B**, correspondingly, fast silver exchange, fast ligand exchange at silver and fast vinyl gold exchange at silver. Sufficiently strong nucleophiles will cause cleavage of **G** to yield **B**.

Protodemetalation of **G** was found to occur by the nucleophile assisted dissociative mechanism (through **B**). Therefore, **G** is considered as an off-cycle intermediate of the catalytic process (same as **D**). Considering the material balance of the catalytic system, it was demonstrated that formation of **G** will induce changes of the concentrations of in-cycle organogold intermediates and H^+ , and only these changes are responsible for the observed effect (not silver itself). The effect can be positive or negative (see explanations in the main text). No silver effect takes place if there is no accumulation of **G** in the reaction mixture. We foresee that formation of mixed silver-gold acetylide complexes $[\text{RC}\equiv\text{C}(\text{AuL})(\text{Ag})]^+$ might account for a silver effect in reactions of some terminal alkynes.¹⁹ This subclass remains to be explored.

Despite the ability to influence the rate of gold catalyzed hydroalkoxylation, Ag^+ is found to be essentially innocent with regard to the mechanism of the catalytic process itself. This is supposed to be valid for many reaction types, including those for which the simultaneous presence of silver and gold components was previously (erroneously) suggested to be crucial.⁴ Some reactions that are

separately catalyzed either by silver or by gold are beyond the scope of this conclusion (for those reactions a "true" silver effect associated with direct participation of silver in the catalytic process would indeed take place).²⁰

Besides formation of **G**, a silver effect may be associated with incomplete equation 1 (negative outcome) or reactivation of a gold catalyst by silver from halogenide poisoning (positive outcome). Whatever reason applies, the chemical sense of a silver effect is always the same: a change (decrease or increase) of the concentration of non-silver catalytic cycle participants.

ASSOCIATED CONTENT

Supporting Information. Complete experimental procedures and detailed NMR spectra. This material is available free of charge via the Internet at <http://pubs.acs.org>.

AUTHOR INFORMATION

Corresponding Author

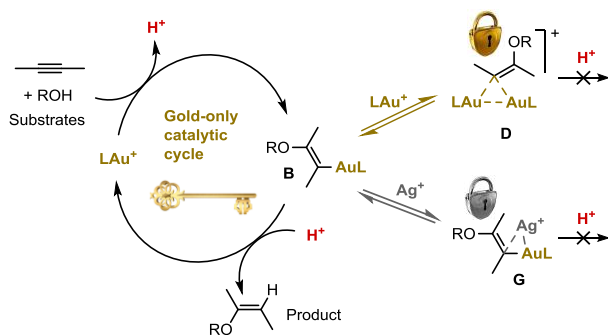
* E-mail: vinceero@gmail.com, martin.e.maier@uni-tuebingen.de

Funding Sources

Financial support by the state of Baden-Württemberg is greatly acknowledged.

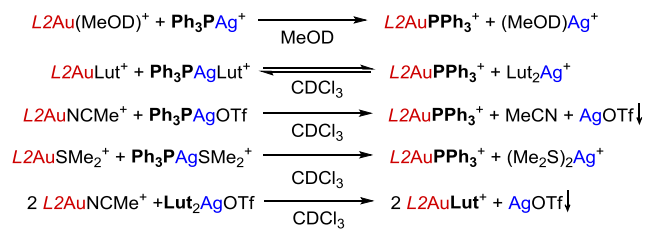
ACKNOWLEDGMENT

We thank Dr. K. Eichele and the Institut für Anorganische Chemie for giving us access to their NMR spectrometer.



REFERENCES

- ¹ For reviews on gold catalysis, see: (a) Rudolph, M.; Hashmi, A. S. K. *Chem. Soc. Rev.* **2012**, *41*, 2448-2462. (b) Corma, V.; Leyva-Peréz, A.; Sabater, M. J. *Chem. Rev.* **2011**, *111*, 1657-1712. (c) Bandini, M. *Chem. Soc. Rev.* **2011**, *40*, 1358-1367. (d) Boorman, T. C.; Larrosa, I. *Chem. Soc. Rev.* **2011**, *40*, 1910-1925. (e) Shapiro, N. D.; Toste, F. D. *Synlett* **2010**, 675-691. (f) Sengupta, S.; Shi, X. *ChemCatChem* **2010**, *2*, 609-619. (g) Bongers, N.; Krause, N. *Angew. Chem., Int. Ed.* **2008**, *47*, 2178-2181. (h) Gorin, D. J.; Sherry, B. D.; Toste, F. D. *Chem. Rev.* **2008**, *108*, 3351-3378. (i) Jiménez-Núñez, E.; Echavarren, A. M. *Chem. Rev.* **2008**, *108*, 3326-3350. (j) Li, Z.; Brouwer, C.; He, C. *Chem. Rev.* **2008**, *108*, 3239-3265. (k) Arcadi, A. *Chem. Rev.* **2008**, *108*, 3266-3325. (l) Muzart, J. *Tetrahedron* **2008**, *64*, 5815-5849. (m) Shen, H. C. *Tetrahedron* **2008**, *64*, 7847-7870. (n) Widenhoefer, R. A. *Chem. Eur. J.* **2008**, *14*, 5382-5391. (o) Gorin, D. J.; Toste, F. D. *Nature* **2007**, *446*, 395-403. (p) Fürstner, A.; Davies, P. W. *Angew. Chem., Int. Ed.* **2007**, *46*, 3410-3449. (q) Jiménez-Núñez, E.; Echavarren, A. M. *Chem. Commun.* **2007**, 333-346. (r) Hashmi, A. S. K. *Chem. Rev.* **2007**, *107*, 3180-3211. (s) Hashmi, A. S. K.; Hutchings, G. J. *Angew. Chem., Int. Ed.* **2006**, *45*, 7896-7936.
- ² Weber, D.; Gagne, M. R. *Org. Lett.* **2009**, *11*, 4962-4965.
- ³ Examples of Au-Ag complexes with a bridging carbon: (a) Contel, M.; Garrido, J.; Gimeno, M. C.; Jones, P. G.; Laguna, A.; Laguna, M. *Organometallics* **1996**, *15*, 4939-4943. (b) Contel, M.; Jiménez, J.; Jones, P. G.; Laguna, A.; Laguna, M. *J. Chem. Soc., Dalton Trans.* **1994**, 2515-2518. (c) Fernández, E. J.; Hardacre, C.; Laguna, A.; Lagunas, M. C.; López-de-Luzuriaga, J. M.; Monge, M.; Montiel, M.; Olmos, M. E.; Puelles, R. C.; Sánchez-Forcada, E. *Chem. Eur. J.* **2009**, *15*, 6222-6233. (d) Fernández, E. J.; Laguna, A.; López-de-Luzuriaga, J. M.; Montiel, M.; Olmos, M. E.; Pérez, J.; Puelles, R. C. *Organometallics* **2006**, *25*, 4307-4315. (e) Ruiz, J.; Riera, V.; Vivanco, M.; García-Granda, S.; García-Fernández, A. *Organometallics* **1992**, *11*, 4077-4082. (f) Vicente, J.; Chicote, M. T.; Alvarez-Falcón, M. M.; Jones, P. G. *Organometallics* **2005**, *24*, 4666-4675. (g) Xie, Z.-L.; Wei, Q.-H.; Zhang, L.-Y.; Chen, Z.-N. *Inorg. Chem. Commun.* **2007**, *10*, 1206-1209. (h) Mazhar-Ul-Haque; Horne, W.; Abu-Salah, O. M. J. *Crystallogr. Spectrosc. Res.* **1992**, *22*, 421-425.
- ⁴ Wang, D.; Cai, R.; Sharma, S.; Jirak, J.; Thummanapelli, S. K.; Akhmedov, N. G.; Zhang, H.; Liu, X.; Petersen, J. L.; Shi, X. *J. Am. Chem. Soc.* **2012**, *134*, 9012-9019.
- ⁵ Homs, A.; Escofet, I.; Echavarren, A. M. *Org. Lett.* **2013**, *15*, 5782-5785.
- ⁶ Kumar, M.; Hammond, G. B.; Xu, B. *Org. Lett.*, **2014**, *16*, 3452-3455.
- ⁷ For activation of gold hydroxo complexes with a Brønsted acid: Gaillard, S.; Bosson, J.; Ramón, R. S.; Nun, P.; Slawin, A. M. Z.; Nolan, S. P. *Chem. Eur. J.* **2010**, *16*, 13729-13740.
- ⁸ For anion exchange of LAuCl with an alkali metal salt: (a) Fürstner, A.; Alcarazo, M.; Goddard, R.; Lehmann, C. W. *Angew. Chem., Int. Ed.* **2008**, *47*, 3210-3214. (b) Kleinbeck, F.; Toste, F. D. *J. Am. Chem. Soc.* **2009**, *131*, 9178-9179. (c) Lau, V. M.; Gorin, C. F.; Kanan, M. W. *Chem. Sci.* **2014**, DOI: 10.1039/C4SC02058H. For activation of LAuCl by other Lewis acids: (d) Lavallo, V.; Frey, G. D.; Kousar, S.; Donnadiou, B.; Bertrand, G. *Proc. Natl. Acad. Sci. U.S.A.* **2007**, *104*, 13569-13573. (e) Guérinot, A.; Fang, W.; Sircoglou, M.; Bour, C.; Bezenine-Lafollée, S.; Gandon, V. *Angew. Chem., Int. Ed.* **2013**, *52*, 5848-5852. (f) Fang, W.; Passet, M.; Guérinot, A.; Bour, C.; Bezenine-Lafollée, S.; Gandon, V. *Chem. Eur. J.* **2014**, *18*, 5439-5446. For activation of LAu(phthalimide) by Brønsted and Lewis acids: (g) Han, J.; Shimizu, N.; Lu, Z.; Amii, H.; Hammond, G. B.; Xu, B. *Org. Lett.*, **2014**, *16*, 3500-3503.
- ⁹ Zhdanko, A.; Maier, M. E. *Chem. Eur. J.* **2014**, *20*, 1918-1930.
- ¹⁰ Zhdanko, A.; Maier, M. E. *Chem. Eur. J.* **2013**, *19*, 3932-3942.
- ¹¹ Seidel, G.; Lehmann, C. W.; Fürstner, A. *Angew. Chem., Int. Ed.* **2010**, *49*, 8466-8470.
- ¹² Blanco, M. C.; Camara, J.; Gimeno, M. C.; Jones, P. G.; Laguna, A.; Lopez-de-Luzuriaga, J. M.; Olmos, M. E.; Villacampa, M. D. *Organometallics* **2012**, *31*, 2597-2605.
- ¹³ Stability of various diaurated species was quantitatively evaluated: Zhdanko, A.; Maier, M. E. *Organometallics* **2013**, *32*, 2000-2006.
- ¹⁴ In connection with this intermetallic ligand exchange of Nu between formal LAu⁺ and Ag⁺ we established that the LAu⁺ unit has higher potency than a "naked" Ag⁺ to bind a Nu, as evidenced by the following almost stoichiometric reactions (four of the five equilibria were entirely shifted to the right):



¹⁵ Zhdanko, A.; Ströbele, M.; Maier, M. E. *Chem. Eur. J.* **2012**, *18*, 14732-14744.

¹⁶ Weber, S. G.; Rominger, F.; Straub, B. F. *Eur. J. Inorg. Chem.* **2012**, 2863-2867.

¹⁷ Zhu, Y.; Day, C. S.; Zhang, L.; Hauser, K. J.; Jones, A. C. *Chem. Eur. J.* **2013**, *19*, 12264-12271.

¹⁸ Isomerization of **E1** is found to be purely gold and not a proton catalyzed process under these conditions (unpublished).

¹⁹ Jašíková, L.; Roithová, J. *Organometallics* **2013**, *32*, 7025-7033.

²⁰ Example of such a reaction: Pennell, M. N.; Turner, P. G.; Sheppard, T. D. *Chem. Eur. J.* **2012**, *18*, 4748-4758.

Manuscript 10

For the Sections 6.3.6., 6.3.7., 6.3.8.

Pd, Pt, Hg Catalysis

Experimental Investigation of Gold(I), Palladium(II), Platinum(II) and Mercury(II) Catalyzed Spirocyclizations

Alexander Zhdanko^{*a}, Markus Ströbele^b, Cécilia Maichle-Mössmer^b, Martin E. Maier^{*a}

^a Institut für Organische Chemie Universität Tübingen Auf der Morgenstelle 18, 72076 Tübingen (Germany)

^b Institut für Anorganische Chemie Universität Tübingen Auf der Morgenstelle 18, 72076 Tübingen (Germany)

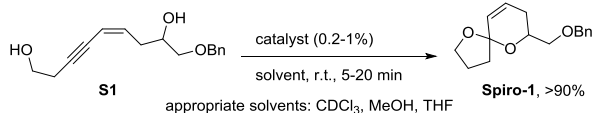
Supporting Information Placeholder

ABSTRACT: Experimental mechanistic investigations of gold(I), palladium(II), platinum(II) and mercury(II) catalyzed spirocyclization reactions of 5-en-3-yn-1,8-diols was conducted in order to observe various organometallic species and explain the differences in the reactivity of each metal catalyst and the corresponding organometallic species.

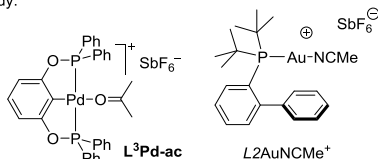
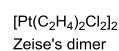
Introduction

In our laboratory we recently investigated spirocyclizations of internal enyne diols and found that 5-en-3-yn-1,8-diol systems furnished the corresponding [5,6]-spiroacetal products very efficiently with a number of gold(I), palladium(II), platinum(II) and mercury(II) catalysts.¹ Herein, using this well-functioning reaction (Scheme 1) we disclose mechanistic investigations and try to make an attempt to compare the differences of action of each of these metal catalysts, defining their weaknesses and advantages.

Scheme 1. Spirocyclization of the Model 1,3-Enyne Diol **S1**.



Catalysts used in this study:



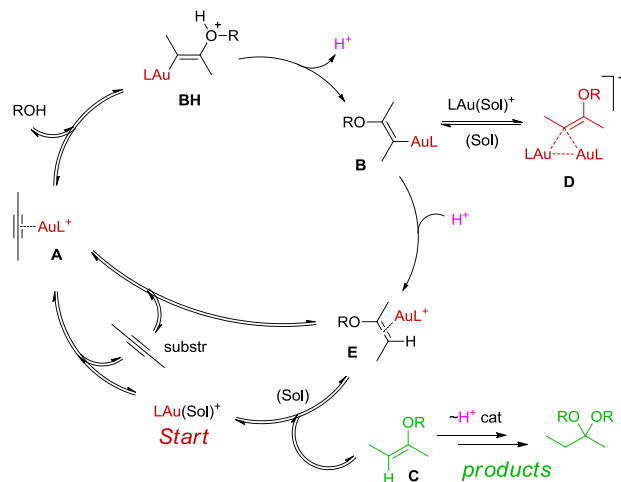
Catalysis by Cationic Gold Complexes

Recently we reported a thorough experimental study of gold catalyzed inter- and intramolecular hydroalkoxylation of alkynes reaching a high level of understanding of the process (Scheme).² Now, we would like to report on a mechanistic study of a related gold catalyzed spirocyclization which involves an intramolecular hydroalkoxylation step as well.

Here our studies also began with the detection and characterization of a relevant organogold intermediate in the presence of a base. Indeed, treatment of the substrate **S1** with freshly prepared Ph₃PAuOTf (1 equiv) in the presence of 1,8-bis(dimethylamino)naphthalene (PrSp, 1.3 equiv) in CDCl₃ allowed direct observation of a single organogold compound. In complete accordance with the previously published research, this appeared to be diaurated species **D1**, which was characterized in situ by ¹H, ¹³C and ³¹P NMR, H,H-COSY and HMBC spectra and exhibited typical spectral values (³¹P = 37.19 ppm). Also a high

resolution ESI MS spectrum showed a signal at 1177.248, consistent with the presence of **D1** cation.

Scheme 2. Previously Established Mechanism of Gold Catalyzed Hydroalkoxylation.



Besides formation of diaurated species, which is presently a trivial fact, interesting transformations were discovered upon continuous monitoring the reaction mixture during a 30 h period. The complete panorama of the reaction is presented in Figure 1. At first, Ph₃PAuOTf reacts with the substrate in a fast manner (<6 min) to give **D1** and results in binding only 50% of **S1** according to reaction stoichiometry. By this time yet 21% of dienol ether **5-endo-1** was formed competitively. The remainder of the substrate disappears in a 7 – 8 h period to give dienol ether **5-endo-1**. Then another process becomes evident, namely isomerization of **5-endo-1** to **6E-1**. Yet, very minor amount of another isomer **6Z-1** was observed (starting from <0.01 equiv at 7 h till 0.05 equiv at 25 h). The stereochemical assignment of these compounds was confirmed by NOESY spectra. Notably, during the entire time of the monitoring no traces of **Spiro-1** were formed. Simply, the reaction conditions were not acidic enough to trigger the proton-assisted spirocyclization of any of the dienol ethers.

A number of important conclusions were already suggested by this single experiment: 1) the starting enynediol first cyclizes in a 5-*endo-dig* manner to give the corresponding dienol ether as a single primary product (>99% regioselectivity); 2) all other dienol ether regioisomers are products of isomerization of this dienol ether and not the products of cyclization of the starting enynediol; 3) the isomerization of the dienol ether into another dienol ether is a gold but not a Brønsted acid catalyzed process; 4) formation of a spiroacetal final product is rather a Brønsted acid and not a gold catalyzed process.

In order to corroborate these conclusions we conducted a number of control experiments. First, a related enynediol **S2** reacted with Ph₃PAuOTf and PrSp under the same conditions as above to immediately (<5 min) yield a single diaurated species **D2** (³¹P = 37.33 ppm) and a single dienol ether **5-endo-2** as a primary product, further slowly evolving into **6E-2**. This demonstrates, that even a more hindered tertiary alcohol from the alkynyl side chain cyclizes much faster than a primary alcohol from the alkenol side chain.

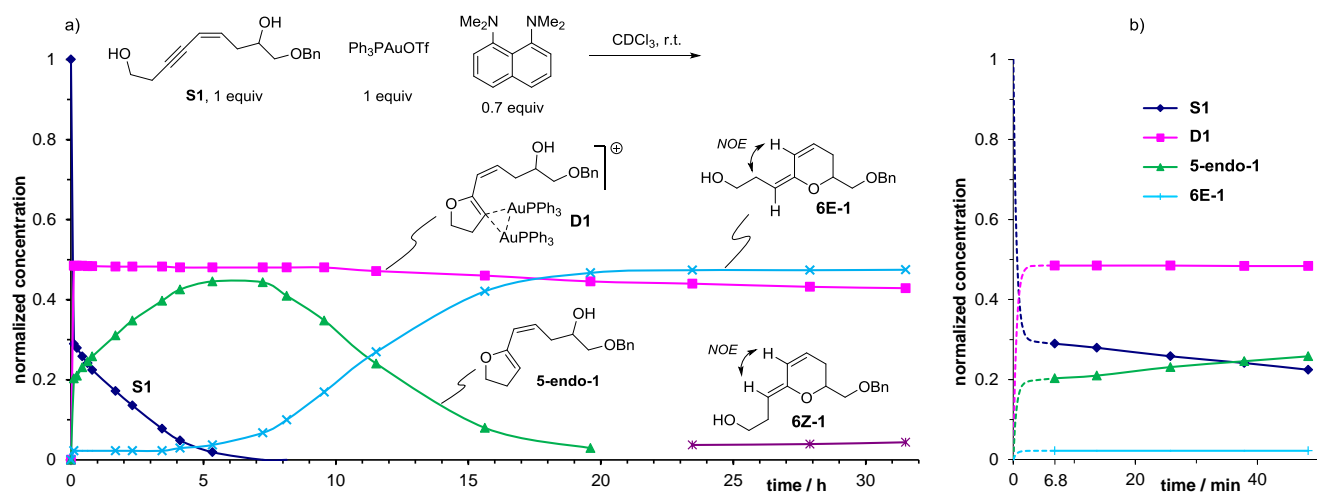
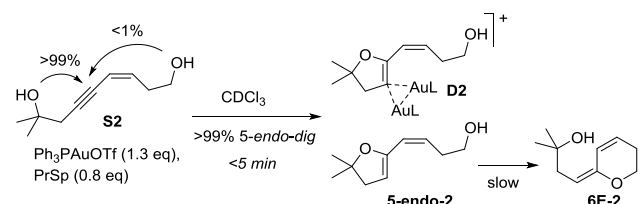


Figure 1. Stoichiometric in situ NMR experiment: a) the entire reaction course, b) first 50 minutes of the same reaction

Scheme 3. Demonstration of a Selective 5-*endo-dig* Cyclization.



To study the enol ether isomerization, various catalysts were added to a solution of **5-endo-3** and the reaction mixtures were monitored by NMR. The starting **5-endo-3** was prepared in situ by palladium catalysis (to be discussed below in Table 2). The results are given in Table 1, that shows conversions and the ratio of products calculated with regard of the starting dienol ether (referenced as “1 equiv”).³ Thus, addition of *t*Bu₂PyH⁺ OTf⁻ at 4% level led to a sluggish reaction, yielding no dienol ether isomerization products, but only the **Spiro-3** (entry 1). In contrast, all gold catalysts yielded only dienol ether isomerization products **6E-3** and **6Z-3** and no spiroacetal (entries 1-3). The formation of **Spiro-3** in the presence of Brønsted acid and its inability to form in the gold catalyzed conditions is the main criterion to differentiate the reaction mechanisms. It clearly indicates that Brønsted acid catalysis was switched off under gold catalyzed conditions,⁴ confirming that the isomerization of **5-endo-3** into the other dienol ethers is a gold catalyzed process, being orthogonal to the Brønsted acid catalyzed spirocyclization.

Table 1. Control Experiments on Isomerization of Dienol Ether.

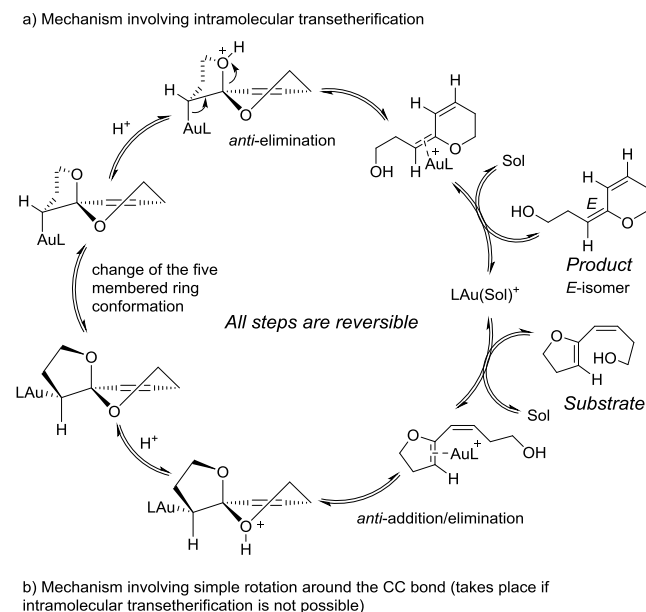
| N | Catalyst | conv. at time | 6E:6Z:Spiro, equiv |
|---|--|---------------|--------------------|
| 1 | <i>t</i> Bu ₂ PyH ⁺ (4%) | 17%, 60 min | 0 : 0 : 0.17 |
| 2 | L5AuNCMe ⁺ (33%) ^a | 100%, 5 min | 0.1 : 0.9 : 0 |
| 3 | Ph ₃ PAuNCMe ⁺ (36%) | 100%, 5 min | 0.1 : 0.9 : 0 |
| 4 | L2AuNCMe ⁺ (41%) | 62%, 20 min | 0.58 : 0.06 : 0 |

^a) L5 = (3,5-(CF₃)₂C₆H₃)₃P

The rate and outcome of gold catalyzed isomerization clearly depended on the ligand at gold. Application of the relatively electron deficient catalysts (entries 2, 3) rapidly led to the equilibrium mixture of **6E-3/6Z-3** dienol ethers, of which the **6Z-3** appears as the major isomer (being thermodynamically more stable). The electron rich catalyst (entry 4) led to a slow reaction, yielding **6E-3** as the major product, that very slowly further transforms into **6Z-3**. Yet, the **6E-** type was the major isomer during the isomerization within the aforementioned stoichiometric experiments (Figure 1 and Scheme 3). These results

imply, that gold stereoselectively catalyzes isomerization of **5-endo** into **6E** as the first relatively fast step and then **6E** into **6Z** as the second slower step (automatically indicating the following order of thermodynamic stability for the dienol ethers: **5-endo** < **6E** < **6Z**).

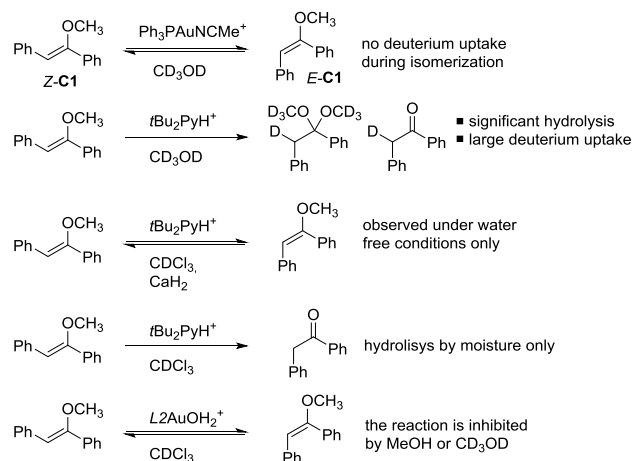
Scheme 4. Two Mechanisms of Enol Ether Isomerization.



The stereoselective **6E** formation can be rationalized by the catalytic cycle shown on Scheme 4, a). It includes formation of dienol ether π -complexes, stereospecific and reversible intramolecular *anti*-addition/elimination of the alcohol at the C=C bond and conformation changes. As a whole this process represents a case of intramolecular transesterification. All the steps are seen as reversible and the thermodynamic driving force is provided by the release of the unsaturated ring strain from the **5-endo** dienol ether. Formation of dienol ether π -complexes and their fast ligand exchange equilibria are well observable on ^1H and ^{31}P NMR spectra of the reaction mixtures. Clear to see, that if a Brønsted acid enters this catalytic cycle same way as gold (take H^+ instead of LAu^+ in all parts of the scheme), the system arrives at the stable spirocycle which is unable to ring-open in any direction.

Formation of **6Z** from **6E** cannot be rationalized by the transesterification mechanism. Rather, it requires isomerization through simple bond rotation at the dienol ether π -complex (meaning that the double bond character is partially lost), as exemplified on Scheme 4, b). This was corroborated in a series of control experiments on a model substrate **Z-C1** to especially ensure that isomerization was caused by gold and not by a Brønsted acid (and yet does not require any intermolecular transesterification). Short summary of these experiments is given on Scheme 5. Surely, protonation of dienol ether by Brønsted acid can also cause isomerization through bond rotation in the arising carbocation and lead to the corresponding enol ether isomer, but this is only possible under alcohol free and water free conditions, otherwise an acetal or ketone are formed.

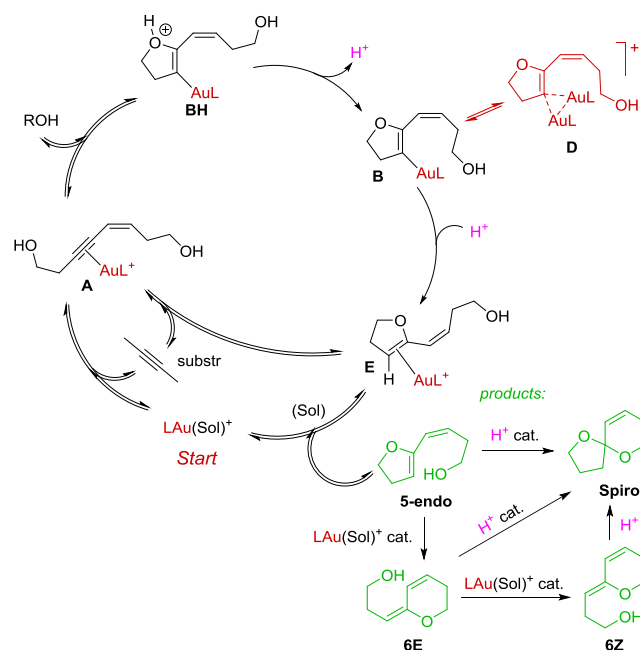
Scheme 5. Model Study of Gold Catalyzed Enol Ether Isomerization.



This study indicated very weak intrinsic reactivity of a gold enol ether π -complex toward nucleophilic attack, which makes intermolecular transesterification almost impossible (at room temperature). However, it can slowly occur at elevated temperature according to a single report.⁵

Based on these experimental facts and also knowledge from our mechanistic study of gold catalyzed hydroalkoxylation we can give a detailed view of the mechanism of gold catalyzed spirocyclization (Scheme 6). It features the main catalytic cycle that produces **5-endo** dienol ether as a single regioisomer. Other regioisomers **6E** and **6Z** are (competitively) produced by gold catalyzed enol ether isomerization of **5-endo** by the mechanisms shown above (Scheme 4). The isomerization of **5-endo** to **6E** is considered as stereospecific intramolecular transesterification of the enol ether. This stereochemical result, however, can be spoiled by a competitive isomerization of **6E** into **6Z**. The final spirocycle is produced by a classical Brønsted acid catalyzed acetalization of each of the dienol ether regioisomers (cyclization of **5-endo** being the fastest process).

Scheme 6. Mechanism of Gold Catalyzed Spirocyclization.

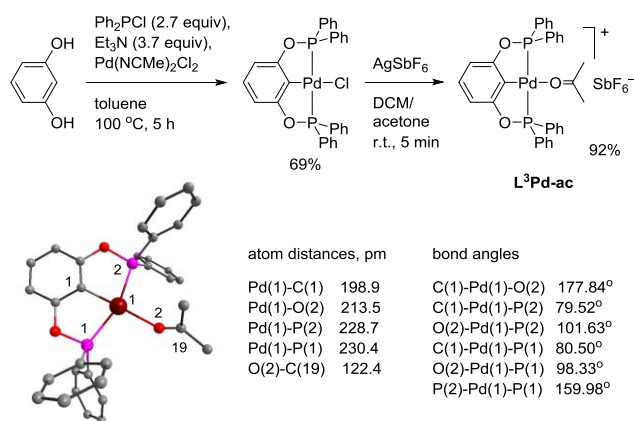


Catalysis by a Cationic Palladium Pincer Complex

Palladium catalyzed hydroalkoxylation of alkynes is known since 1983 from the work of Utimoto and only associated with the use of neutral Pd complexes.⁶ Although the reactions mostly required elevated temperatures and long reaction times (hours or days) the chemistry achieved considerable progress mainly due to *in situ* combination with cross-coupling processes. Simple intramolecular alcohol addition was proposed to take place through alkoxypalladation with subsequent protodepalladation. However until now this mechanism has not been investigated and verified. The only evidence for formation of vinylpalladium species was obtained in palladium mediated stereoselective addition of methanol to activated acetylenes giving the corresponding stable complexes, which were isolated and characterized.⁷

We hypothesized, that the drawback of previously employed palladium catalysts for hydroalkoxylation is mainly associated with poor affinity of the catalysts to a triple bond and β -hydride elimination, which gives catalytically even less active Pd(0) species.⁸ Also alkyne trimerization is known to be catalyzed by Pd.⁹ To address these problems we proposed to use cationic Pd(II) pincer complexes. This idea was inspired by a report from Michael and Cochran concerning the hydroamination of alkenes catalyzed by cationic palladium pincer complexes.¹⁰ They supposed that the cationic nature of these complexes should enhance the activation of a triple bond while the tridentate nature of the ligands would prevent β -hydride elimination and alkyne oligomerization processes. Simply saying, installation of a tridentate pincer ligand reduces the intrinsic "specialization" of the palladium center by blocking any Pd(II)/Pd(0) redox processes. After such a "restyle", cationic pincer complexes should become similar to simple gold catalysts LAu⁺.

Scheme 7. Preparation and X-ray Structure of Pd Catalyst.



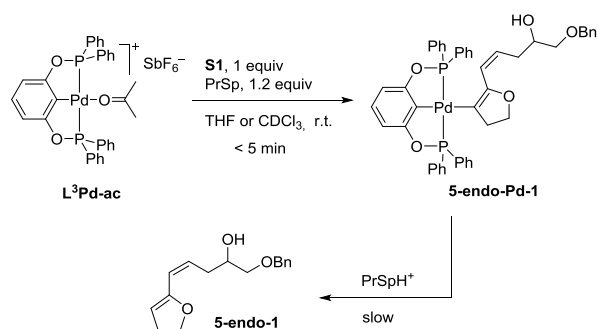
In our preceding publication we introduced a simple palladium catalyst **L³Pd-ac** for activation of alkynes at room temperature.¹ This catalyst is the complex of palladium with the tridentate pincer ligand and the weakly bound acetone ligand. The molecular composition of the complex as 1:1 adduct with acetone was initially suggested from integration of the ¹H NMR spectrum but not from the chemical shift of acetone, because it gets displaced by residual water in solution. Here we confirm coordination of acetone to Pd by single crystal X-ray analysis (Scheme 7).

In the current paper we used this catalyst to get insight into the mechanism of palladium catalyzed spirocyclization. We again applied the tactics of catching an organometallic intermediate in

the presence of a base. Indeed, treatment of the substrate **S1** with **L³Pd-ac** (1 equiv) in the presence of 1,8-bis(dimethylamino)naphthalene (PrSp, 1.3 equiv) in CDCl₃ or THF led to immediate formation of a single organopalladium compound. This turned out to be simple vinyl palladium species **5-endo-Pd-1** which was characterized *in situ* by ¹H, ¹³C, ³¹P and various two dimensional NMR spectra. Remarkably, protonolysis of **5-endo-Pd-1** by PrSpH⁺ occurs slowly enough to allow characterization in solution during extended period of time, but eventually all **5-endo-Pd-1** is transformed to the corresponding dienol ether **5-endo-1**. The fact that vinyl-palladium species tolerates PrSpH⁺ indicates its much higher resistance to protonolysis in comparison to the corresponding vinyl-gold species, that are known to undergo protodeauration by PrSpH⁺ immediately.

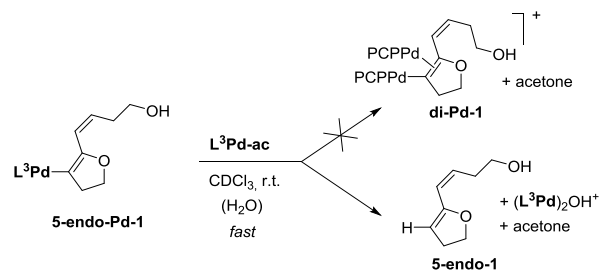
The ¹H NMR spectrum of **5-endo-Pd-1** exhibits a molar ratio pincer ligand:dienol ether core of 1:1. In the ³¹P NMR it exhibits one singlet at 146.31 ppm (which is 1.4 ppm lowfield from **L³Pd-ac**). Furthermore, the species does not react with PPh₃ or Cl⁻ (to exclude formation of any cationic dipalladium species which would be similar to diaurated species).

Scheme 8. Formation of Vinyl Palladium Intermediate 5-endo-Pd-1 in the Presence of a Base.



In order to test the existence of cationic dipalladium species, fresh catalyst **L³Pd-ac** was added to a solution of **5-endo-Pd-1**. Instead of giving new organopalladium species **di-Pd-1**, complete protodepalladation immediately occurred (Scheme 9). This indicates that cationic dipalladium species (if able to exist) must be extremely unstable and will certainly not arise under real catalytic conditions. Given the fact that diaurated species exist even with very bulky ligands, the existence of any dipalladium species is likely precluded by nature of the metal rather than by simple steric reasons.

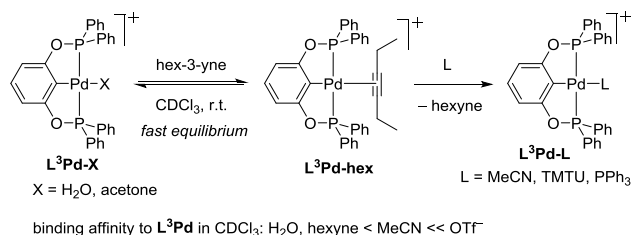
Scheme 9. Reactivity of Vinyl Palladium Species Toward Pincer Palladium Cation.



After finding the key vinyl palladium intermediate we turned our attention to formation of a palladium alkyne π -complex, the

precursor of vinyl palladium in the catalytic cycle. When hexyne-3 was added to solutions of cationic $L^3Pd\text{-ac}$ or $L^3Pd\text{-H}_2O$ in $CDCl_3$, a dynamic situation took place as indicated by NMR spectrum. Free and bound hexyne gave separate sets of broadened signals, demonstrating that the alkyne interacts readily and reversibly with the cationic metal center (Scheme 10). The arising palladium hexyne complex $L^3Pd\text{-hex}$ was characterized *in situ* by 1H and ^{31}P NMR. The bound hexyne signals appear at 0.85 and 1.85 ppm, both being shifted upfield in comparison to free hexyne. Attempts to isolate this complex by crystallization were unsuccessful. Addition of a stronger nucleophile (MeCN, TMTU or PPh_3) to $L^3Pd\text{-hex}$ /hexyne mixtures led to complete displacement of the bound hexyne.

Scheme 10. Coordination Chemistry of Palladium Catalyst.



After these stoichiometric experiments we proceeded to study palladium catalysis in action. We found that application of the corresponding $[L^3Pd\text{-MeCN}]^+ SbF_6^-$ or the neutral $L^3Pd\text{-OTf}$ complex causes much slower reactions than $L^3Pd\text{-ac}$. A model ligand exchange study was conducted to establish the binding affinity series to L^3Pd in $CDCl_3$: acetone, H₂O, hexyne < MeCN << OTf⁻ (Scheme 10). The inability of hexyne (a model substrate) to readily displace MeCN and OTf⁻ nicely explains the decrease of catalytic activity of $L^3Pd\text{-X}$ observed in the same order X = acetone > MeCN >> OTf⁻. Moreover, this finding confirms that a palladium alkyne π -complex must be the necessary intermediate of the catalytic cycle (similarly as gold alkyne π -complex in gold catalysis). It can be concluded that catalysis by $L^3Pd\text{-ac}$ is less tolerable to the presence of MeCN and OTf⁻, the nucleophiles that are well compatible with gold catalysis (at room temperature). This aspect limits the scope of solvents applicable as a reaction medium. For example, palladium catalyzed reactions running fast in a non-coordinating solvent like CH_2Cl_2 become drastically inhibited in methanol. In case of gold catalysis, fast reactions are possible in both solvents.

Further we conducted a catalytic study under buffered conditions. Pleasingly we found that $L^3Pd\text{-ac}$ in combination with a mild base *t*Bu₂Py allows the cyclization of **S3** and **S4** to stop at the stage of **5-endo** dienol ethers, that are selectively formed *in situ* in ca. 90% yield (Table 2).¹¹ Only minor amounts of the corresponding **6Z** dienol ethers and spiroacetal are competitively formed. These dienol ethers are sensitive and could not be isolated in individual state. The corresponding vinyl palladium species could be directly observed by 1H and ^{31}P NMR as the resting state of this reaction. This means that protodepalladation is the rate determining step under these mildly buffered conditions. Addition of a high amount of fresh $L^3Pd\text{-ac}$ catalyst (35 mol %) to **5-endo-3** caused a slight shift and broadening of the dienol ether signals. This indicates formation of a palladium enol ether π -complex undergoing fast ligand exchange within the $[L^3Pd\text{-diene}]^+/diene$ system. Importantly, no fast catalytic transformation of the dienol ether followed. After 80 minutes of reaction time only ca. 30%

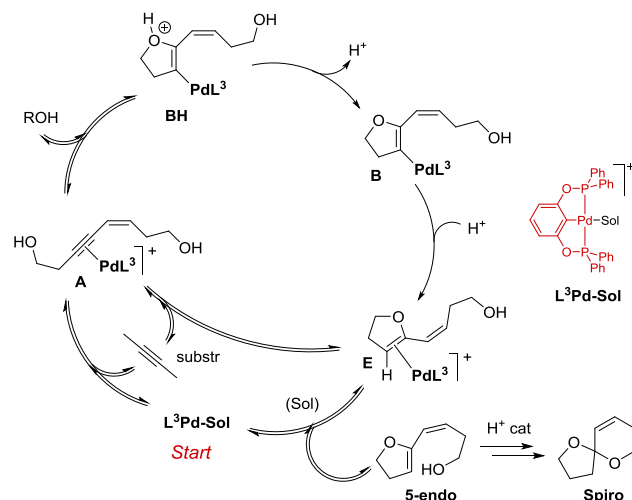
conversion of the dienol ether directly to the spiroacetal was observed.¹² This reveals the very mild nature of L^3Pd that can hardly cause isomerization of the very sensitive 5-endo dienol ether (unlike gold catalysts).

Table 2. Palladium Catalyst Enables Selective Synthesis of 5-Endo Dienol Ether 5-endo-3 and 5-endo-4.

| N | Substrate (conc., M) | Catalytic system | Solvent | conv. at time | 5-endo : 6Z : Spiro mol ratio |
|---|----------------------|--|------------|---------------|-------------------------------|
| 1 | S3 , 0.14 M | $L^3Pd\text{-ac}$ (1%), <i>t</i> Bu ₂ Py (5%) | $CDCl_3$ | 100%, 20 min | 0.92 : 0.08 : <0.02 |
| 2 | S3 , 0.09 M | $L^3Pd\text{-ac}$ (2%), <i>t</i> Bu ₂ Py (5%) | CD_2Cl_2 | 100%, 10 min | 0.90 : 0.1 : <0.02 |
| 3 | S4 , 0.04 M | $L^3Pd\text{-ac}$ (2%), <i>t</i> Bu ₂ Py (6%) | $CDCl_3$ | 100%, 40 min | 0.94 : 0.06 : <0.01 |

Based on these experimental facts and also knowledge from gold catalysis we can propose the mechanism for palladium catalyzed spirocyclization (Scheme 11). It is essentially the same as the mechanism of the gold catalyzed version but without formation of any off-cycle bimetallic species and without any dienol ether isomerization steps. Similarly to gold, all ligand exchange processes at $L^3Pd\text{-Sol}$ appear to be fast.

Scheme 11. Mechanism of Palladium Catalyzed Spirocyclization that are Consistent With Experimental Findings.

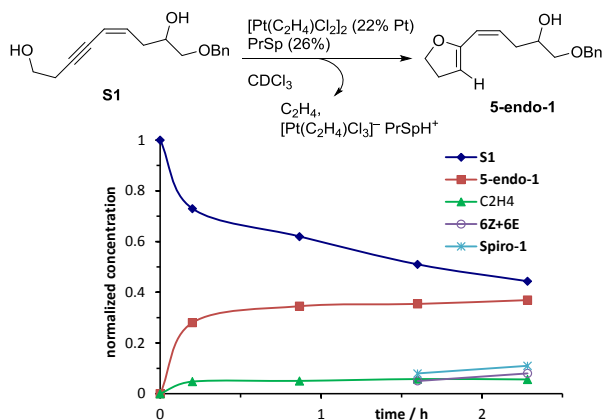


Catalysis by Zeise's Dimer and Other Platinum Compounds

Here again we tried to obtain a key organoplatinum intermediate in the presence of a base. Unfortunately this tactic was not fruitful in this case. Mixing the substrate **S1**, Zeise's dimer and 1,8-bis(dimethylamino)naphthalene (PrSp) triggered a fast catalytic reaction which soon retarded and left no organoplatinum intermediate in solution (Scheme 12). Rather, the base and Zeise's dimer reacted with traces of water to produce a salt which was identified as $[Pt(C_2H_4)Cl_3]^- PrSpH^+$. Partial formation of dienol ether product indicates that catalysis was running competitively until all the platinum bound into catalytically less active species. Absence of organoplatinum intermediate implies that no

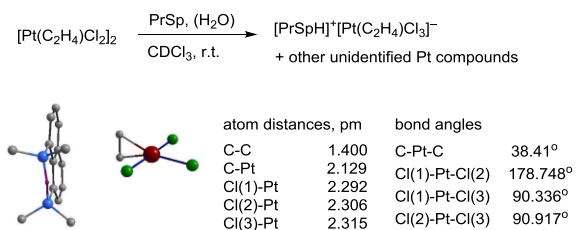
compound resistant to protodeplatination was formed. So the hypothetical vinyl platinum intermediate must be highly reactive. Interestingly, a part of ethylene became free but we could not identify what other complementary complex of platinum should have been formed according to the balance.

Scheme 12. Reaction of Zeise's Dimer With Substrate in the Presence of PrSp.



The identity of $[\text{Pt}(\text{C}_2\text{H}_4)\text{Cl}_3]^- \text{PrSpH}^+$ was confirmed by independent synthesis from Zeise's dimer and either PrSp or PrSpH⁺ Cl⁻ and also by the X-ray analysis (Scheme 13). Formation of $[\text{Pt}(\text{C}_2\text{H}_4)\text{Cl}_3]^-$ is rather unexpected because the known *trans*- $[\text{Pt}(\text{C}_2\text{H}_4)(\text{OH})\text{Cl}_2]^-$ would be formed upon the action of a base and water on Zeise's dimer.¹³ A control reaction of Zeise's dimer and PrSp in CD₂Cl₂ performed under NMR control did not give stoichiometrical amount of $[\text{Pt}(\text{C}_2\text{H}_4)\text{Cl}_3]^-$ (there is no Cl⁻ source in the system) but showed some other unidentified products. The uptake of OH⁻ (0.58 equiv) was also less than 1 equiv per 1 equiv of Pt (as evidenced by the PrSpH⁺ peak). Based on this fact we conclude, that *trans*- $[\text{Pt}(\text{C}_2\text{H}_4)(\text{OH})\text{Cl}_2]^-$ would be too basic to exist with PrSpH⁺ as a counterion in CDCl₃ or CD₂Cl₂. Correspondingly, $[\text{Pt}(\text{C}_2\text{H}_4)\text{Cl}_3]^-$ possibly arises as a result of the incomplete OH⁻ uptake and the subsequent Cl⁻ and OH⁻ redistribution among several species. Unfortunately, those new products could not be identified.

Scheme 13. Synthesis and Structure of $[\text{Pt}(\text{C}_2\text{H}_4)\text{Cl}_3]^- \text{PrSpH}^+$



Coordination chemistry of platinum complexes. Importance of *trans*-effects in rates of ligand exchange at Pt. In order to achieve a deeper understanding of the behaviour of various platinum species in solution we further studied coordination chemistry of Zeise's dimer (Scheme 14). We found that this complex is highly reactive toward ligand exchange in solution. Thus, it reacts immediately with hexyne, Me₂S, PPh₃, PrSp and MeCN. In reactions with Me₂S or PPh₃ the exchange goes till the final PtL₂Cl₂ (L = Me₂S or PPh₃), no monosubstitution product PtL(C₂H₄)Cl₂ could be detected as intermediate. In contrast, the reaction with MeCN stopped rigorously at the stage of

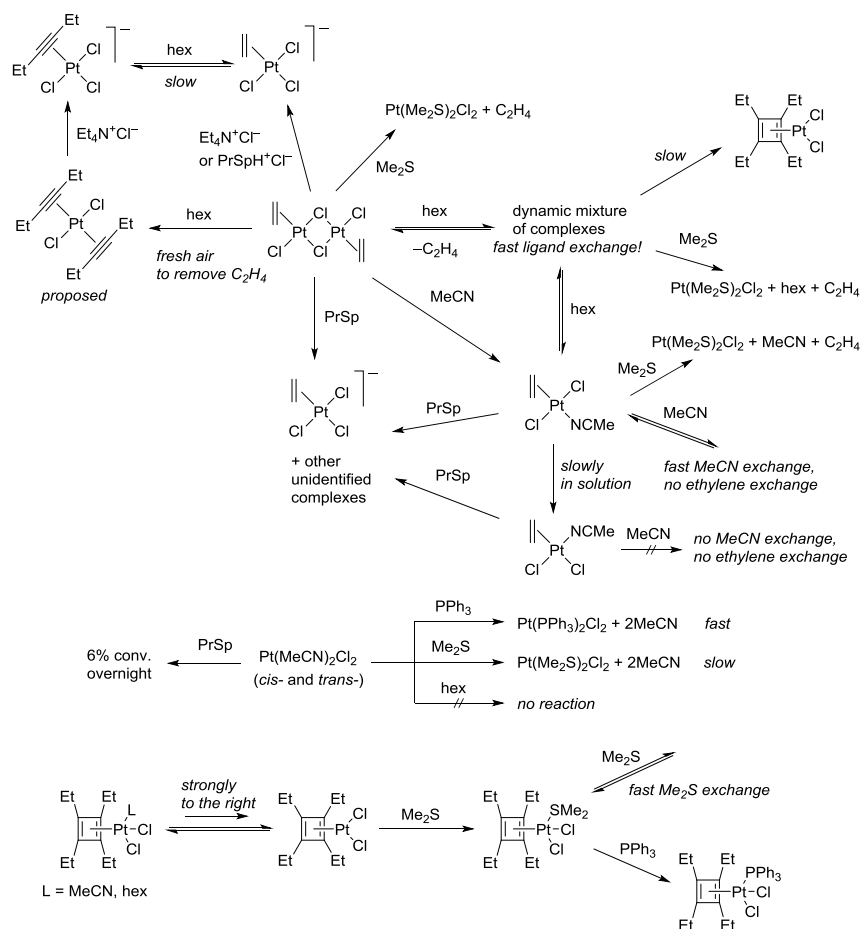
monosubstituted product *trans*-Pt(C₂H₄)(MeCN)Cl₂. In the presence of an excess of MeCN it undergoes fast ligand exchange as evidenced by a single averaged signal of bound and free MeCN, but no ethylene exchange occurs. *Trans*-Pt(C₂H₄)(MeCN)Cl₂ slowly isomerizes to *cis*-Pt(C₂H₄)(MeCN)Cl₂ in solution (56% conversion over 4 days at 40 °C in CDCl₃). Notably, *cis*-Pt(C₂H₄)(MeCN)Cl₂ was inert toward ligand exchange. For example, it does not liberate MeCN when dissolved in CD₃CN, unlike *trans*-Pt(C₂H₄)(MeCN)Cl₂.

Next, an NMR spectrum of a Zeise's dimer/hexyne mixture was recorded to observe dynamic situation, that also would indicate fast ligand exchange processes. The exact composition of this mixture remained unknown. However we did obtain useful information from the reactivity of the mixture. We found that in the presence of a sufficient excess of hexyne the ethylene gets almost completely liberated (as evidenced by the common ethylene signal approaching the chemical shift value of pure ethylene at 5.39 ppm in CDCl₃). Passing fresh air into Zeise's dimer/hexyne mixtures led to complete elimination of ethylene from the solution, leaving only alkyne complexes. Initially there are at least two compounds, but in the presence of a large excess of hexyne only one compound remains. Based on the recently reported data, this was tentatively identified as $[\text{Pt}(\text{hex})_2\text{Cl}_2]$, while the former temporary intermediate is suggested to be a Zeise's dimer analogue $[\text{Pt}(\text{hex})\text{Cl}_2]_2$.¹⁴ Both these complexes exhibit slow mode of hexyne exchange as evidenced by separate sets of free/bound hexyne signals (but the hexyne signals remain slightly broadened). When Et₄N⁺ Cl⁻ was added to this mixture, immediate reaction followed to form a single platinum complex, which was identified as $[\text{Pt}(\text{hex})\text{Cl}_3]^-$.¹⁵ All the dynamic ligand exchanges got frozen, sharp signals of hexyne excess were completely restored.

These facts point to the importance of *trans*-effects in platinum chemistry, which means that any ligand in a square platinum(II) complex directly influences the rate of ligand exchange specifically at the opposite position.¹⁶ Simply MeCN or Cl⁻, have a much lower *trans*-effect than ethylene or alkyne and this makes the ligand exchange at the *trans*- position to MeCN or Cl⁻ rather slow. This conclusion was additionally verified in experiments with a simple complex Pt(MeCN)₂Cl₂ (available as a mixture of *cis*- and *trans*-isomers).¹⁷ Indeed, this complex was completely unreactive towards hexyne. Pt(MeCN)₂Cl₂/MeCN mixtures exhibited separate signals for bound and free MeCN, indicating slow ligand exchange. In contrast to Pt(C₂H₄)(MeCN)Cl₂, the complex reacted slowly with Me₂S but quickly with PPh₃ to provide the corresponding PtL₂Cl₂. It demonstrates that ligand exchange with sufficiently strong ligands may occur smoothly regardless of the *trans*-effects. In contrast, the presence of a suitable *trans*-ligand (e.g. ethylene) becomes crucial when weak ligands (MeCN, alkyne, alkene) come to play! Typical substrates and products in platinum catalyzed alkyne chemistry would qualify as weak ligands, therefore we suggest that the huge *trans*-effects in ligand exchange at Pt is a very important factor controlling catalytic activity of Pt compounds. Due to the knowledge of the *trans*-effects, we may suggest that simple PtCl₂, the most often used catalyst for alkyne reactions, simply does not allow the best exploitation of intrinsic Pt abilities. Solid PtCl₂ has a polymeric structure, where Pt is surrounded only by the Cl ligands with their poor *trans*-effects, making PtCl₂ to be reluctant in ligand exchange. It makes sense because PtCl₂ requires boiling in MeCN for several minutes to

become $\text{Pt}(\text{MeCN})_2\text{Cl}_2$.¹⁷ And it does not give $\text{Pt}(\text{alkene})_2\text{Cl}_2$ upon reaction with alkenes.

Now it is easier to understand what happens in Zeise's dimer/hexyne mixtures. The NMR line broadening of all components in the system indicates that both ethylene and hexyne should have comparable binding affinities and a high *trans*-effect to **Scheme 14. Coordination Chemistry of Platinum Compounds.**^a



trans- effect: low (MeCN, Cl^-), moderate (Me_2S), high (alkene, alkyne)

^aAll reactions in CDCl_3 at r.t. All reactions are immediately fast except otherwise noted

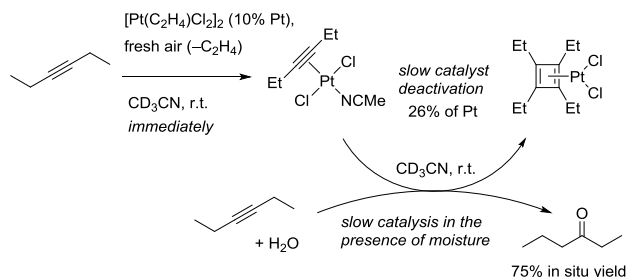
Formation of platinum cyclobutadiene complex as a side-process in catalysis. Encouraged by the fast Zeise's dimer/hexyne reaction we attempted to isolate the possible hexyne complexes by evaporation of the reaction mixture. However, this led to complete formation of the known cyclobutadiene complex $[\text{Pt}(\text{C}_4\text{Et}_4)\text{Cl}_2]$ (shown on Scheme 14).¹⁸ It appears that formation of this complex is slow in a diluted solution, but becomes fast upon concentration. Indeed, if the Zeise's dimer/hexyne solution is left to stay overnight, all initial dynamic processes disappear and $[\text{Pt}(\text{C}_4\text{Et}_4)\text{Cl}_2]$ is formed as a sole product. This complex was inert toward weak ligands like hexyne-3 or MeCN, but it did react with Me_2S to give $[\text{Pt}(\text{C}_4\text{Et}_4)(\text{Me}_2\text{S})\text{Cl}_2]$. The mixture $[\text{Pt}(\text{C}_4\text{Et}_4)(\text{Me}_2\text{S})\text{Cl}_2]/\text{Me}_2\text{S}$ exhibited fast mode of ligand exchange as evidenced by a single common Me_2S peak. Based on this result it was concluded, that $[\text{Pt}(\text{C}_4\text{Et}_4)\text{Cl}_2]$ may additionally coordinate only sufficiently strong ligands, while binding of weak alkyne or MeCN is strongly disfavored.

enable fast ligand exchange. As soon as a third strong ligand is added (Cl^-), it quickly substitutes only one alkyne or alkene from one side of platinum. Because of the low *trans*-effect of Cl^- the second ligand is left without ability to undergo fast exchange.

Since this dimerization of an alkyne could be a competitive side process during platinum catalyzed transformations in general, we investigated if $[\text{Pt}(\text{C}_4\text{Et}_4)\text{Cl}_2]$ possesses any catalytic activity. Control experiments indicated that it possesses very poor catalytic activity. For instance, after 19 h only 37 % conversion of 3-pentynol-1 (a very reactive substrate) was achieved in the presence of $[\text{Pt}(\text{C}_4\text{Et}_4)\text{Cl}_2]$ (1.7 %) in CDCl_3 . This complex was unable to catalyze intermolecular hydroalkoxylation of hexyne in MeOH. In light of the aforementioned inertness of $[\text{Pt}(\text{C}_4\text{Et}_4)\text{Cl}_2]$ to accept additional weak ligands it is not surprising that its catalytic activity is drastically decreased. Therefore, formation of Pt cyclobutadiene complexes can be regarded as catalyst deactivation. In order to check the occurrence of this undesired process under catalytic conditions, Zeise's dimer was mixed with a large excess of hexyne in acetonitrile and ethylene was eliminated by passing fresh air through the solution. Immediate formation of *trans*-Pt(hexyne)(MeCN) Cl_2 occurred as evidenced by NMR. When the reaction mixture was allowed to stay overnight, a high conversion of hexyne to hexanone occurred as a result of hydration by the

moisture in the system. After this time 26% of all Pt had transformed into $[\text{Pt}(\text{C}_4\text{Et}_4)\text{Cl}_2]$, while the other 74% remained as *trans*-Pt(hexyne)(MeCN)Cl₂. Based on this result we suggest that alkyne dimerization should be generally slow and should not compete if the desired catalytic reaction is fast (especially in case of more complicated substrates).

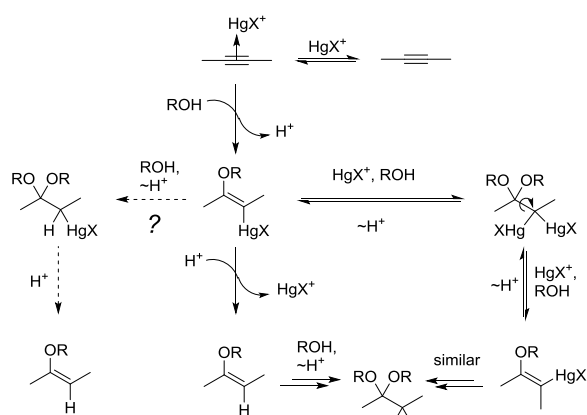
Scheme 15. Competitive Formation of $[\text{Pt}(\text{C}_4\text{Et}_4)\text{Cl}_2]$ During Alkyne Hydration.



Mechanism of Mercury (II) Catalyzed Reaction

Introduction. Although mercury catalyzed hydroalkoxylation of alkynes is known for a century, it has not gained widespread application in laboratory synthesis. Primarily this is associated with the lack of efficient catalysts being able to operate efficiently at low catalyst loadings and mild conditions. In fact, most of the research work done in the past involved harsh conditions (HgO , H_2SO_4 , heat) or substantial (if not stoichiometric) amounts of toxic mercury(II) salts, the reason for which these methods have been practically banned.^{6a} Only recently milder methods dealing with active, highly electrophilic salts, such as mercury triflate, appeared in the literature.¹⁹ However the mechanism or the corresponding reactions has not been investigated in detail. Our current understanding of catalytic hydroalkoxylation process is primarily based on the knowledge of solvomercuration/demercuration processes, which have long been known as reactions being stoichiometric in mercury (Scheme 16).²⁰

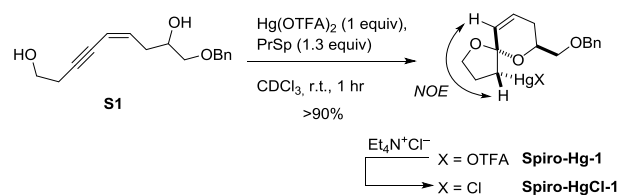
Scheme 16. Preliminary Consideration of Possible Mechanisms for Mercury Catalyzed Reaction.



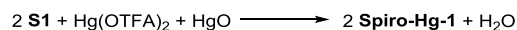
Stoichiometric experiments with $\text{Hg}(\text{OTFA})_2$. At first we conducted stoichiometric reactions with $\text{Hg}(\text{OTFA})_2$ with the aim to observe some intermediates directly by NMR.²¹ According to the proposed catalytic cycle, protonolysis of vinylmercury species is required to release the product from the metal center. Therefore, addition of a base should inhibit this process and allow observation of some organomercury intermediates. Indeed, treatment of

substrate **S1** with $\text{Hg}(\text{OTFA})_2$ (1 equiv) in the presence of proton sponge (PrSp, 1.3 equiv) in CDCl_3 allowed direct observation of an organomercury compound (Scheme 17). However the product appeared to be not a vinylmercury species, but a mercurated spirocycle **Spiro-Hg-1** formed as a single diastereomer (as confirmed by ^1H , ^{13}C NMR, H_1H -COSY, HMBC and NOESY spectra). In the ^1H NMR spectrum it exhibits a characteristic triplet at 2.76 ppm, corresponding to the CH-Hg fragment (the accurate position of mercury satellites was not located because of signal overlapping), and the alkene CH=CH fragment gives a coupling pattern corresponding to a cyclized product. Also, in the ^{13}C spectrum it exhibits a characteristic acetal signal at 104.5 ppm. In the ^{19}F NMR spectrum a single signal at -73.50 ppm is observed (which is distinctive from pure $\text{Hg}(\text{OTFA})_2$ at -71.91 and free OTFA^- at -74.87). Together with reaction stoichiometry it proves that the compound is monoalkyl mercury with OTFA^- being covalently bound to the metal. Upon addition of $\text{Et}_4\text{N}^+\text{Cl}^-$ it completely transformed into the corresponding chloride.

Scheme 17. Formation of the Key Organomercury Intermediate in the Presence of a Base.

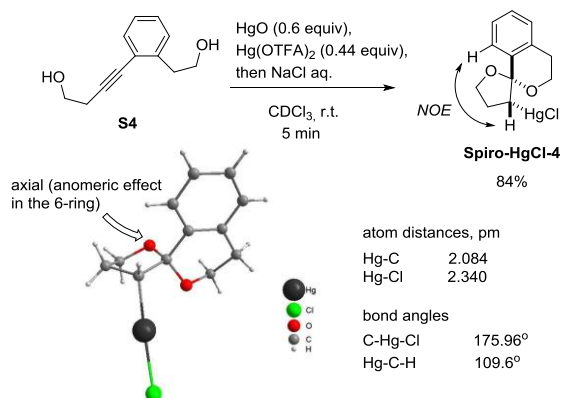


Subsequently we found that yellow oxide HgO can be used as a base and mercury source in combination with $\text{Hg}(\text{OTFA})_2$ to synthesize **Spiro-Hg-1**. While in CDCl_3 and especially in CD_2Cl_2 the reaction is accompanied with competitive formation of **Spiro-1**, in THF the competition is highly suppressed so it becomes possible to generate **Spiro-Hg-1** virtually free of any side products, according to the equation:



Using this method, crystalline **Spiro-HgCl-4** was synthesized in individual state (84% yield, counting on $\text{Hg}(\text{OTFA})_2$ as a limiting reagent). It was characterized by various NMR spectra (^1H , ^{13}C , NOESY and other) and its structure was additionally confirmed by X-ray analysis (Scheme 18). The unambiguously determined relative stereochemistry of **Spiro-HgCl-4** in connection with the NOESY spectrum makes us sure that the stereochemistry of **Spiro-HgCl-1** was also determined correctly.

Scheme 18. Synthesis and X-ray Structure of Spiro-HgCl-4.



Catalytic experiments with Hg(OTFA)₂ and the role of Spiro-Hg-1 in the catalytic cycle. Reaction of **S1** with Hg(OTFA)₂ (0.3 equiv) in CDCl₃ led to complete conversion of the starting material already after 18 min, giving a mixture of **Spiro-1** and **Spiro-Hg-1** (an equivalent amount of TFA is also formed). **Spiro-Hg-1** (0.27 equiv after 18 min) further slowly transformed to **Spiro-1**, but even after 4.7 h 0.07 equiv of **Spiro-Hg-1** still remained (Scheme 19). At a lower loading of Hg(OTFA)₂ (4%) in CDCl₃ the reaction was monitored for 1.3 h till 92% conversion. Again, **Spiro-Hg-1** was detected as a single organomercury compound but no organic intermediates were detected. Formation of any dienol ether intermediate could not be detected because of the fast spirocyclization catalyzed by TFA. The overall reaction was found to be half-order in **S1**.

Scheme 19. Catalytic Reaction at High Hg(OTFA)₂ Loading.

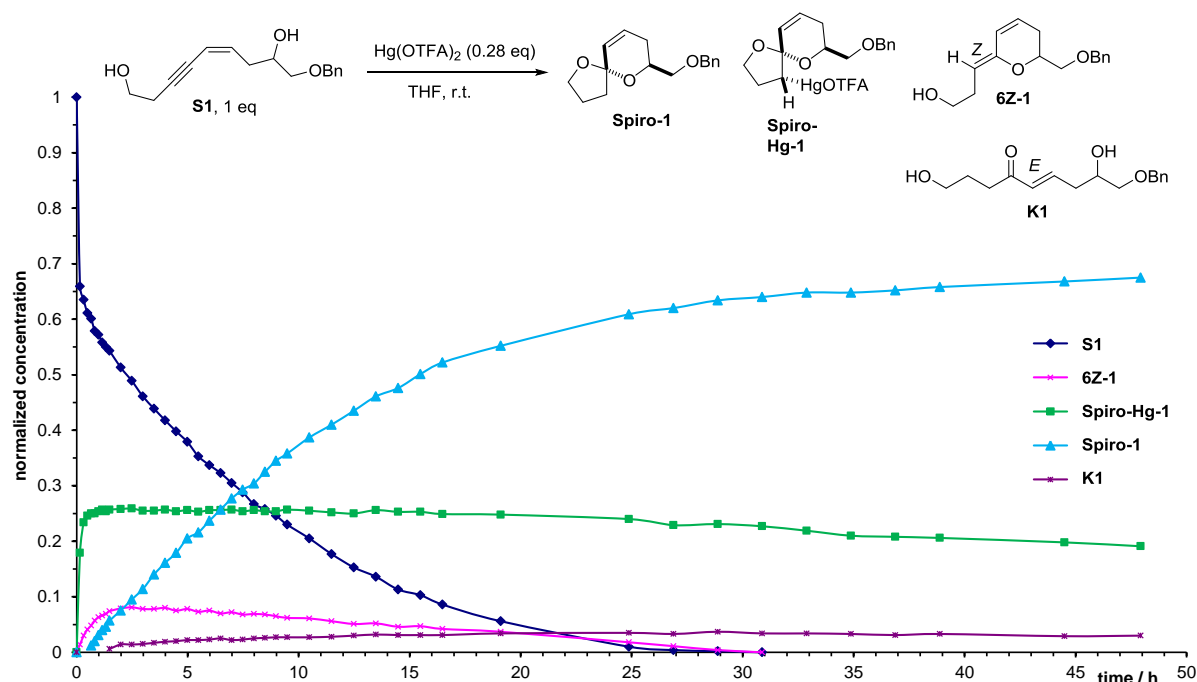
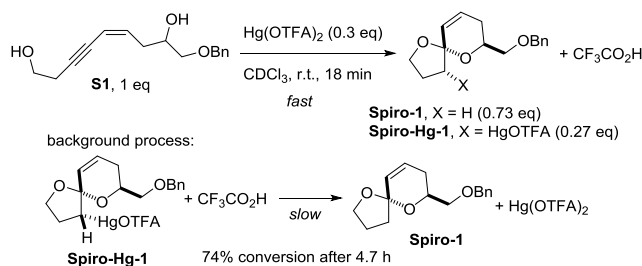


Figure 2. Complete Panorama of Hg(OTFA)₂ Catalyzed Reaction at High Catalyst Loading, Showing the Intermediate Products.

The high resistance of **Spiro-Hg-1** toward protodemercuration might question whether it is a necessary intermediate of the catalytic cycle. Therefore, we turned our attention to study the reactivity of this species (Scheme 20). We found that addition of an excess of TMTU to a solution of **Spiro-Hg-1**/TFA 1:1, generated from **S1** and Hg(OTFA)₂ in THF, led to instant conversion of **Spiro-Hg-1** to a **6Z-1/6E-1** dienol ether 1:0.07 mixture (which is close to the 1:0.1 equilibrium mixture). The same result was obtained upon treatment of **Spiro-Hg-1** with excess of PrSpH⁺ Cl⁻. Importantly, treatment of **6Z-1** with Hg(OTFA)₂ in the presence of PrSp furnished **Spiro-Hg-1** back

Replacing CDCl₃ as solvent with THF slowed down the Brønsted acid catalyzed processes and allowed observation of both organomercury and organic intermediates. We performed a catalytic run with 0.28 equiv catalyst loading in THF and monitored the reaction during a 50 h period. The complete diagram is shown in Figure 2. As can be seen, the reaction starts with a characteristic "rush" period, which lasts *ca.* 20 min. During this short period a number of organomercury intermediates were observed: dimercurated species and its ring opening products evolving toward **Spiro-Hg-1** as a single organomercury species at the end of this period. Then a slow phase begins, which is characterized by almost constant concentration of **Spiro-Hg-1**. Notably, **6Z-1** was all the time observed as a single regioisomer of a dienol ether intermediate (the configuration of the double bond was established by a NOESY experiment). After all the substrate had reacted, **Spiro-Hg-1** still remained stable for many hours.

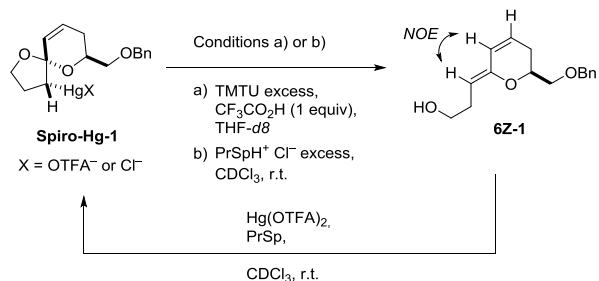
as a sole product. This reaction corresponds to an alkoxymercuration of an enol ether, which was previously represented in literature with few examples.²² The alkoxymercuration/elimination are believed to be the mechanistic steps of mercury catalyzed enol ether transesterification.²³

In addition to these stoichiometric experiments, we also performed some manipulations on catalytic mixtures. We noted that addition of *t*Bu₂PyH⁺ to a mixture of **S3** and Hg(OTFA)₂ in THF greatly accelerates conversion of the substrate. Under these conditions we noted fast scrambling of mercury between **Spiro-**

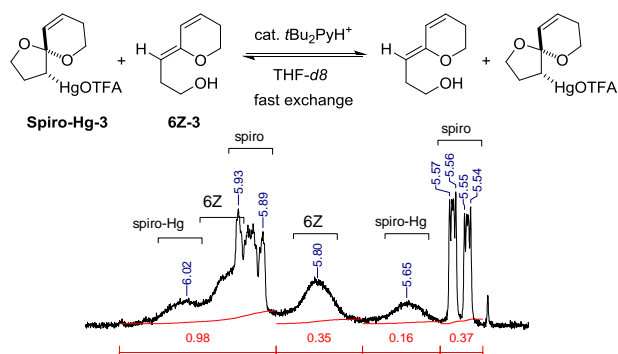
Hg-3 and **6Z-3**, which is evidenced by the line broadening of their signals (Scheme 21). This phenomenon was not observed in the presence of TFA that arises during catalysis by $\text{Hg}(\text{OTFA})_2$ alone, indicating the higher strength of $t\text{Bu}_2\text{PyH}^+$ as acid. Notably, $t\text{Bu}_2\text{PyH}^+$ catalyzes the mercury scrambling faster than spirocyclization of **6Z-3**, but eventually **6Z-3** disappears and the signal of **Spiro-Hg-3** sharpens. A mixture of **Spiro-Hg-3** and *epi*-**Spiro-Hg-3** was found to immediately and completely epimerize toward **Spiro-Hg-3** in the presence of $t\text{Bu}_2\text{PyH}^+$ (Scheme 22). This process occurs in the absence of mercury scavengers and is not accompanied by protodemercuration.

These observations indicate, that **Spiro-Hg** is amenable to fast protodemercuration but only in the presence of a suitable nucleophile as mercury scavenger. This process involves a regioselective opening of the 5-membered ring. If there is no suitable mercury scavenger in the mixture, **Spiro-Hg** keeps integrity but can undergo fast epimerization of the acetal carbon (which is believed to occur also through the 5-membered ring opening). Within the catalytic cycle, the substrate should play the role of a nucleophile, taking mercury from **Spiro-Hg** and starting a new catalytic cycle. The aforementioned mercury scrambling would be considered as a "passive" background process, because it does not contribute to productive conversion of the substrate.

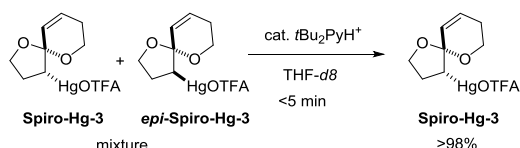
Scheme 20. Stereoselective Protodemercuration of Spiro-Hg-1 in the Presence of TMTU or Cl^- as Mercury Scavengers. Stereoselective Mercuration of 6Z-1 Back to Spiro-Hg-1.



Scheme 21. Observation of Fast Brønsted Acid Catalyzed Mercury Scrambling.

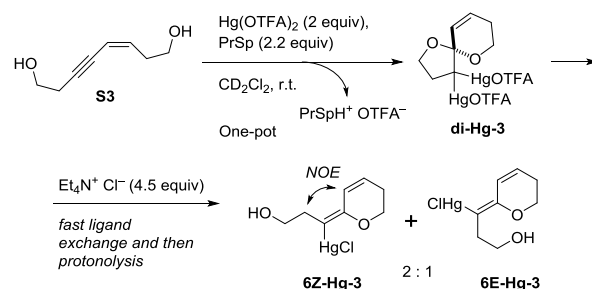


Scheme 22. Fast Brønsted Acid Catalyzed Epimerization of Spiro-Hg-3.



Attempts to detect vinyl mercury species. Formation and chemistry of gem-dimercurated species. In order to confirm the origin of **Spiro-Hg** we turned our attention towards detection of vinyl mercury a possible precursor. Because of the possible high reactivity of this hypothetical species we sought to detect it under essentially acid free conditions. Thus, substrate **S1** was first treated with 1 equiv of MeLi in THF in order to stoichiometrically and irreversibly transform it to the corresponding alkoxide *in situ*. This was treated with 1 equiv $\text{Hg}(\text{OTFA})_2$. Unfortunately, no vinyl mercury resulted, but instead, formation of half equivalent of *gem*-dimercurated species **di-Hg-1** was observed. The other half equivalent of the substrate remained simply unreacted. Obviously, even though acid free conditions precluded protonolysis of any vinyl mercury, it reacted with another half of mercury instead.

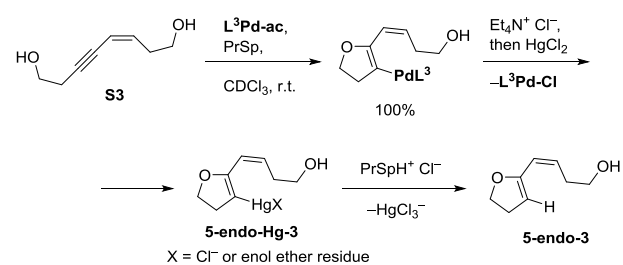
Scheme 23. Formation of Dimercurated Species and its Protonolysis in the Presence of Cl^- .



The identity of **di-Hg-1** and **di-Hg-3** was confirmed by stoichiometric synthesis from the substrate, MeLi (or PrSp) and $\text{Hg}(\text{OTFA})_2$ taken in 1:2:2 molar ratio (Scheme 23). It was characterized *in situ* by ^1H and ^{13}C NMR spectra. Protonolysis of **di-Hg-3** in the presence of TMTU excess was not stereoselective and yielded two vinyl-mercury isomers **6Z-Hg-3** and **6E-Hg-3** (stereochemical assignment of **6Z-Hg-3** was confirmed by a NOESY spectrum).

Finally, a vinyl mercury compound could be generated *in situ* by transmetalation of a vinyl palladium species by HgCl_2 (taken as a limiting reagent). Currently it remains unknown if this is an R_2Hg or RHgCl type of species. This material undergoes immediate protodemercuration by $\text{PrSpH}^+ \text{Cl}^-$ to yield pure **5-endo-3** free of any isomerization products (Scheme 24). This interesting finding suggests that the intermediate α -mercurated oxonium ion can be intercepted by a strong nucleophile prior to cyclization/isomerization. This finding does not contradict the failure to form traces of **5-endo** under catalytic condition, because formation of **5-endo** may be precluded by the absence of strong nucleophiles, that would bind mercury prior than **5-endo-Hg** would cyclize into **Spiro-Hg**.

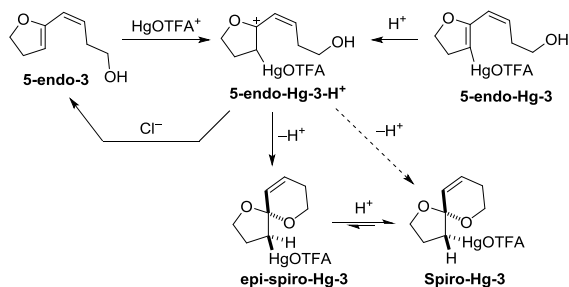
Scheme 24. Transmetalation of Vinyl Palladium Species by HgCl_2 and Subsequent Mild Protodemercuration of the Vinyl Mercury in the Presence of an Excess of Cl^- .



Further stoichiometric experiments with $\text{Hg}(\text{OTFA})_2$ and the origin of Spiro-Hg in the catalytic cycle. The above experiments clearly showed how Spiro-Hg further evolves first into **6Z** and then into the final Spiro. Unfortunately, they do not give a clue about how the substrate transforms into Spiro-Hg. Being unable to detect the primary vinyl mercury that arises upon the first cyclization event, we have no better idea other than appealing to catalysis by other metals. We know that the first cyclization event in gold, palladium and platinum catalyzed reactions is a *5-endo-dig* cyclization. It is reasonable to suggest that mercury may not be an exception. However, **5-endo** dienol ethers were never observed even in trace amounts in all experiments with $\text{Hg}(\text{OTFA})_2$, which is seemingly inconsistent with our reasoning. Given the high affinity of mercury to carbon, we propose that the primary vinyl mercury intermediate does not release the **5-endo** upon protodemercuration, but rather undergoes the second alcohol addition eventually leading to Spiro-Hg. Given this consideration we conclude that **6Z** may not be the primary product of cyclization of the substrate, but the result of ring opening of Spiro-Hg.

In order to get some experimental support to this explanation, we reasoned to perform experiments on alkoxymercuration of a **5-endo** dienol ether. Our reasoning is based on an assumption, that either protonation of vinyl mercury or mercuration of enol ether both occur through the same α -mercured oxonium ion, and that the eventual products originating from this ion in both processes should be the same (Scheme 25). Thus, **5-endo-3** was selectively prepared *in situ* by palladium catalysis. It was further treated with 0.5 equiv of $\text{Hg}(\text{OTFA})_2$ in the presence of excess PrSp (Scheme 26). This led to instant (<5 min) formation of two organomercury products: Spiro-Hg-3 and epi-Spiro-Hg-3 at full mercury loading. In parallel, the remaining **5-endo-3** slowly (30 min) isomerized to give a mixture of **6E-3**/**6Z-3**. After **5-endo-3** had finished, the reaction mixture continued to slowly evolve toward **6Z-3** and Spiro-Hg-3. As we already mentioned before, epi-Spiro-Hg-3 immediately epimerizes into Spiro-Hg-3 in the presence of a stronger acid $t\text{Bu}_2\text{PyH}^+$, and this process appears to be just slower in the presence of PrSpH⁺.

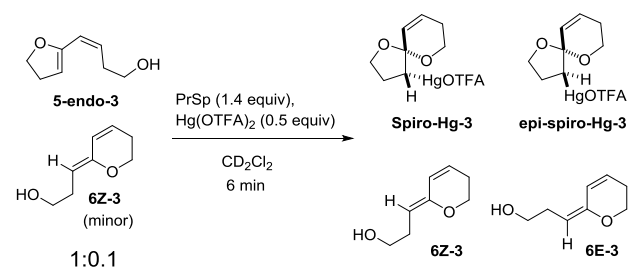
Scheme 25. Assumption that Protonation of Vinyl Mercury or Mercuration of Enol Ether Both Occur Through the Same α -Mercured Oxonium Ion, Eventually Giving the Same Products.



Formation of epi-Spiro-Hg-3 at least as a predominant organomercury product suggests that it must also arise upon protonolysis of hypothetical **5-endo-Hg-3**. However, epi-Spiro-Hg-3 was never observed as intermediate under real catalytic conditions, suggesting it is immediately epimerized by acid. It also remains unknown whether protonolysis of **5-endo-Hg** as well as mercuration of **5-endo-3** are both intrinsically

stereospecific processes that would yield epi-Spiro-Hg-3, followed by the acid catalyzed epimerization to Spiro-Hg-3. Anyway, this experiment provided some basis to conclude, that Spiro-Hg must eventually arise from **5-endo-Hg** during the catalytic process.

Scheme 26. Alkoxymercuration of 5-Endo Dienol Ether.



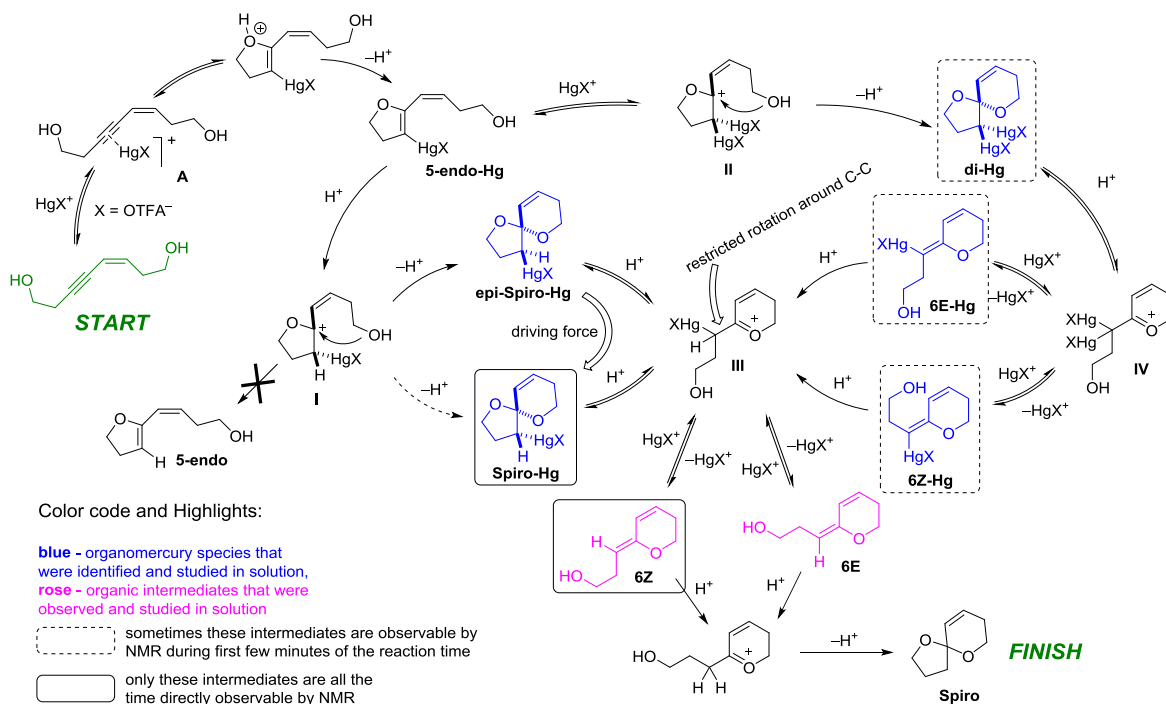
- 6E/6Z/spiro-Hg/epi-spiro-Hg/5-endo = 1 : 0.35 : 0.53 : 0.79 : 0.15 at 6 min
- 5-endo disappears at 30 min
- reaction mixture slowly evolves toward 6Z/spiro-Hg
- epi-spiro-Hg rapidly isomerizes into spiro-Hg in the presence of a stronger acid $t\text{Bu}_2\text{PyH}^+$

Mechanism of $\text{Hg}(\text{OTFA})_2$ catalyzed spirocyclization.

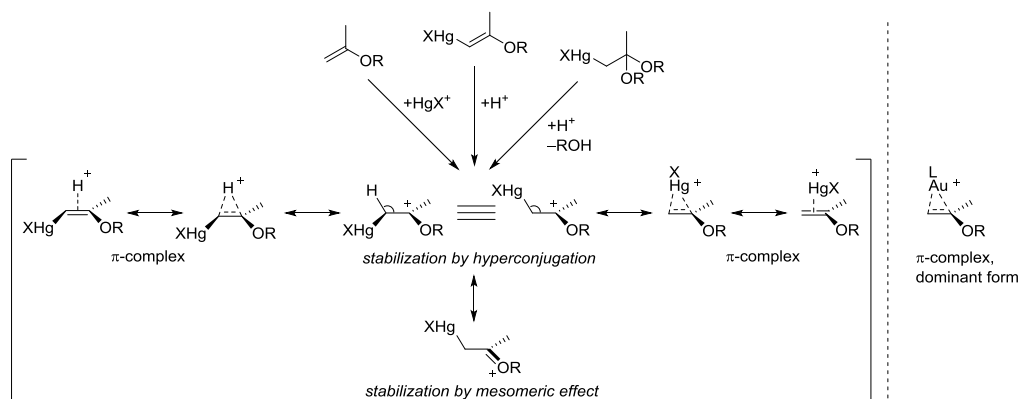
Based on the above experimental evidence we propose a mechanistic scheme for the whole catalytic process (Scheme 27). It starts by means of *5-endo-dig* cyclization essentially the same way as all other gold, palladium, platinum catalyzed versions, forming **5-endo-Hg** as the primary organomercury intermediate, concomitantly liberating acid in solution. Further, **5-endo-Hg** undergoes two competitive processes, occurring without the cleavage of the C–Hg bond. Thus, **5-endo-Hg** undergoes mercuration to deliver *gem*-dimercurated species **di-Hg**. As a second option it undergoes protonolysis to deliver epi-Spiro-Hg, and possibly Spiro-Hg. Notably, the protonolysis cannot end up with the mercury cleavage to deliver **5-endo** (because the opposite process is rather favored). This property constitutes the major difference from the other transition metal catalyzed versions.

Further, **di-Hg** evolves toward Spiro-Hg through a series of ring-opening/ring-closing events (involving neutral **6E-Hg** and **6Z-Hg** on the way). In parallel, any epi-Spiro-Hg formed from protonolysis is immediately epimerized by acid to form Spiro-Hg as a single thermodynamically stable epimer. The total mixture of **di-Hg**, **6E-Hg** and **6Z-Hg** quickly evolves toward Spiro-Hg, which is observed as the single resting state during the whole remaining reaction time. This evolution period was found to be very fast in CDCl_3 (<5 min, no **di-Hg**, **6E-Hg** and **6Z-Hg** are observed at all), but slower in THF (ca. 20 min).

Spiro-Hg is rather resistant to protodemercuration by itself. Only in the presence of a HgOTFA^+ scavenger it would quickly react releasing the **6Z** dienol ether as the major regioisomer (>90%). Indeed, the opposite reaction is alkoxymercuration of **6Z**, giving Spiro-Hg 100% back. It is the diol substrate to bind the arising HgOTFA^+ moieties, to provide the fundamental basis for the catalytic turnover of mercury. The **6Z** released on this step is further transformed to the Spiro final product by means of classical Brønsted acid catalysis.



Scheme 27. Mechanism of Hg(OTFA)₂ Catalyzed Spirocyclization.



Scheme 28. Formation of α -Mercurated Oxonium Ion and Its Resonance Structures. Comparison With Gold Enol Ether π -Complex.

Overall, the mechanism of mercury catalyzed spirocyclization looks a bit complicated. Several steps include formation of a single type of intermediate: α -mercurated oxonium ion (species **I**, **III**). These species are formed by three processes, from three different types of precursors (Scheme 28). The structure of the α -mercurated oxonium can be displayed as a series of resonance structures. This species is believed to be involved in the known mercury(II)-catalyzed transesterification of enol ethers. The exact structure of this species was never established. But from the reactivity patterns we may suggest that it should be best described as α -mercurated oxonium ion and not as a π -complex (a situation similar to that of α -aurated iminium ion).²⁴ In contrast, gold complexes of enol ethers are qualified rather as π -complexes.

In addition to α -mercurated oxonium ions there are also α,α -dimercurated oxonium ions possible (species **II**, **IV**), which are formed by mercuriation of any vinyl mercury intermediate. These ions must be even more stabilized by hyperconjugation with mercury.

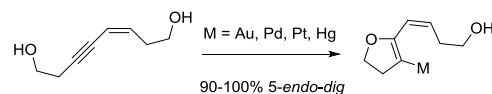
We suggest that the double bond character in α -mercurated oxonium ions should be partially lost, enabling rotation around

the C–C bond as shown in Scheme 27. Therefore eventually they must give a thermodynamic mixture of alkene isomers upon elimination of mercury by ligand exchange. Therefore, protodemercuration should not be considered as a stereospecific process (but it can be very selective if the difference in thermodynamic stabilities of the competing products is sufficiently big, such as in our case with **6E/6Z**). The situation resembles that described for α -aurated iminium ions and the conjunct isomerization of enamines.

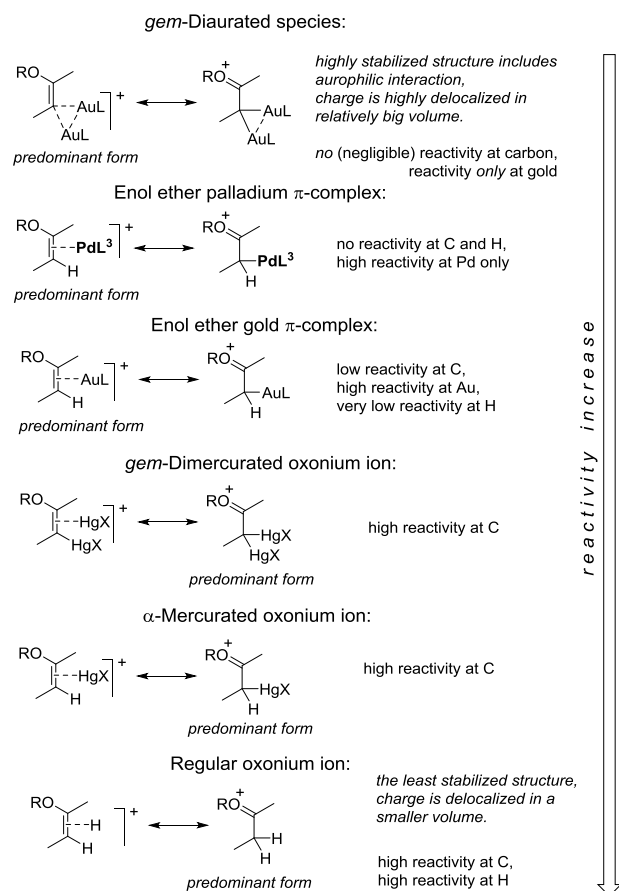
Conclusion

We investigated mechanisms of gold(I), palladium(II), platinum(II) and mercury(II) catalyzed spirocyclizations. From our broad mechanistic survey we can draw comparisons of catalysis by each of these metals, defining similarities and differences, advantages and disadvantages. A few of them are listed below.

1. First cyclization event is 5-endo-dig for each of the metals:



2. Comparison of reactivity of various cationic species toward nucleophilic addition at the C–O carbon is suggested:



- Au, Pd and Hg complexes all undergo fast ligand exchange. In contrast, Pt complexes do not always undergo fast ligand exchange, being strongly dependent on the *trans*-effect.
- L^3Pd-ac catalysis does not inhibit itself by building up any off-cycle species like Au.
- L^3Pd-ac catalysis is ineffective to promote isomerization of **5-endo**, but the other metals do cause isomerization. Therefore, L^3Pd-ac catalysis can be more suitable for synthesis of sensitive enol ethers.
- Among these metals Hg seems to have the highest ability to activate the substrate but the lowest ability to liberate the product.
- Despite some differences in mechanistic details, all the metals are suitable as catalysts for synthesis of **Spiro**.

ACKNOWLEDGMENT

We thank Dr. D. Wistuba for HRMS analysis, Dr. K. Eichele and the Institut für Anorganische Chemie for allowing us to use the NMR spectrometer.

REFERENCES

- Zhdanko, A.; Maier, M. E. *Eur. J. Org. Chem.* **2014**, 3411-3422.
- Zhdanko, A.; Maier, M. E. *Chem. Eur. J.* **2014**, *20*, 1918-1930.
- Since the starting dienol ether solution was contaminated with minor amounts of 6Z and spiroacetal, the amounts of these minor components were taken into account when calculating the conversions of the starting dienol ether and its product ratios.

⁴ Traces of Brønsted acid that can be imagined to form by a gold catalyst hydrolysis ($3LAu^+ + H_2O \rightleftharpoons (LAu)_3O^+ + 2H^+$, strongly shifted to the left if no base is present) or as a participant in gold-catalyzed enol isomerization catalytic cycle appears to be not enough for running any Brønsted acid catalysis at a competitive speed.

⁵ Nakamura, A.; Tokunaga, M. *Tetrahedron Lett.* **2008**, *49*, 3729-3732.

⁶ (a) Alonso, F.; Beletskaya, I. P.; Yus, M. *Chem. Rev.* **2004**, *104*, 3079-3160. (b) Chinchilla, R.; Nájera, C. *Chem. Rev.* **2014**, *114*, 1783-1826.

⁷ (a) Avshu, A.; O'Sullivan, R. D.; Parkins, A. W.; Alcock, N. W.; Countryman, R. M. *J. Chem. Soc., Dalton Trans.* **1983**, 1619-1624. (b) Kataoka, Y.; Tsuji, Y.; Matsumoto, O.; Ohashi, M.; Yamagata, T.; Tani, K. *J. Chem. Soc., Chem. Commun.* **1995**, 2099-2100.

⁸ Although hydroalkoxylation catalyzed by Pd(0) is known as well, this reaction requires an acid (benzoic acid) as a co-catalyst, occurs at elevated temperatures and/or requires long reaction times (Ref. 6a).

⁹ (a) Saito, S.; Yamamoto, Y. *Chem. Rev.* **2000**, *100*, 2901-2916. (b) Malatesta, L.; Santarella, G.; Vallarino, L.; Zingales, F. *Angew. Chem.* **1960**, *72*, 34-34.

¹⁰ Michael, F. E.; Cochran, B. M. *J. Am. Chem. Soc.* **2006**, *128*, 4246-4247.

¹¹ By the end of conversion of the starting substrate only <2 % of the spiroacetal is formed. The dienol ether will slowly continue to form spiroacetal, if the reaction mixture is not quenched by a stronger base (e.g. PrSp).

¹² Slow but direct formation of spiroacetal suggests that this process is most likely catalyzed by traces of Brønsted acid.

¹³ Benedetti, M.; Barone, C. R.; Antonucci, D.; Vecchio, V. M.; Ienco, A.; Maresca, L.; Natileb, G.; Fanizzi, F. P. *Dalton Trans.*, **2012**, *41*, 3014-3021.

¹⁴ König, A.; Bette, M.; Bruhn, C.; Steinborn, D. *Eur. J. Inorg. Chem.* **2012**, 5881-5895.

¹⁵ Steinborn, D.; Tschöerner, M.; Zweidorf, A. v.; Sieler, J.; Bögel, H. *Inorg. Chim. Acta* **1995**, *234*, 47-53.

¹⁶ (a) Chernyaev, I. I. *Ann. inst. platine (USSR)* **1926**, *4*, 243-275. (b) Kauffman, G. B. *J. Chem. Educ.* **1977**, *54*, 86-89.

¹⁷ Muñoz, M. P.; Méndez, M.; Nevado, C.; Cárdenas, D. J.; Echavarren, A. M. *Synthesis* **2003**, 2898-2902.

¹⁸ (a) Steinborn, D.; Gerisch, M.; Heinemann, F. W.; Scholz, J. Z. *Anorg. Allg. Chem.* **1995**, *621*, 1421-1425. (b) Gerisch, M.; Steinborn, D. Z. *Anorg. Allg. Chem.* **1995**, *621*, 1426-1430. (c) Steinborn, D.; Nünthel, R.; Sieler, J.; Kempe, R. *Chem. Ber.* **1993**, *126*, 2393-2396.

¹⁹ (a) Nishizawa, M.; Skwarczynski, M.; Imagawa, H.; Sugihara, T. *Chem. Lett.* **2002**, 12-13. (b) Imagawa, H.; Kurisaki, T.; Nishizawa, M. *Org. Lett.* **2004**, *6*, 3679-3681. (c) Ravindar, K.; Reddy, M. S.; Deslongchamps, P. *Org. Lett.* **2011**, *13*, 3178-3181.

²⁰ Larock, R.C. *Solvomercuration / Demercuration Reactions in Organic Synthesis*, Springer, **1986**.

²¹ Although mercury trifluoroacetate is a much less active catalyst for the spirocyclization, we have chosen this salt for mechanistic investigation because it was available in individual state as an easy to handle solid from commercial sources.

²² (a) Mlynarski, J.; Banaszek, A. *Carbohydrate Research* **1996**, *295*, 69-75. (b) Khripach, N. B.; Galitskii, N. M. *Zh. Org. Khim.* **1987**, *23*, 195-205. (c) Paquet, F.; Sinay, P. *J. Am. Chem. Soc.* **1984**, *106*, 8313-8315.

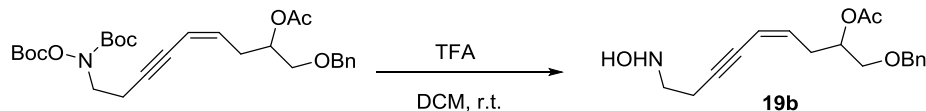
²³ Watanabe, W. H.; Conlon, L. E. *J. Am. Chem. Soc.* **1957**, *79*, 2828-2833.

²⁴ Zhdanko, A.; Maier, M. E. *Angew. Chem. Int. Ed.* **2014**, *53*, 7760-7764.

Appendix 1. Synthesis of hydroxylamine 19b and pyrrole 20b

The information of Appendix 1 concerns the Section 6.2.3.

(3Z)-1-[(benzyloxy)methyl]-8-(hydroxyamino)oct-3-en-5-ynyl acetate (19b)



The bis-Boc protected hydroxylamine (93 mg, 0.18 mmol) was dissolved in CH_2Cl_2 (1 mL) and TFA (0.2 mL, ca. 14 equiv) was added. The reaction mixture was left to stay at room temperature for several hours until TLC indicated complete conversion. The reaction mixture was diluted with EtOAc and extracted with aqueous NaHCO_3 . The organic phase was dried with Na_2SO_4 and evaporated. The residue was purified by flash chromatography (DCM/MeOH 20:1) to yield the title product as oil (51.7 mg, 91% yield). Figure A1 shows ^1H and ^{13}C NMR spectra of **19b**.

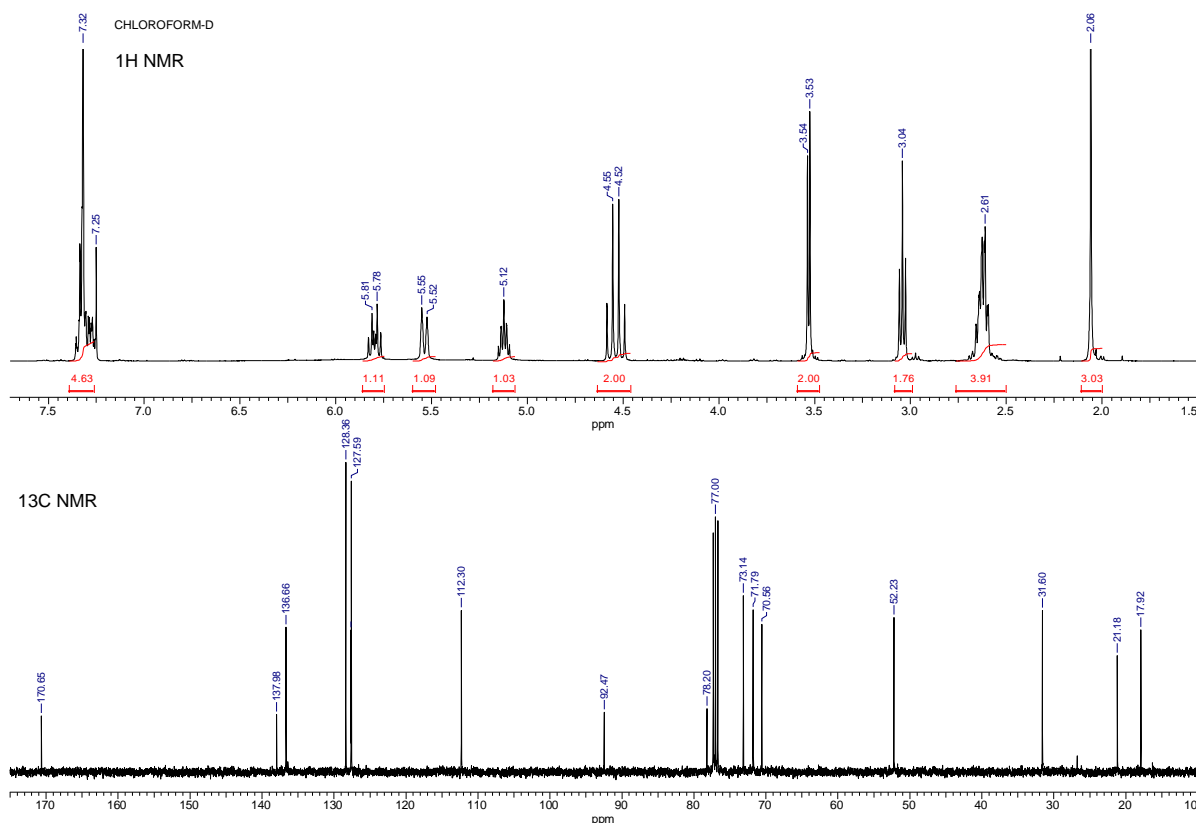
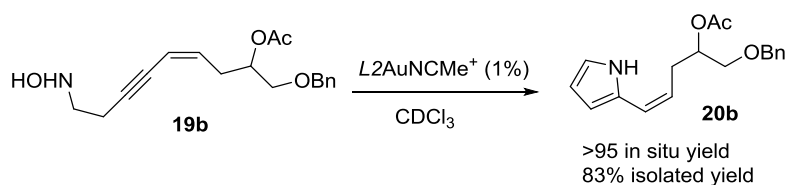


Figure A1. ^1H and ^{13}C NMR spectra of **19b**.

(3Z)-1-[(benzyloxy)methyl]-8-(hydroxyamino)oct-3-en-5-ynyl acetate (**19b**). R_f (DCM/MeOH 20:1) 0.4, R_f (EtOAc) 0.46. ^1H NMR (400 MHz, CDCl_3): 7.26-7.36 (m, 5H), 5.79 (dt, $J = 7.4, 10.7$ Hz, 1H), 5.53 (d, $J = 10.9$ Hz, 1H), 5.12 (m, 1H), 4.56 (d, $J = 12.2$ Hz, 1H), 4.51 (d, $J = 12.2$ Hz, 1H), 3.53 (app d, $J = 5.1$ Hz, 2H), 3.04 (t, $J = 6.4$ Hz, 2H), 2.59-2.66 (m, 4H), 2.06 (s, 3H). ^{13}C NMR (CDCl_3): 170.7, 138.0, 136.7, 128.4, 127.7, 127.6, 112.3, 92.5, 78.2, 73.1, 71.8, 70.6, 52.2, 31.6, 21.2, 17.9.

(3Z)-1-[(benzyloxy)methyl]-4-(1H-pyrrol-2-yl)but-3-enyl acetate (20b)



Catalyst $L2AuNCMe^+ SbF_6^-$ (0.5 mg, 0.65 μ mol, 1%) was added to a solution of hydroxylamine **19b** (15.2 mg, 47.9 μ mol) in $CDCl_3$ (0.55 mL). The reaction mixture was left to stay at room temperature. After 2 h NMR spectrum indicated *ca.* 95% conversion to the title product (Figure A2). The reaction mixture was evaporated and the pure product was obtained by flash chromatography (petroleum ether/EtOAc 2:1) as colorless oil (13 mg, 83% yield).

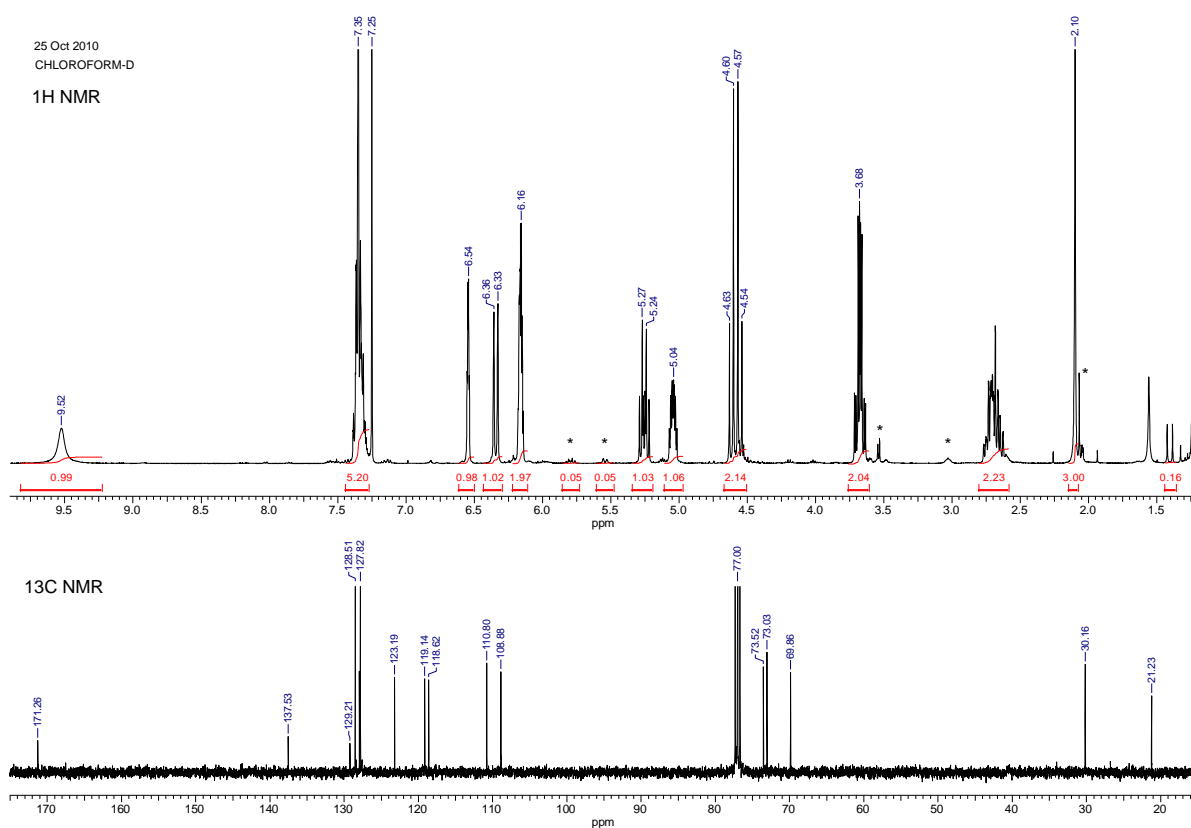


Figure A2. 1H and ^{13}C NMR spectra of the crude reaction mixture after 2 h reaction time showing 95% conversion of **19b** into **20b**. The signals of the residual **19b** are marked with (*).

(3Z)-1-[(benzyloxy)methyl]-4-(1H-pyrrol-2-yl)but-3-enyl acetate (**20b**). R_f (petroleum ether/EtOAc 4:1) 0.32, R_f (petroleum ether/EtOAc 2:1) 0.61. 1H NMR (400 MHz, $CDCl_3$): 9.52 (br, 1H), 7.29-7.38 (m, 5H), 6.54 (m, 1H), 6.35 (d, $J = 11.6$ Hz, 1H), 6.14-6.18 (m, 2H), 5.25 (dt, $J = 8.4, 11.8$ Hz, 1H), 5.04 (dddd, $J = 8.3, 5.6, 4.2$ Hz, 1H), 4.61 (d, $J = 11.9$ Hz, 1H), 4.55 (d, $J = 11.9$ Hz, 1H), 3.69 (dd, $J = 10.7, 4.4$ Hz, 1H), 3.65 (dd, $J = 10.7, 3.8$ Hz, 1H), 2.63-2.77 (m, 2H), 2.10 (s, 3H). ^{13}C NMR ($CDCl_3$): 171.3, 137.5, 129.2, 128.5, 128.0, 127.8, 123.2, 119.1, 118.6, 110.8, 108.9, 73.5, 73.0, 69.9, 30.2, 21.2.

I would like to thank all the teachers who contributed to my education. I especially thank the following teachers:

Ripich T. A. (Рипич Т. А.) – my first teacher.

Krivoshejeva V. A. (Кривошеева В. А.) – for the knowledge acquired on the wonderful mathematics lessons in school.

Ldokova V. P. (Льдокова В. П.) – for the piano lessons.

Zelenoi K. V. – for the unusually impressive and touching lectures on the history of arts.

Bakhtina T. P. (Бахтина Т. П.) – for the knowledge acquired on the unforgettable mathematics lessons in the Lyceum.

Kolevich T. A. (Колевич Т. А.) – for the discovery of the Lyceum for me and her overall support on my way.

Khvaluk V. N. (Хвалюк В. Н.) – for providing the Roberts Caserio book and inspiring me towards International Chemistry Olympiads.

Pukin A. V. (Пукин А. В.) – for providing the Mandelstam book and the inspiring lectures in organic chemistry during the summer school.

Presniakov I. A. (Пресняков И. А.) – for the seminars and colloquiums in inorganic chemistry in the MSU.

Zolotova G. A. (Золотова Г. А.) – for the seminars and colloquiums in analytical chemistry in the MSU.

Kitaev L. E. (Китаев Л. Е.) – for the seminars and colloquiums in physical chemistry in the MSU.

Nenajdenko V. G. (Ненайденко В. Г.) – for providing the starting projects for my diploma thesis.

Maier M. E. – for providing the starting projects for my PhD thesis.

I thank my cousin Maxim for bringing home chemicals from school to make chemical experiments on my 9th birthday that lighted up the enthusiasm for chemistry in me.

I thank Kirill for sharing the fun of doing chemical synthesis and other experiments in our home laboratory.

I thank the authors of the books, whom I did not know in person but who contributed the most in my chemistry education and especially organic chemistry. Among others, my most important and inspiring chemistry books were:

Shimanovich, I. E.; Pavlovich, M. L.; Tikaviy V. F.; Malashko P. M. General chemistry (“Общая химия в формулах, определениях, схемах”), 1996.

Roberts, J. D.; Caserio, M. C. Basic Principles of Organic Chemistry (translated to Russian).

Химическая энциклопедия (Chemistry encyclopedia), 5 volumes, 1988-1998.

Мандельштам Т.В. Стратегия и тактика органического синтеза (Strategy and tactics of organic synthesis), 1989.

Я выражаю благодарность всем учителям и научным руководителям, которые участвовали в моем образовании. Особую благодарность выражаю учителям:

Ришич Т. А. – моя первая учительница.

Кривошеева В. А. – за знания, полученные на увлекательных уроках математики в школе.

Льдокова В. П. – за уроки фортепиано, давшие мне понимание музыки в будущем.

Зеленой К. В. – за необычно трогательные лекции по истории искусств.

Бахтина Т. П. – за знания, полученные на увлекательных уроках математики в Лицее.

Колевич Т. А. – за знакомство с Лицеем и всеобщую поддержку на моем пути.

Хвалюк В. Н. – за предоставление книги Робертса и Касерио, которая во многом преопределила выбор органической химии как моей специальности.

Пукин А. В. – за предоставление книги Манделъштам и за вдохновляющие лекции по органической химии в летней школе.

Пресняков И. А. – за интересные семинары и коллоквиумы по неорганической химии в МГУ.

Золотова Г.А. – за интересные семинары и коллоквиумы по аналитической химии в МГУ.

Китаев А. Е. – за интересные семинары и коллоквиумы по физической химии в МГУ.

Ненайденко В. Г. – за предоставление начальных проектов для дипломной работы, за предоставление творческой свободы и поддержку всех моих инициатив..

Maier M. E. – за предоставление начальных проектов для докторской работы, за предоставление творческой свободы и поддержку всех моих инициатив.

Я благодарю моего двоюродного брата Максима за совместные занятия в детстве и знакомство с интересными объектами (включая электричество), и за то, что он принес химические вещества для проведения экспериментов на мой 9 день рождения, что и вызвало интерес к химии и послужило отправной точкой в ее самостоятельном изучении по книгам.

Я благодарен Кириллу за совместные интересные эксперименты в домашней лаборатории.

Я благодарю авторов, которых я никогда не знал лично, за их книги, которые внесли наибольший вклад в мое химическое образование. Книги, оказавшие наибольшее влияние:

Шиманович, И. Е.; Павлович, М. А.; Тикавый, В. Ф.; Малашко, П. М. Общая химия в формулах, определениях, схемах, 1996.

Робертс, Дж. Д.; Касерио, М. С. Основы органической химии.

Химическая энциклопедия, 5 томов, гл. ред. И. Л. Кнунянц, Н. С. Зефирова, 1988-1998.

Манделъштам Т.В. Стратегия и тактика органического синтеза, 1989.

Alexander Zhdanko

Date of Birth: 14.03.1985

Place of birth: Republic of Belarus, town Kletsk

Language: Russian, English, German

Education

2009 – 2015 University of Tübingen (PhD degree with “*Summa cum laude*”, supervisor: Prof Martin E. Maier).

2003 – 2008 Lomonosov Moscow State University (honour diploma in chemistry, supervisor of the diploma work: Valentine G. Nenajdenko).

2001 – 2003 Lyceum of Belarusian State University, Minsk.

1996 – 2001 Republican College of Arts, Minsk, piano studies.

1991 – 1996 Secondary School N2, Kletsk.

I have studied Chemistry as my hobby since the age of 9.